Scintillation VS Ionisation

- With the previous equations we can define the recombination-independent sum

$$E_0 = (N_q + N_{ph}) \cdot W_{ph}$$

- The recombination-independent energy required to produce a single detectable quantum, N_q or N_{ph} is also called the **W-value** (note that $N_q + N_{ph} = N_i + N_{ex}$ for any value of r)

- We will thus use $W_{ph} = W$ (this assumes that each recombining electron-ion pair produces an exciton, which leads to a photon)

- Later we will see how it can be measured (for example, at fixed energy interactions, by varying the electric field, or using different lines at different energies, for a given field)

Material	Ar	Xe
W-value [eV]	19.5±1.0	13.7±0.2 11.5±0.2

Linear Energy Scale for ER

ENERGY CALIBRATION

- With the energy deposition being described as

$$E_0 = (N_{ph} + N_q) \cdot W$$

  - W is the average energy required to produce a single excited or ionized atom (and for NRs we must also consider the "quenching factor")

- As we shall see, in two-phases TPCs, the observed light and charge signage are called $S1$ and $S2$, respectively, and these are related to the detector-specific gains g_1 and g_2. We then obtain

$$E_0 = \left(\frac{S1}{g_1} + \frac{S2}{g_2} \right) \cdot W$$

- g_1 is the total photon detection efficiency, g_2 is the charge amplification factor,. These are determined by using mono-energetic lines from various calibration sources

  - g_1 and g_2 are typically given in terms of number of photoelectrons (PE) per quantum, or in terms of detected photons (phd) per quantum

  - typical values: g_1 = 0.15 PE/photon (XENON1T), 0.11 phd/photon (LUX), g_1 = 0.16 PE/photon (DarkSide-50); g_2= 10 PE/electron (XENON1T) , g_2 = 12 phd/electron (LUX), g_2 = 23 PE/electron (here per extracted electron, DarkSide-50)

Linear Energy Scale for ER

ENERGY RESOLUTION

- The mean light and charge yields (L_y and Q_y) are then defined as

$$L_y \equiv \frac{S1}{E_0} \qquad Q_y \equiv \frac{S2}{E_0}$$

- And are estimated by 2D gaussian fits to mono-energetic lines, form the measured $S1$ and $S2$

Example XENON100

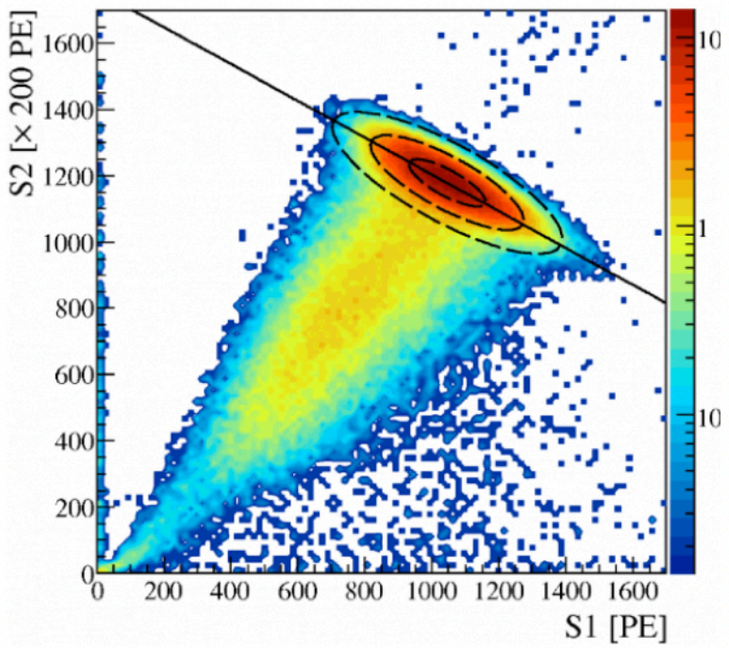

Example EXO-200

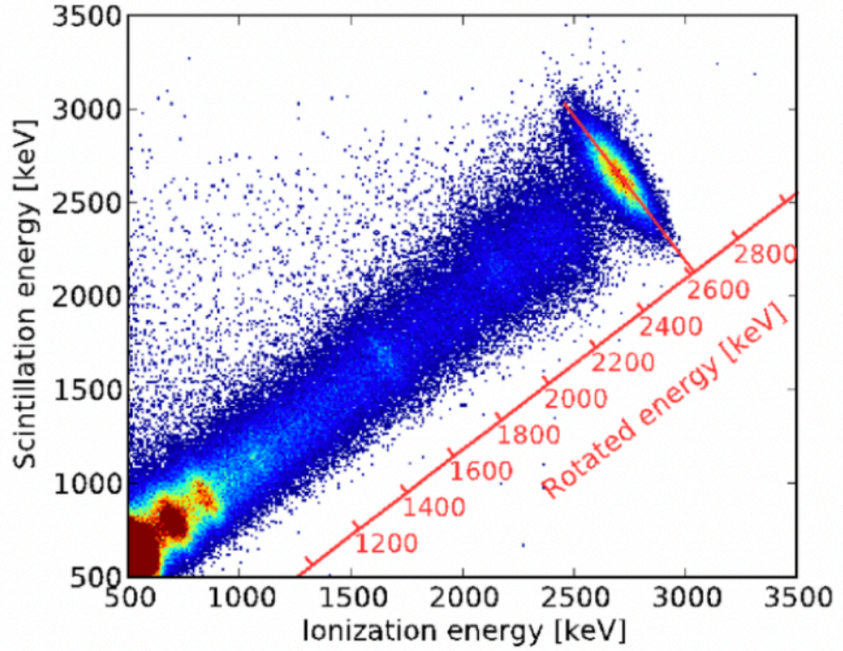

- Knowing L_y, Q_y from mono-energetic lines, one can measure the energy resolution (usually with an empirical fit to a number of measurements at different energies). The relative resolution scales as

$$\frac{\sigma}{E} \propto \frac{a}{\sqrt{E}} + b$$

Example LUX

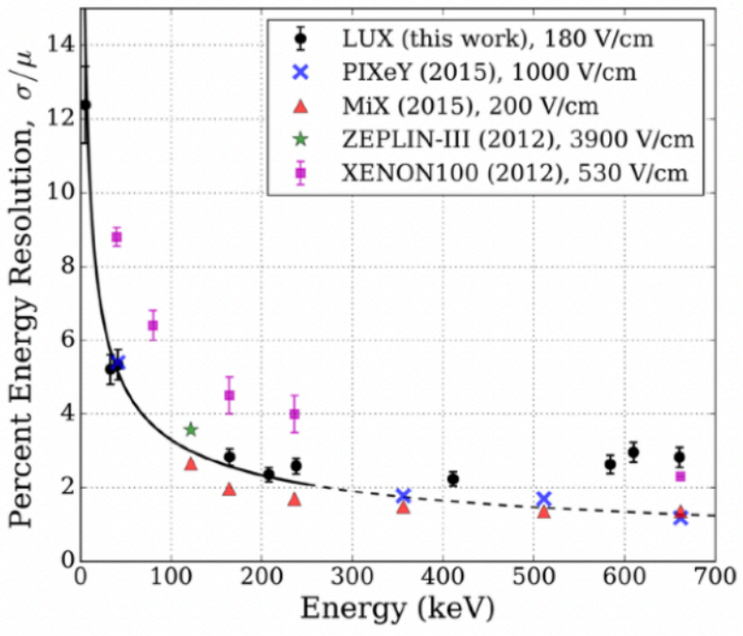

Example EXO-200

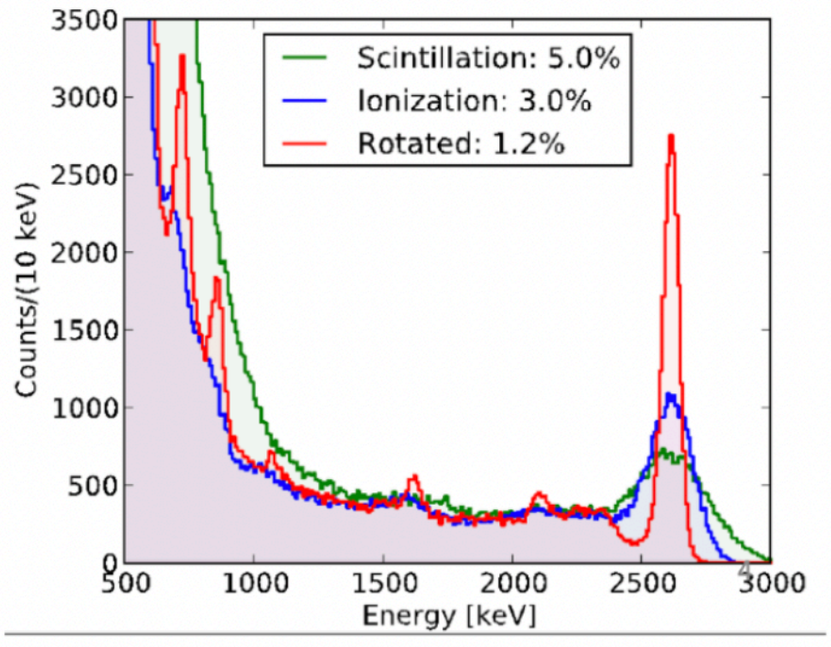

Linear Energy Scale for ER

THE DOKE PLOT

- One can also rewrite the previous equation as follows:

$$Q_y = -\frac{g_2}{g_1} L_y + \frac{g_2}{W}$$

- since we can measure $S1$ and $S2$ for clear spectral features, and E_0 is known, one can estimate g_1 and g_2 from a so-called Doke plot: a plot of $Q_y (= S2/E_0)$ versus $L_y (= S1/E_0)$

- From a linear fit one can thus extract g_1, g_2 and once these are known, reconstruct the energy of an event

$$E_0 = \left(\frac{S1}{g_1} + \frac{S2}{g_2} \right) \cdot W$$

- Hence g_1 and g_2 are simply the proportionality factors between produced number of photons and electrons, and detected ones, for each signal
  - for $S1$: mostly the efficiency of detecting photons
  - for $S2$: it includes the extraction efficiency, secondary amplification, etc

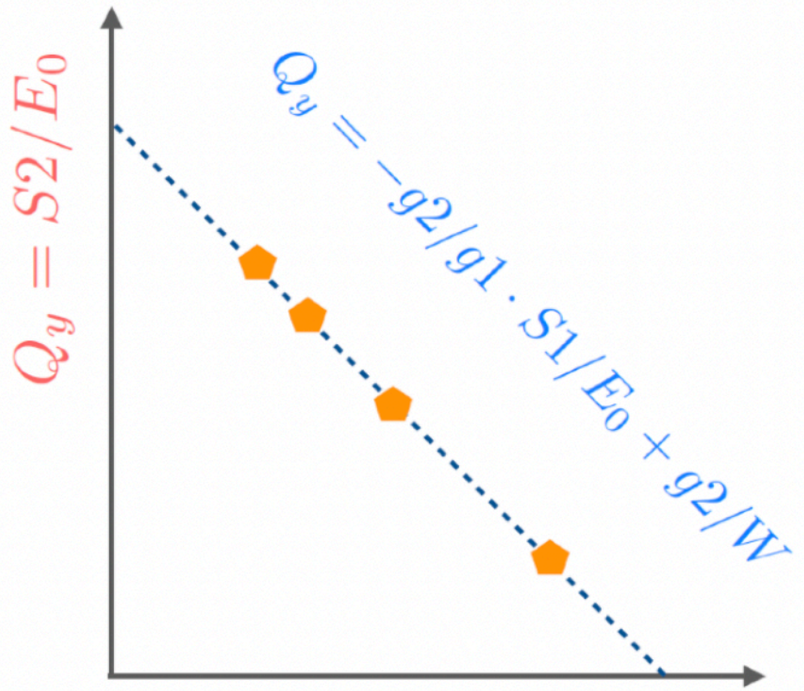

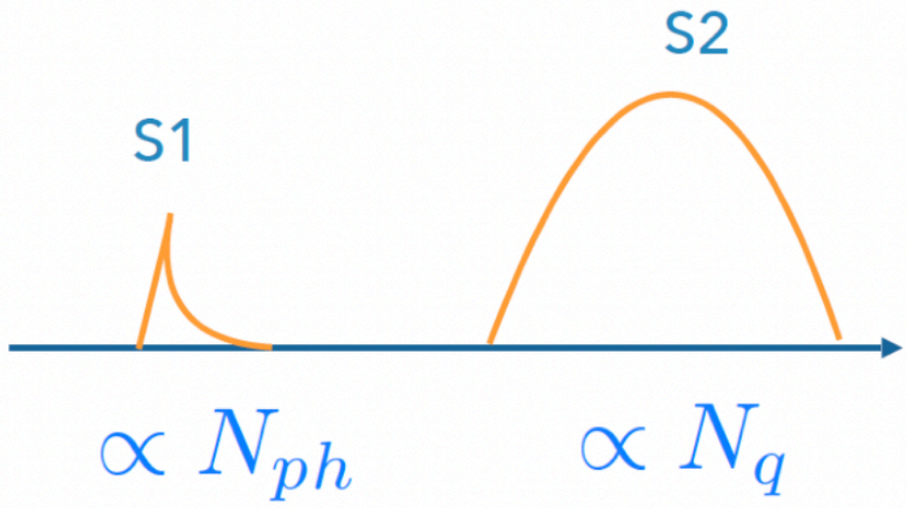

$$N_{ph} = N_{ex} + r \cdot N_i \quad N_q = (1 - r) \cdot N_i$$

Linear Energy Scale for ER

THE DOKE PLOT

- One can also rewrite the previous equation as follows:

$$Q_y = -\frac{g_2}{g_1} L_y + \frac{g_2}{W}$$

- since we can measure $S1$ and $S2$ for clear spectral features, and E_0 is known, one can estimate g_1 and g_2 from a so-called Doke plot: a plot of $Q_y (= S2/E_0)$ versus $L_y (= S1/E_0)$

- From a linear fit one can thus extract g_1, g_2 and once these are known, reconstruct the energy of an event

$$E_0 = \left(\frac{S1}{g_1} + \frac{S2}{g_2} \right) \cdot W$$

- Hence g_1 and g_2 are simply the proportionality factors between produced number of photons and electrons, and detected ones, for each signal
  - for $S1$: mostly the efficiency of detecting photons
  - for $S2$: it includes the extraction efficiency, secondary amplification, etc

Example Doke plot from **XENON1T**

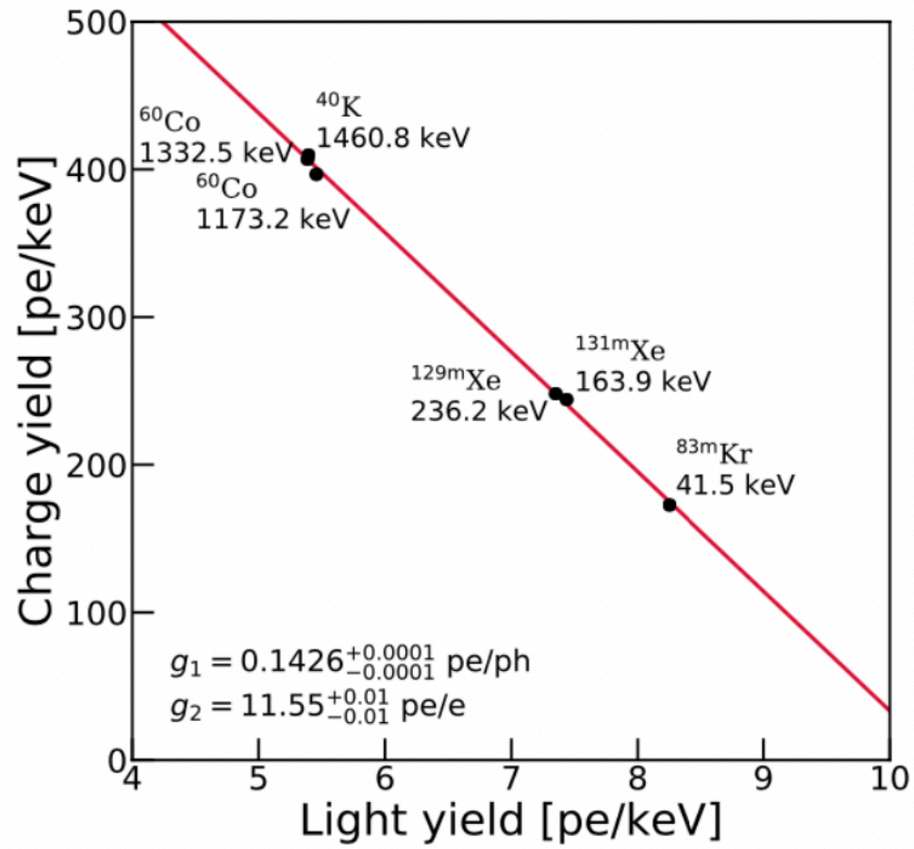

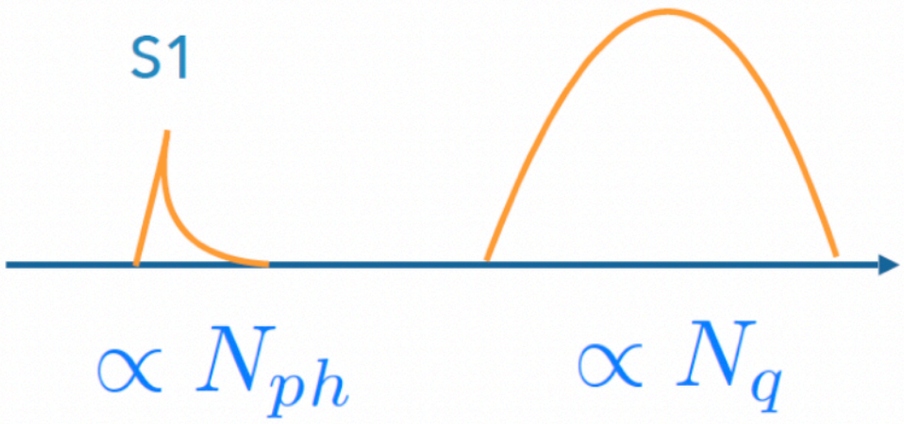

$$N_{ph} = N_{ex} + r \cdot N_i \quad N_q = (1 - r) \cdot N_i$$

Linear Energy Scale for ER

THE DOKE PLOT

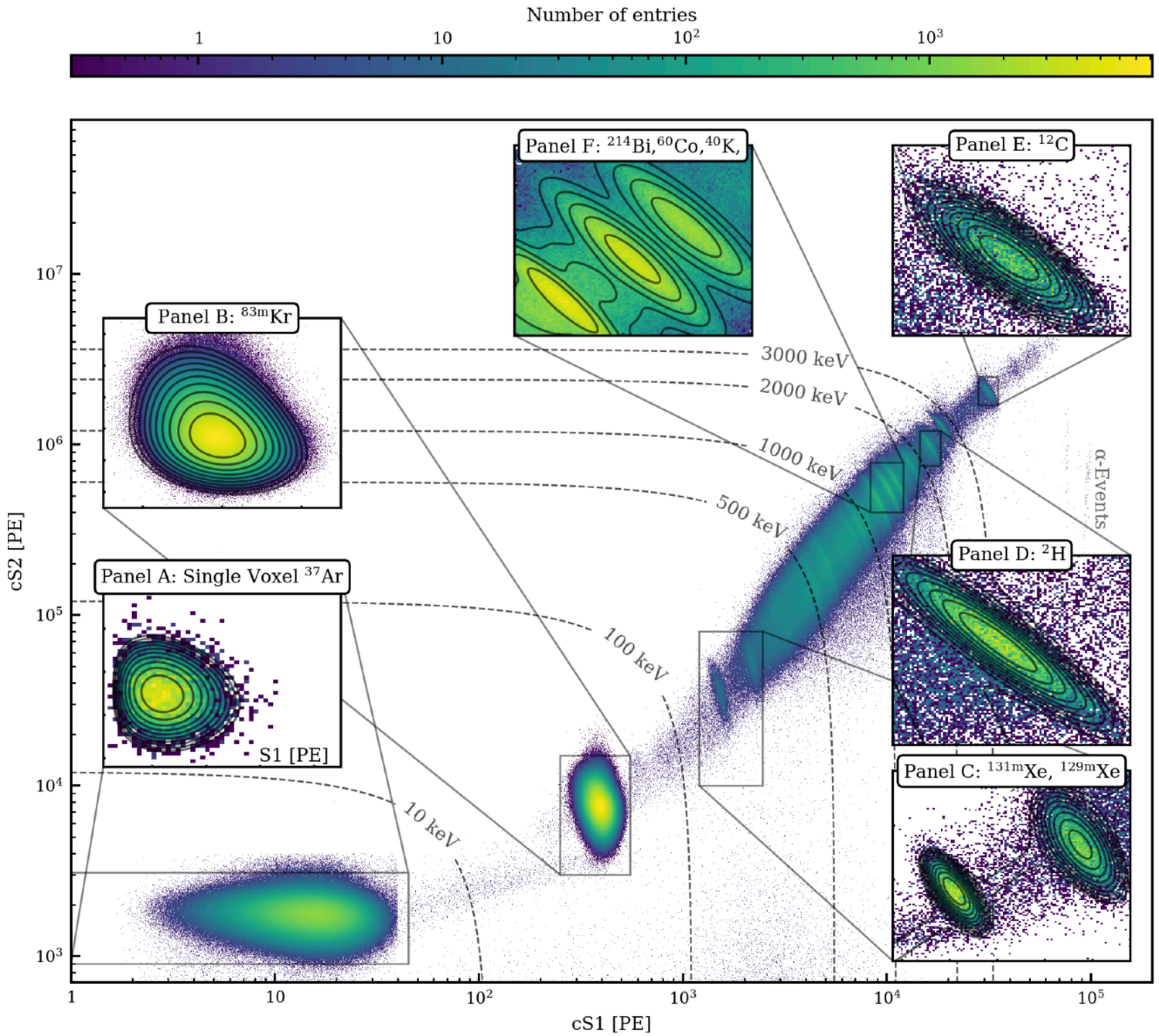

XENONnT:
PRD 111 (2025) 6, 062006

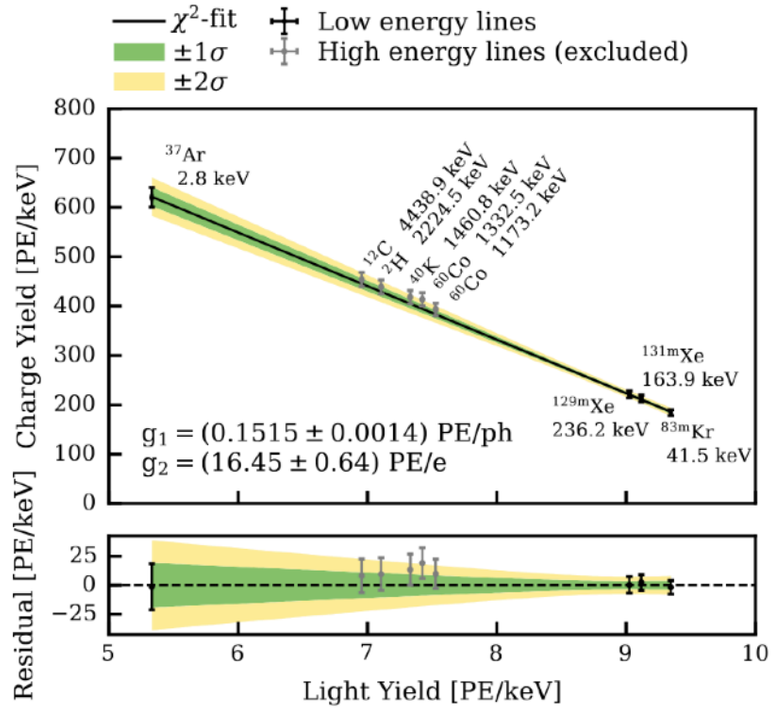

FIG. 22. Anti-correlation between the measured light yield and charge yield using mono-energetic lines. The black solid line represents the best linear fit to the data obtained from ^{37}Ar, ^{83m}Kr, ^{129m}Xe, and ^{131m}Xe low-energy lines. Data points derived from high-energy lines, not included in the fit, are displayed as grey markers. Despite not being used for the fitting process, these high-energy points remain consistent with the fitted model within their uncertainties.

ER vs NR

ELECTRONIC AND NUCLEAR RECOILS IN NOBLE LIQUIDS

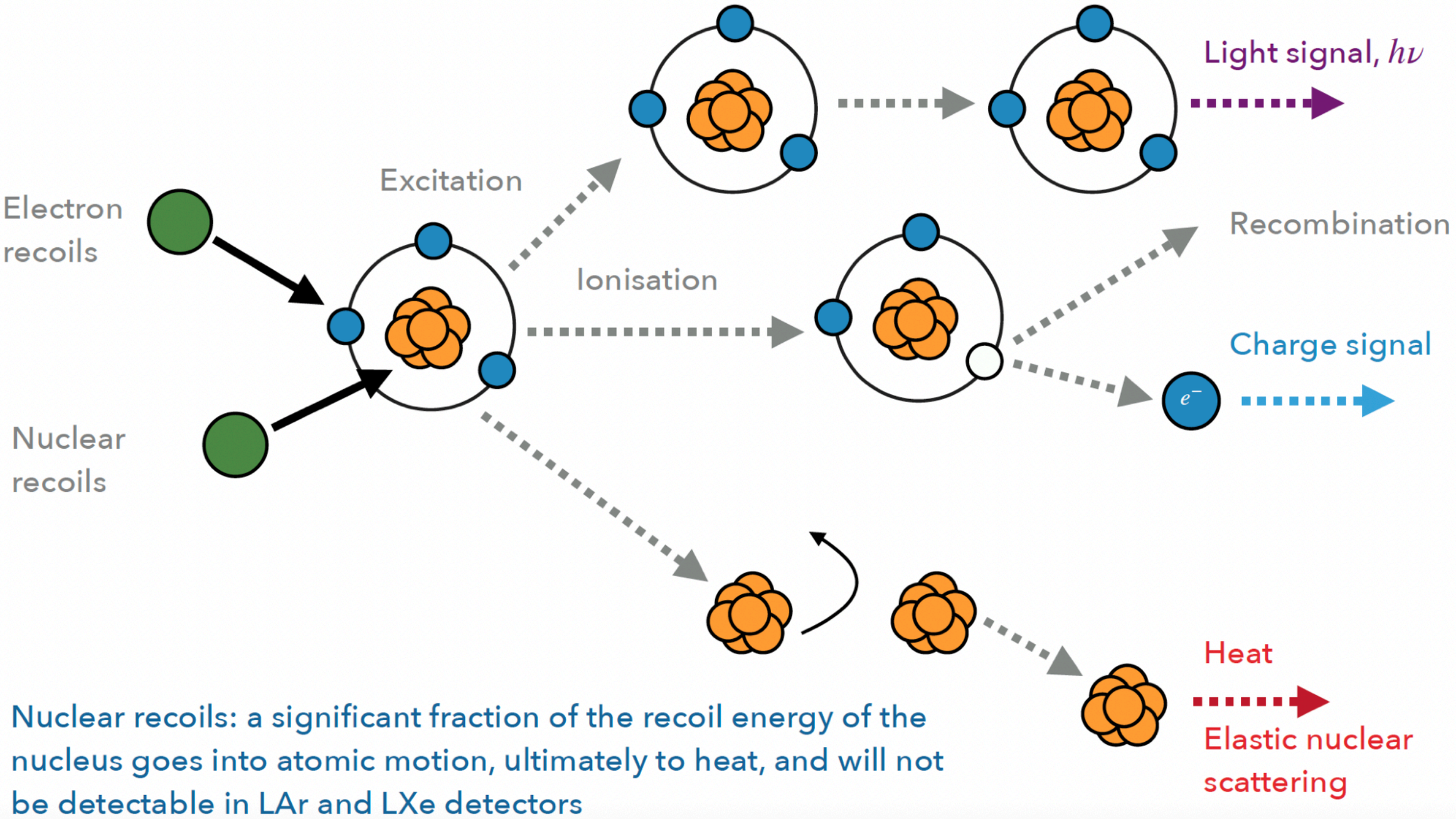

Nuclear recoils: a significant fraction of the recoil energy of the nucleus goes into atomic motion, ultimately to heat, and will not be detectable in LAr and LXe detectors

THE LINDHARD FACTOR IN NOBLE LIQUIDS

- Lindhard prediction works better if the nuclear recoil is reconstructed using both scintillation and ionization signals (hence the total quanta, for example in two-phase TPCs), the so called "combined energy scale":

$$E_{ER} = W \cdot (N_{ph} + N_q)$$

$$E_{NR} = W \cdot (N_{ph} + N_q) \cdot \frac{1}{f_n}$$

$$f_n = \frac{W \cdot (N_{ph} + N_q)}{E_{NR}}$$

- N_q is the number of primary electrons
- N_{ph} is the number of primary UV photons
- W is the average energy to produce an electron or a photon

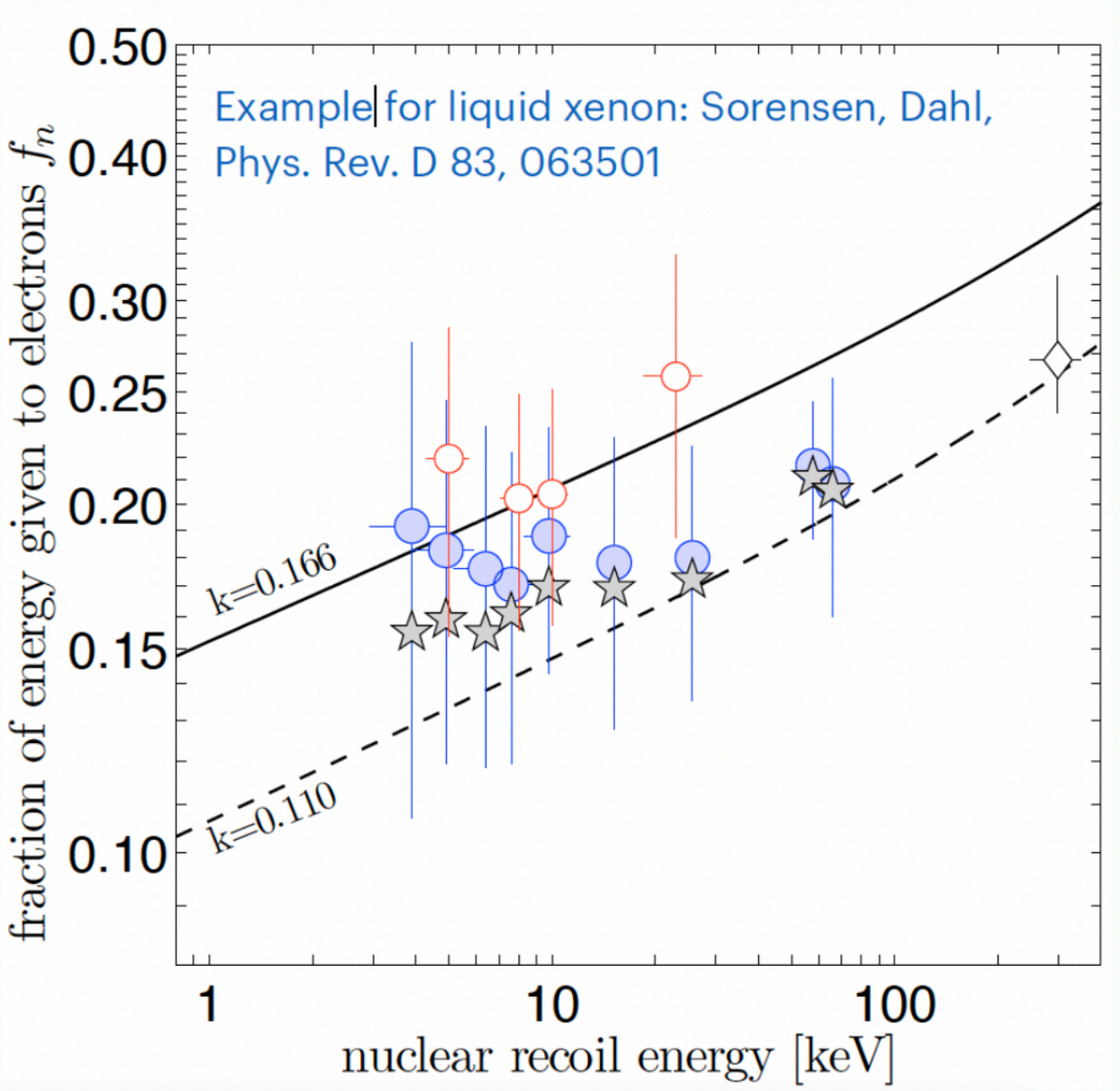

ER vs NR: Larger recombination in NR

- Because the stopping power for electrons increases with decreasing energy below 1 MeV the tracks of ERs in LXe have a high ionization/excitation density near the end of the track. In contrast, alpha and to a certain extent also NRs will have higher density at the beginning of the track.

- At the low energies relevant to DM search the ionization density of NRs is much larger than that of ERs and since the recombination rate increases with ionization density we expect less reduction of scintillation due to E-field for NRs.

- This was indeed observed in the first experiments to measure the ionization and scintillation of NRs in LXe carried out at Columbia at the start of the XENON Dark Matter project (see previous slide).

- New measurements are currently underway at Columbia to measure the charge and light yield of much lower energy NRs and also of ERs with a few keV of energy. Will discuss this experiment along others in Lecture 2

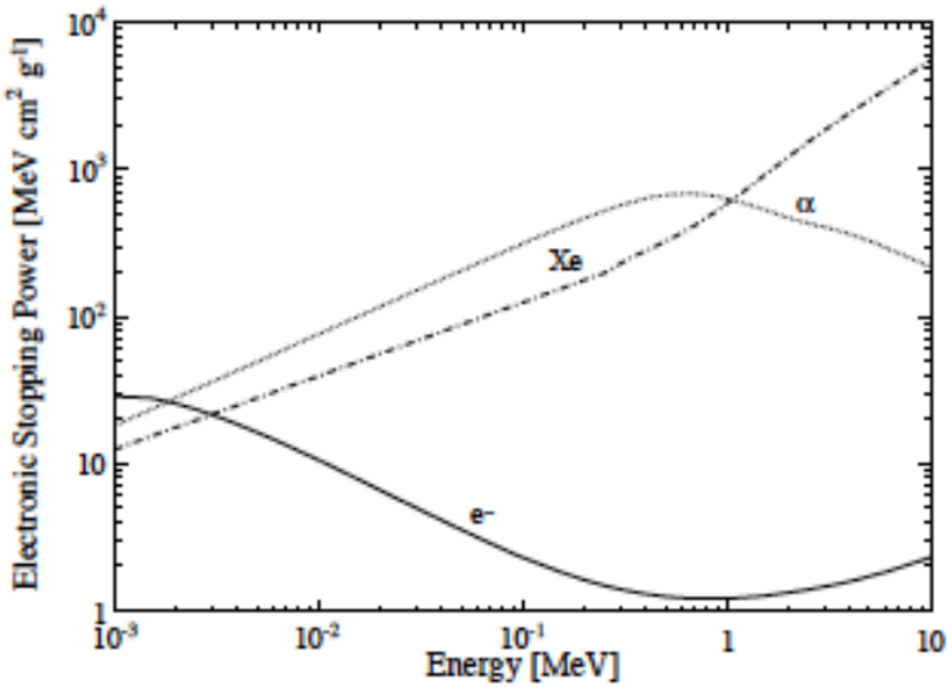

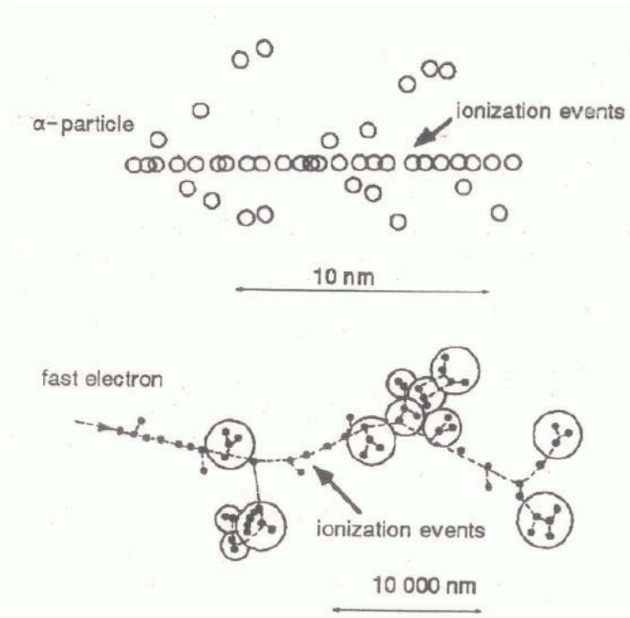

NR: higher dE/dX -> higher recombination -> reduced charge signal compared to light -> smaller charge/light ratio

Light and Charge Yield of NRs

- Must be determined based on NR data, using two methods
- direct: observe mono-energetic neutrons scatters which are tagged with n-detectors
- indirect: measure energy spectra from calibration n-sources, compare with MC predictions

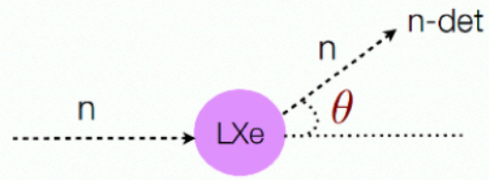

P. Agnes et al., Phys. Rev. D 104, 2021

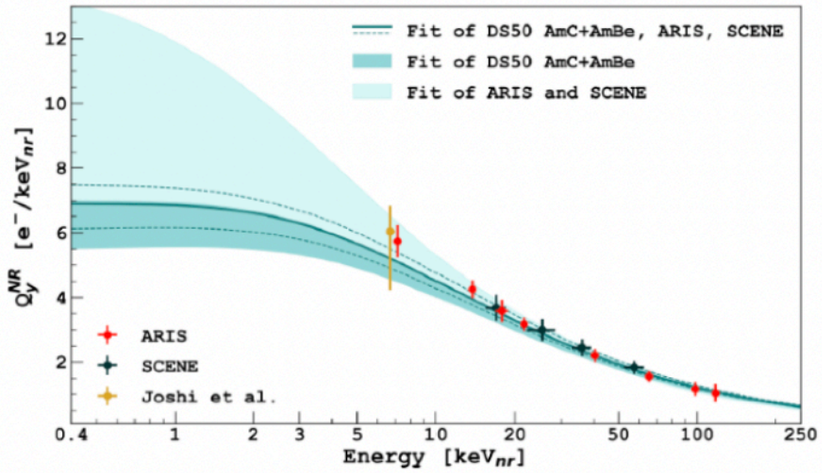

- LAr: charge yield measured down to ~ 0.5 keV$_{NR}$ (≡ 3 ionisation electrons)

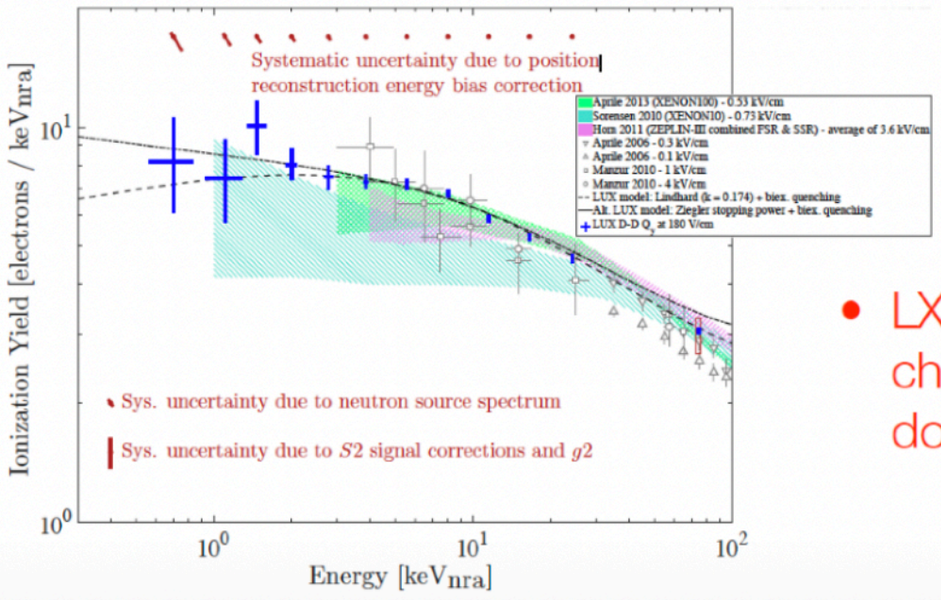

- LXe: here data from LUX; charge yield measured down to 0.7 keV$_{NR}$

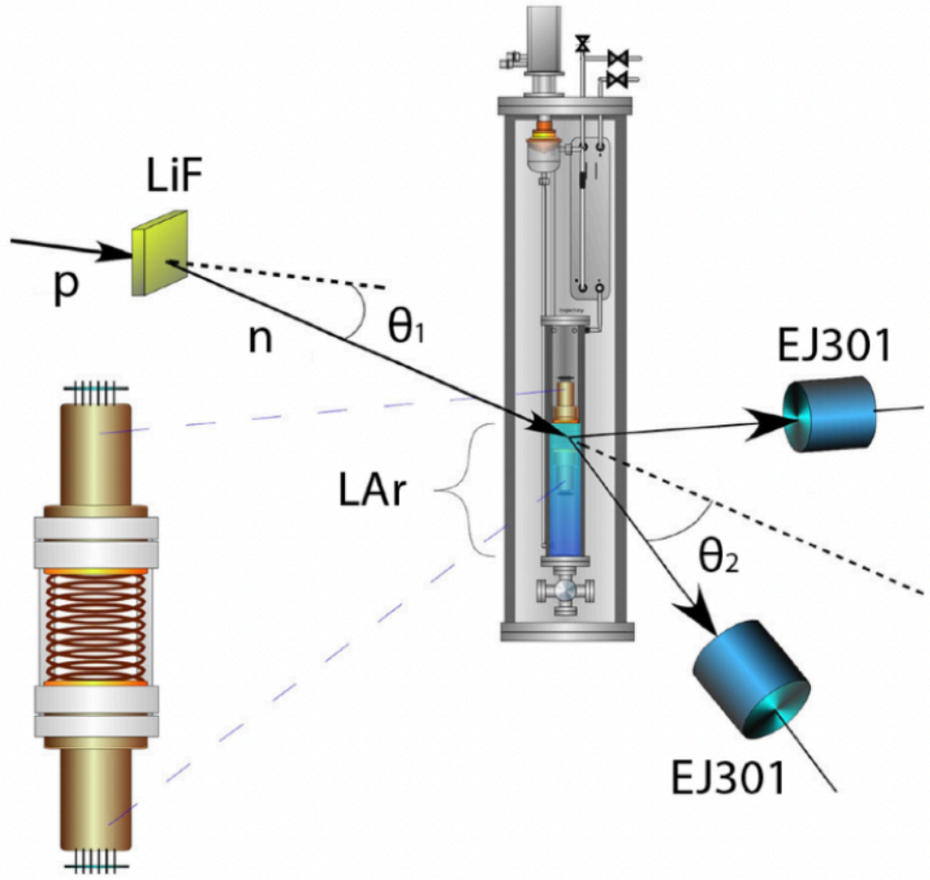

SCENE collaboration, PRD 91, 2015

Light and Charge Yield of NRs

Light yield at low energies: data from LUX

- Use data acquired in situ with monochromatic 2.5 MeV neutrons (D-D generator)
- Calculate energy (via angle) from x-y position and Δt (z separation)
- Light yield measured down to 1 keV

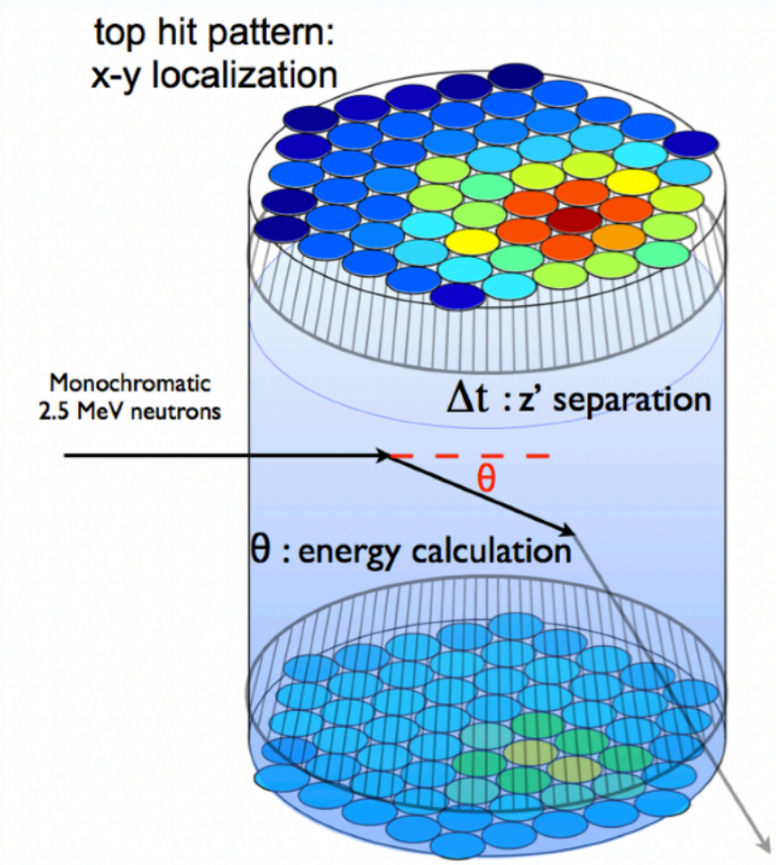

$$E_r = E_n \frac{4 m_n m_{Xe}}{(m_n + m_{Xe})^2} \frac{1 - \cos\theta}{2}$$

D. Huang, UCLA DM2016

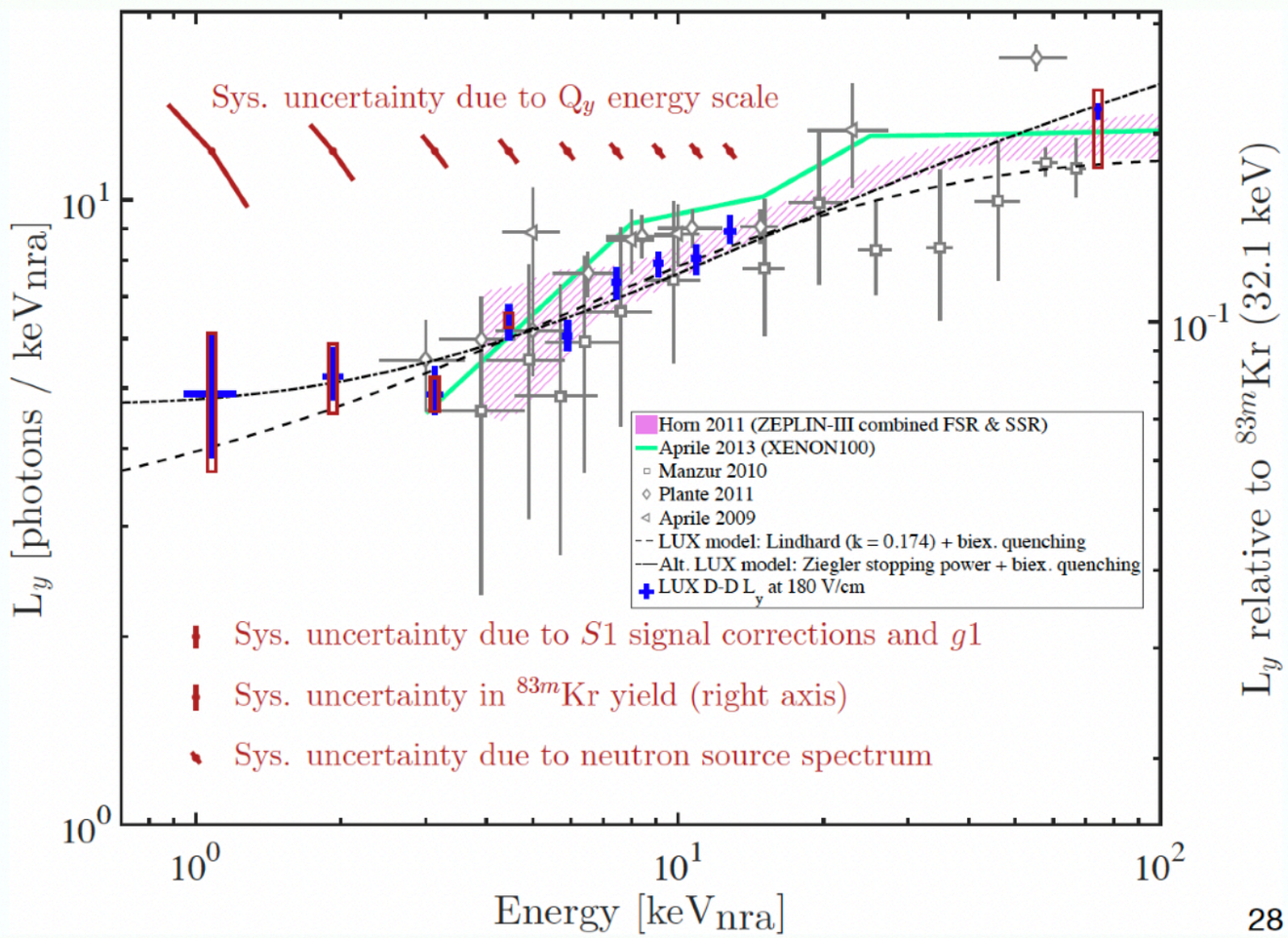

28

Light and Charge Yield of ERs

Light yield for ERs in LXe: data from Xürich

- Light yield decreases with lower deposited energies in the LXe
- Field quenching is ~ 75%, only weak field-dependance

Relative light yield to 32.1 keV of ^{83m}Kr

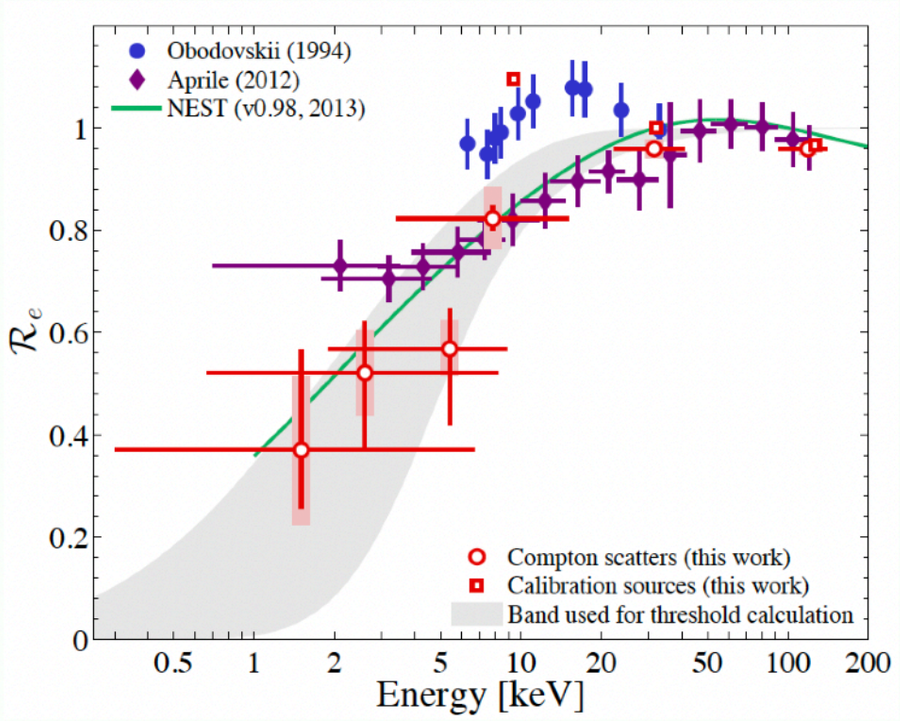

Quenching of the scintillation light at a field of 0.45 kV/cm

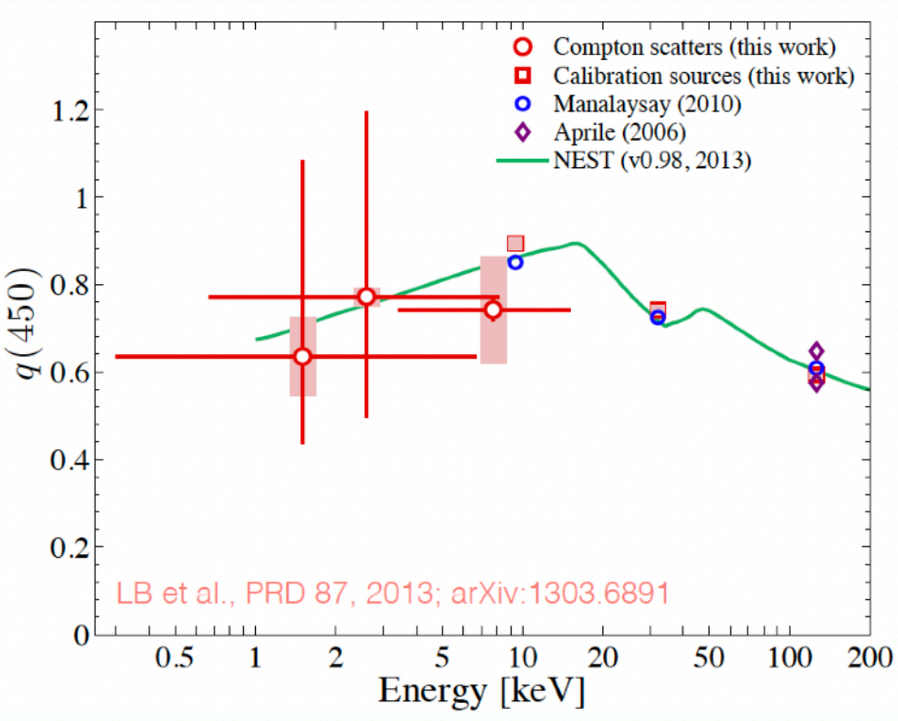

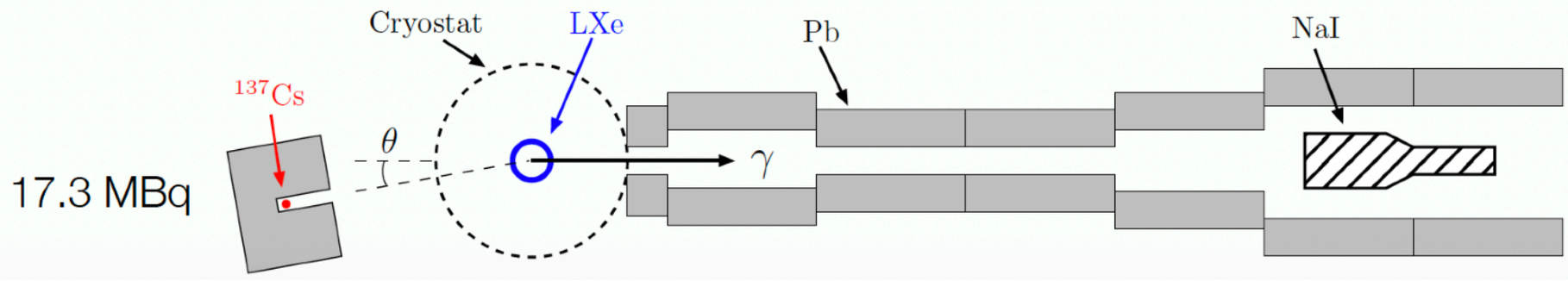

Light and Charge Yield of ERs

Charge yield for ERs in LAr: data from DarkSide-50

- Use data acquired in situ with ^{37}Ar and ^{39}Ar calibration sources
- Fit of the ER ionisation yields
- Charge yield of ERs measured down to ~ 0.179 keV_{ee} (L1-shell Auger electron from ^{37}Ar)

0.27 and 2.8 keV

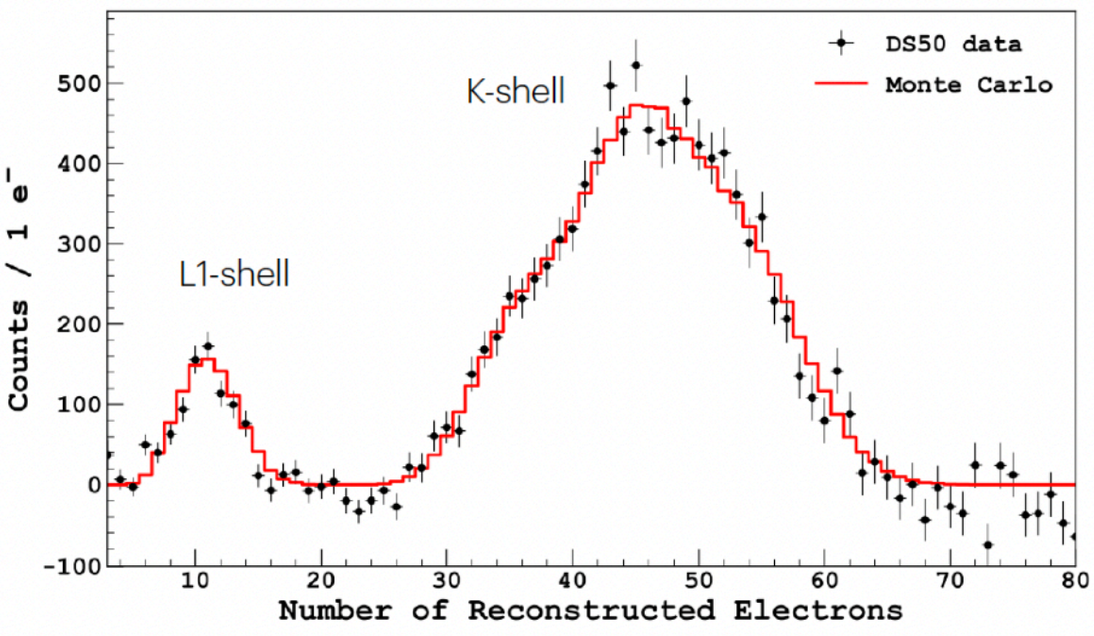

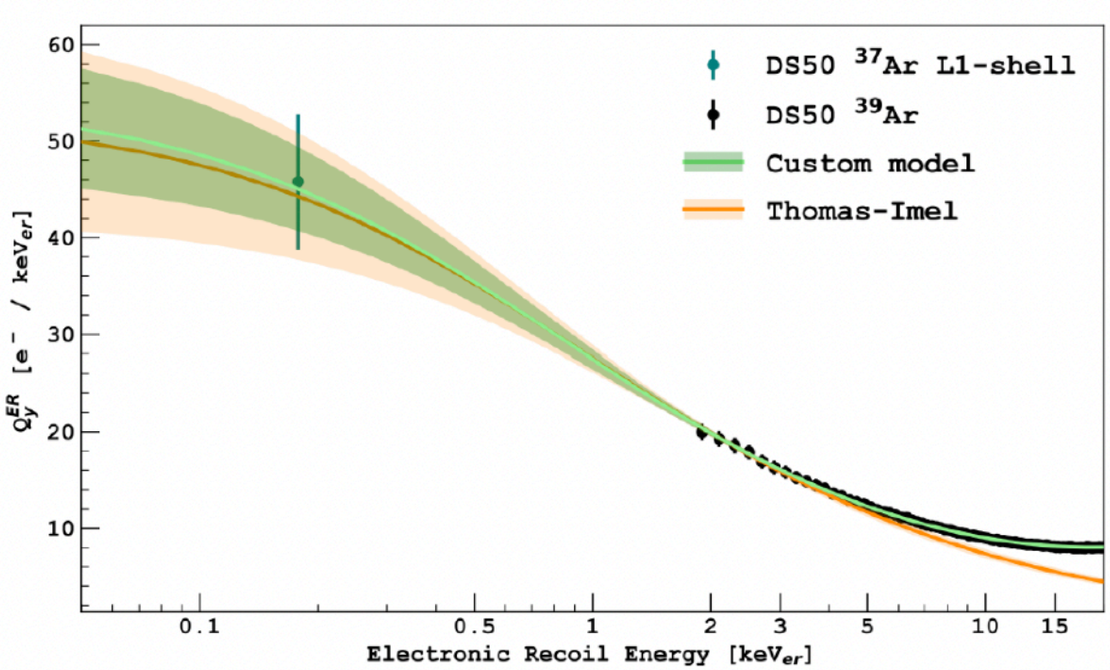

P. Agnes et al., Phys. Rev. D 104, 2021

NEST simulations

LIGHT AND CHARGE YIELDS FROM NEST

NEST: Model Detector

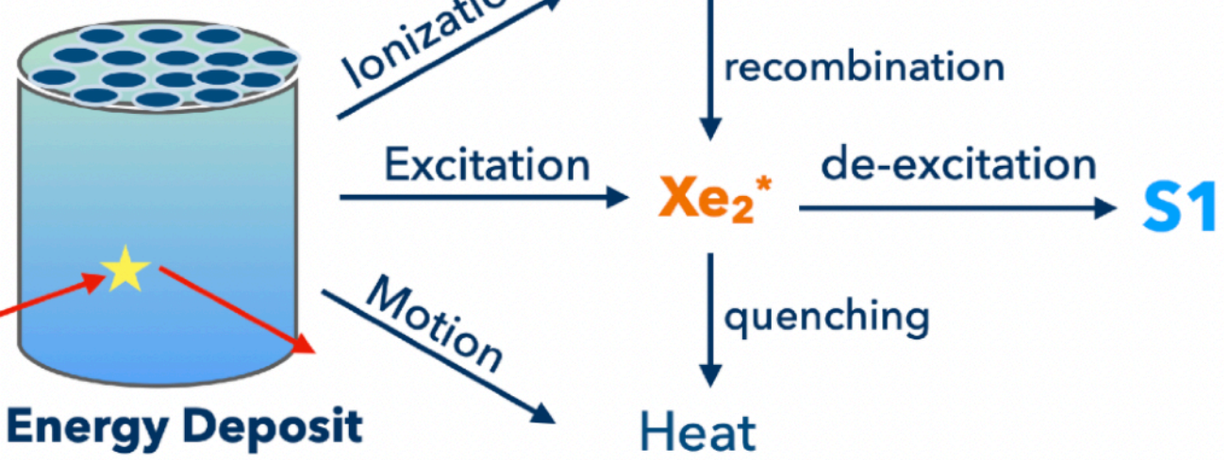

NEST: Simulate Signals

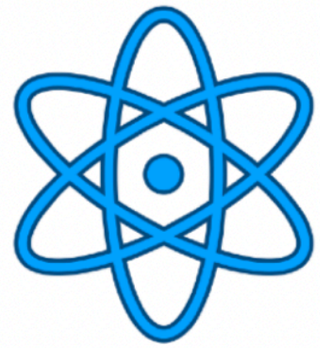

Macroscopic	Microscopic
❖ Fields (drift, gap)	❖ Particle types
❖ Density, Temp, Phase	❖ Recombination, dE/dx
❖ Geometry, PMTs...	❖ Nex/Ni

ER	*NR*	*Other*
Photons (γ)	Neutrons	α (alphas)
β^-, μ^- (leptons)	Heavy Nuclei	^{83m}Kr
expanding...	WIMPs	Protons

Figures by Sophia Andaloro, APS meeting April 2021

https://nest.physics.ucdavis.edu

NEST simulations

HOME ABOUT PEOPLE BENCHMARK PLOTS (XENON) BENCHM

Parameters

Input

ER

Incident Particle	beta/Compton/axion

More Particle Types Available in the C++ Code!

Target Density [g/cm3]	3
Drift Field > 0 V/cm	100
Recoil Energy [keV]	5
S1 gain (g1)	0.16
S2 gain (g2)	30

Output

photons	218.990697832
Ly [ph/keV]	43.798139566
Observed Electron-Equivalent Energy [keVee]	4.999999999999999
Relative to Kr83m	0.668673887
Electrons	154.523407980
Qy [e/keV]	30.90468160
S1 [PE or phe]	35.038511653
S2 [PE or phe]	4635.7022394

HOME ABOUT PEOPLE BENCHMARK PLOTS (XENON) BENCHMA

Parameters

Input

NR

Incident Particle	neutron/WIMP

More Particle Types Available in the C++ Code!

Target Density [g/cm3]	3
Drift Field > 0 V/cm	100
Recoil Energy [keV]	5
S1 gain (g1)	0.16
S2 gain (g2)	30

Output

photons	33.180953110
Ly [ph/keV]	6.636190622
Observed Electron-Equivalent Energy [keVee]	0.8833505539540563
Relative to Kr83m	0.096470806
Electrons	31.303637329
Qy [e/keV]	6.26072747
S1 [PE or phe]	5.308952498
S2 [PE or phe]	939.1091199

https://nest.physics.ucdavis.edu

NEST simulations

LIGHT AND CHARGE YIELDS FROM NEST: XENON

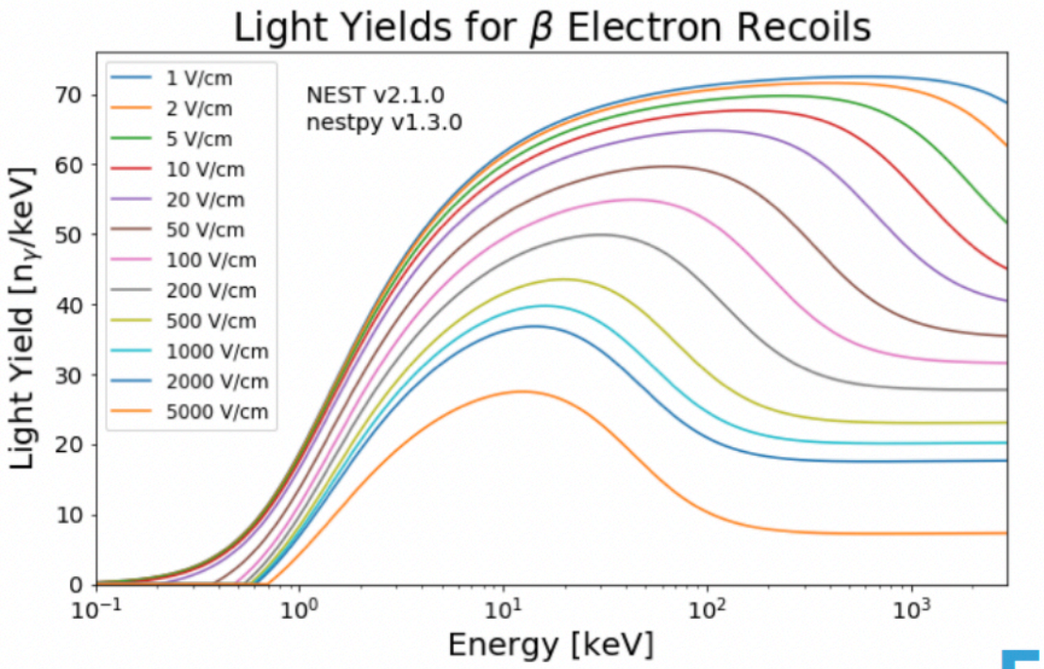

Light yield

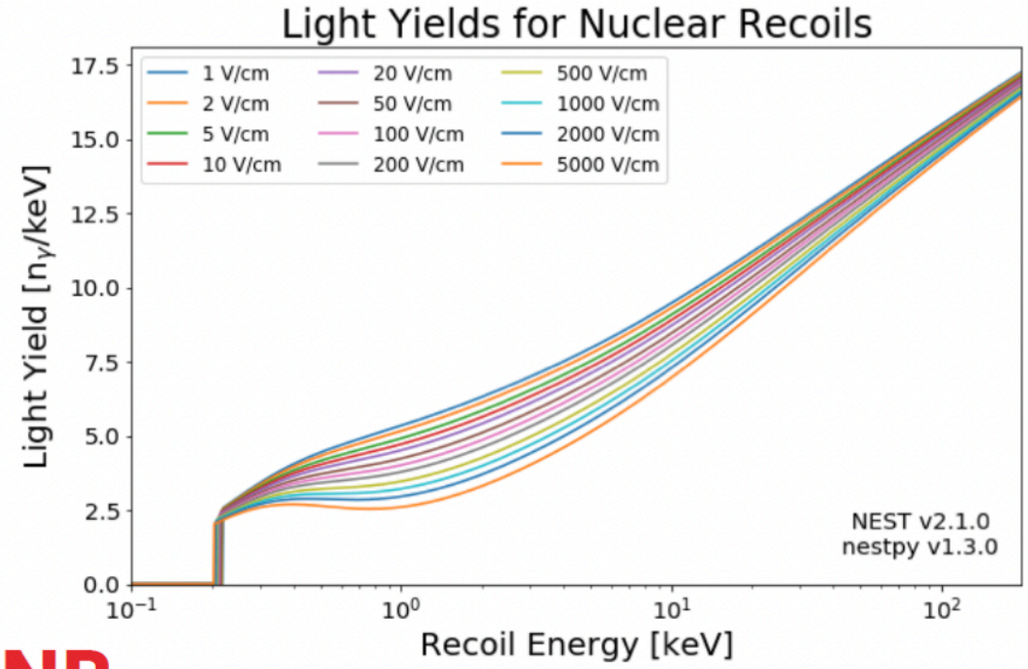

ER **NR**

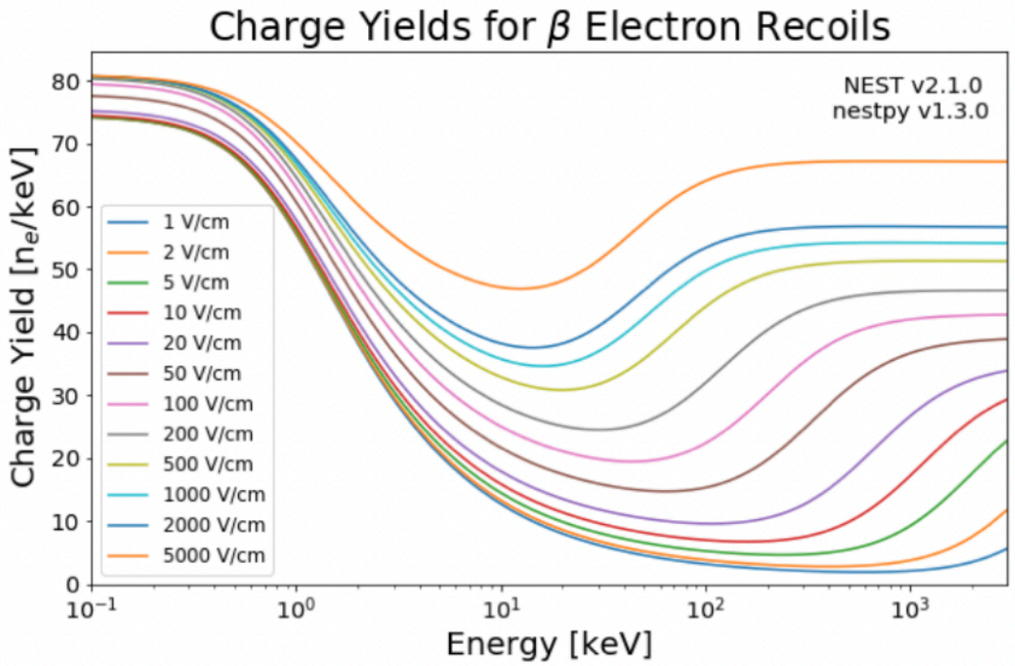

Charge yield

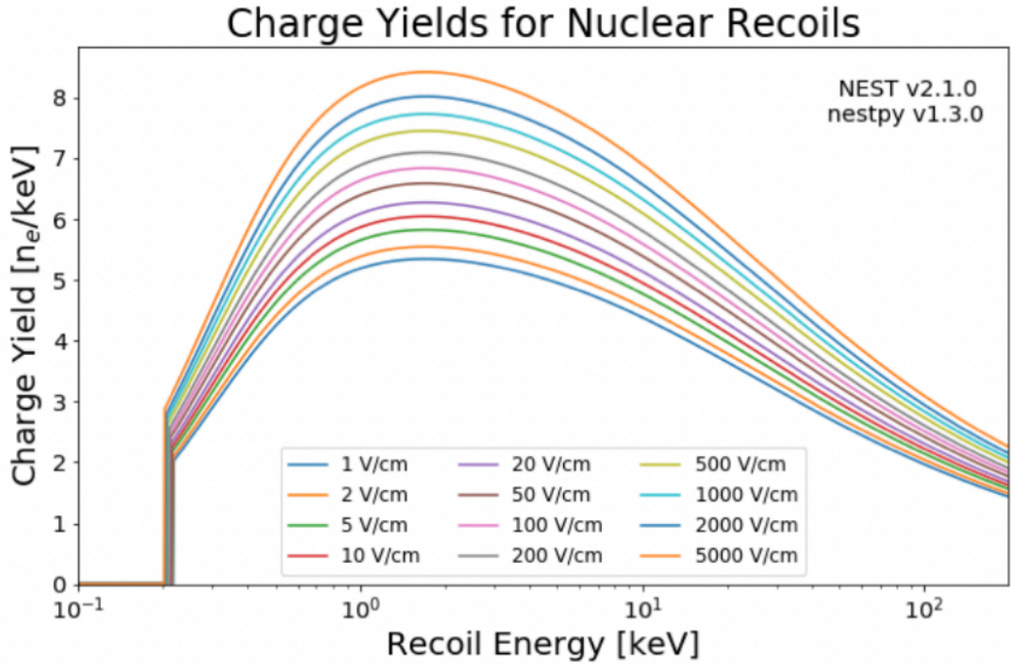

https://nest.physics.ucdavis.edu

NEST simulations

LIGHT AND CHARGE YIELDS FROM NEST: ARGON

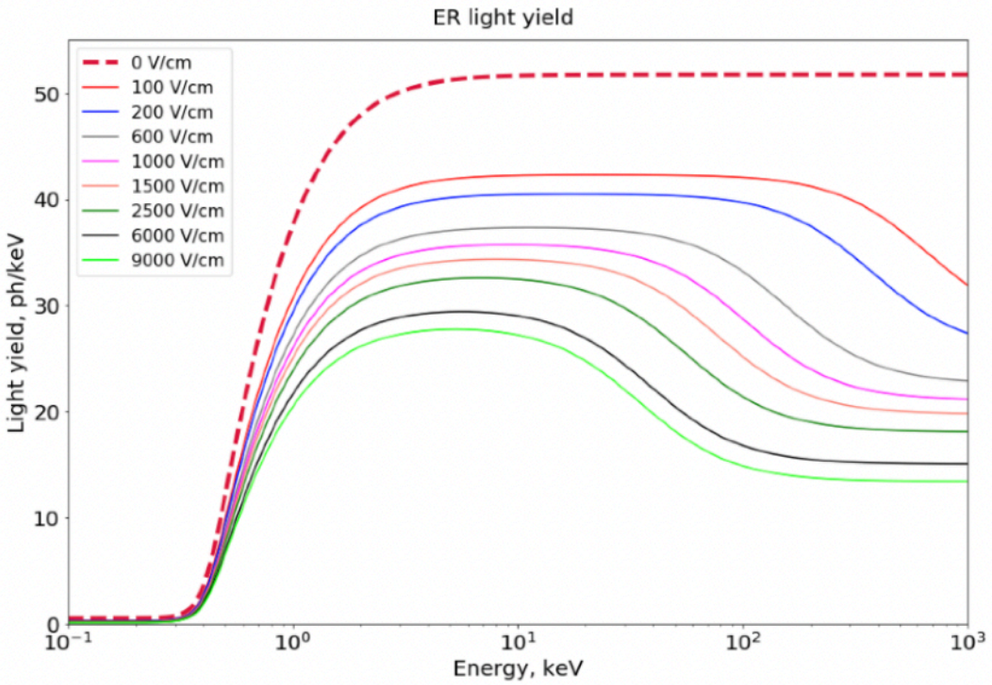

Light yield

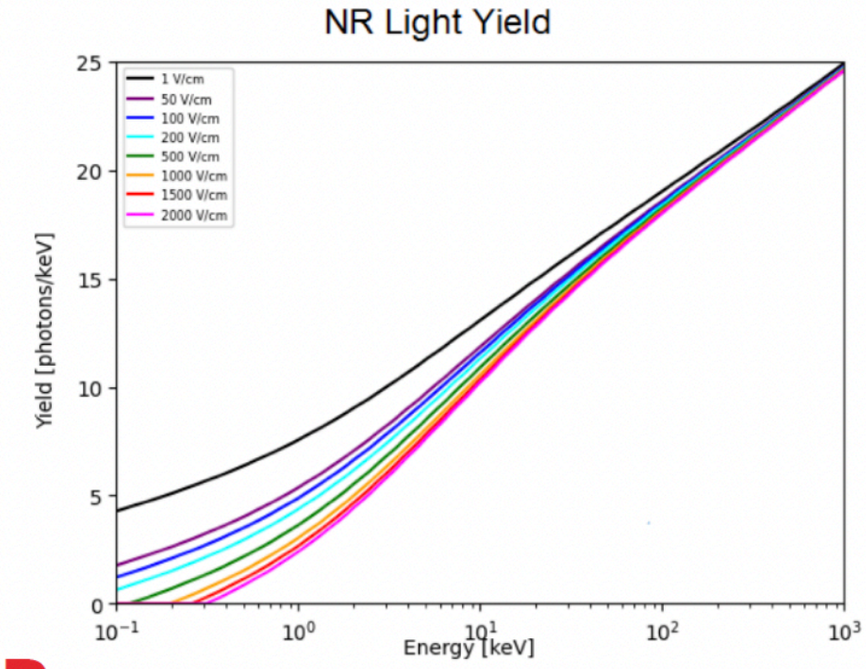

ER **NR**

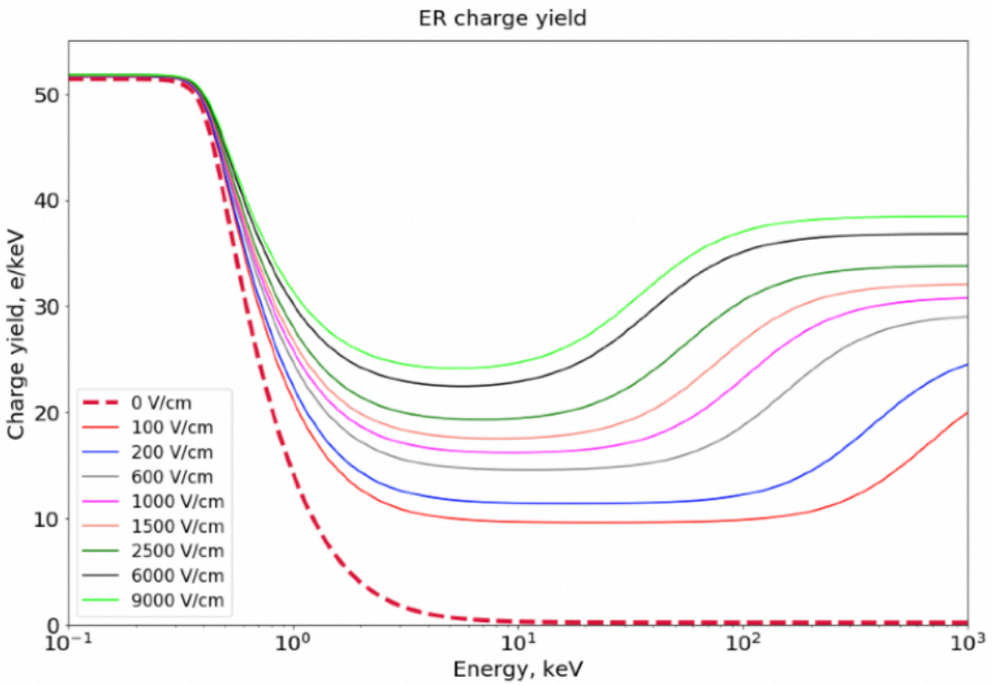

Charge yield

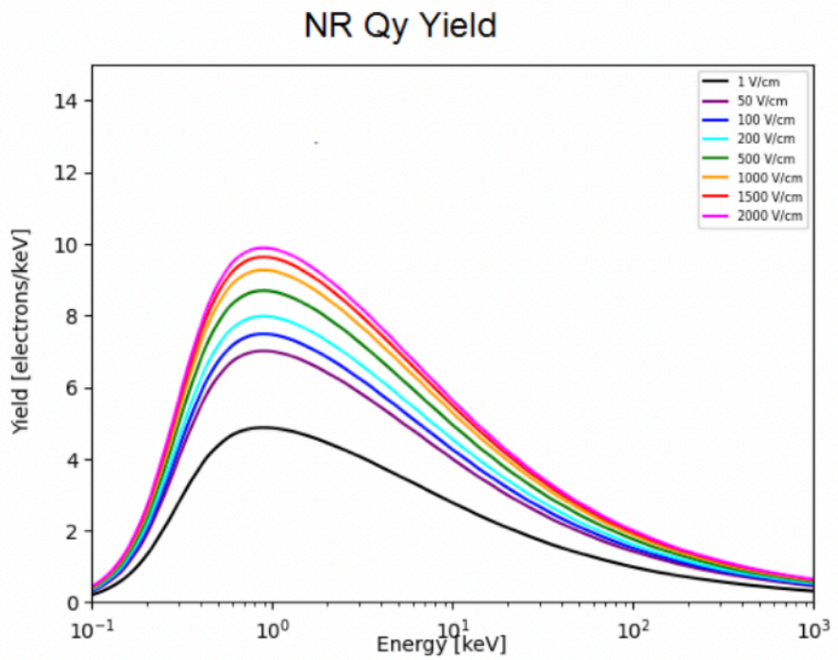

https://nest.physics.ucdavis.edu

NEST simulations

SUMMARY LIGHT AND CHARGE YIELDS IN XENON

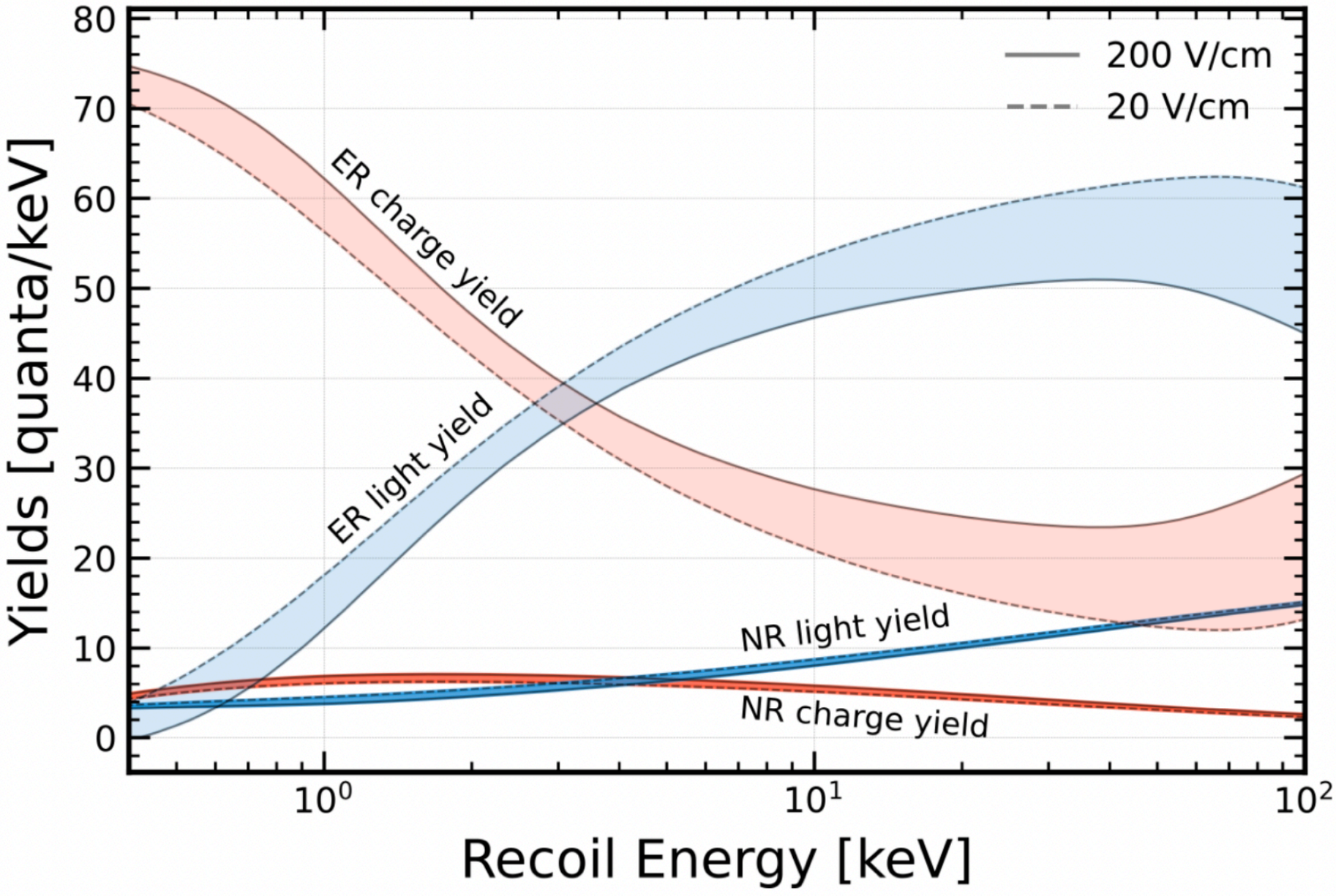

Figure by G. Volta with NEST

https://nest.physics.ucdavis.edu

Electron Drift Velocity and Diffusion

- Under irradiation, atomic electrons are excited in the conduction band becoming free electrons. If not trapped by electronegative impurities, they can drift freely under an external field inducing a detectable charge signal.

- At low field, vd= muE. Electron mobility is highest in LXe (2000 cm2/V/s similar to the mobility in Si (in LAr it is about 500 cm2/V/s)

$$V_d = O(mm/us)$$

- The e-velocity in LAr and LXe is much higher than the velocity in gas phase, The addition of organic molecule in noble liquids leads to increased velocity as collisions reduce average electron excitation energy.

- The spread of the drifting electrons is the ultimate limitation to position resolution in noble liquid detectors operated as TPCs (Lecture 2 and 3). Electron diffusion depends on field direction. The longitudinal diffusion coefficient (along E) is ~1/10 of the transverse one. O a distance d, electron cloud spread due to transverse diffusion is negligible in LXe (a few mm over 1 m)

$$\sigma_{D_T} = \sqrt{D_T t_d}$$

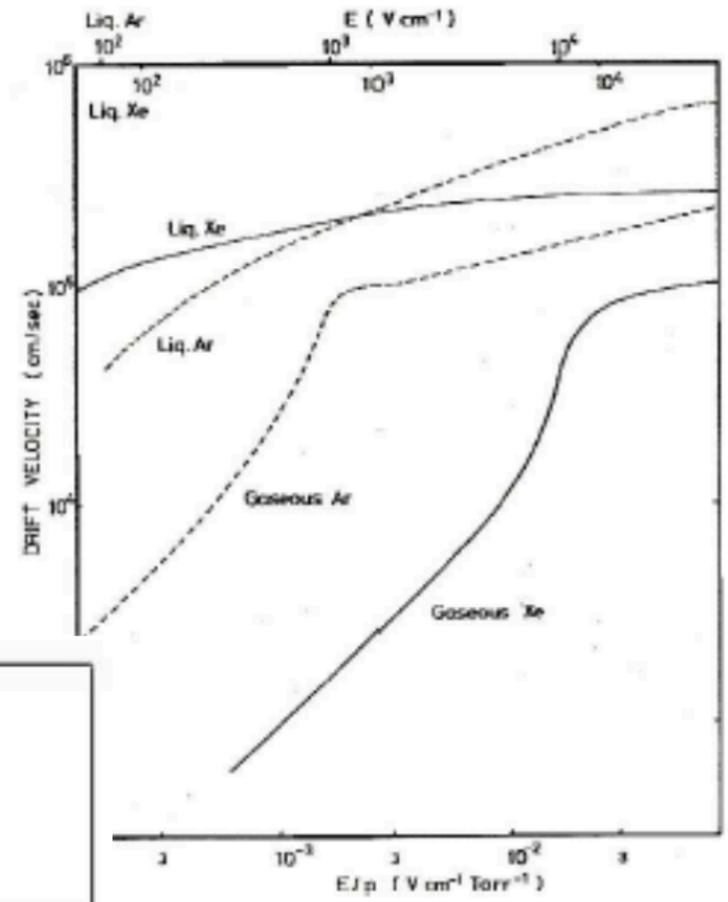

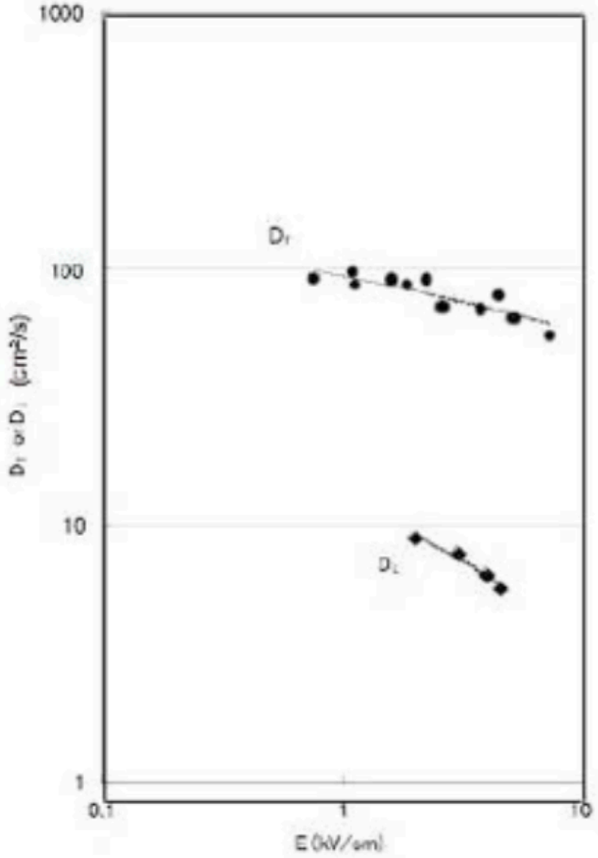

Light Absorption and e- Attachment

Impurities dissolved in the liquid absorb UV photons, reducing the light yield. Light attenuation described as

$$I(x) = I(0)\exp(-x/\lambda_{att})$$

Strong absorption by H2O, even stronger at 128 nm of LAr

Electronegative impurities dissolved in the liquid also trap electrons reducing the charge yield

$$[e(t)] = e(0)exp(-k_S[S]t)$$

We define electron lifetime in terms of the impurity concentration [S] and an attachment rate constant k

$$\tau = (k_S[S])^{-1}$$

The electron attenuation length is related to the lifetime via the electron mobility and the electric field

$$\lambda_{att} = \mu E \tau$$

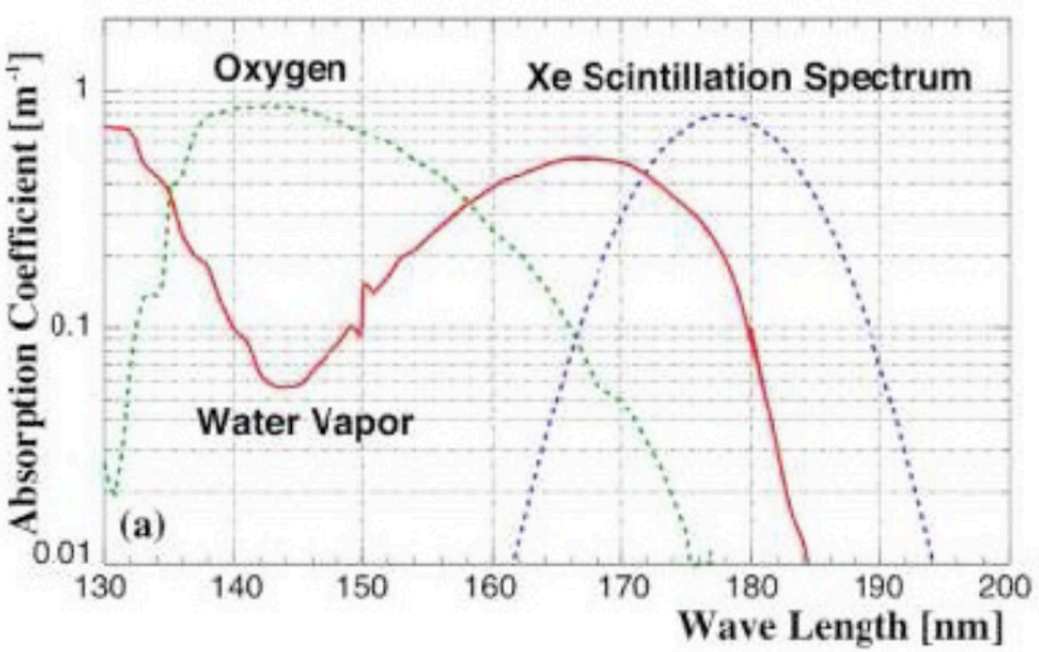

FIG. 25 Absorption coefficient for VUV photons in 1 ppm water vapor and oxygen and superimposed Xe emission spectrum (Ozone, 2005).

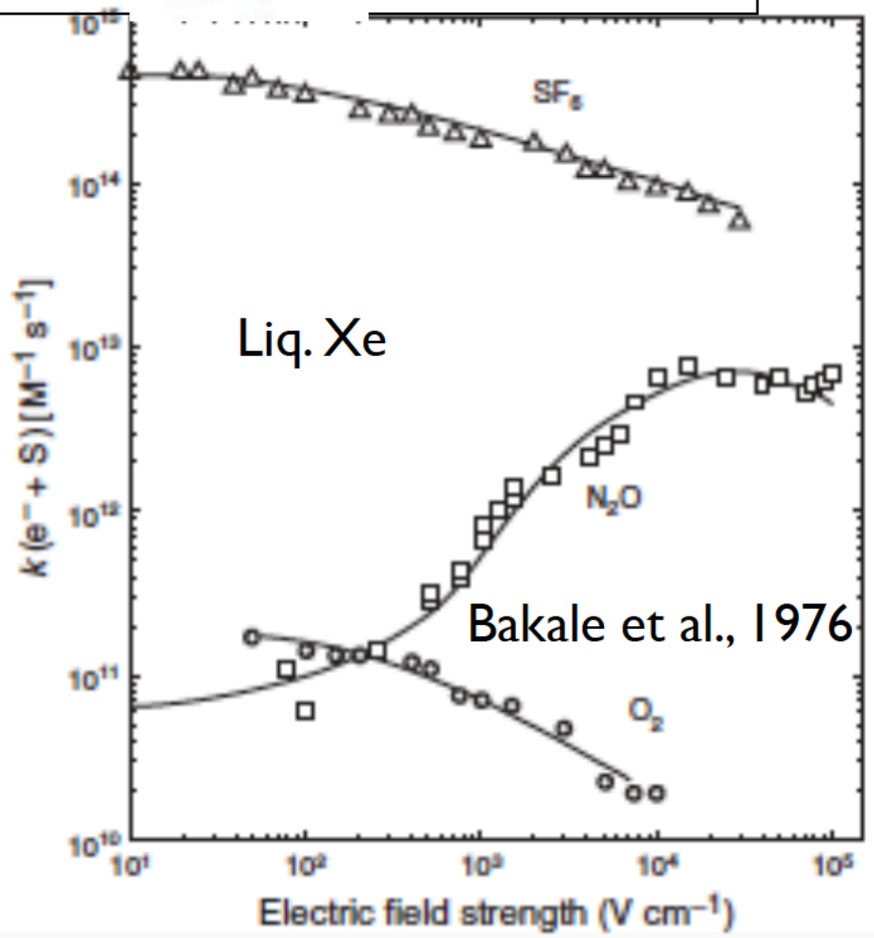

Light Absorption and e- Attachment

Light: 1 ppm of H2O would result in strong absorption hence water vapor must be well below ppm level for efficient light detection

$$\lambda_{\mathrm{abs,H_2O}} = \frac{1}{10^{-6} \cdot n_{\mathrm{Xe}} \sigma_{\mathrm{H_2O}}} = \frac{131\,\mathrm{g\,mol^{-1}}}{10^{-6} N_A \cdot 2.83\,\mathrm{g\,cm^{-3}} \cdot 2 \times 10^{-18}\,\mathrm{cm^2}} \approx 38\,\mathrm{cm}$$

Charge: 1 ppb of O2 equivalent impurities would result in a reasonable electron lifetime,taking the attachment rate constant value at a field of 0.5 kV/cm from Bakale et al.

$$\tau_e = \frac{1}{10^{-9} \cdot n_{\mathrm{Xe}} k_{\mathrm{O_2}}} = \frac{131\,\mathrm{g\,mol^{-1}}}{10^{-9} \cdot 2.83\,\mathrm{g\,cm^{-3}} \cdot 1 \times 10^{11}\,\mathrm{mol^{-1}\,L\,s^{-1}}} \approx 463\,\mu\mathrm{s}$$

Purification System

Xe gas used to fill a DM detector, such as XENON100, is of research grade (99.999%) purity with ppm levels of H_2O, O_2, N_2, CO_2 and Ar. Hence a purification system is used to reduce the level to the ppb required for long electron drift

Because H_2O has high binding energy to surfaces, pumping does not help desorption of H_2O. High T bake-out is necessary. Surfaces in contact with the cold LXe will have low outgassing. However not all materials and surfaces are at this low temperature hence outgassing from warm surfaces contributes to the impurities.

To help removal of impurities the gas is continuously circulated through a high temperature getter, with a diaphragm gas pump. LXe from the bottom of the detector is evaporated in the gas line connecting the detector to the buffer volume of the recirculation system. The pump draws GXe from the buffer volume and circulates it though the getter for purification. The GXe at the output of the getter is fed back into the detector. THe recircualtion rate is kept stable with a flow controller at the input of the pump.

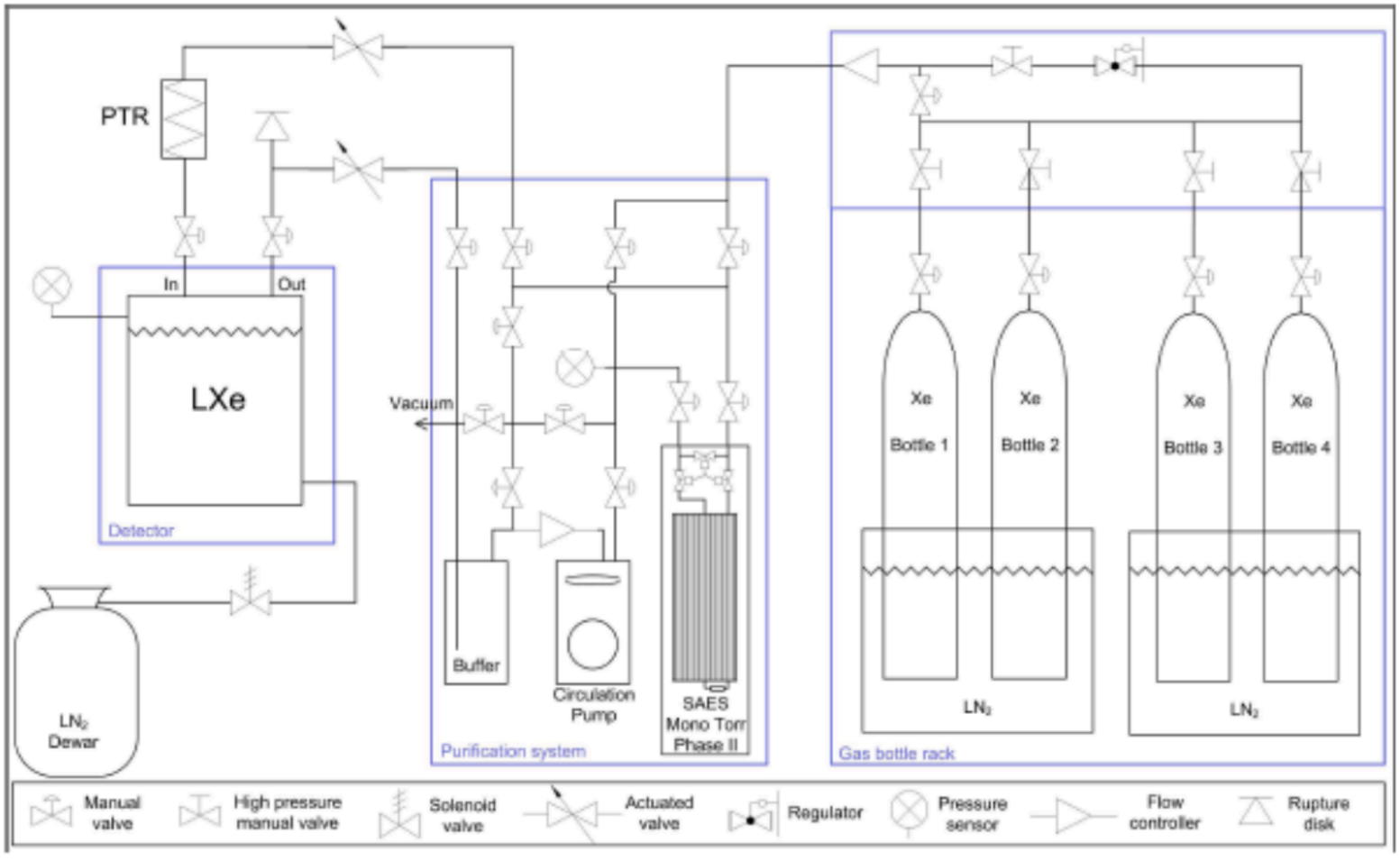

XENON100

Purification System

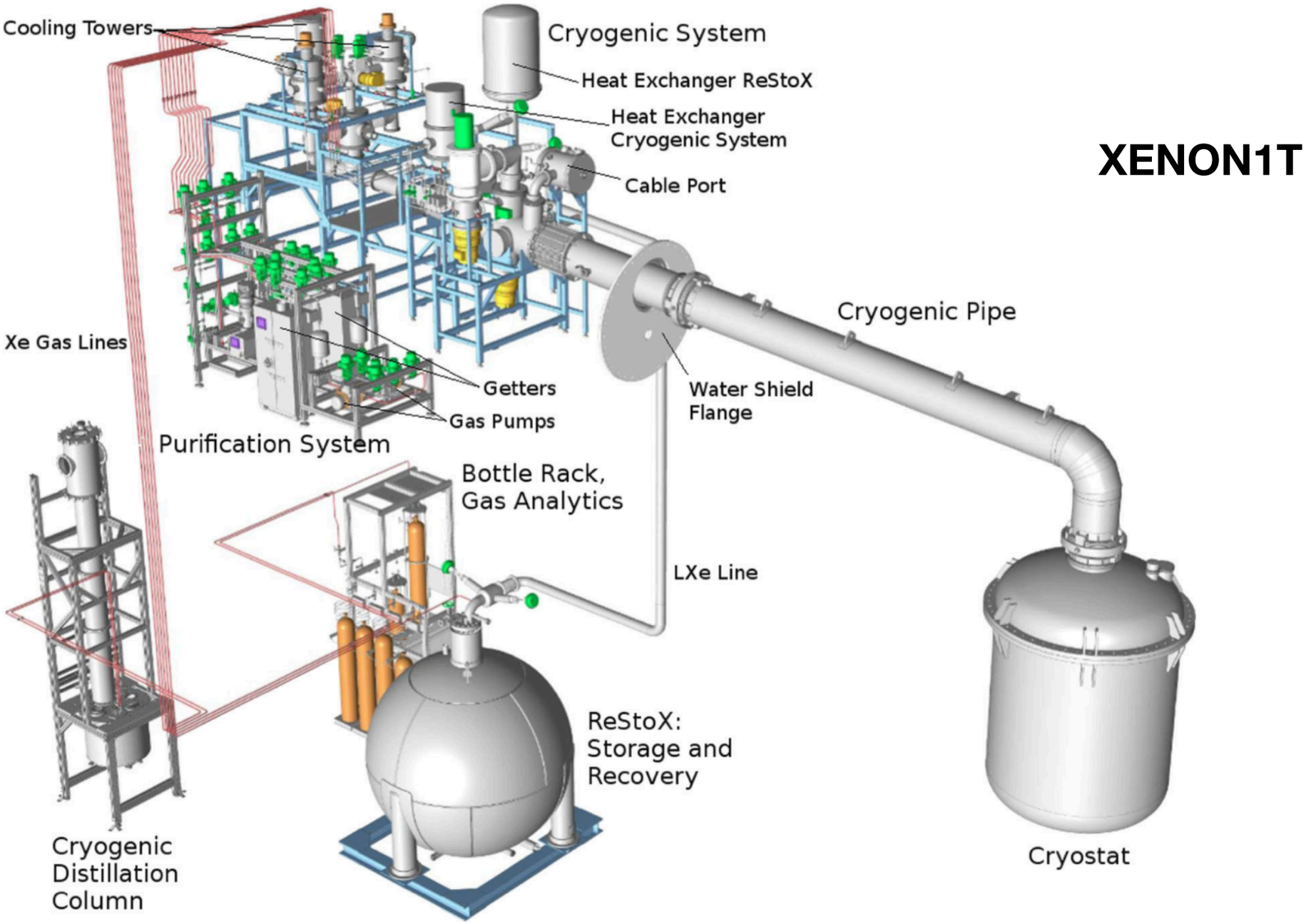

XENON1T

Fig. 9 The gas-handling system of XENON1T consists of the cryogenic system (cooling), the purification system (online removal of electronegative impurities), the cryogenic distillation column (^{nat}Kr removal), ReStoX (LXe storage, filling and recovery), the gas bottle rack (injection of gas into the system) and gas analytics station (gas chromatograph). The cryostat inside the water shield accomodates the TPC

Purification System

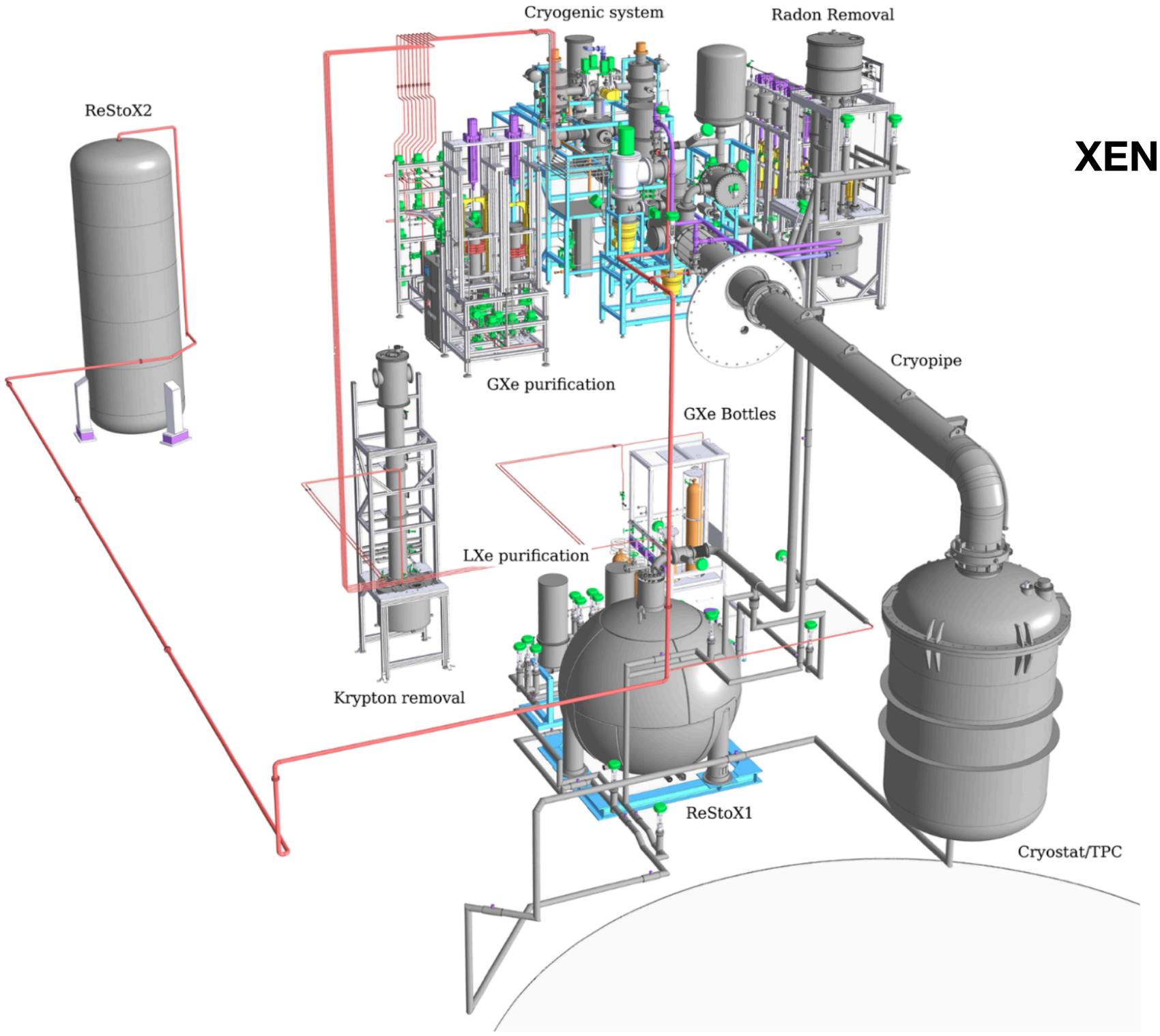

XENONnT

Istituto Nazionale di Fisica Nucleare

ALMA MATER STUDIORUM
UNIVERSITÀ DI BOLOGNA

Noble liquid detectors (mostly LAr and LXe double-phase TPC)

Type of Liquid Noble Detectors

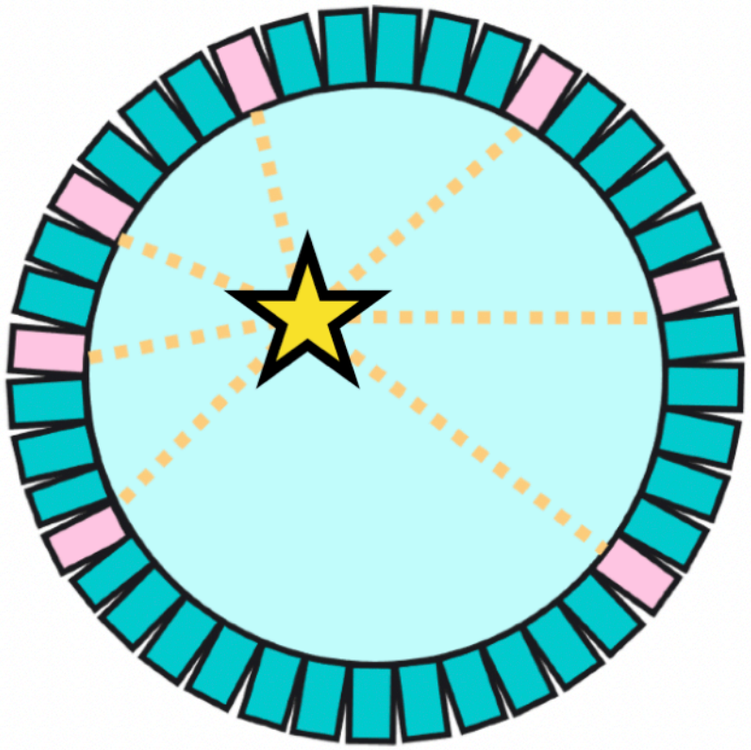

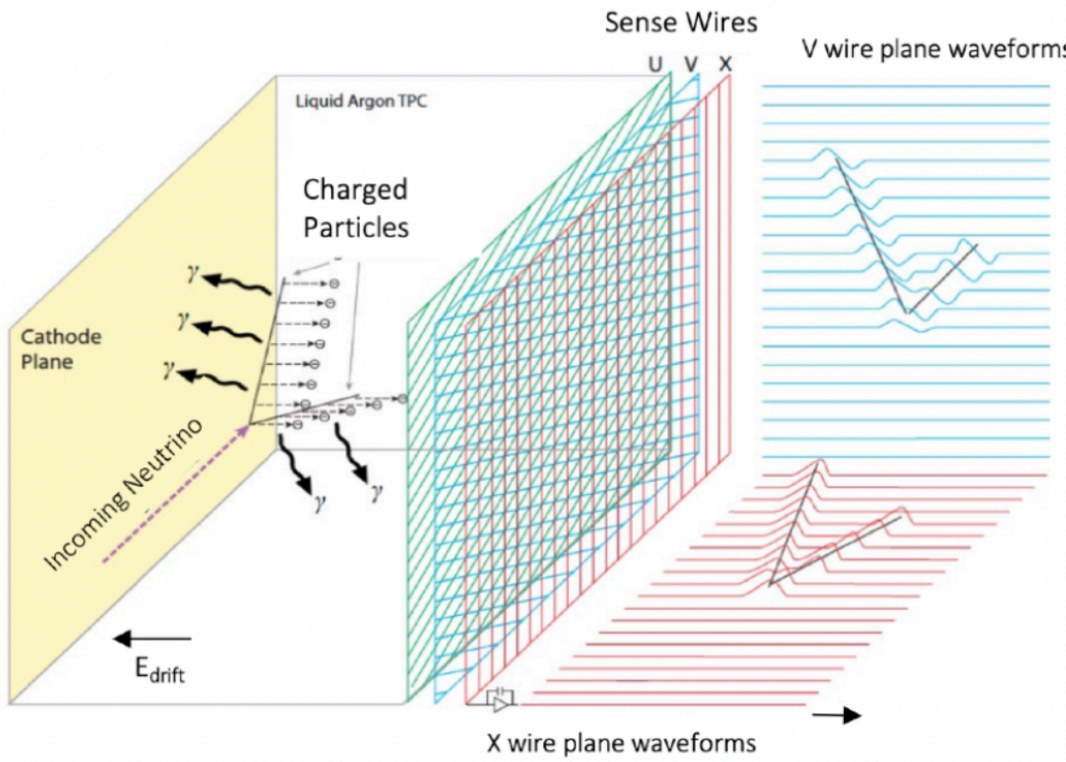

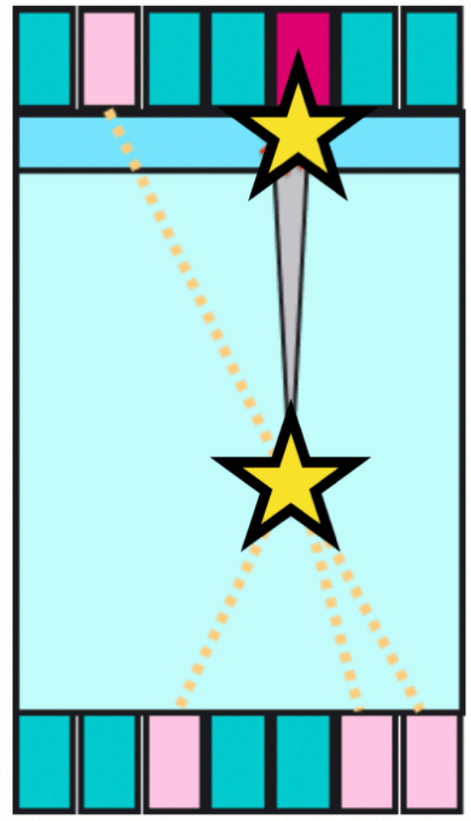

Single phase detector

Single phase TPC

Double phase TPC

DOUBLE PHASE DETECTION PRINCIPLE

Time projection chambers

- Prompt scintillation light signal in the liquid from the direct excitation process (S1 signal)
- Electrons drifted away from the interaction site via an electric drift field ~ $\mathcal{O}(100\,\mathrm{V/cm})$
- Electrons extracted from the condensed liquid into the vapor phase by a stronger electric field ~ $\mathcal{O}$(few kV/cm), also called "extraction field" (e^- need sufficient momentum to overcome the potential barrier at the liquid/gas interface)
- Electrons in the gas phase are accelerated by the electric field and gain sufficient energy to excite atoms in collisions
- These create electroluminiscence (EL; also called proportional scintillation), with similar emission spectra to those of direct scintillation (S2 signal)

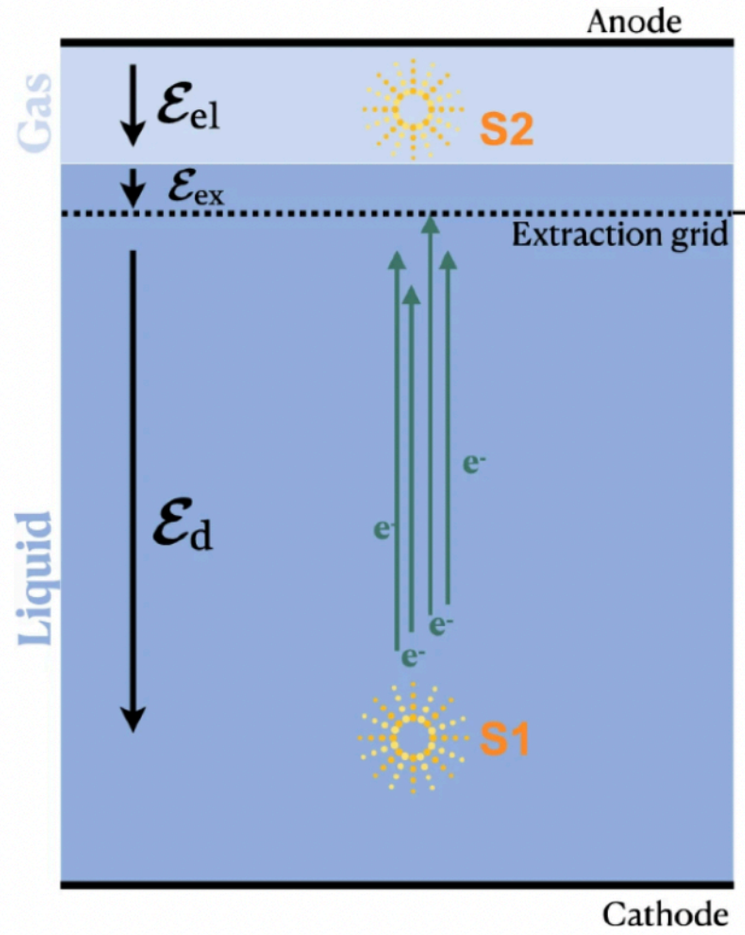

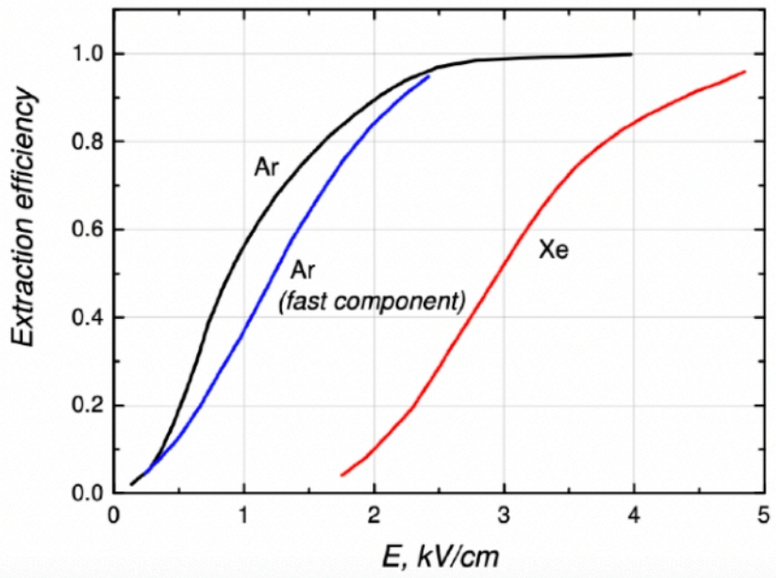

Probability of e- emission. Chepel and Araujo, JINST 2013

LNoble Detectors: Double Phase TPC

DOUBLE PHASE DETECTION PRINCIPLE

Time projection chambers

- A single extracted e- can produce ~ $\mathcal{O}(100)$ of photons, which then produce tens of photoelectrons in the photosensors
- The number of generated S2 photons will depend on the drift path, the field strength E (in V/cm) and the gas density. The yield per cm can be written as:

$$\frac{1}{n}\frac{dN_{ph}}{dx} = a\frac{E}{n} - b$$

- with n being the number of gas atoms/cm^3, n = N_A ρ/A, a and b being gas-specific empirical coefficients
- Important: the EL process is linear, since *the energy of the drifting e- is dissipated via photon emissions* (and these do not participate further in the process)

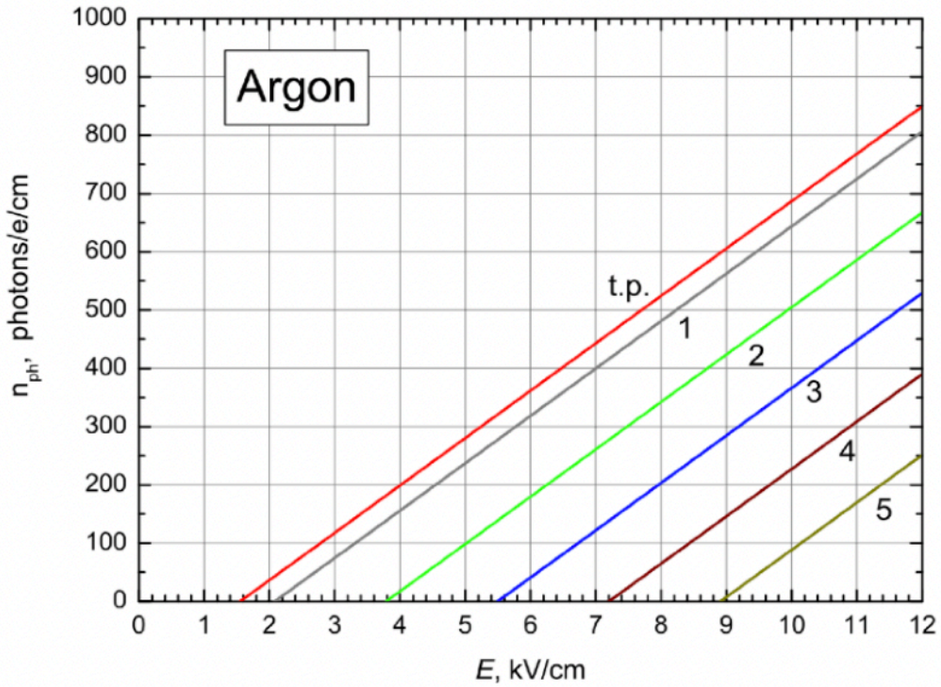

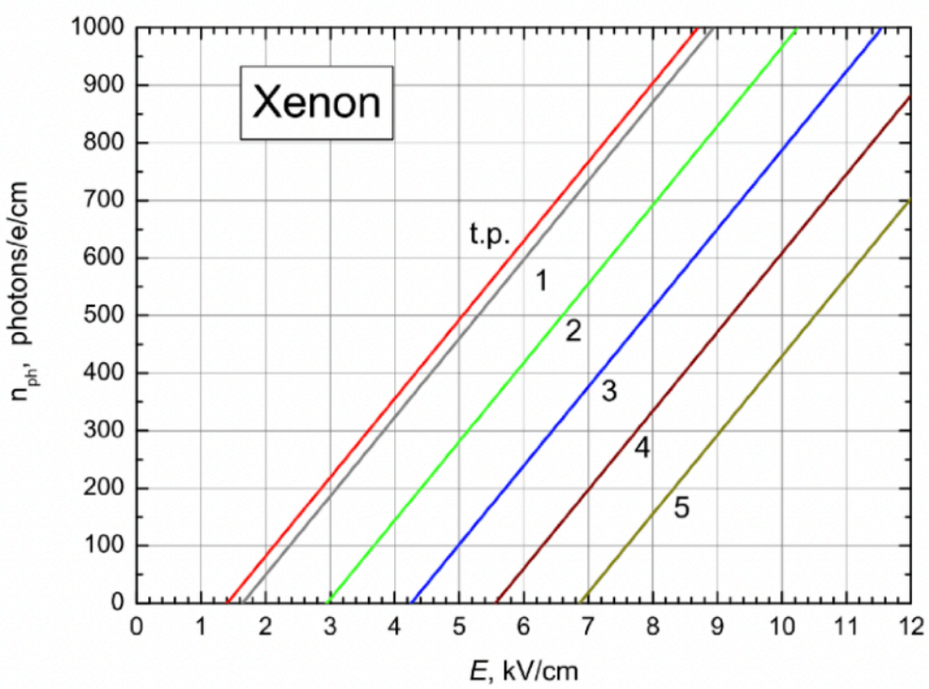

Number of photons generated in 1 cm, as a function of the field and of the gas pressure. Chepel and Araujo, JINST 2013

LNoble Detectors: Double Phase TPC

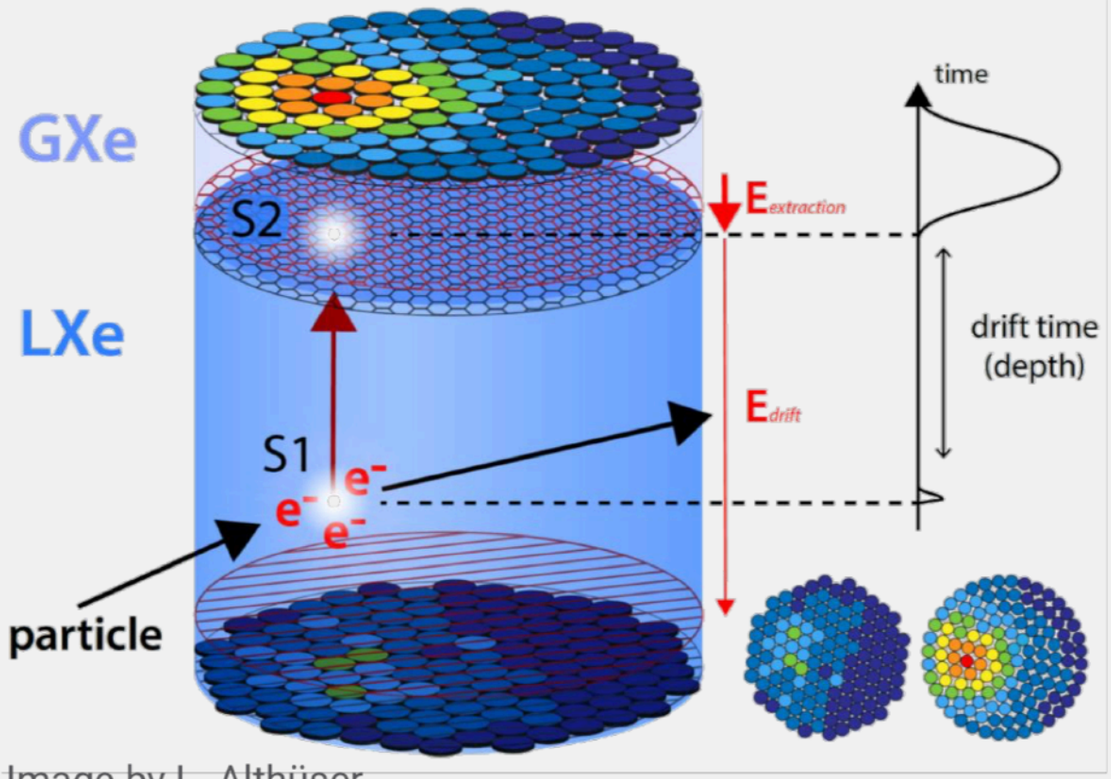

Image by L. Althüser

S1 light signal:

- prompt scintillation photons

S2 charge signal:

- secondary scintillation photons from electroluminescence in GXe due to drifted electrons

3D vertex reconstruction:

- X,Y: S2 hit pattern
- Z: drift time S2-S1

NR (Nuclear Recoils)
WIMP signal, neutrons, CEvNs

ER (Electronic Recoils)
γ, β backgrounds

Discrimination from S2/S1
Larger for ER than NR

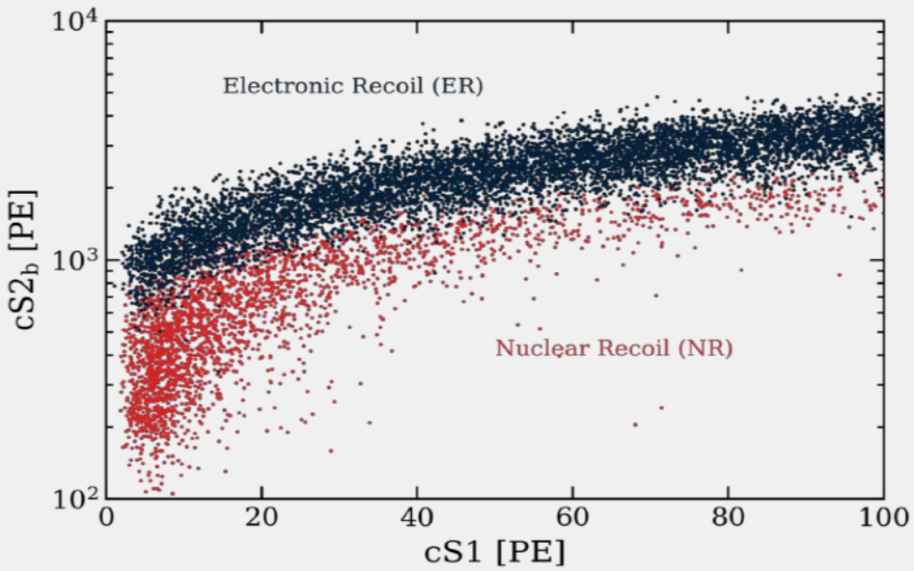

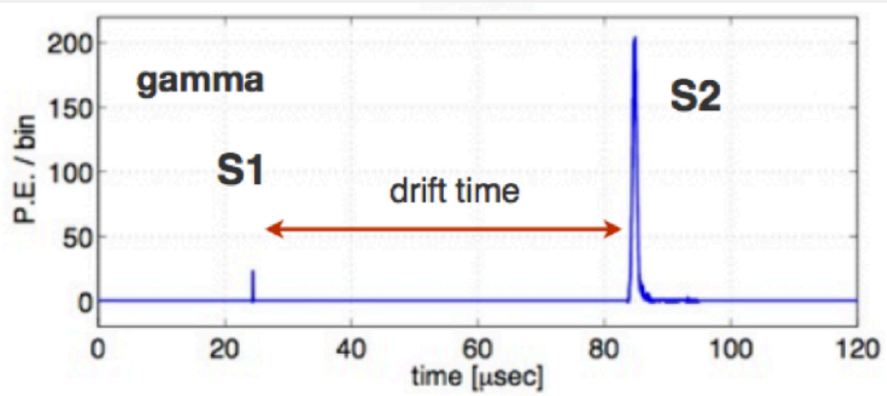

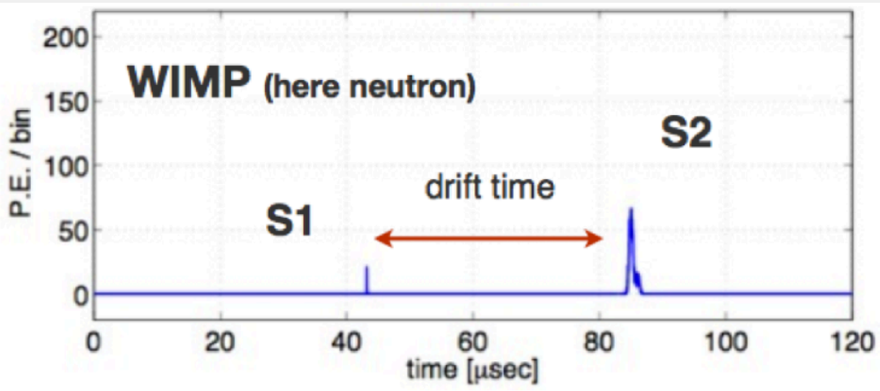

Particle Discrimination in 2-phase TPC

IONIZATION/SCINTILLATION

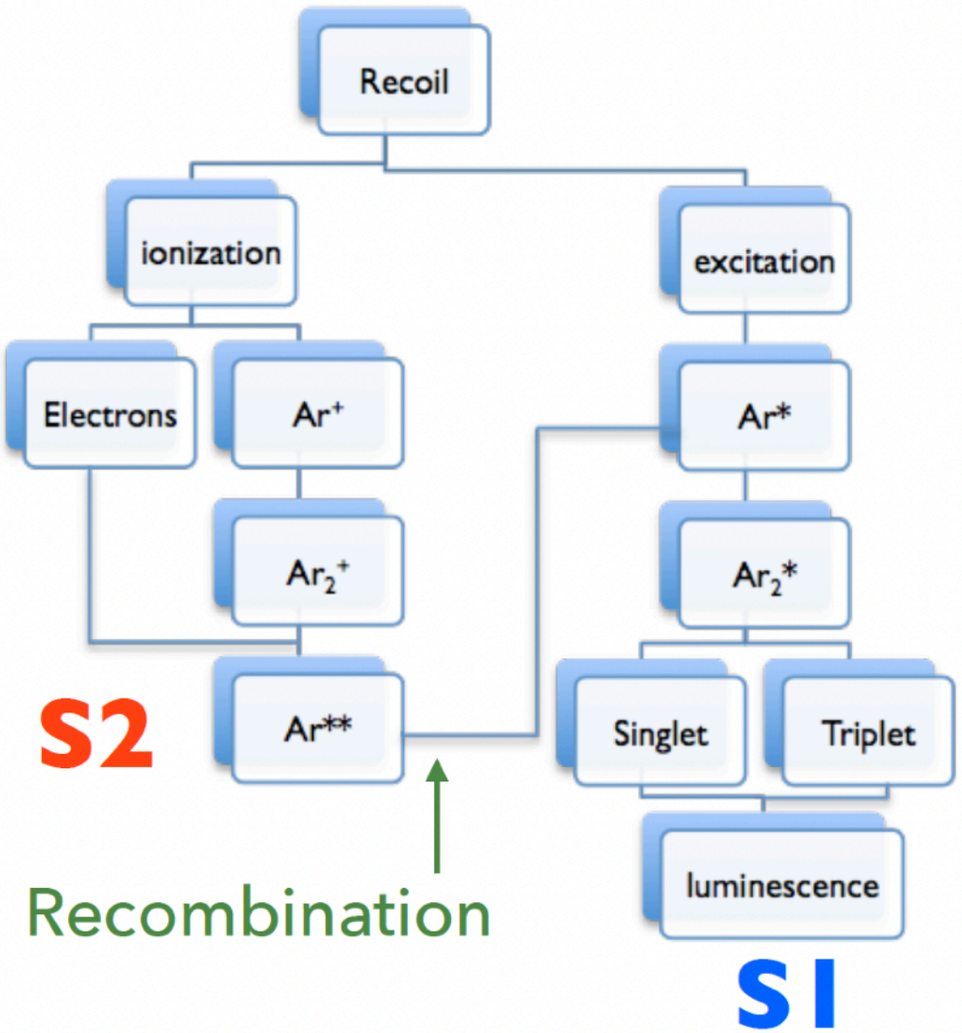

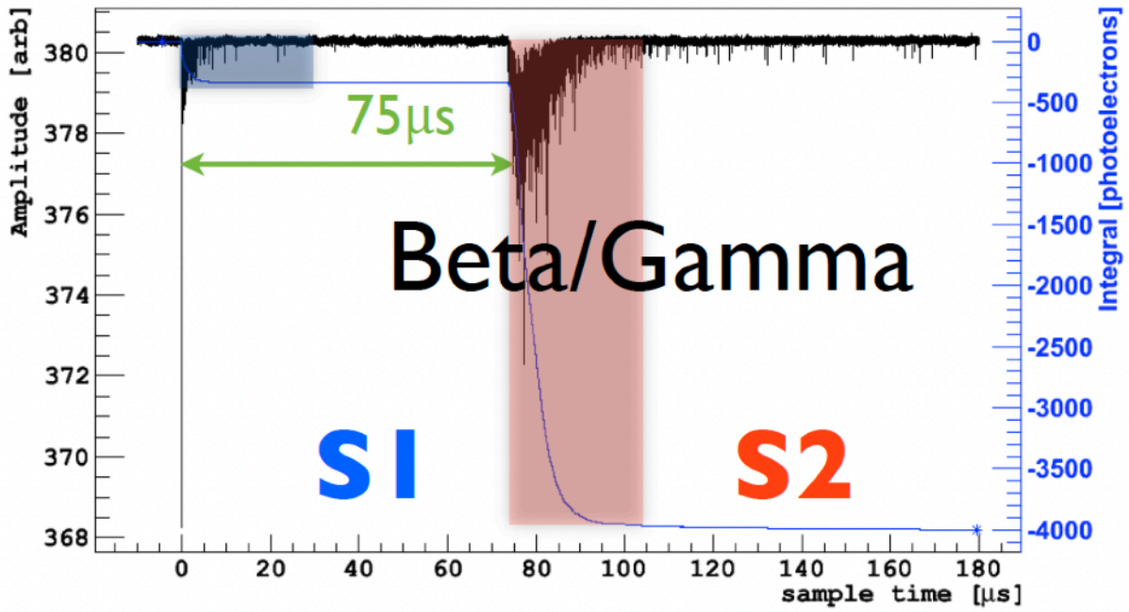

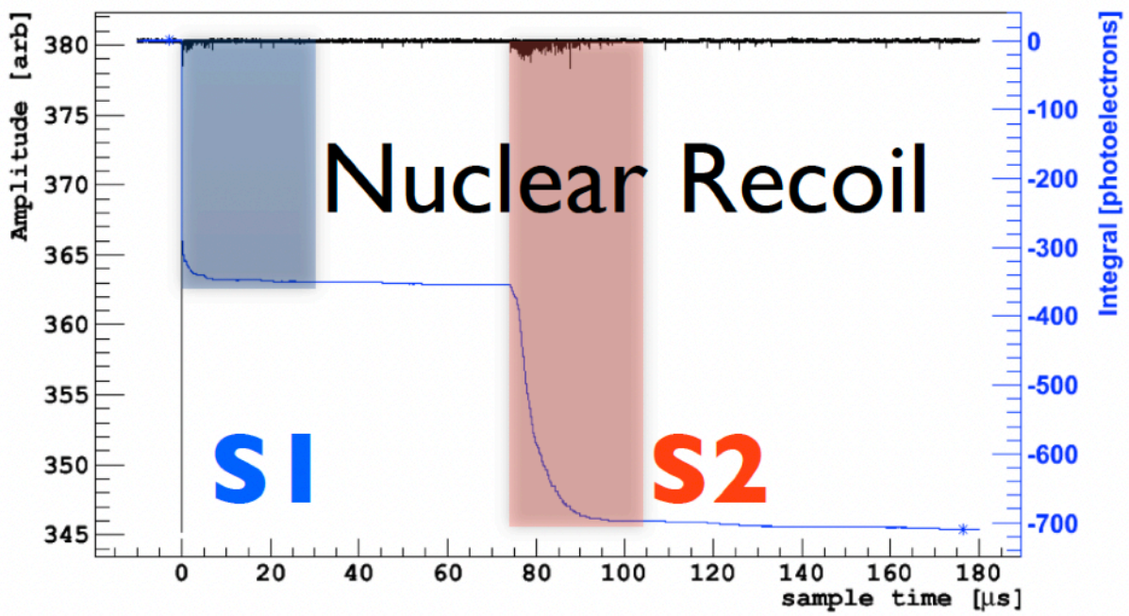

The ratio of S2 to S1 depends on ionization density

Particle Discrimination in 2-phase TPC

PULSE SHAPE DISCRIMINATION

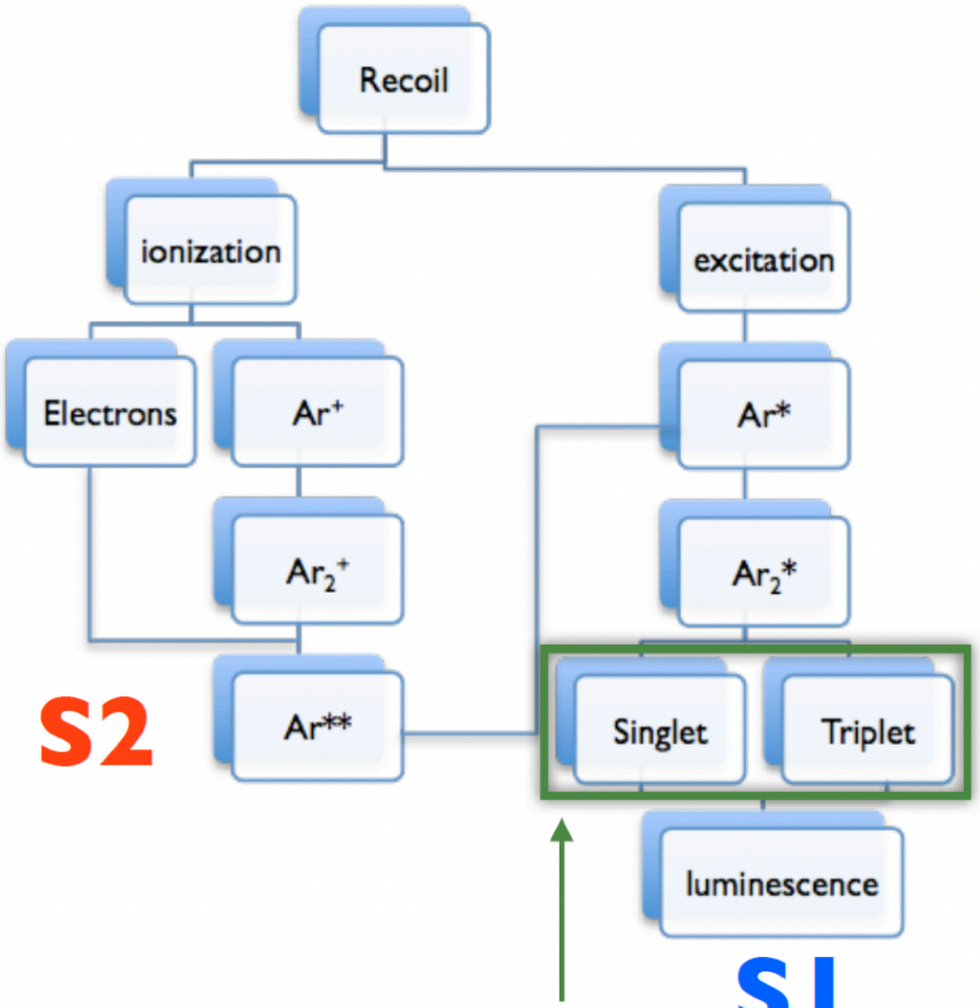

The ratio of light from singlet and triplet depends on ionization density

Ar $t_{singlet} = 7$ ns $t_{triplet} = 1600$

Xe $t_{singlet} = 3$ ns $t_{triplet} = 27$ ns

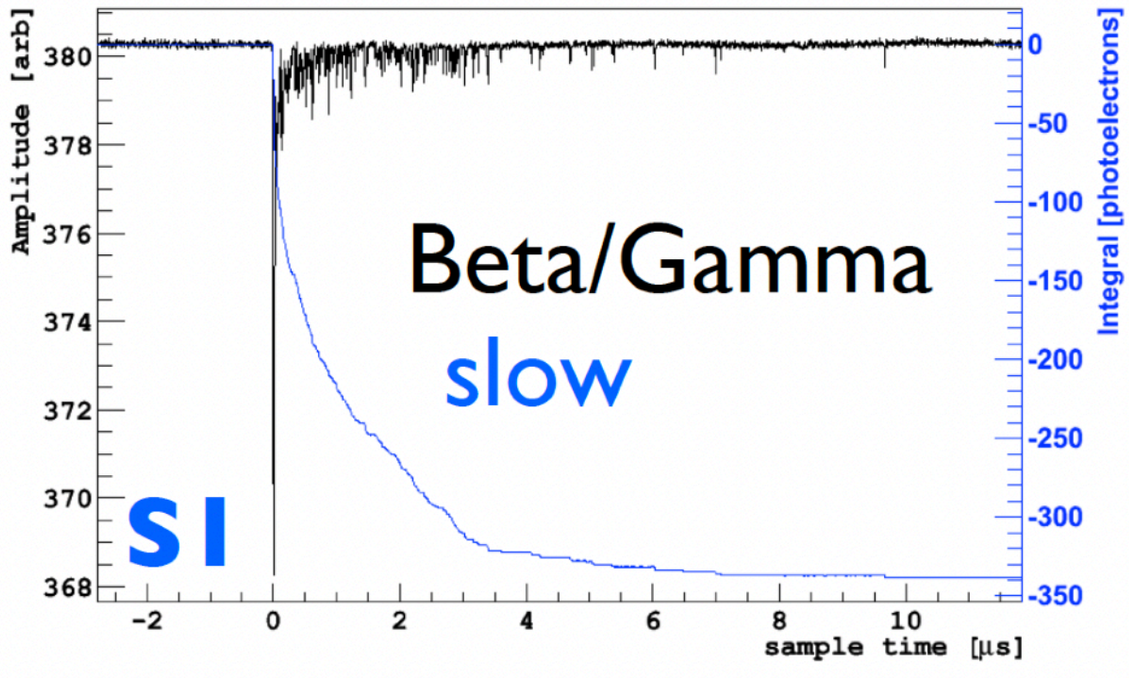

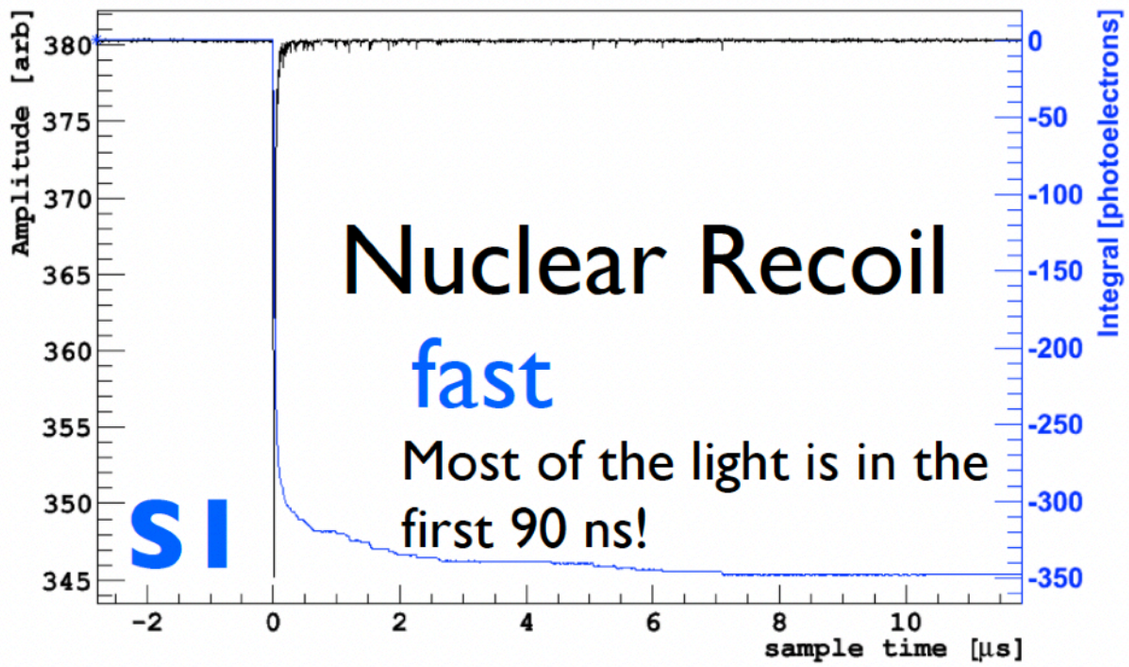

Particle Discrimination in 2-phase TPC

PARTICLE DISCRIMINATION IN NOBLE LIQUIDS

Ratio of charge to light in LXe:

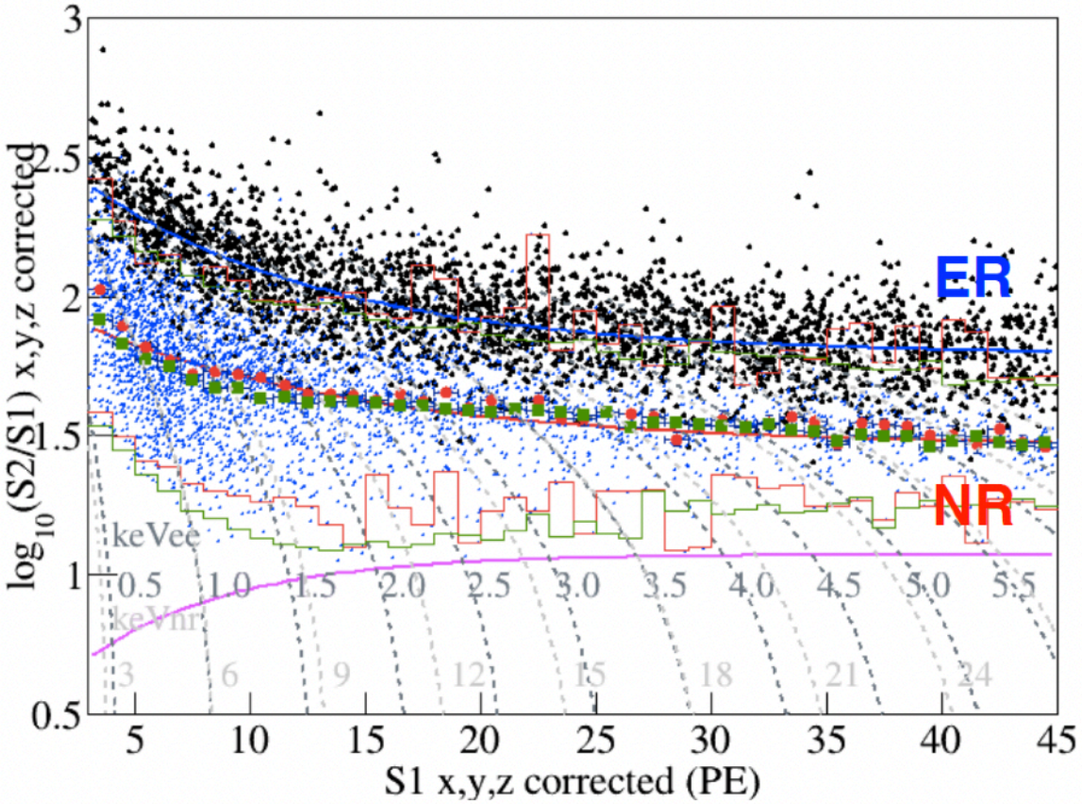

Tritium and AmBe calibrations in PandaX

Discrimination power ~ 10^3

Pulse Shape Discrimination in LAr:

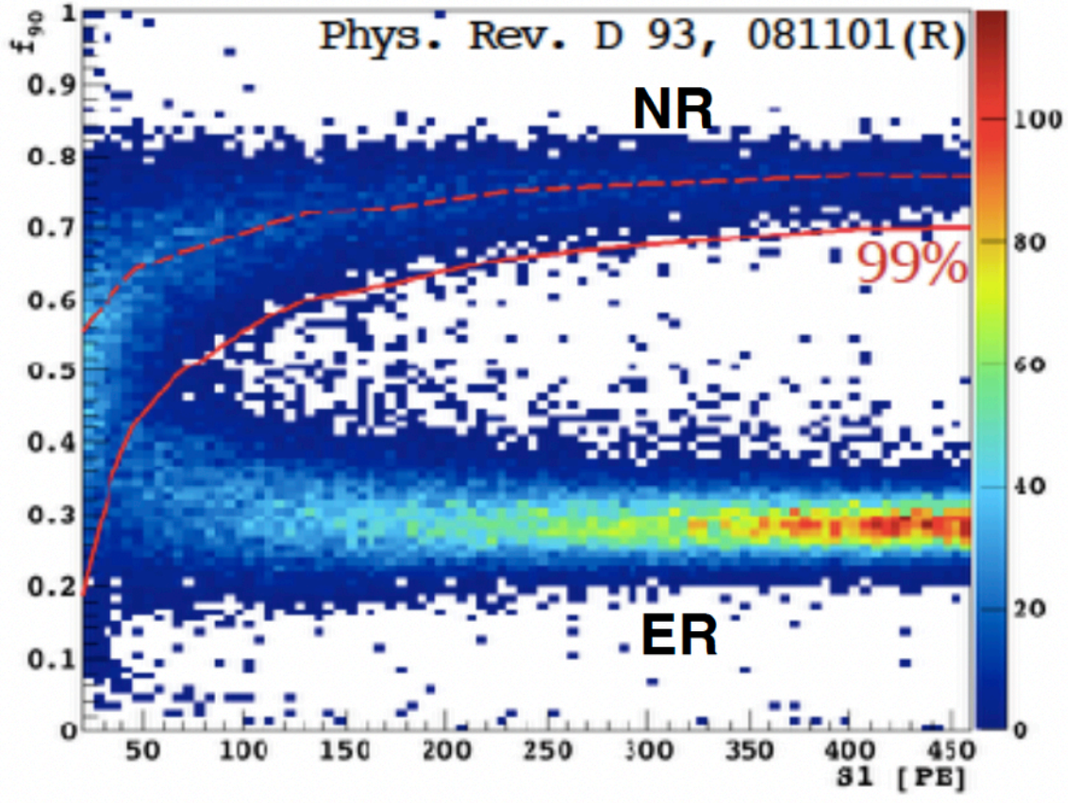

NR band from the AmBe calibration and lower ER band from β-γ backgrounds in DarkSide-50

Discrimination power > 10^8

LAr TPC evolution

ARGON DETECTORS

LAr high mass: background discrimination

10 kg — 2010 — **DarkSide-50** (50 kg, LNGS)

100 kg — **ArDM** (1t, LSC)

1000 kg — 2015 — **DEAP-3600** (3.6t, SNOLAB)

10000 kg — 2020 — **DarkSide-20k** (50t, LNGS)

100000 kg — **ARGO**: 400 t, SNOLAB

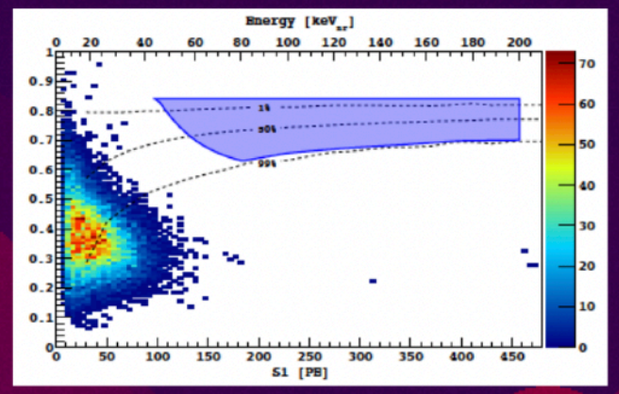

Phys. Rev. D 98, 102006 (2018)

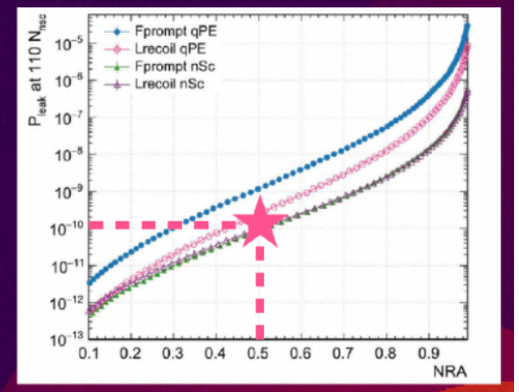

Eur. Phys. J. C 81, 823 (2021)

DS50 low mass: leading SI limit at 1.2-3.6 GeV/c^2

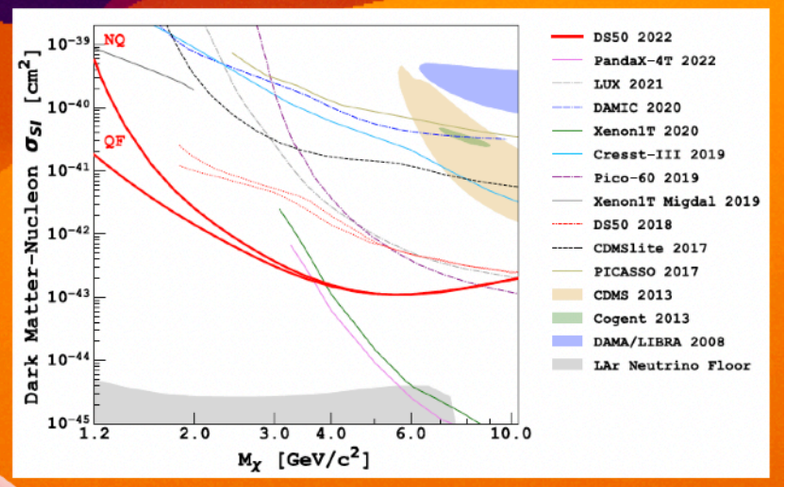

Phys. Rev. D 107, 063001 (2023)

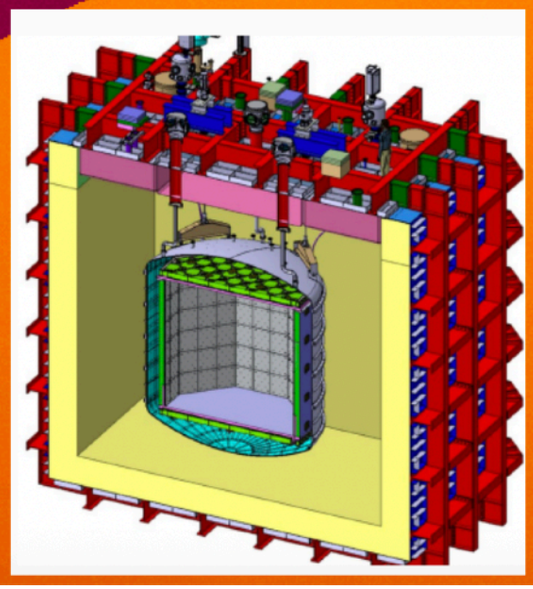

Global Argon Dark Matter Collaboration formed

Credits: Jocelyn Monroe

DarkSide-50 and -20k

DarkSide-50

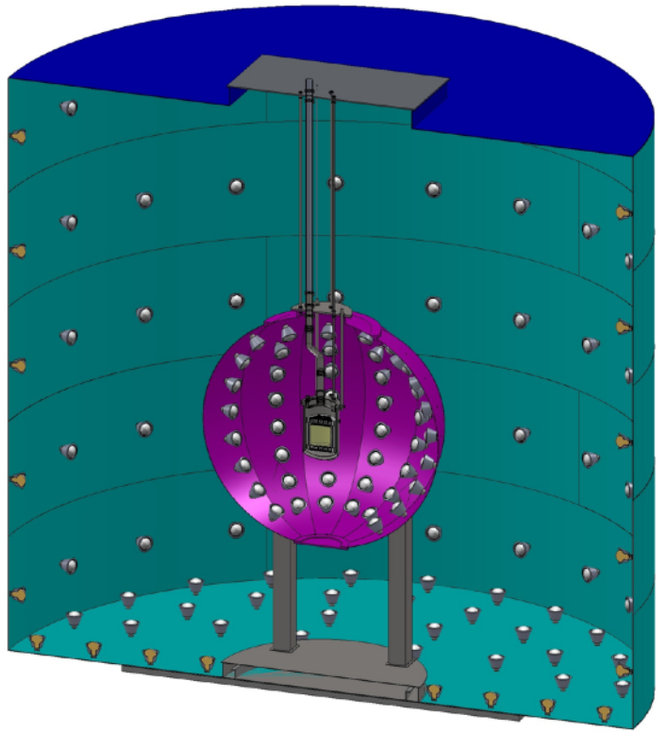

- Detector inside Borexino counting facility at LNGS (Italy)
- 50 kg depleted argon from underground sources

  > 1000 reduction in ^{39}Ar level
- Pulse shape & charge/light ratio for particle discrimination

  Pulse-shape separation > 10^7
- Hamamatsu R11065 as photosensor

  Challenge: operation of PMTs at LAr temperatures

  → plan to use SiPMs in the next generation detector

- **DarkSide-20k**
  - Scheduled for 2021
  - Utilizing underground argon
  - Atmospheric LAr veto, DUNE style cryostat possible
  - Background free
- Global Argon Dark Matter Collaboration
  - 300 t in 2027

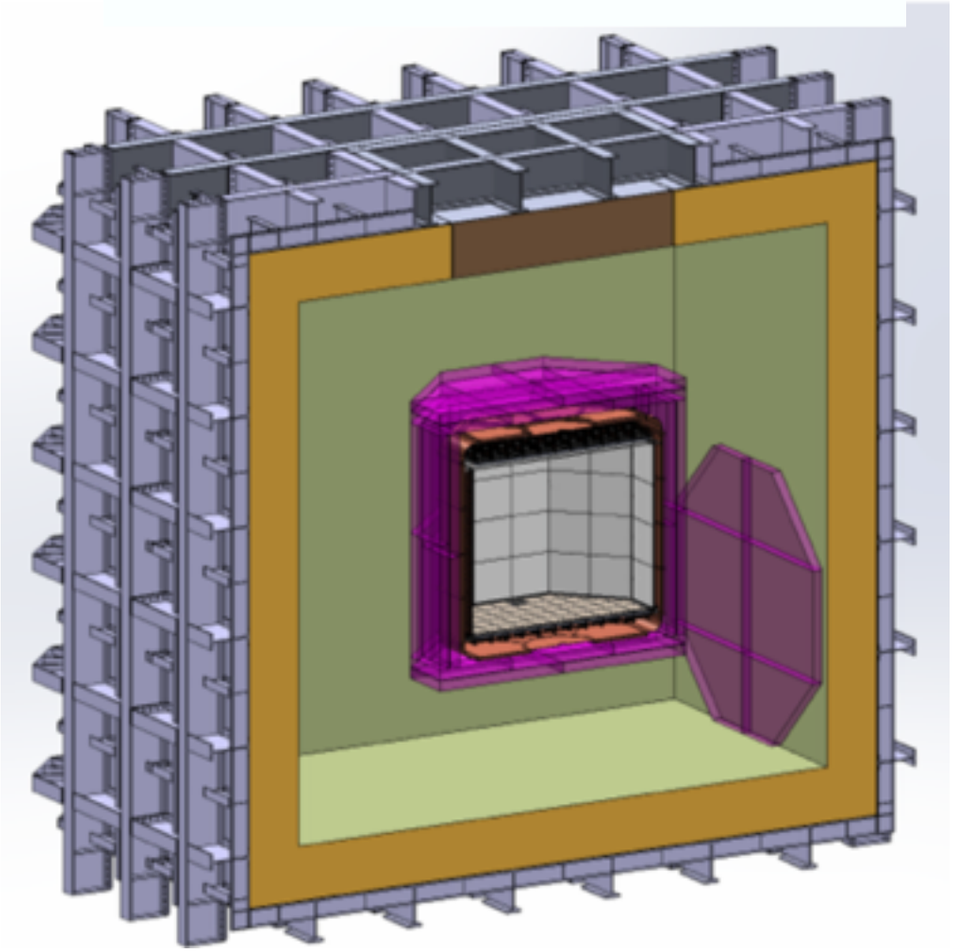

LAr results: DarkSide-50 & DEAP-3600

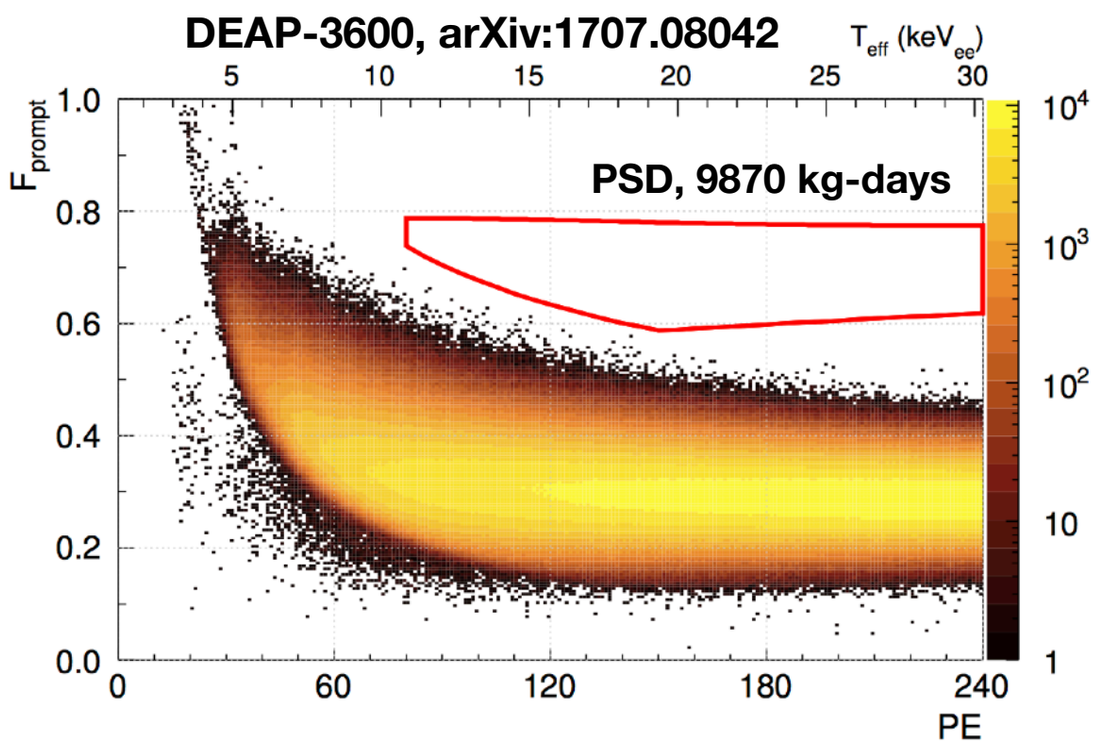

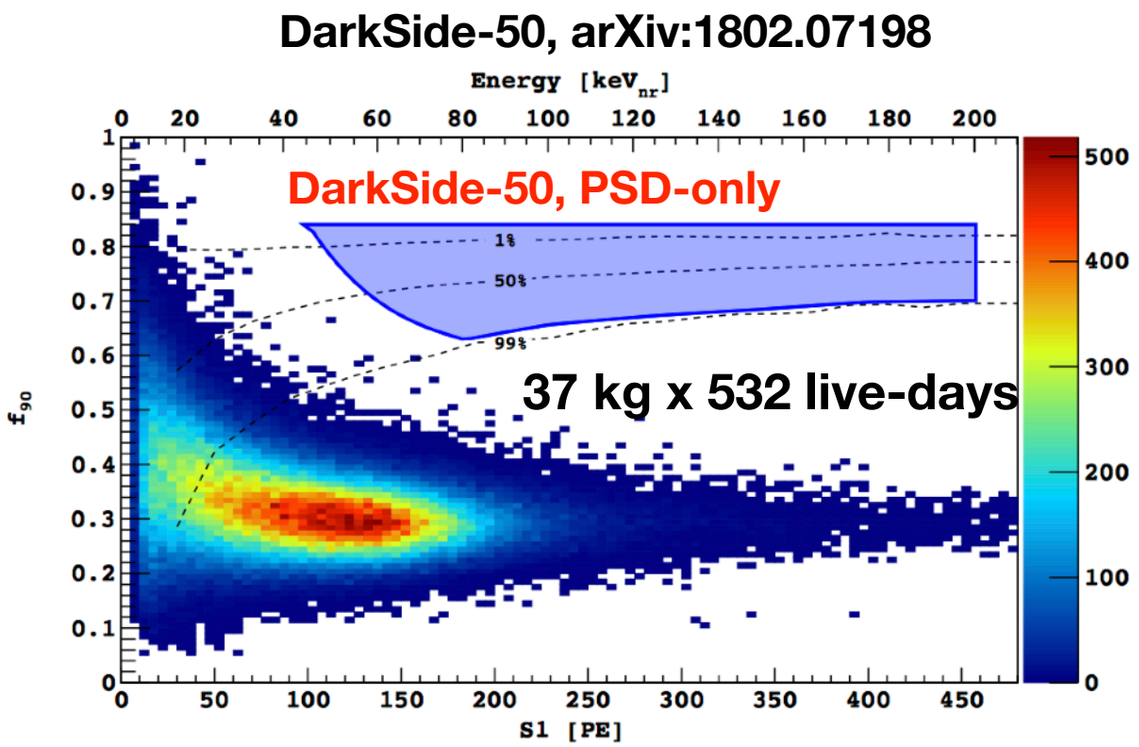

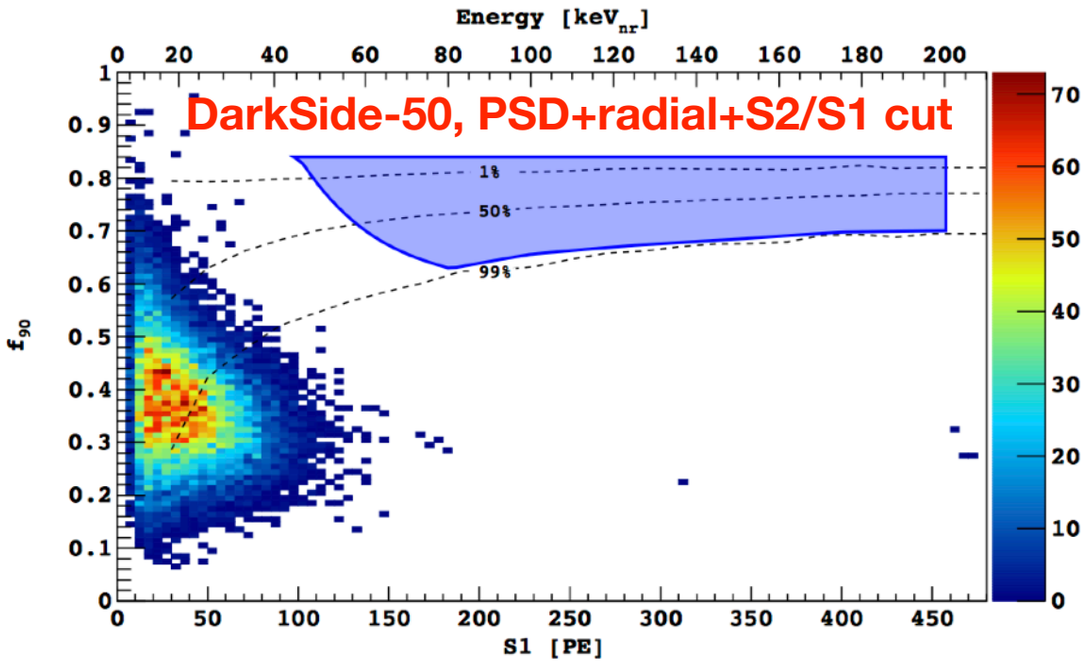

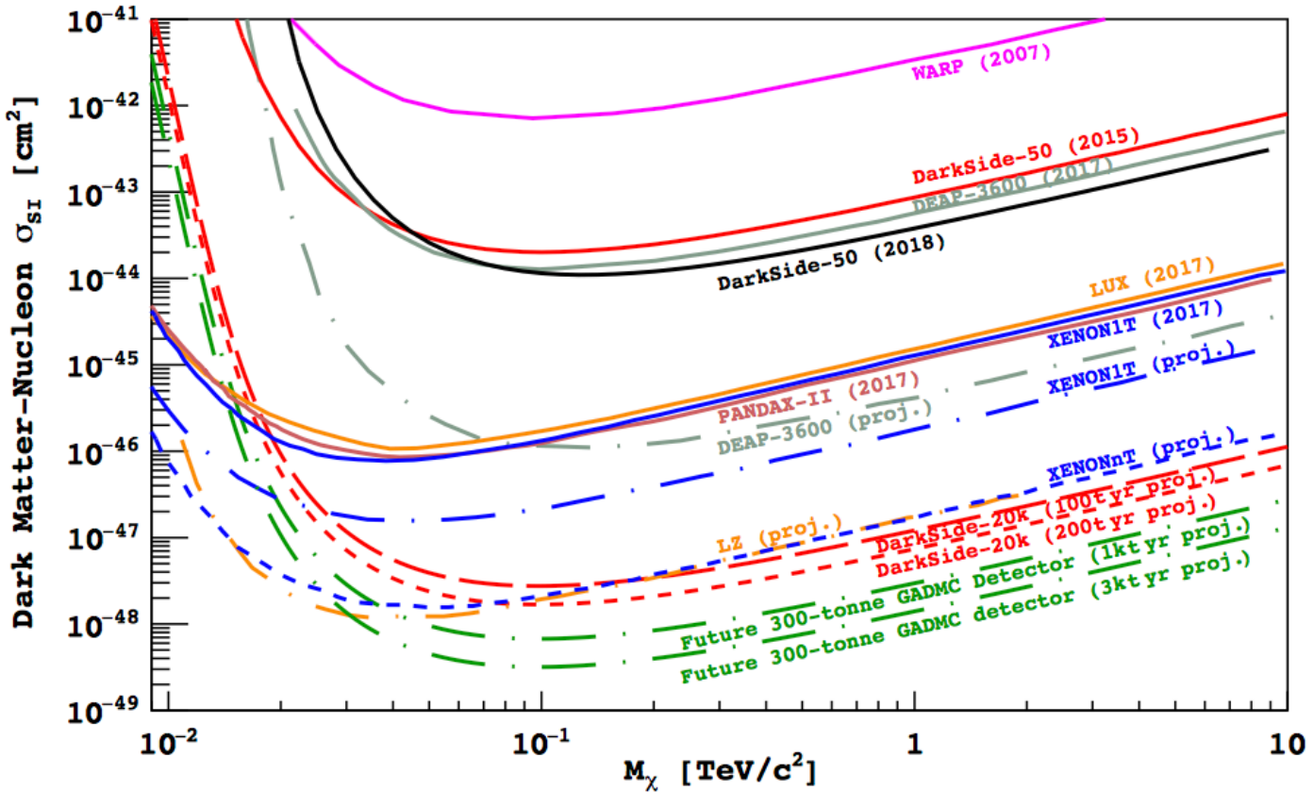

LAr: DarkSide-50 S2-only result

Phys.Rev.D 107 (2023) 6, 6

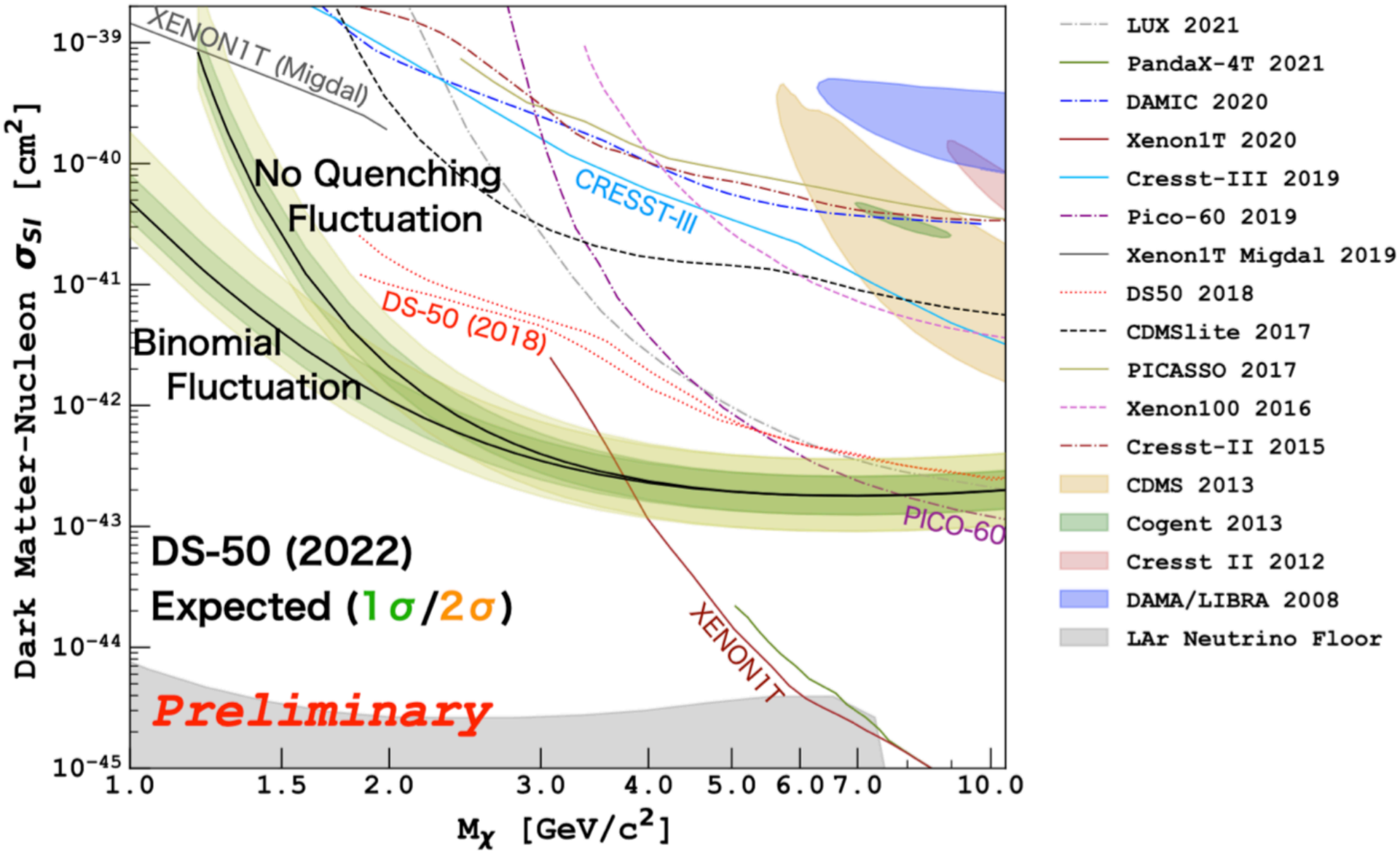

Underground Argon

RADIOPURE ARGON FROM UNDERGROUND SOURCES

- ^{39}Ar β decay (Q = 570 keV, half-life 269 yr)
- ~1Bq/kg in atmosferic Ar
- Origin from $^{40}Ar(n,2n)^{39}Ar$ in atmosphere
- Extraction of Ar from underground sources, where such processes are suppressed
- DS50 used 157 kg of UAr
- Depletion factor in ^{39}Ar : 1400 ± 200

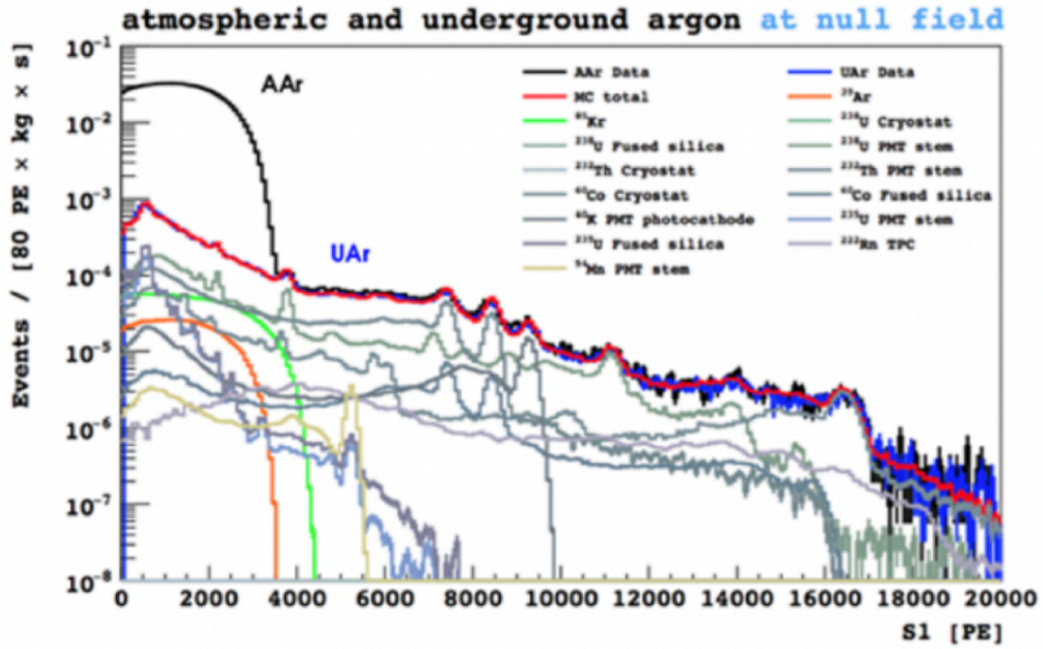

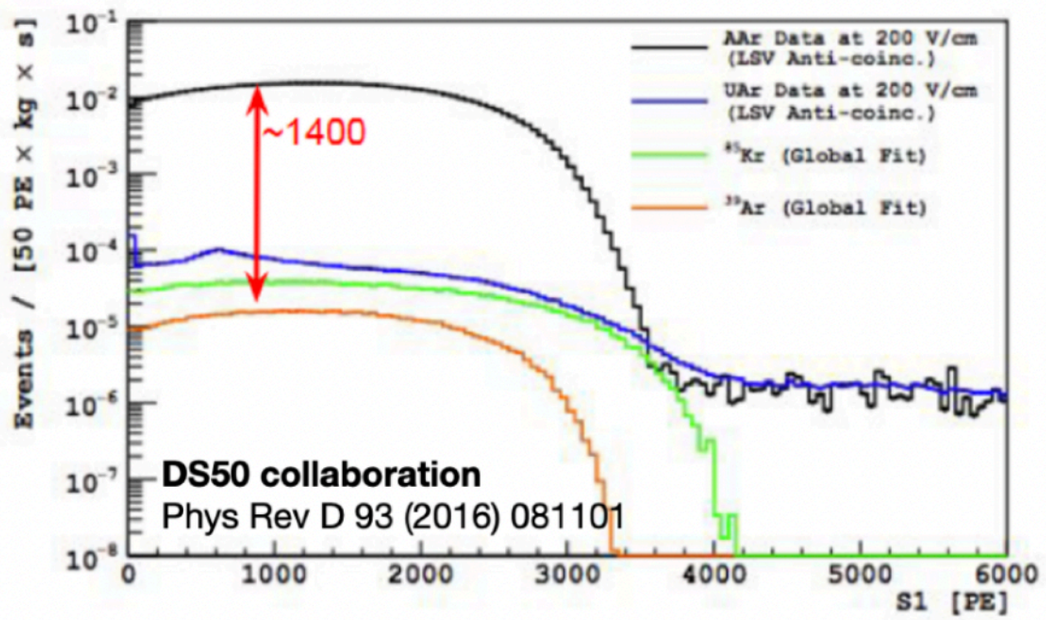

Underground Argon

LOW RADIOACTIVITY ARGON: URANIA & ARIA

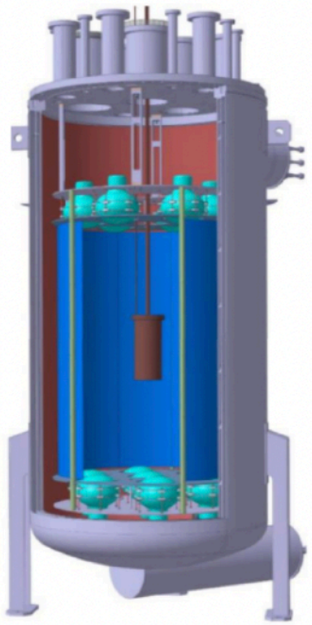

1) UAr extraction at the URANIA plant.

^{39}Ar (β-decay) suppressed by $\sim 10^3$ in underground CO2 reservoir in Cortez, Colorado

UAr extraction rate: 250-330 kg/day

Expected argon purity at outlet: 99.99%

3) Qualification at Canfranc, DArT in ArDM

A single-phase LAr detector with active volume ~1L, capable of measuring UAr to AAr ^{39}Ar depletion factors of the order of 1000 with 10% precision in weeks *JINST 15 P02024*

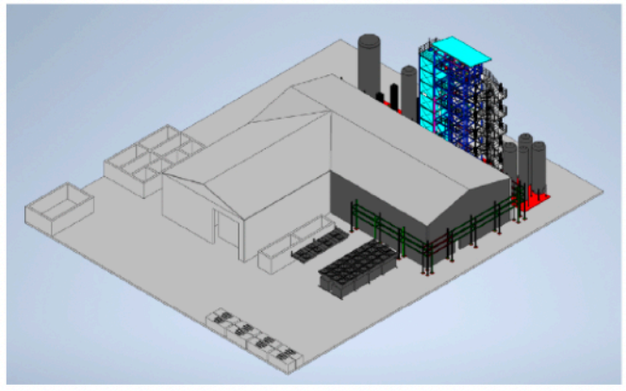

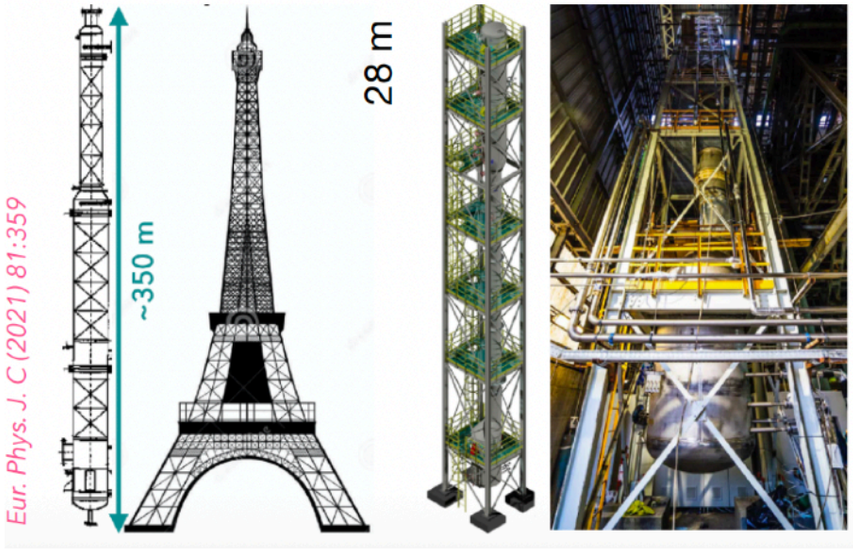

Eur. Phys. J. C (2021) 81:359

2) Cryogenic distillation at the ARIA facility

Installed in the shaft of a coal mine

Chemical purification rate: 1 t/day

First module operated according to specs with nitrogen

Run completed with Ar at the end of 2020 *Eur. Phys. J. C (2023) 83:453*

Full assembly about to start

LAr: DarkSide-20k

THE DARKSIDE-20K DETECTOR @ LNGS

Inner Veto

Radiogenic n's

32-ton underground LAr

- Membrane (ProtoDUNE-like) cryostat
- Atmospheric argon (AAr) volume (≈700 t)
- Vacuum vessel containing UAr and TPC/Veto
- Underground argon (UAr) volume (≈100 t)
- Inner detectors TPC and Neutron Veto with >25 m² SiPM arrays
- Outer Veto with SiPM arrays near the cryostat walls

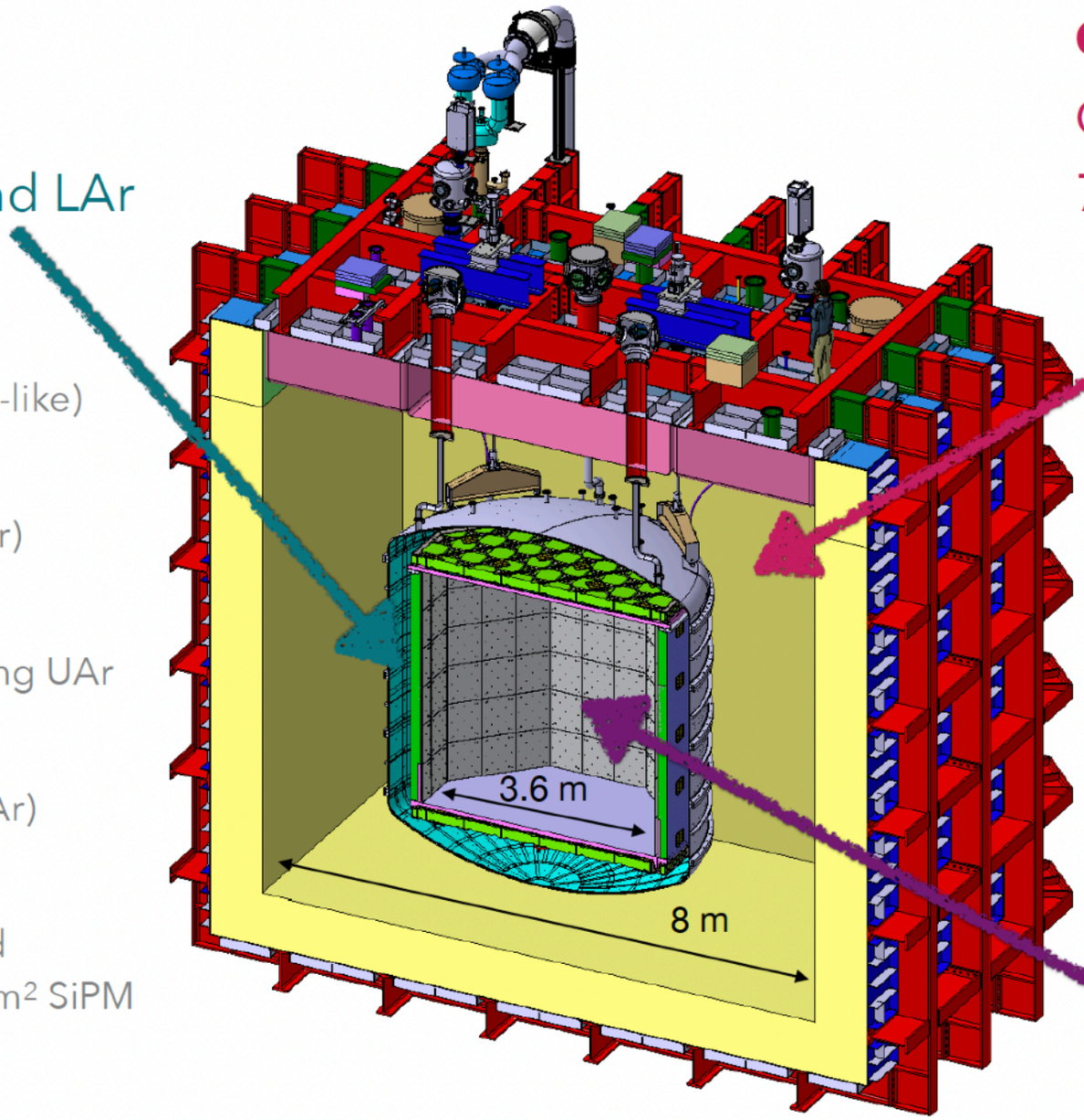

Outer Veto

Cosmic μ's and showers

700-ton atmospheric LAr

TPC

Dark matter detector

50-ton underground LAr/GAr, PMMA walls

(20-ton fiducial mass)

LAr: DarkSide-20k

THE DARKSIDE-20K DETECTOR @ LNGS

- Octagonal shape dual phase argon TPC:
  - Active UAr mass: 49,7 tonnes
  - Fiducial UAr mass: 20,2 tonnes
- Neutron veto:
  - Active UAr mass: 32 tonnes

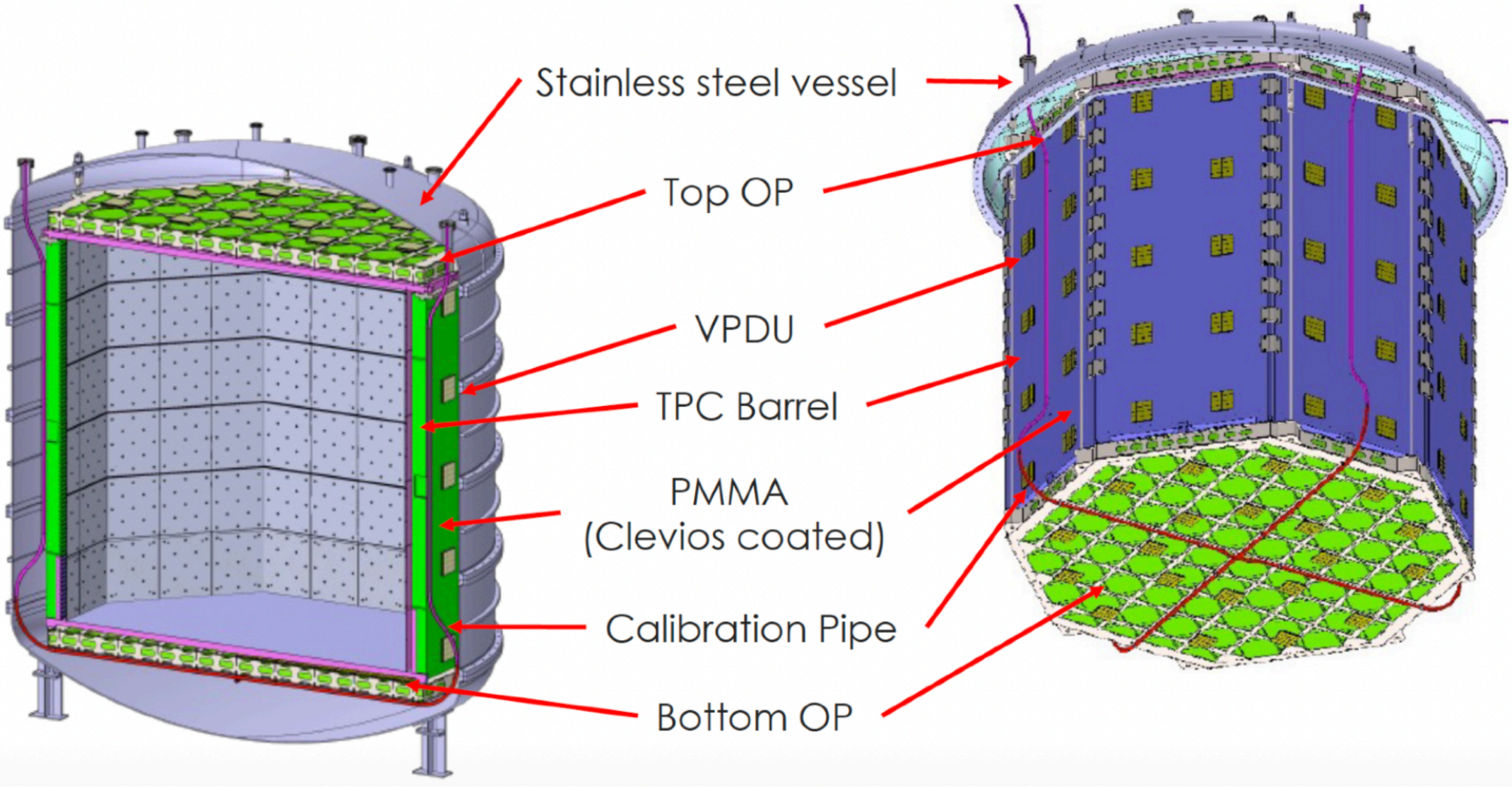

LAr: DarkSide-20k

THE DARKSIDE-20K DETECTOR @ LNGS

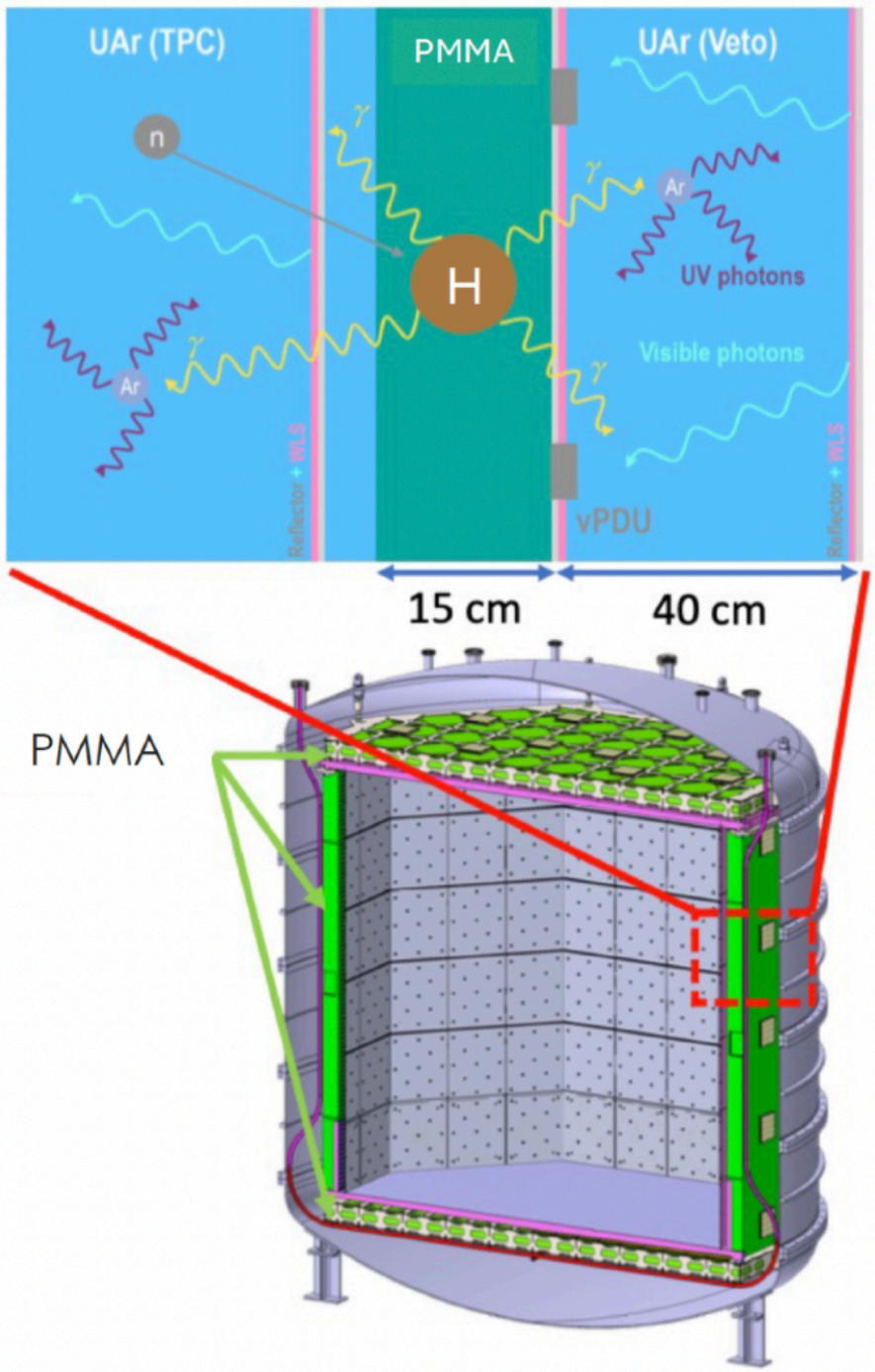

- Acrylic (Hydrogen) + Argon
- Detection of 2,1 MeV gammas from neutron capture on H (53%) in TPC or Veto
  - 4π coverage: TPC walls, top and bottom endcaps
  - 40 cm thick UAr buffer + UAr in TPC
- Produced γ rays interact in UAr in both buffer and TPC
- 3M ESR used as reflector and PEN as wavelength shifter
- Scintillation light detected by SiPMs in both buffer and TPC

LAr: DarkSide-20k

LOW RADIOACTIVITY, HIGH EFFICIENCY SiPM PHOTOSENSORS

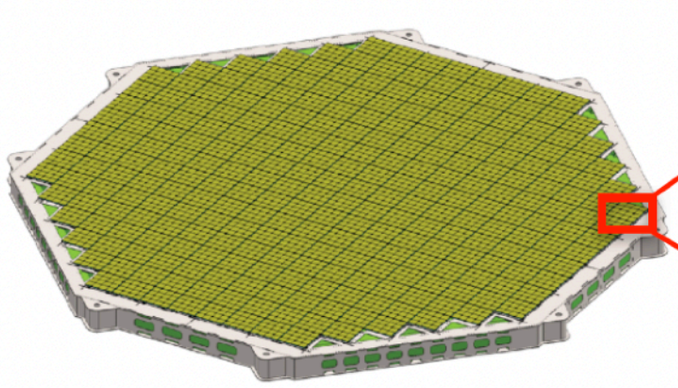

TPC optical plane ($\sim 21\,\mathrm{m}^2$)
525 PDUs

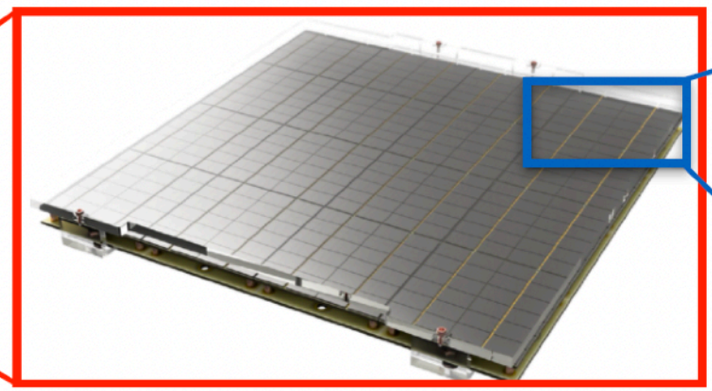

Photo Detection Unit
16 tiles arranged into 4 channels

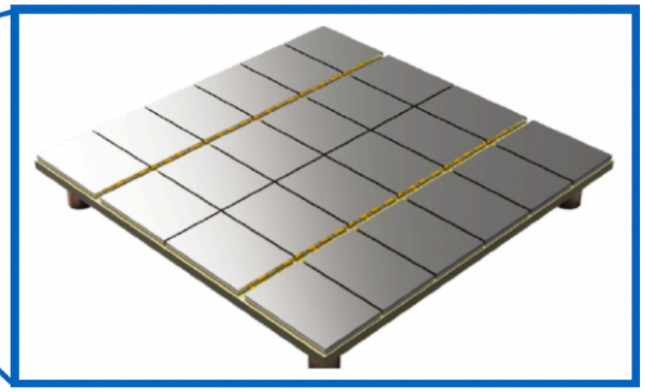

Tile / photo-detector module
24 SiPMs + signal amplifier

- Wafer delivery from LFoundry started in 2022
- Packaging and assembly for TPC sensors: **Nuova Officina Assergi** (NOA), about to start operations
- Packaging and assembly for Veto sensors: RAL and Liverpool, UK
- Several test facilities to qualify production: Naples, Liverpool, Edinburgh, AstroCent

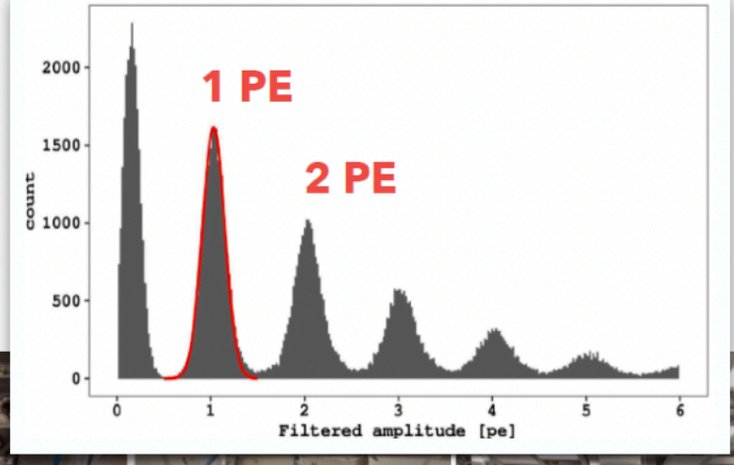

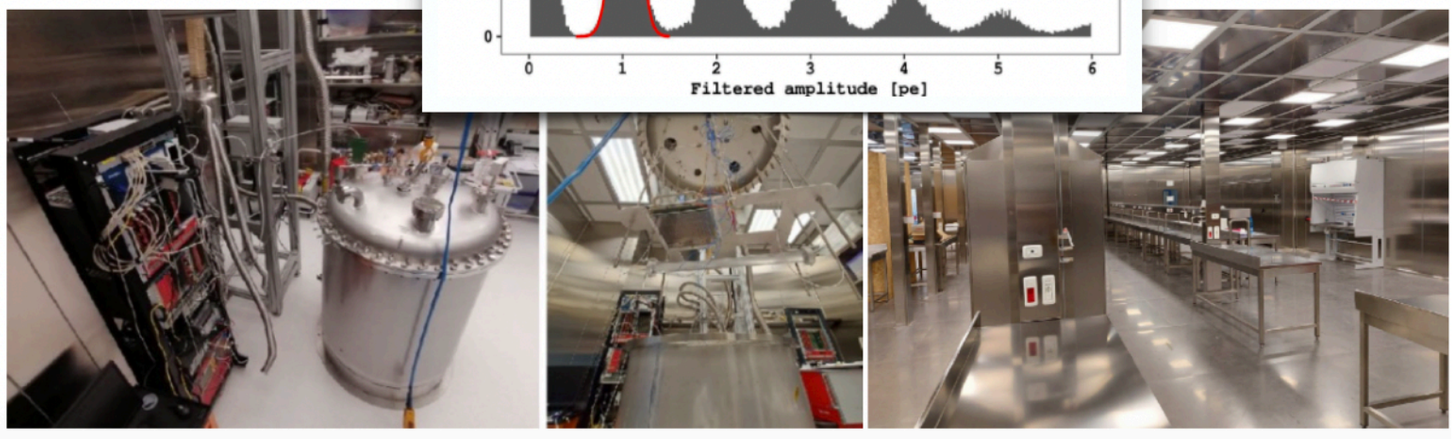

HIGH MASS WIMP SI INTERACTION EXCLUSION LIMITS PROSPECTS

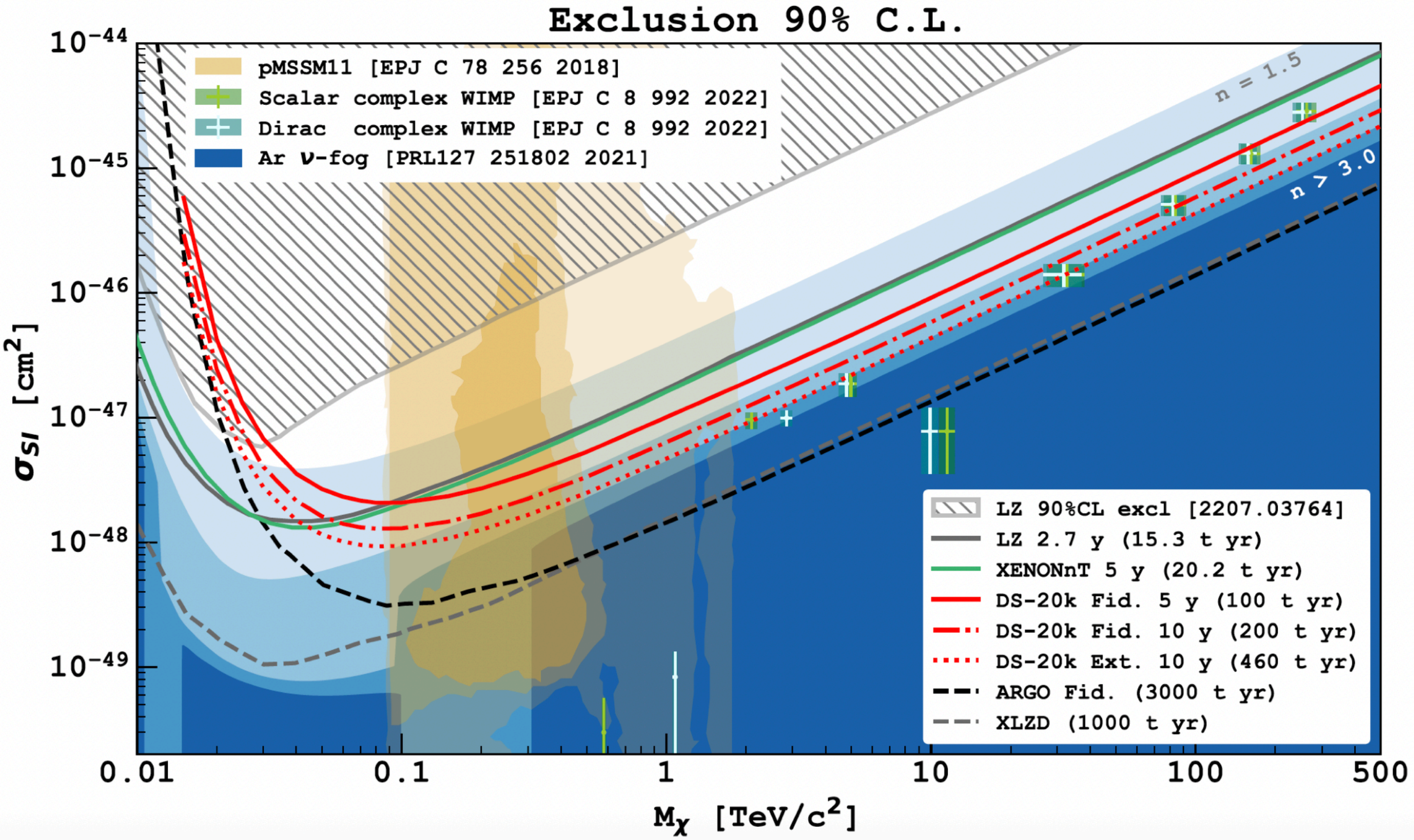

WIMP detectors from the XENON-series

XENON10	XENON100	XENON1T	XENONnT
	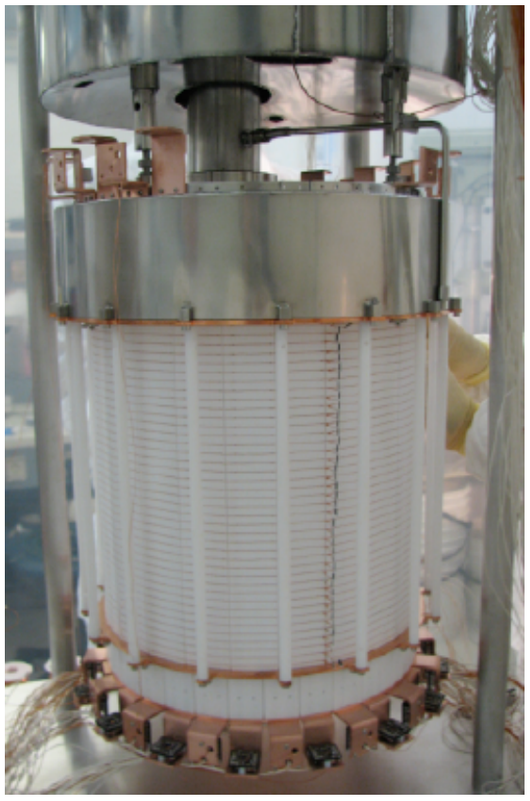	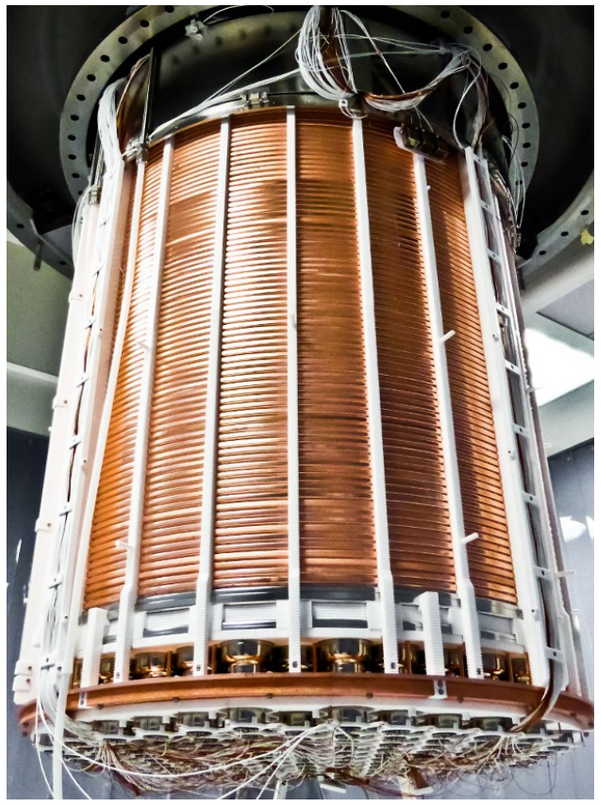	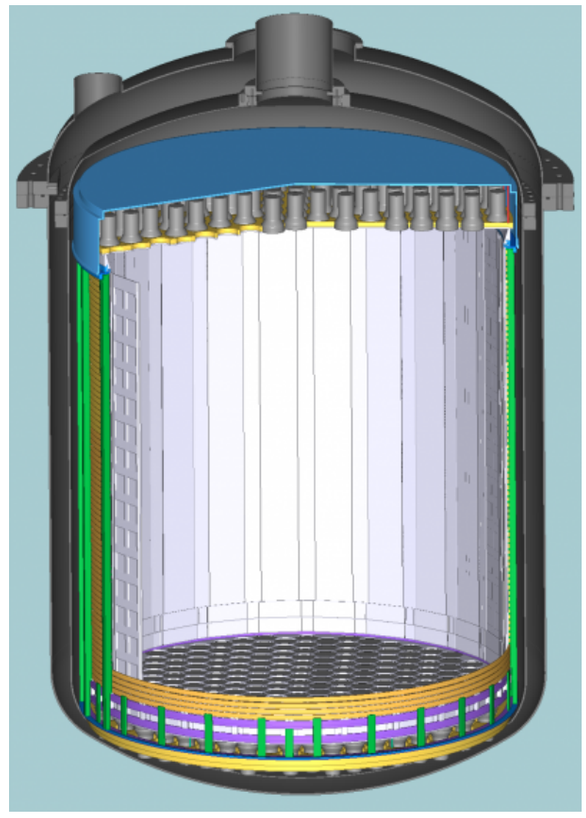
2005-2007	2008-2016	2012-2018	2020-2025
25 kg - 15cm drift	161 kg - 30 cm drift	3.2 ton - 1 m drift	8 ton - 1.5 m drift
~10^{-43} cm^2	~10^{-45} cm^2	~10^{-47} cm^2	~10^{-48} cm^2

Impressive evolution of LXeTPCs

THE EVOLUTION OF SPECIES

TOTAL LXe mass:
3.2 tonnes

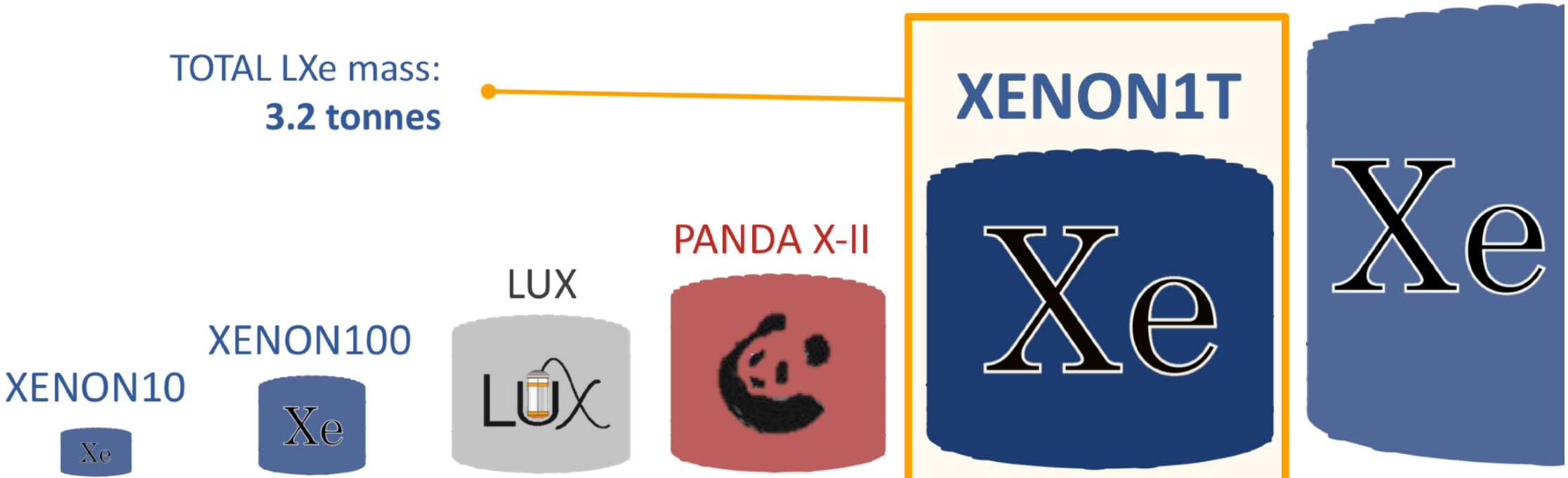

	2005	2008	2013	2016	**2016**	2019
LXe	22 kg	105 kg	250 kg	580 kg	**2000 kg**	6000 kg

ACTIVE LIQUID XENON TARGET MASS

5.3	2.6	1.9		**0.2**	**0.02**

LOW ENERGY ER BACKGROUND $[t \cdot d \cdot keV]^{-1}$

Evolution of LXeTPC detectors

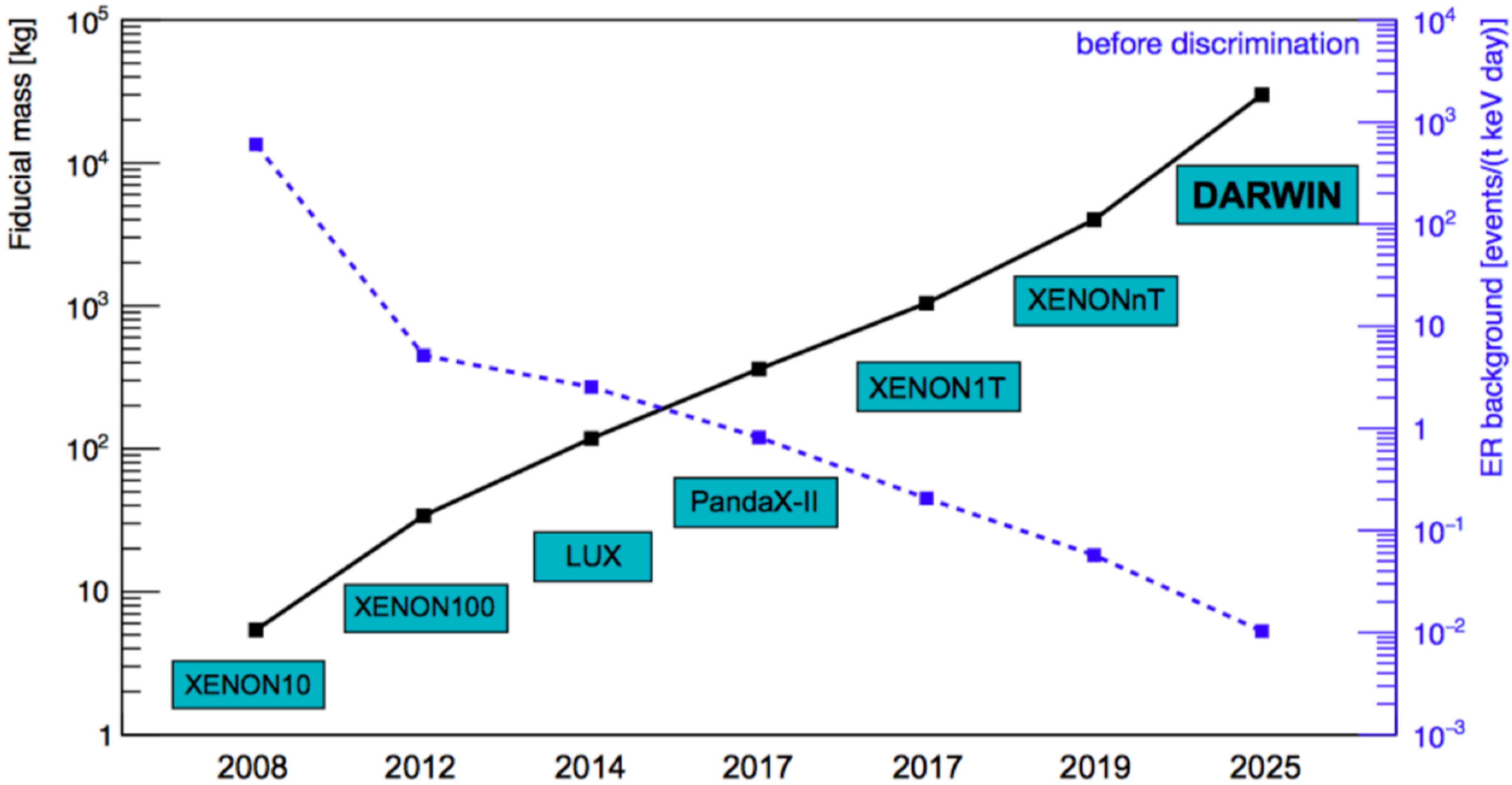

(from T. Marrodan)

(previous) detectors using the LXeTPC

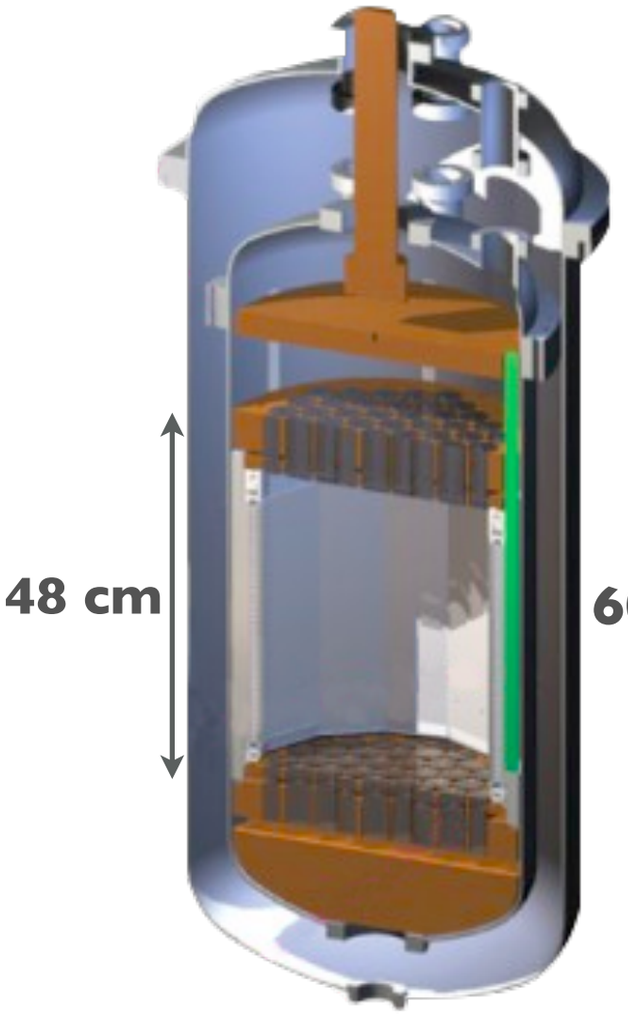

LUX
Active Target: ~250 kg
completed

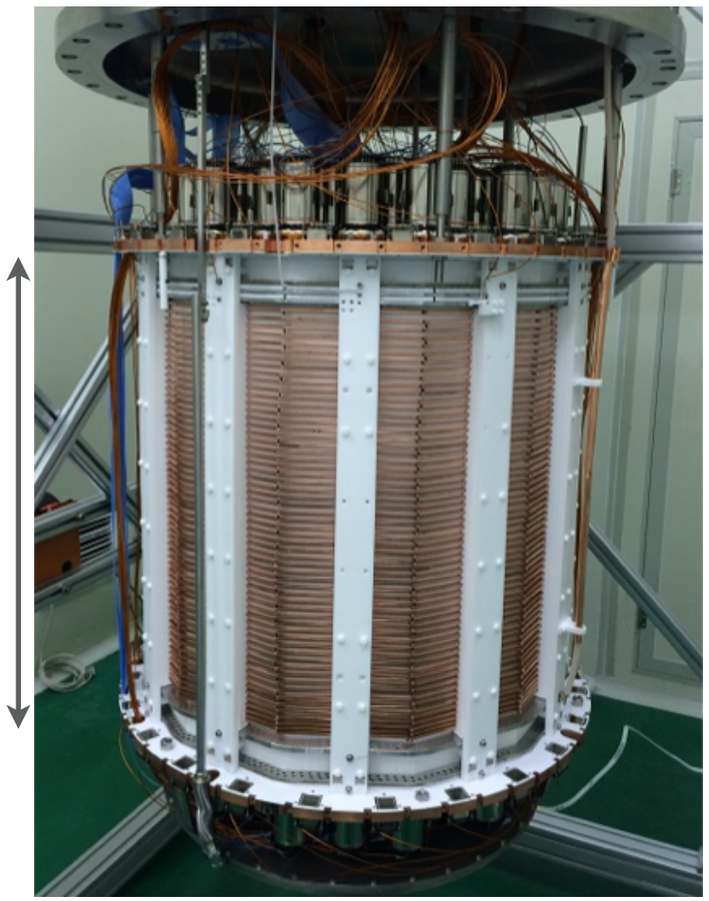

PandaX-II
Active Target: ~580 kg
completed

XENONIT
Active Target: 2000 kg
completed in 2018

The XENON1T Experiment @ LNGS

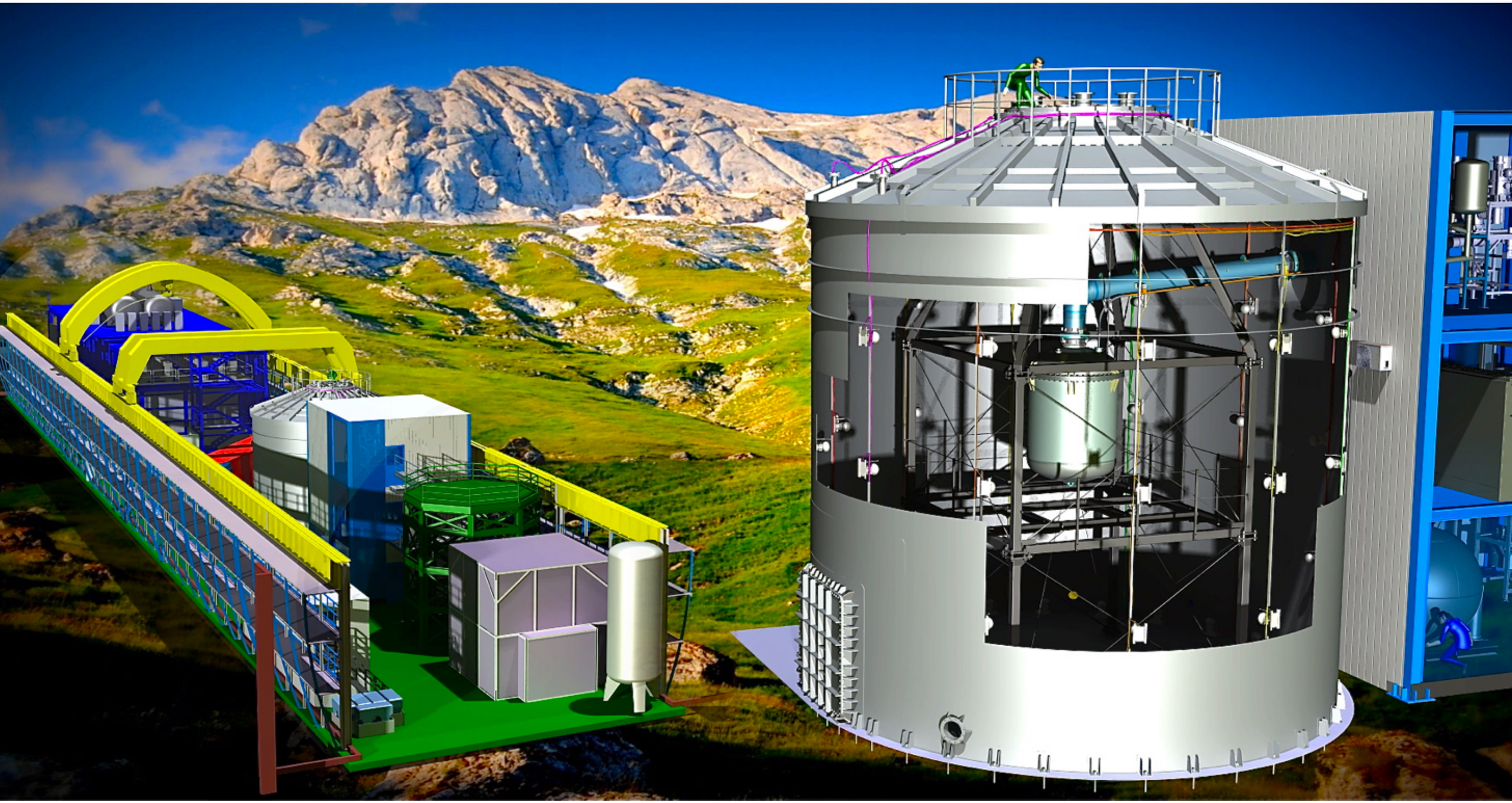

The XENON1T Experiment @ LNGS

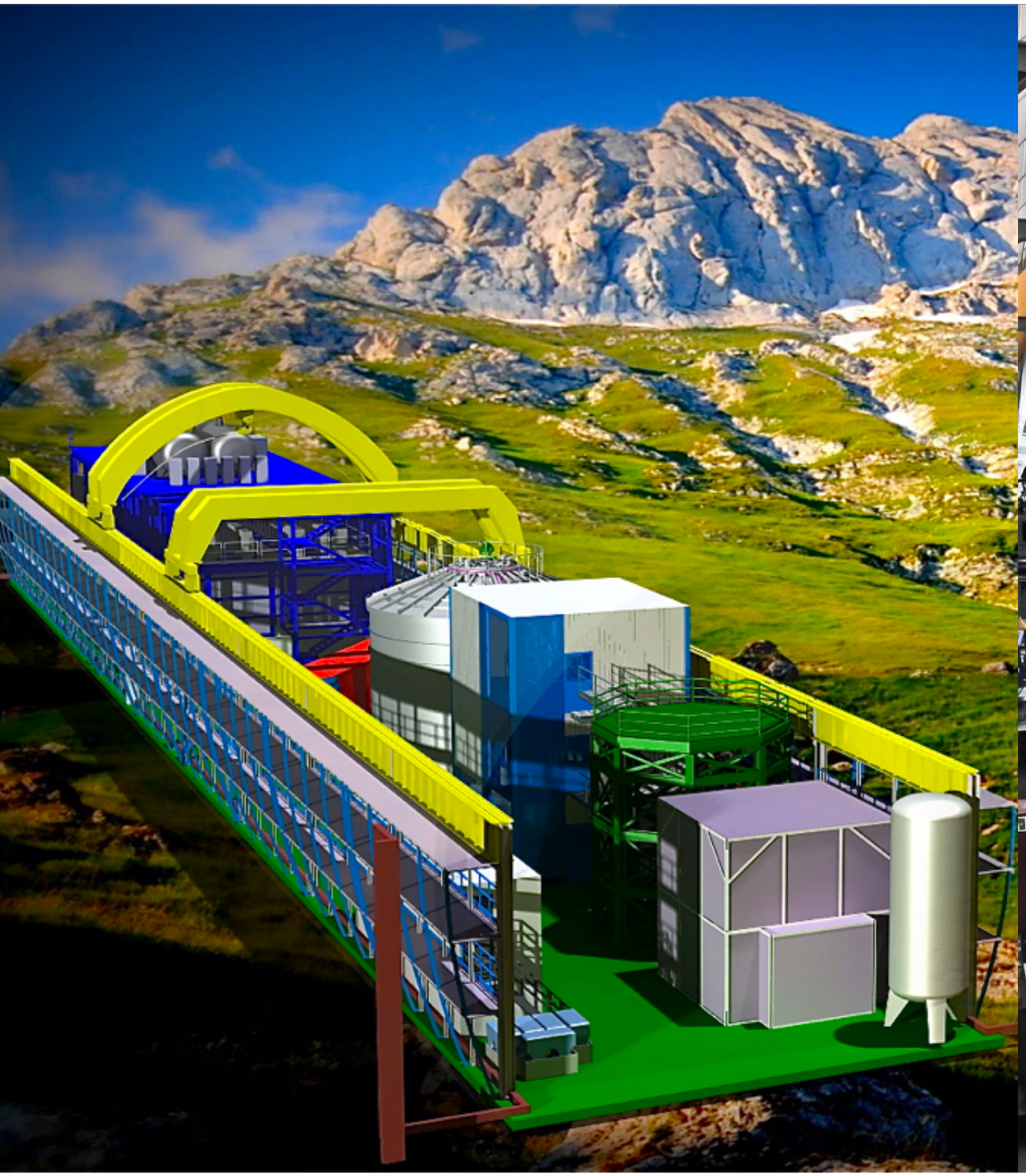

XENON1T: All Systems

E. Aprile et al.,
“The XENON1T Dark Matter Experiment”,
EPJ C 77, 881 (2017).

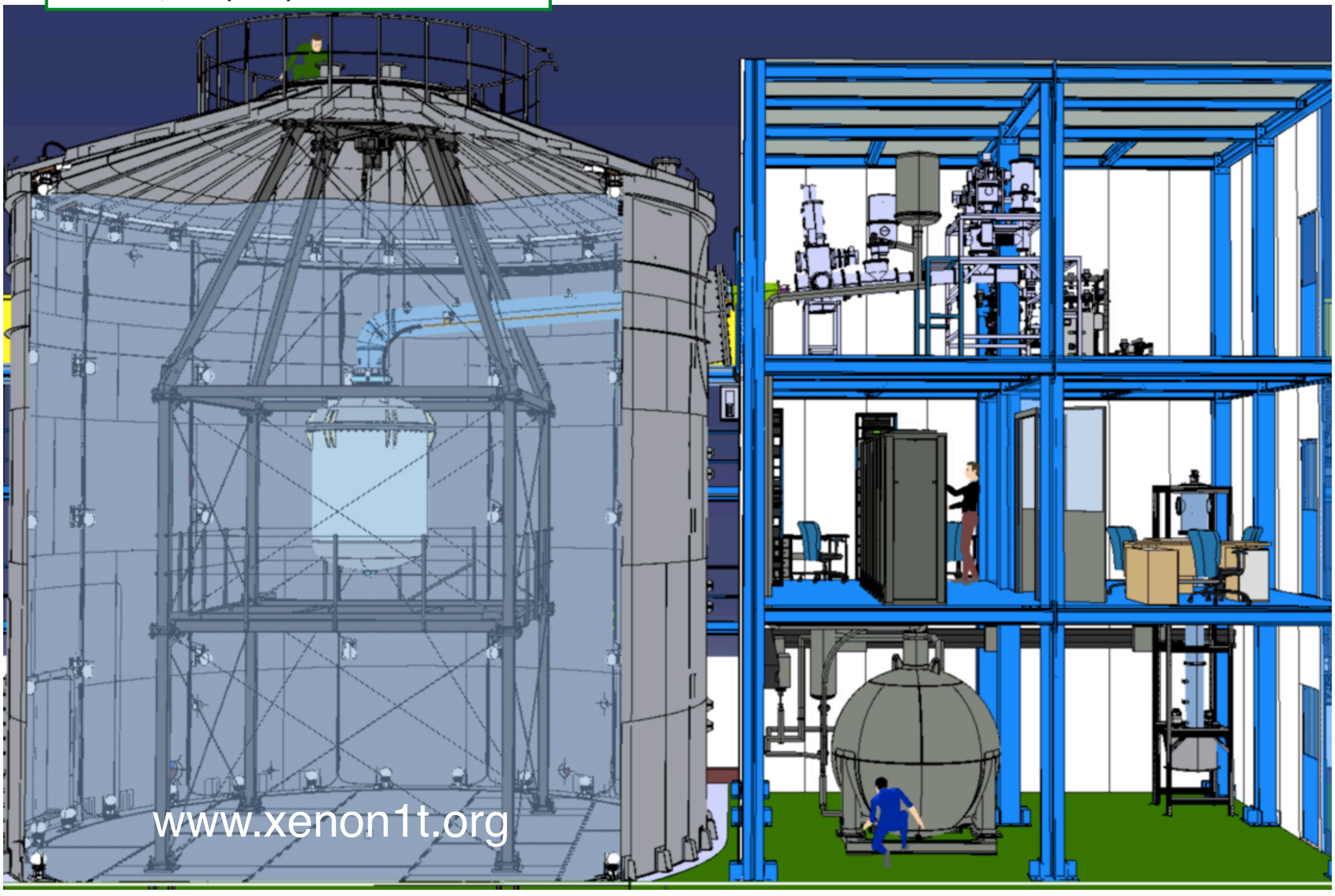

XENON1T: All Systems

E. Aprile et al.,
"The XENON1T Dark Matter Experiment",
EPJ C 77, 881 (2017).

Gd-Water Cherenkov Muon and Neutron Veto

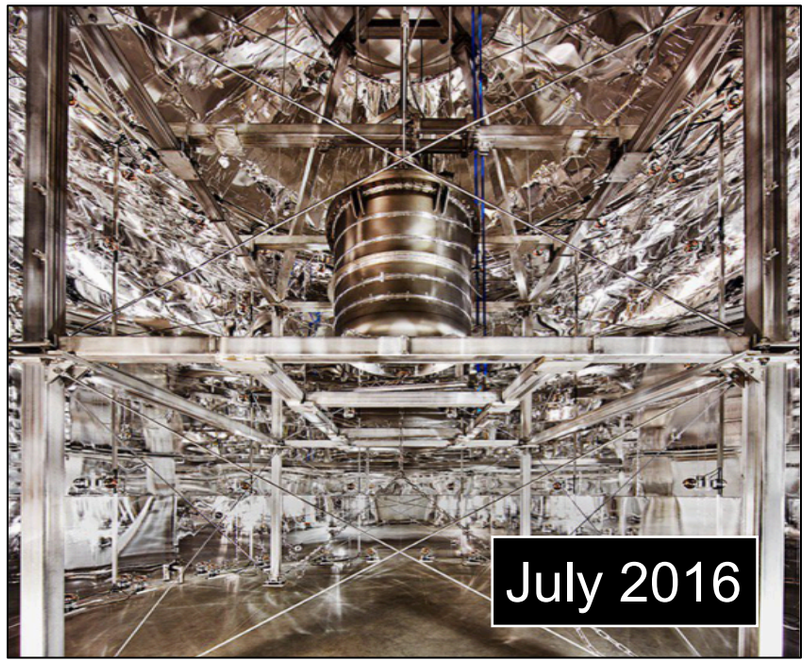

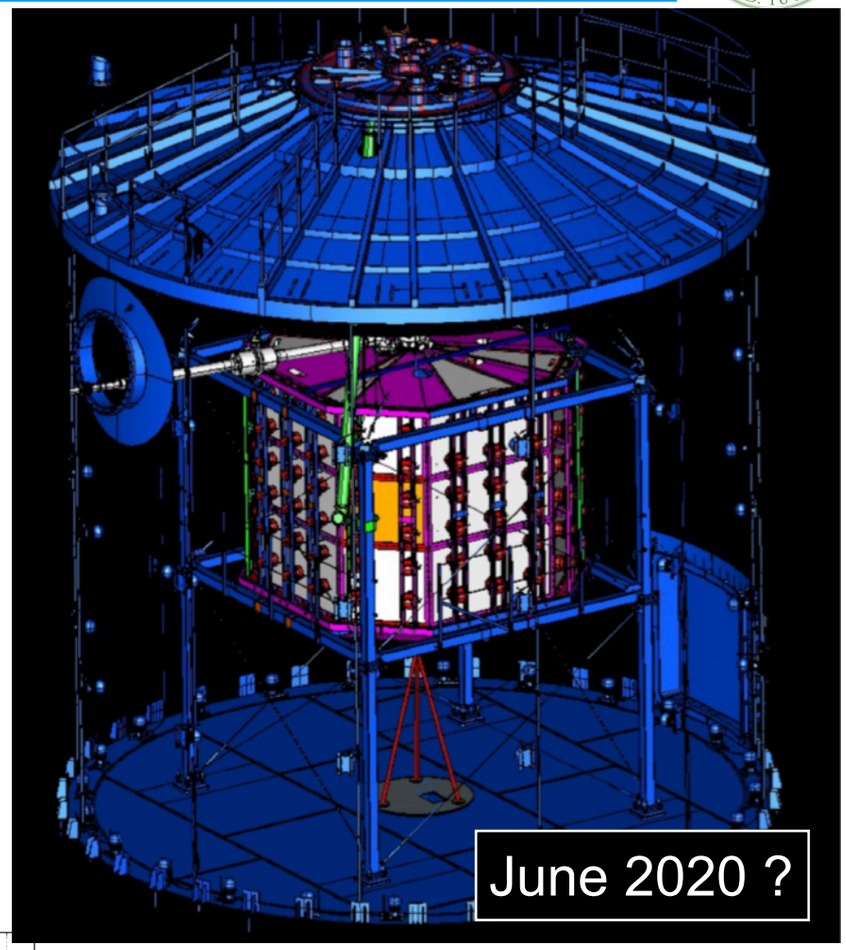

- 700 ton pure water instrumented with 84 high-QE 8'' PMTs
- Trigger efficiency > 99.5% for muons in water tank
- Cosmogenic neutron background suppressed to <0.01 events/ton/yr
- For XENONnT, 120 more PMTs, inner reflective region, and Gd-doping to reduce neutron background

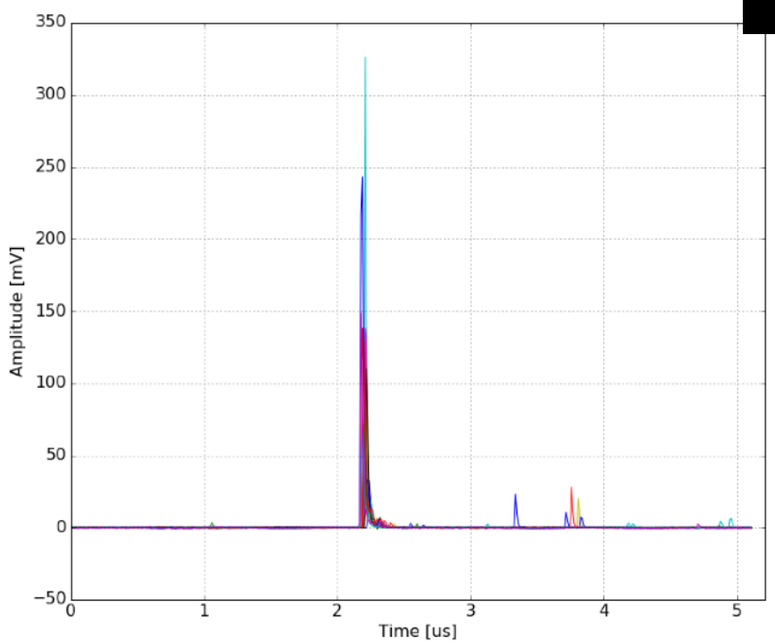

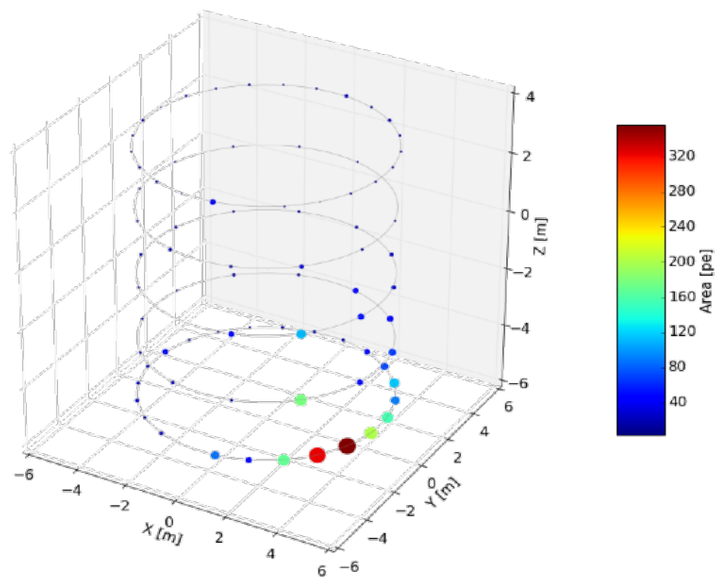

Key contribution of INFN-Bologna researcher and technical staff

JINST 9, 11007 (2014)

Summary of prev-gen LNoble results

arXiv:2104.07634

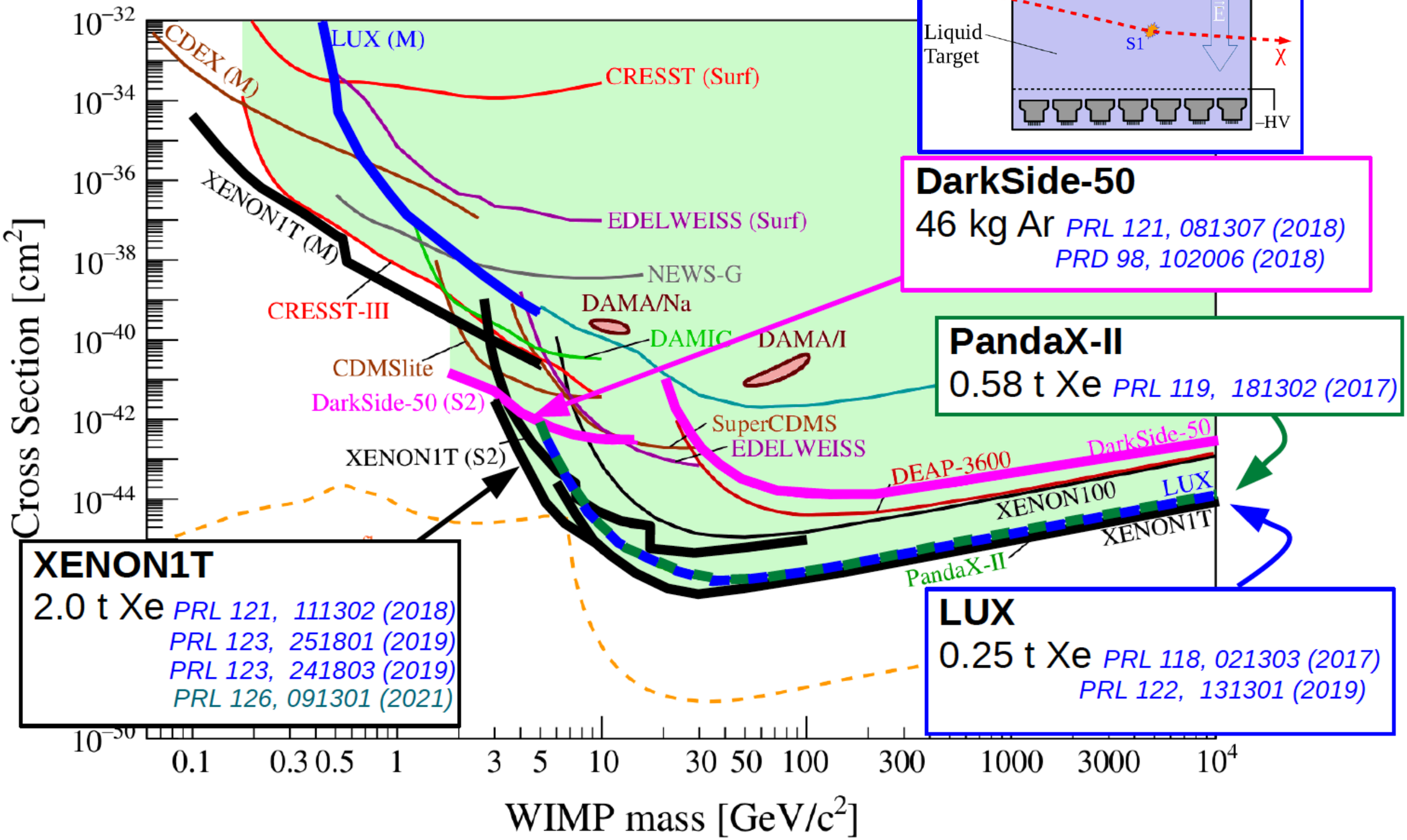

The XENON1T NR band

Detector with:

- Low background: 76 ± 2 events/t/yr/keV
- Low threshold: ~5 keV_{NR}
- Large exposure (mass, livetime): 1 tonne x year

Combination of S1 and S2 signals allow:

- Position reconstruction
- Energy reconstruction
- ER/NR discrimination

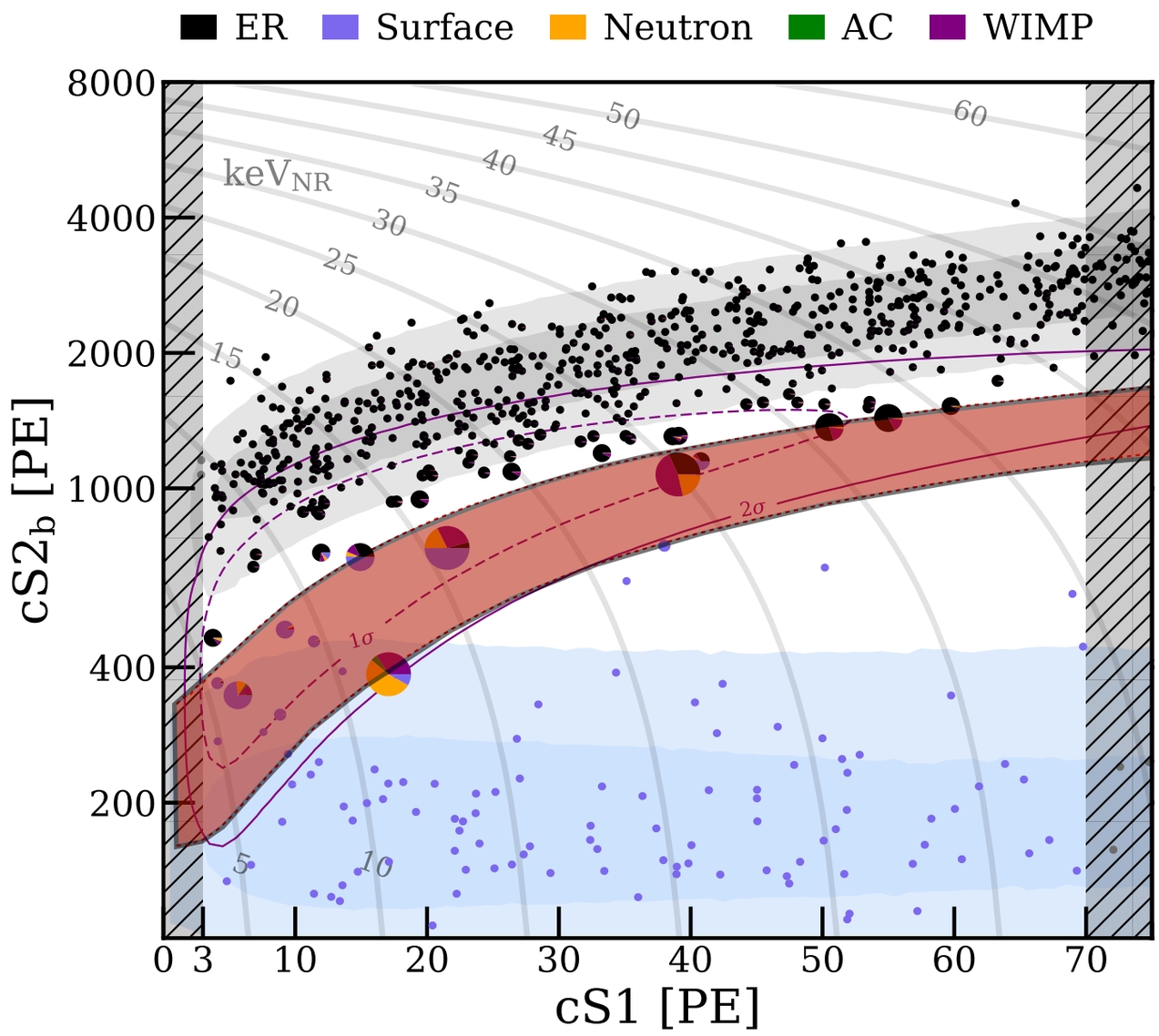

Most stringent result on WIMP Dark Matter down to 3 GeV/c² masses

[PRL 121, 111302 + PRL 123, 251801]

The XENON1T ER band

Detector with:

Low background: 76 ± 2 events/t/yr/keV

Low threshold: 1 keV_{ee}

Large exposure (mass, livetime): 1 tonne x year

Combination of S1 and S2 signals allow:

Position reconstruction

Energy reconstruction

ER/NR discrimination

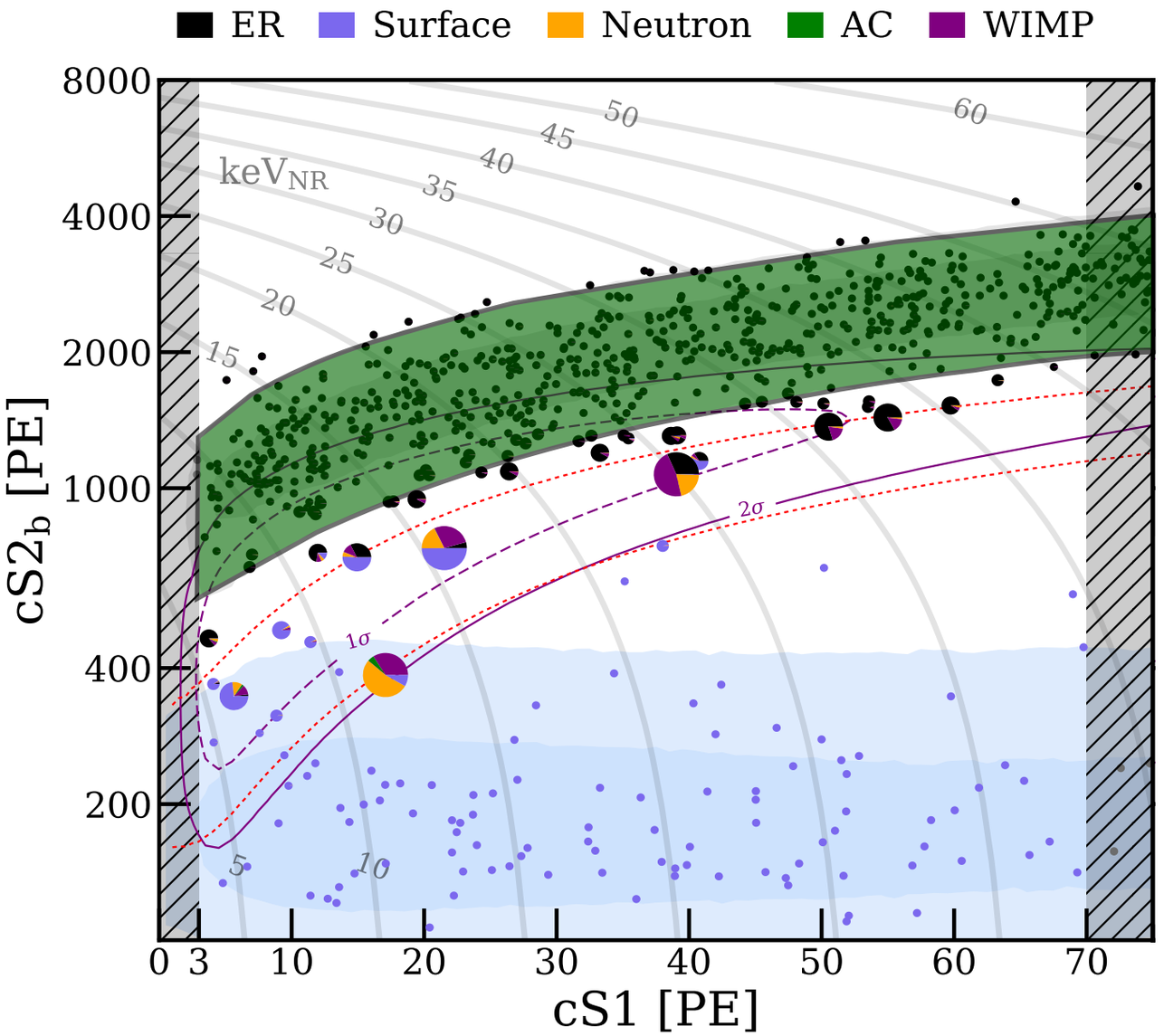

Now use ultra-low ER background to search for excesses in ER band.

The XENON1T ER excess

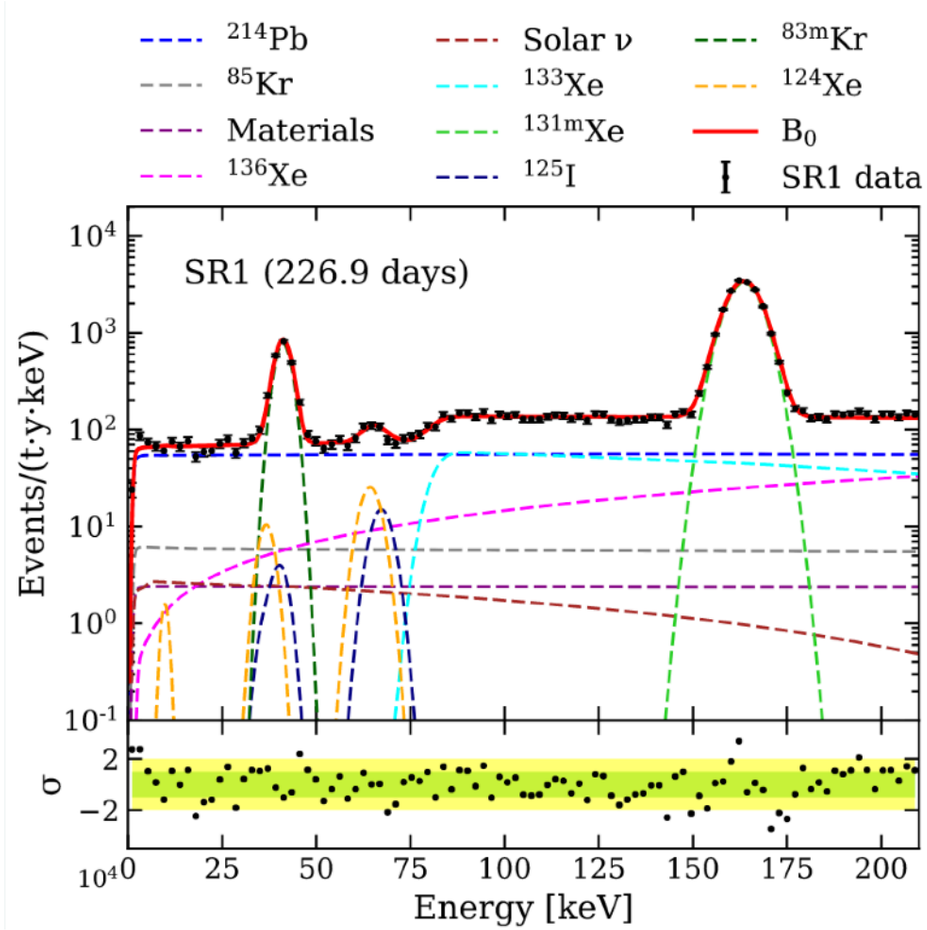

eV$_{ee}$

- **excess in 1-7 keV range**
  285 evts observed vs
  232 ± 15 expected
  → **(naive) 3.3σ fluctuation**

- events uniformly distributed
  – in space
  – in time (but low stats)

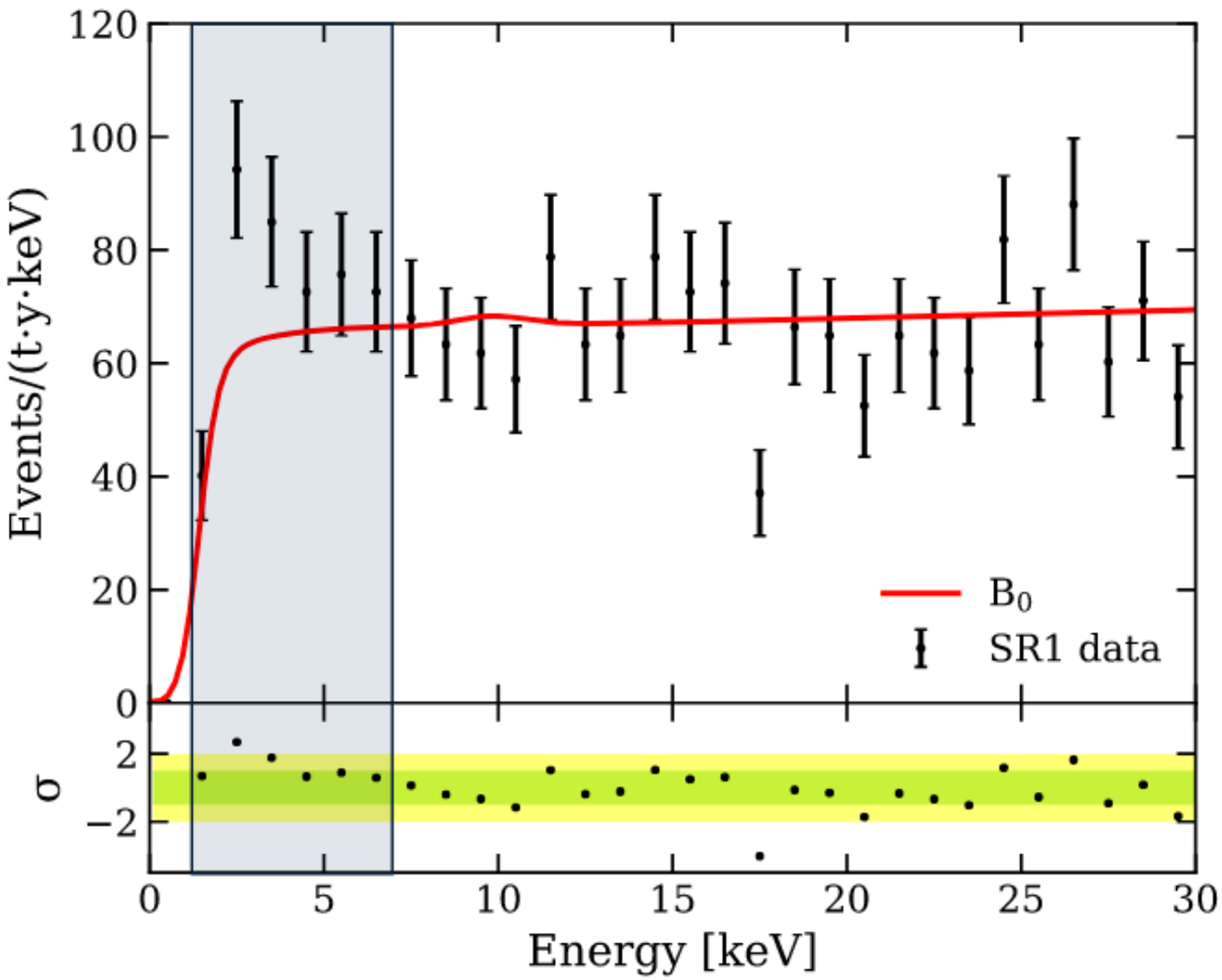

The XENON1T ER excess

Possible interpretations:

PRD 102, 072004 (2020)

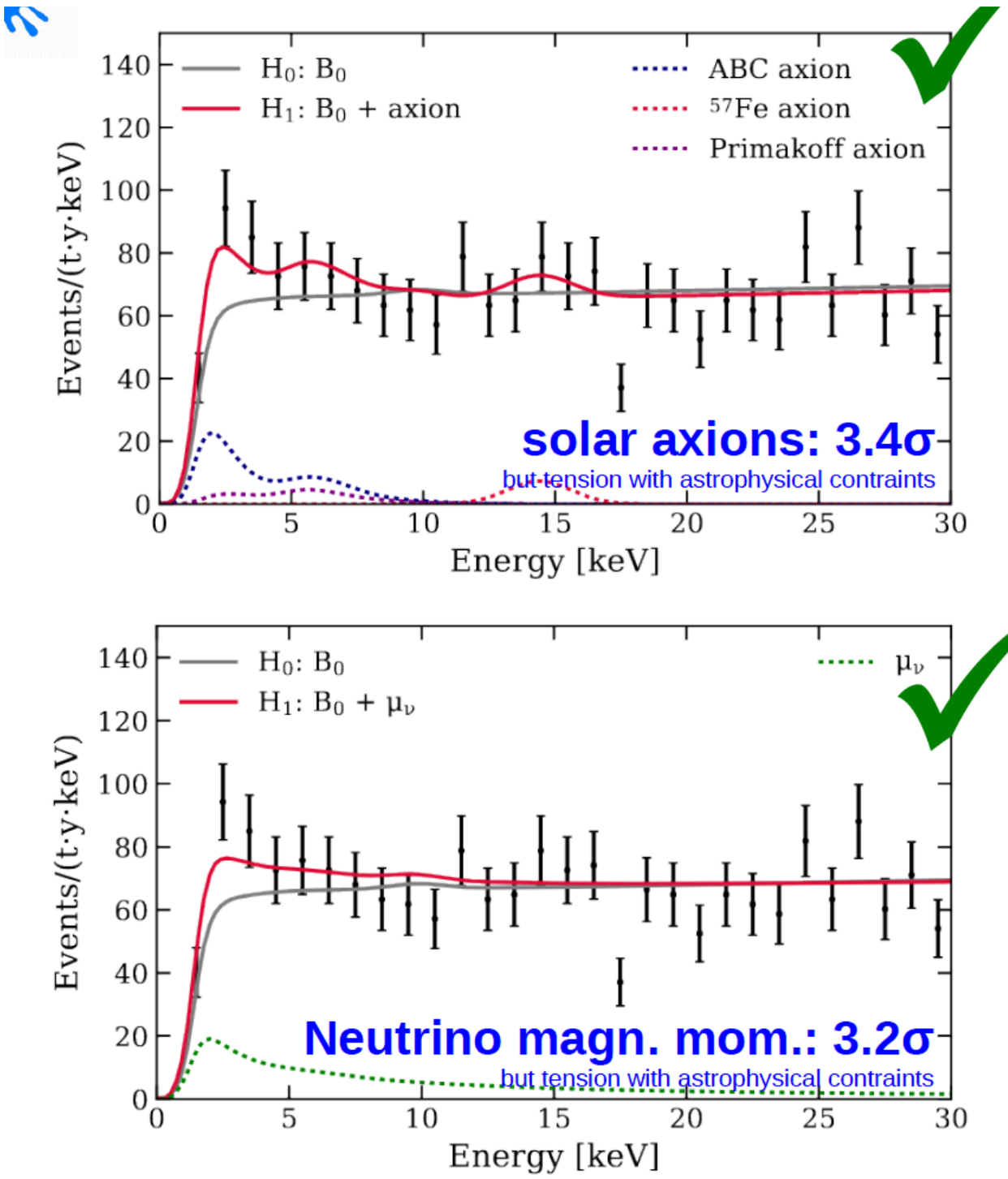

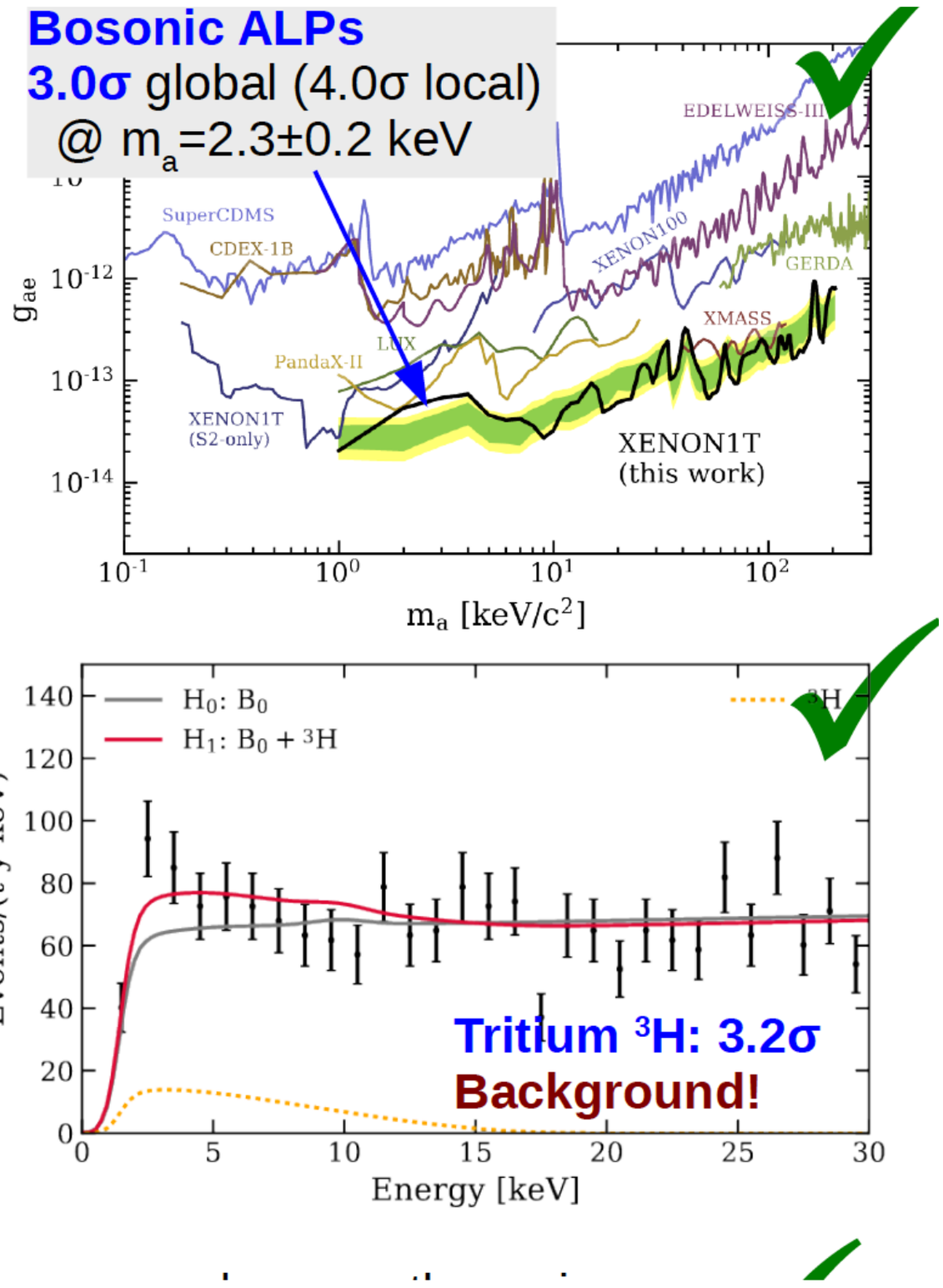

XENONnT ER results (July 2022)

Energy spectrum dominated by 2nd-order weak processes

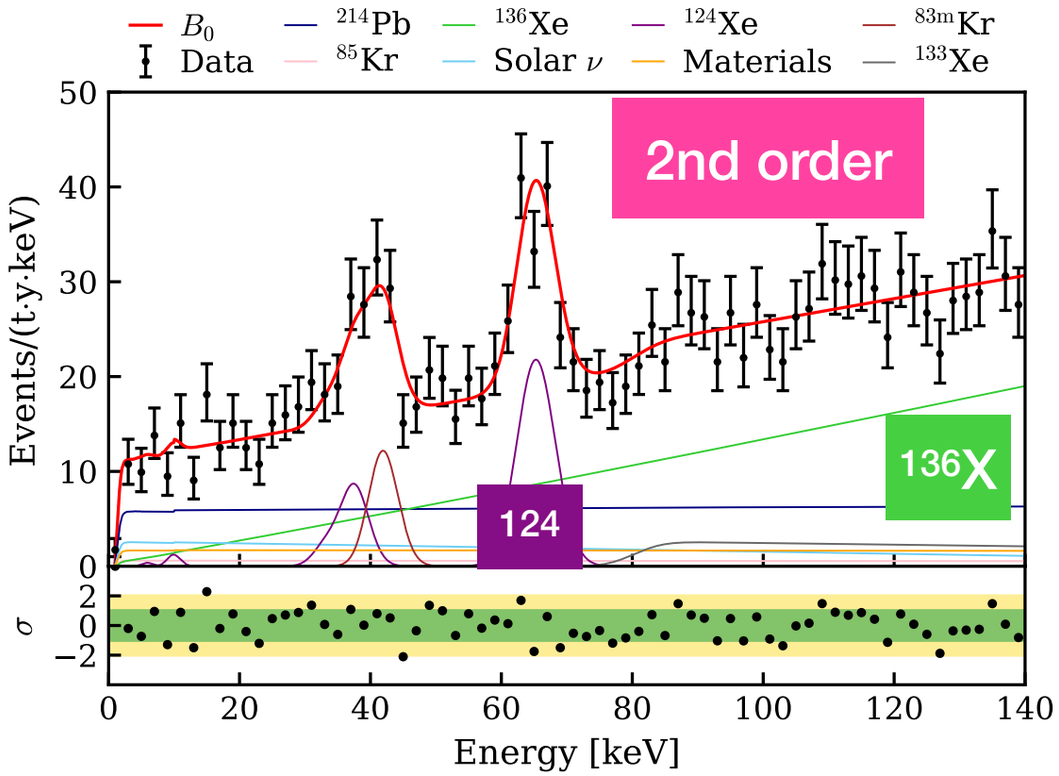

Zoom in the low-energy region: no discrepancy from the bkg model

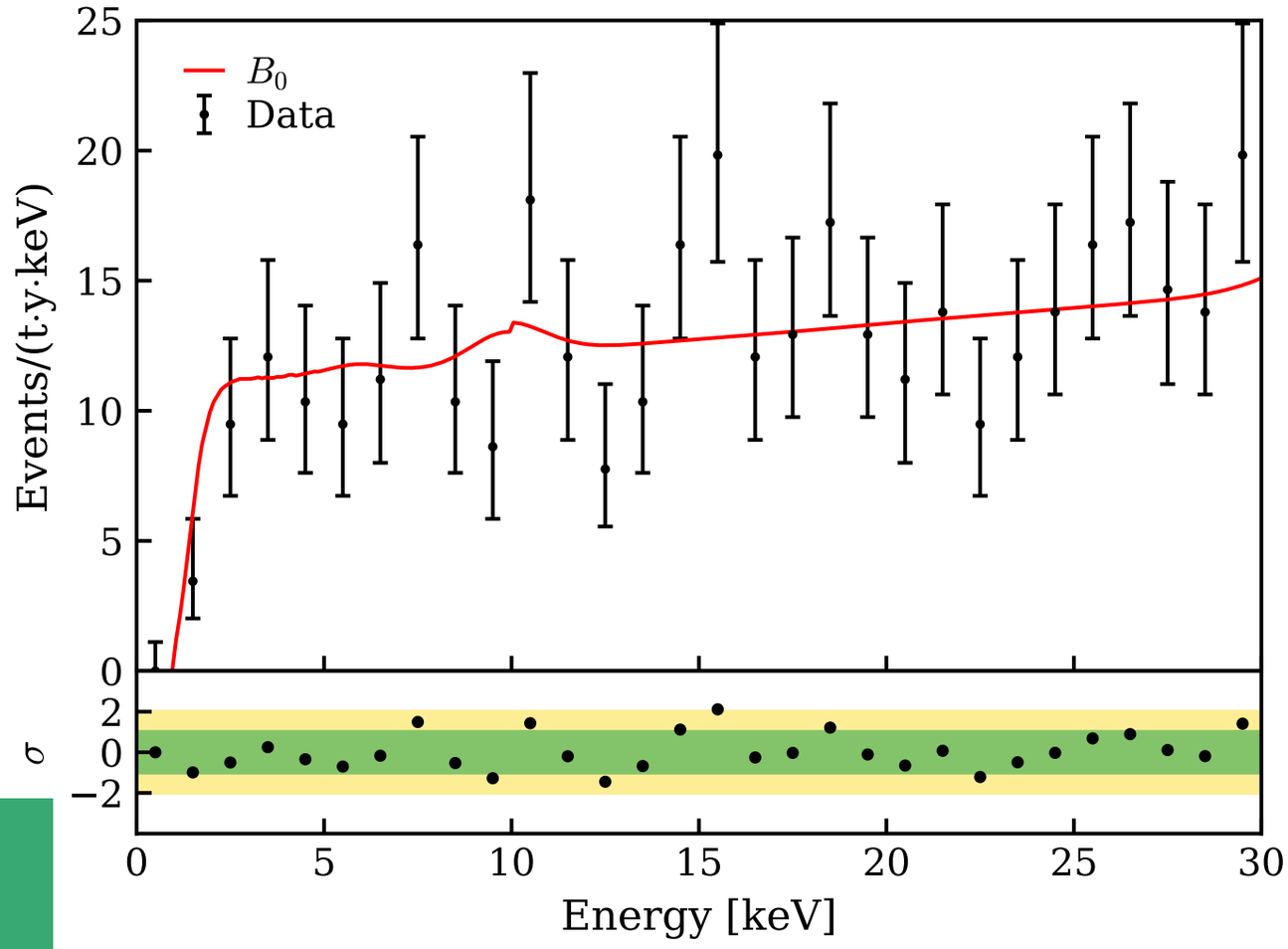

XENONnT key performances in SR0:
> 10 ms **electron lifetime,**
1.77 ± 0.01 μBq/kg **radon concentration**

arXiv:2207.11330, accepted by PRL

Excellent agreement with our background model.
Lowest ER background ever achieved in a DM experiment:
(16.1 ± 0.3) events/(t × yr × keV)

No trace of ^{3}H, even in the Tritium-enhanced run

Set new best limits on Solar Axions, ν magnetic moment, ALPs, …

Nuclear recoil data are still blinded
WIMP search results soon

LXe TPCs: present and future

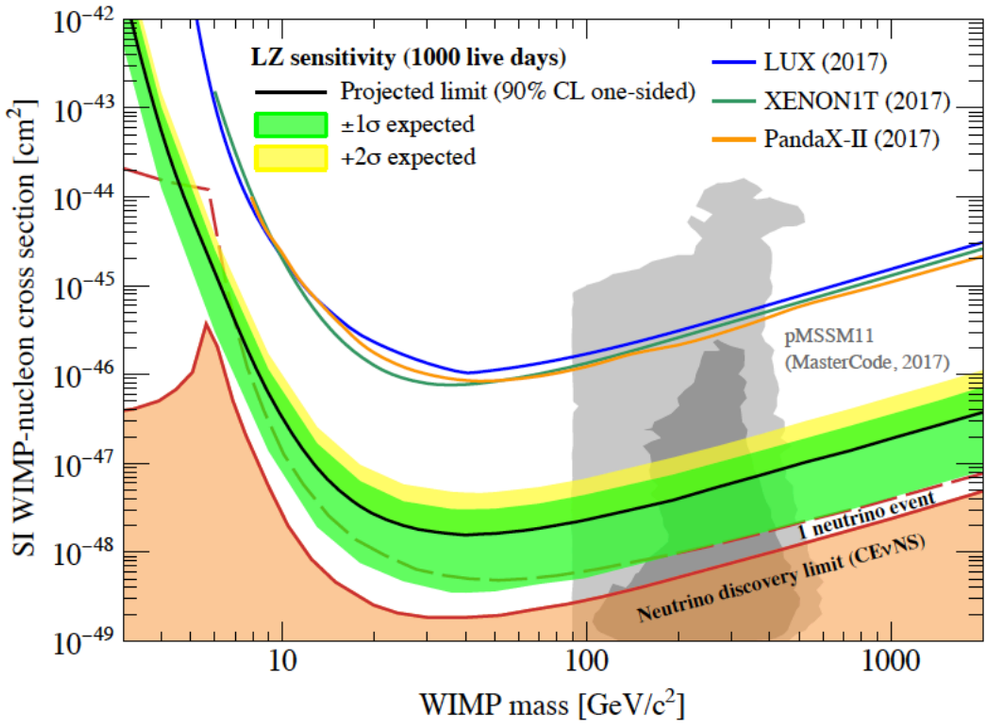

- Results from running experiments and secondary results from completed ones
- XENONnT: 2019 8t, 4t fiducial
- PandaX-4T: 2020 4t
- LZ:2020 10t, 5.6t fiducial
- DARWIN:2024 50t

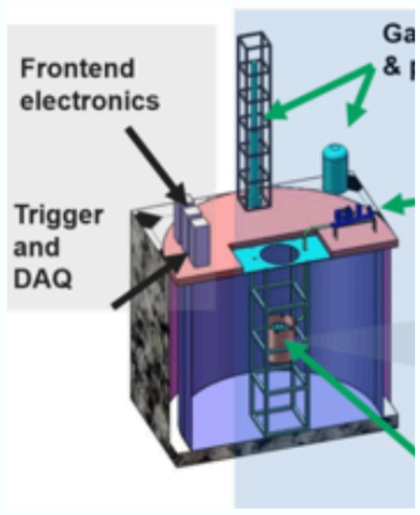

PandaX-4T

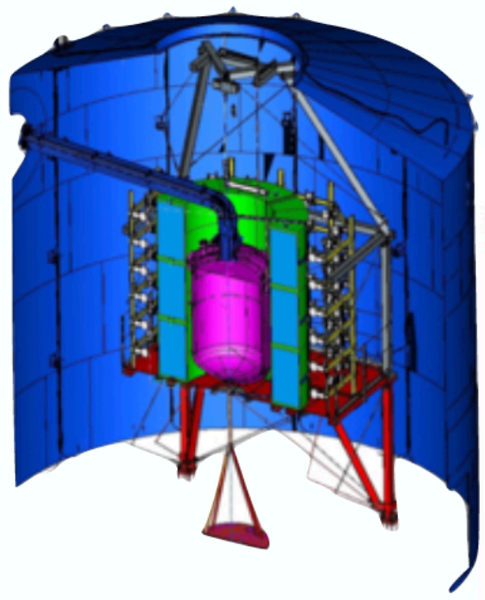

XENONnT

LZ

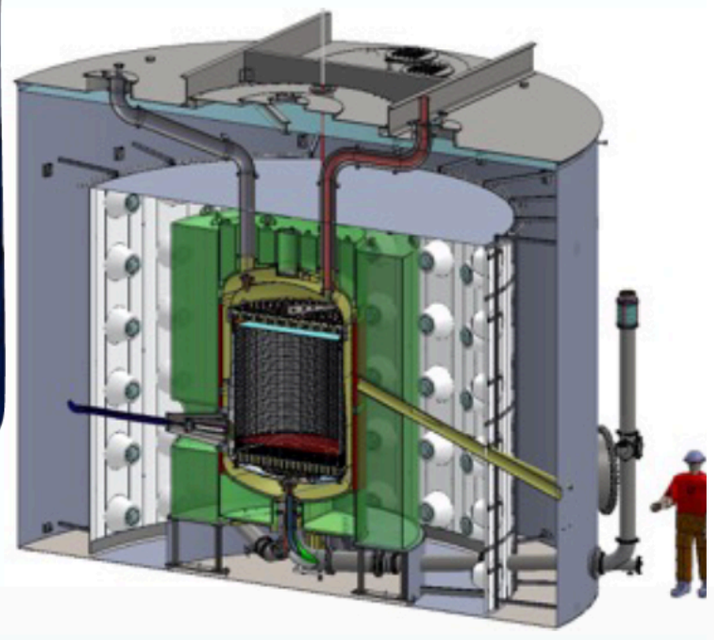

DARWIN

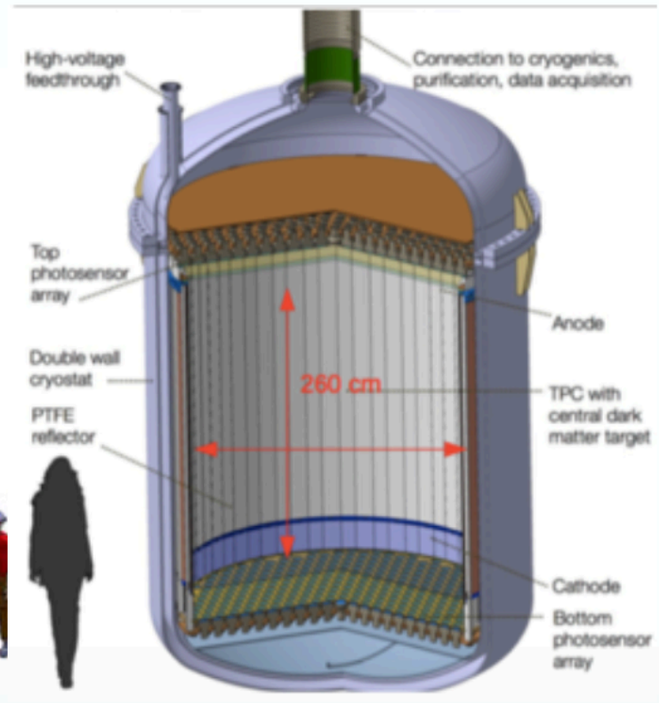

PandaX-4T

PANDA X

PARTICLE AND ASTROPHYSICAL XENON TPC

July 2021/arXiv:2107.13438

- PandaX-4T: A dual-phase Xe TPC based experiment with 3.7 tonne liquid xenon in sensitive volume (see Qing's talk)
- Ultrapure water shield: 13 m (H) x 10 m (D) ~ 900 m^3
- TPC: 1.2 m (H) x 1.2 m (D)
- 3-in PMTs: 169 top/199 bottom

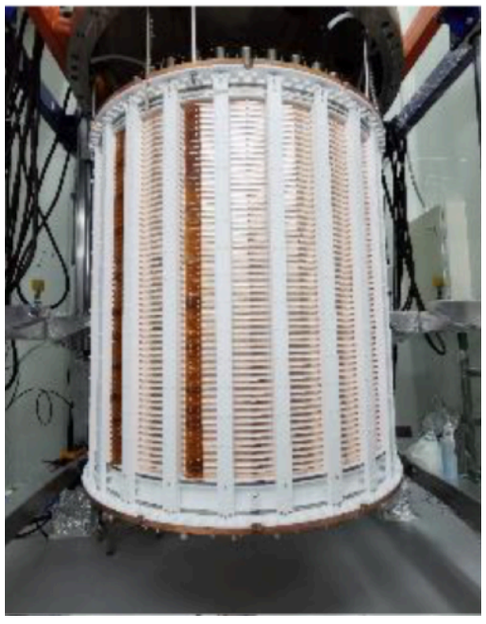

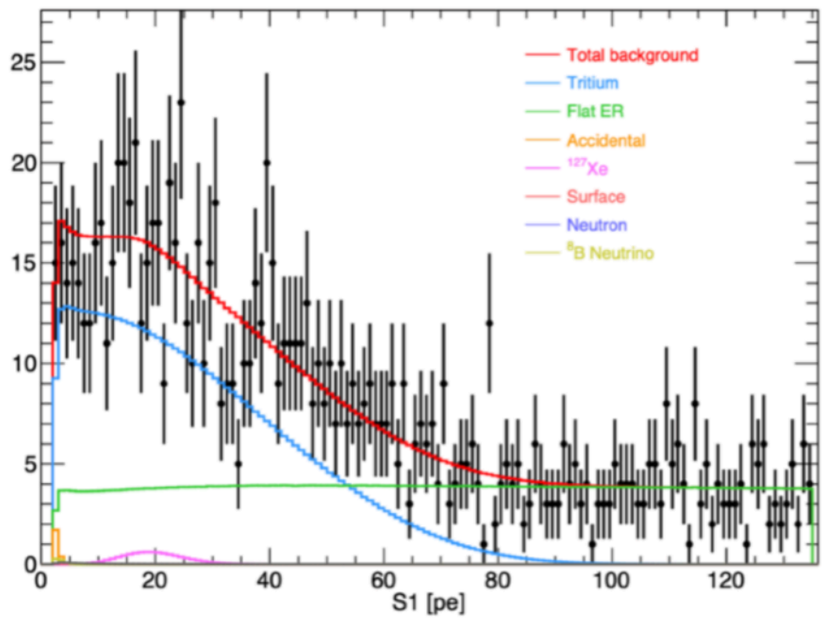

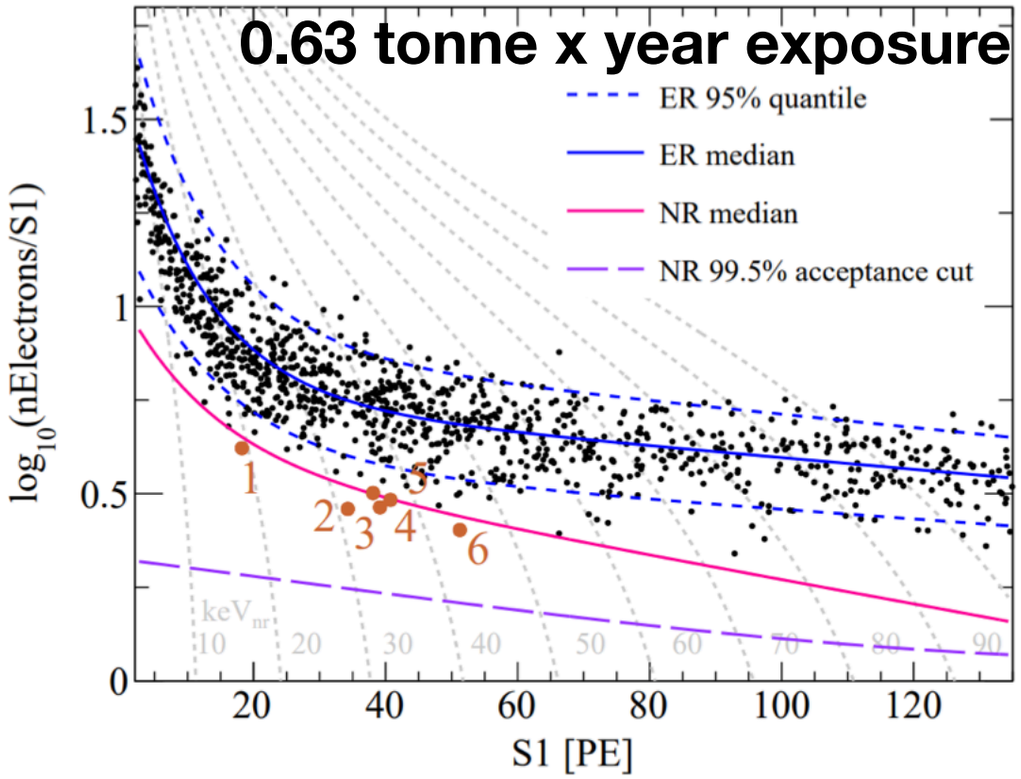

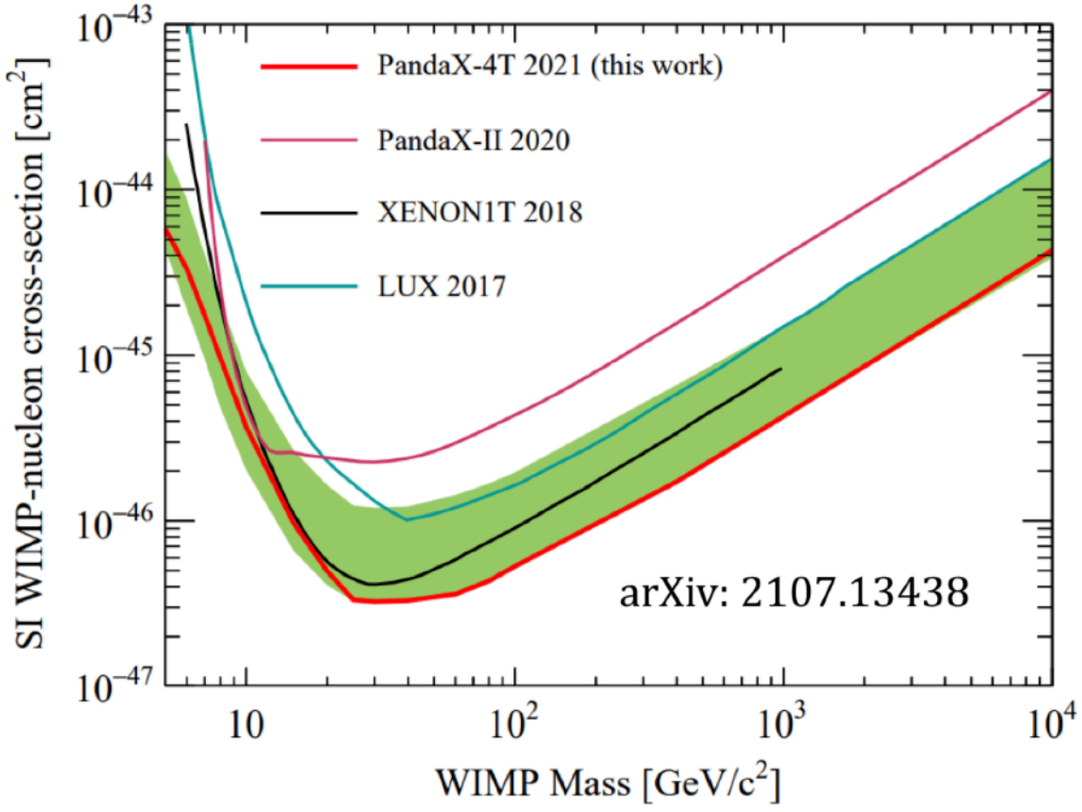

LUX-ZEPLIN

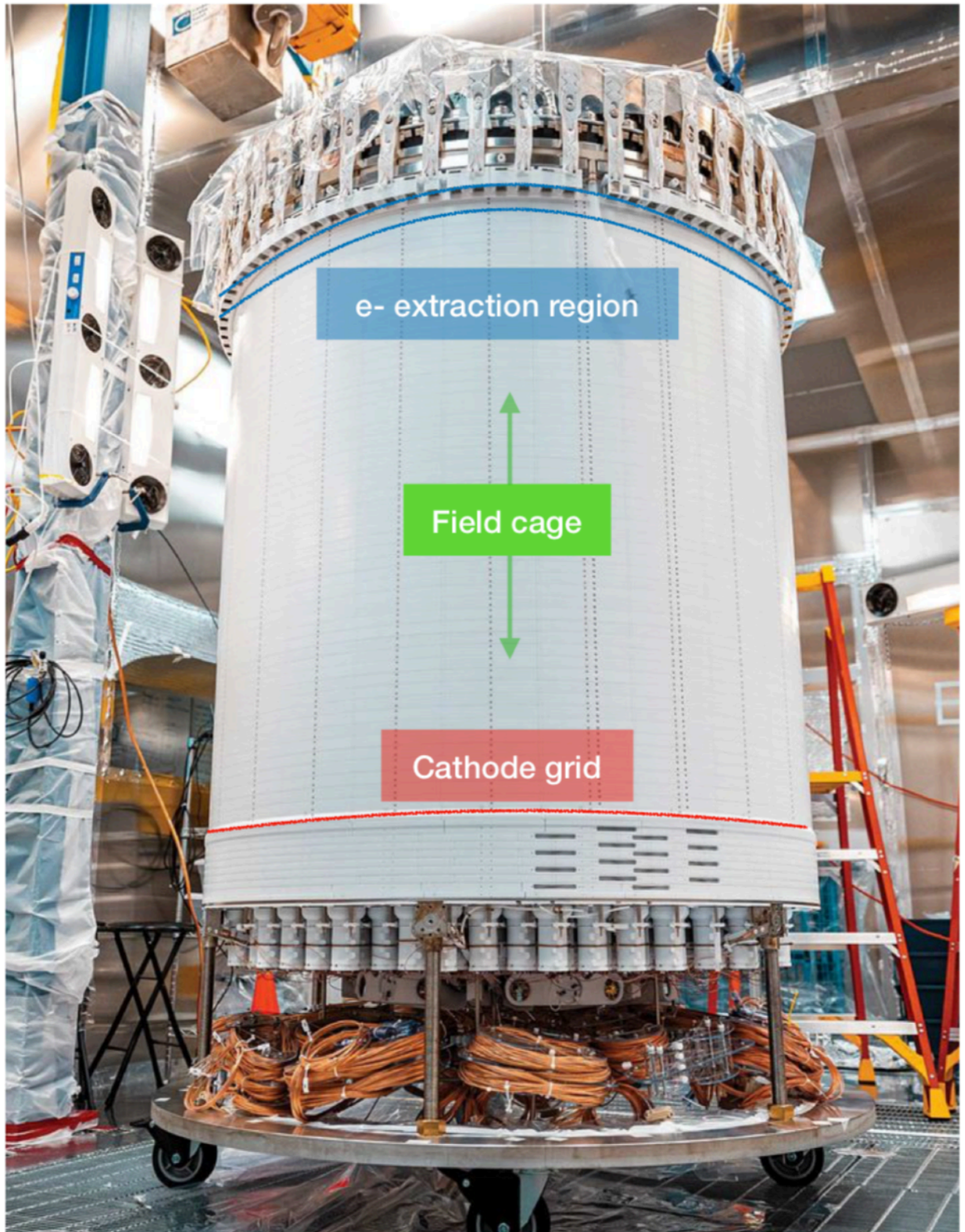

Construction in radon reduced clean room at surface assembly lab completed in 2019

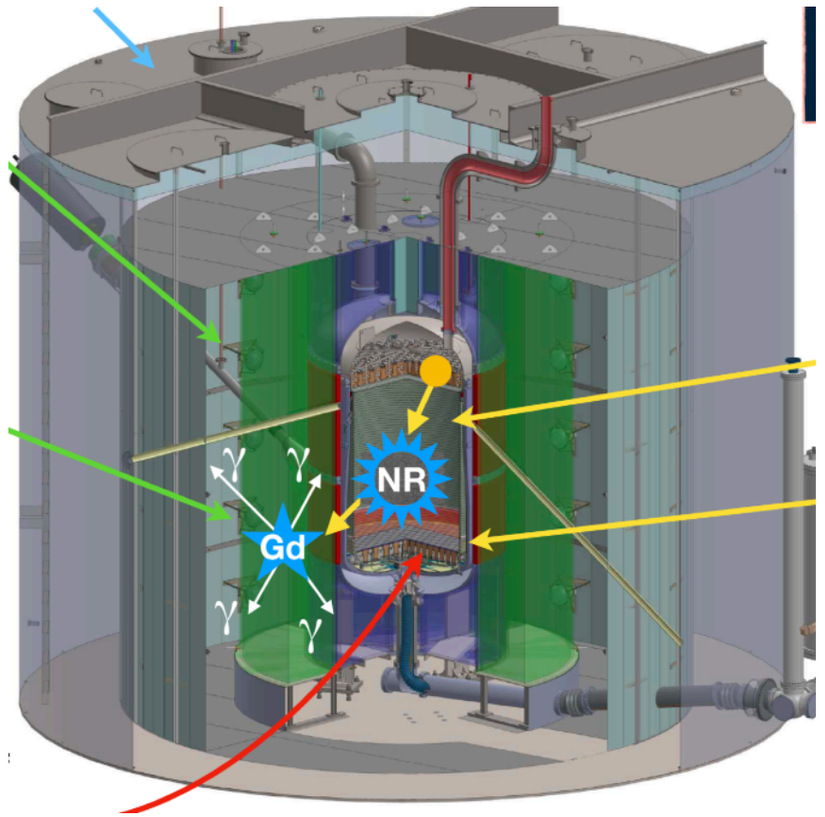

- PTFE field cage maximizes light collection efficiency.
- 494 3” PMTs in total - Hamamatsu R11410-22.
- Woven electrode grids to generate electric-field in the active xenon region (7 tonnes of LXe)
- Nominal cathode voltage of -50 kV (drift field ~ 300 V/cm)
- ~ 2 tonne instrumented skin region between the outside of the TPC and the inner wall of the cryostat vessel.
- First (not blinded) results presented in July ‘22

Recent results from LZ

- Likelihood inference region of interest
  - 3 < S1c < 80 phd
  - S2 > 645 phd (14.5 electrons)*
  - S2c < $10^{4.5}$ phd
- S2 threshold **set above salted ^{8}B & low-mass WIMP region**
- **1220 events** remain after unsalting
- **220 live days x 5.5 t = 3.3 tonne-yr**

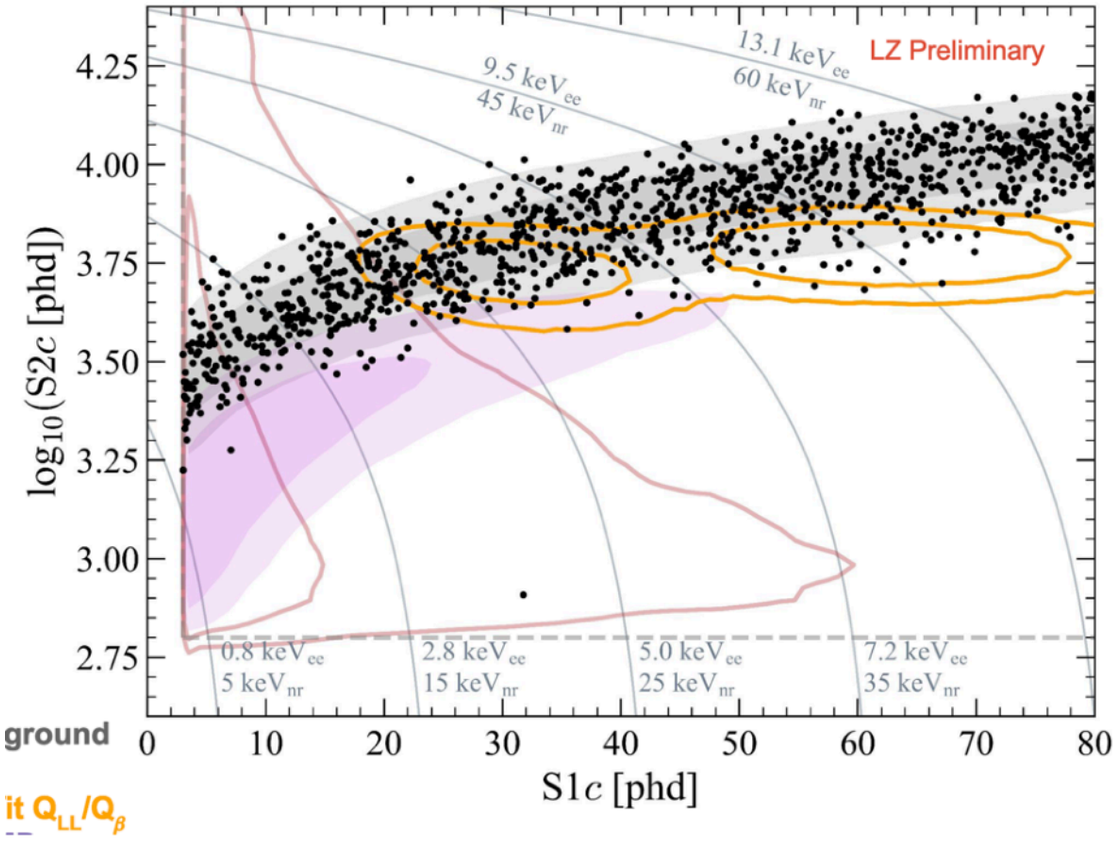

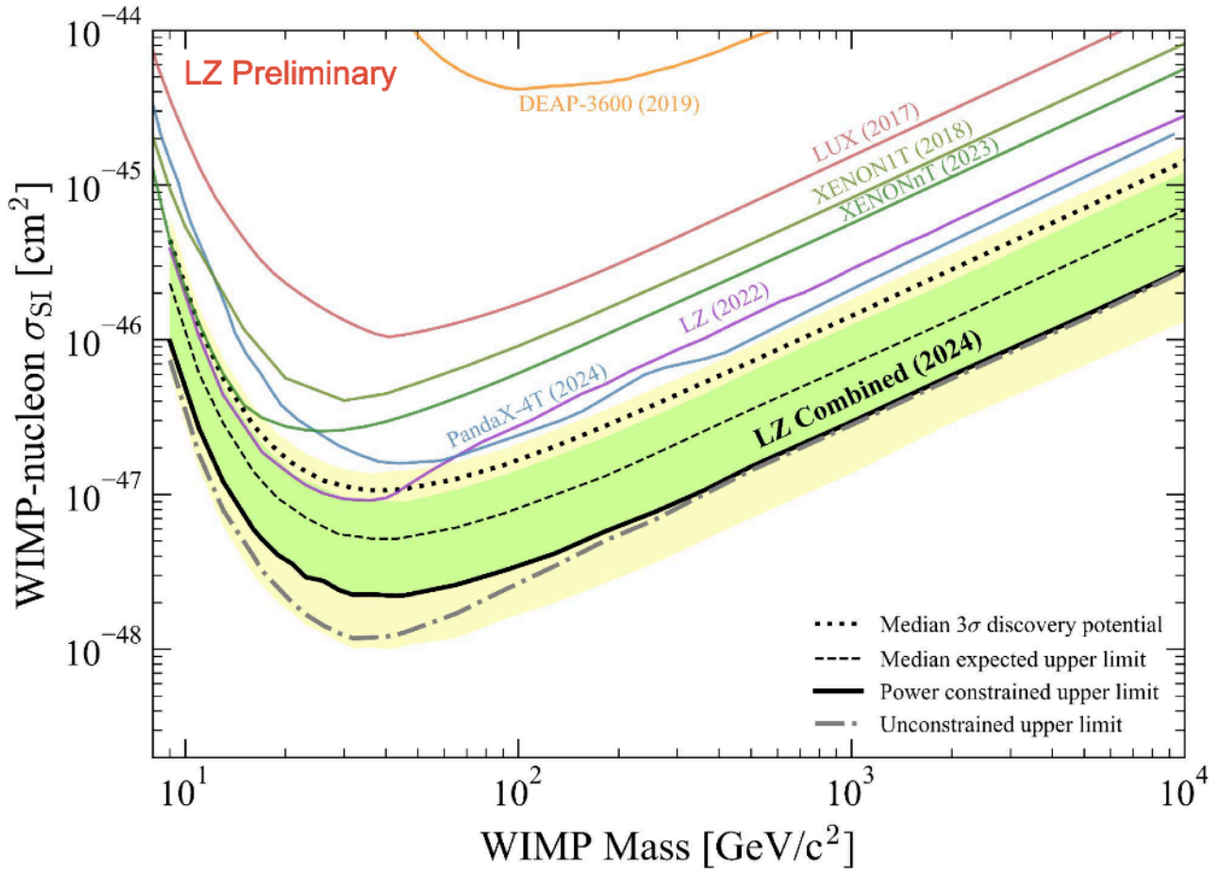

LZ: Phys. Rev. Lett. 135 (2025) 1, 011802

from XENONIT

to XENONnT

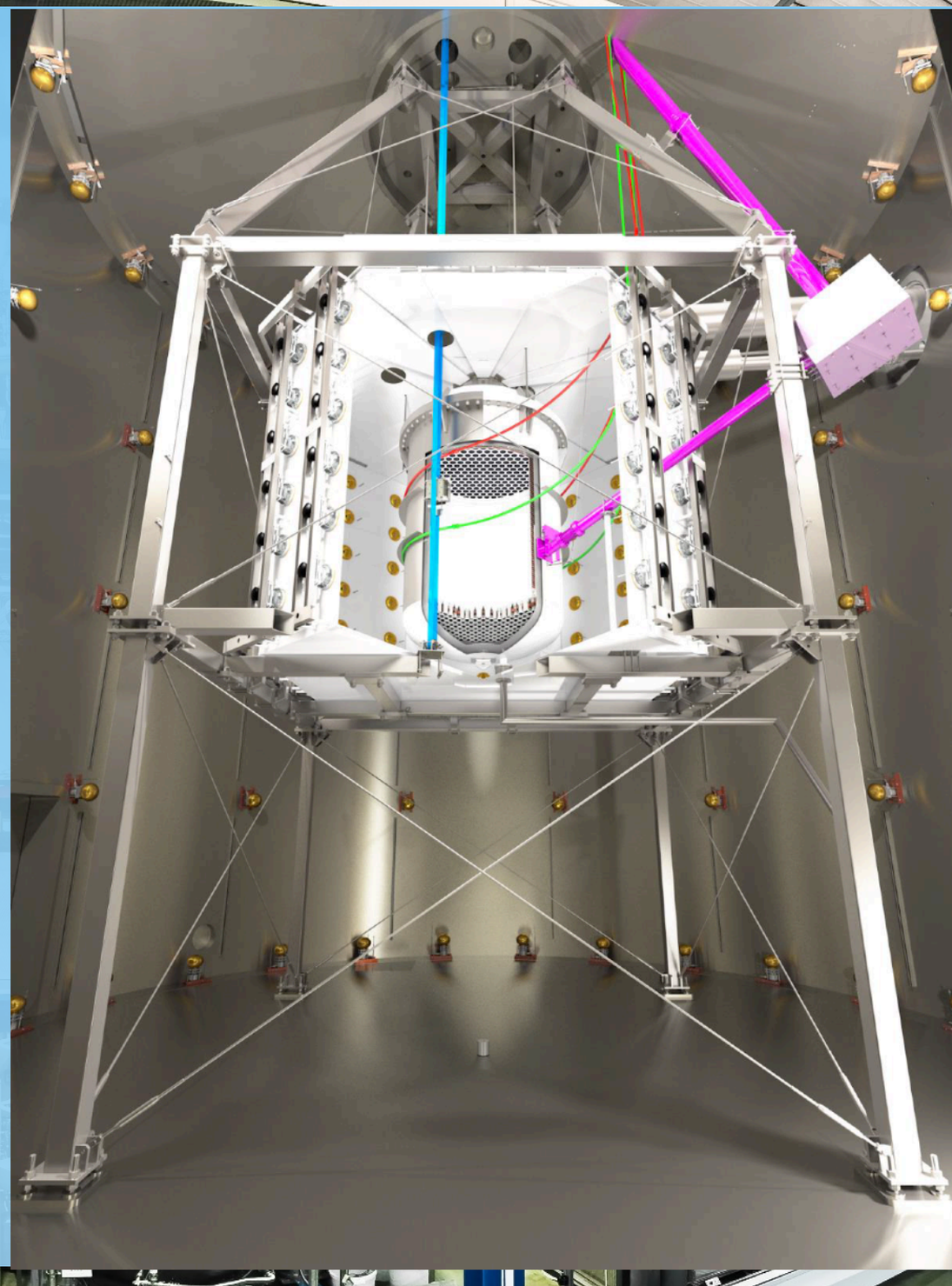

XENONnT: main upgrades

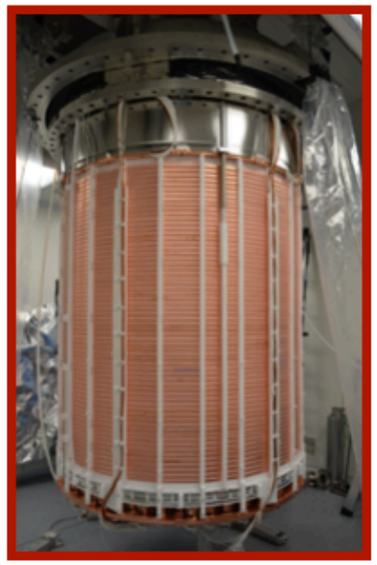

Larger TPC

- Total 8.4 t LXe
- 5.9 t in TPC
- ~ 4 t fiducial
- 248 → 494 PMTs

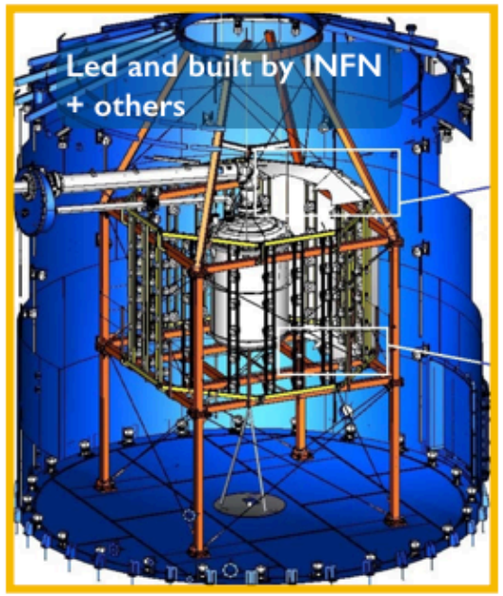

Neutron veto

- Inner region of existing muon veto
- optically separate
- 120 additional PMTs
- Gd in the water tank
- 0.5 % $Gd_2(SO_4)_3$

^{222}Rn distillation

- Reduce Rn (^{214}Pb) from pipes, cables, cryogenic system
- New system, PoP in XENON1T

LXe purification

- Faster xenon cleaning
- 5 L/min LXe (2500 slpm)
- XENON1T ~ 100 slpm

XENONnT TPC

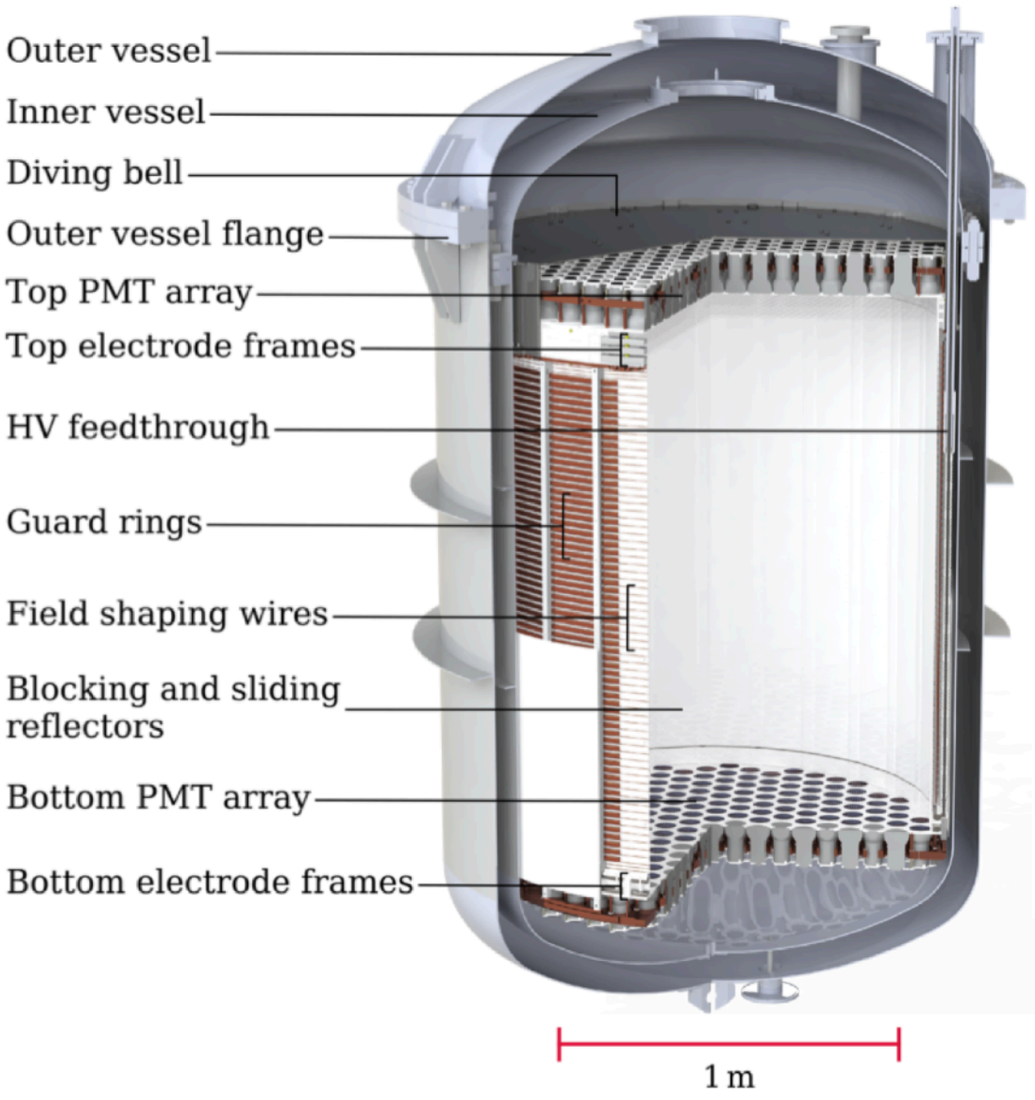

PMTs: almost all of the 494 PMTs are working very well, apart from 7.
Single PhotoElectron acceptance > 90%.

HVdrift 15 kV (100 V/cm)
Light yield larger than what obtained in XENON1T: 0.16 pe/photon.

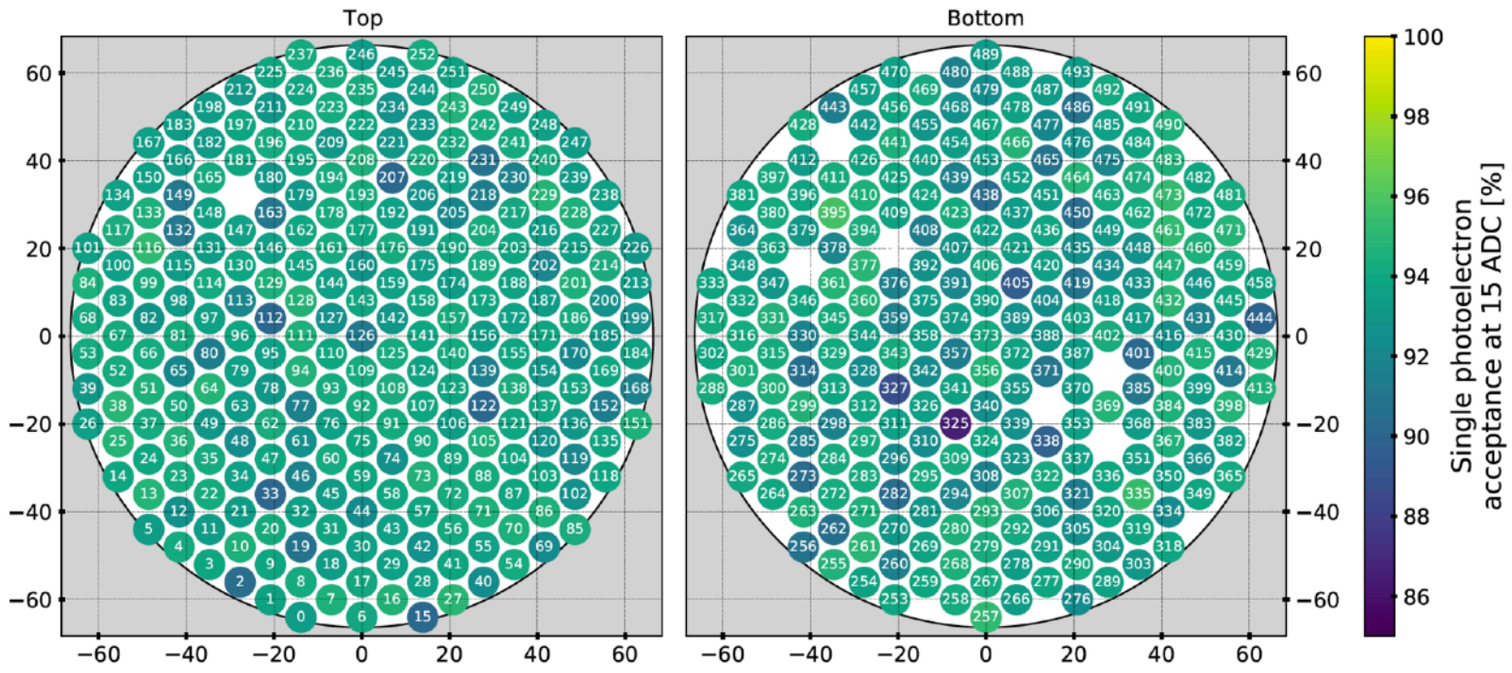

The making of the XENONnT TPC
https://www.youtube.com/watch?v=58OjXiONghU

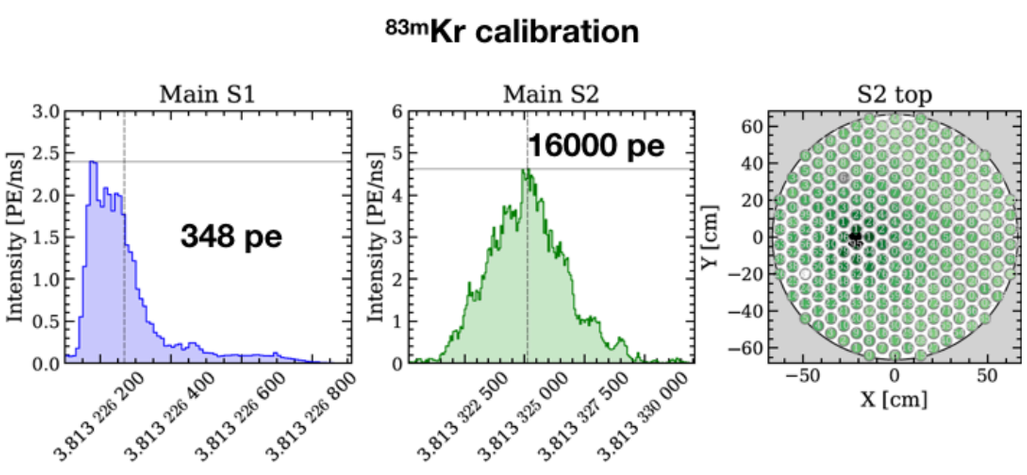

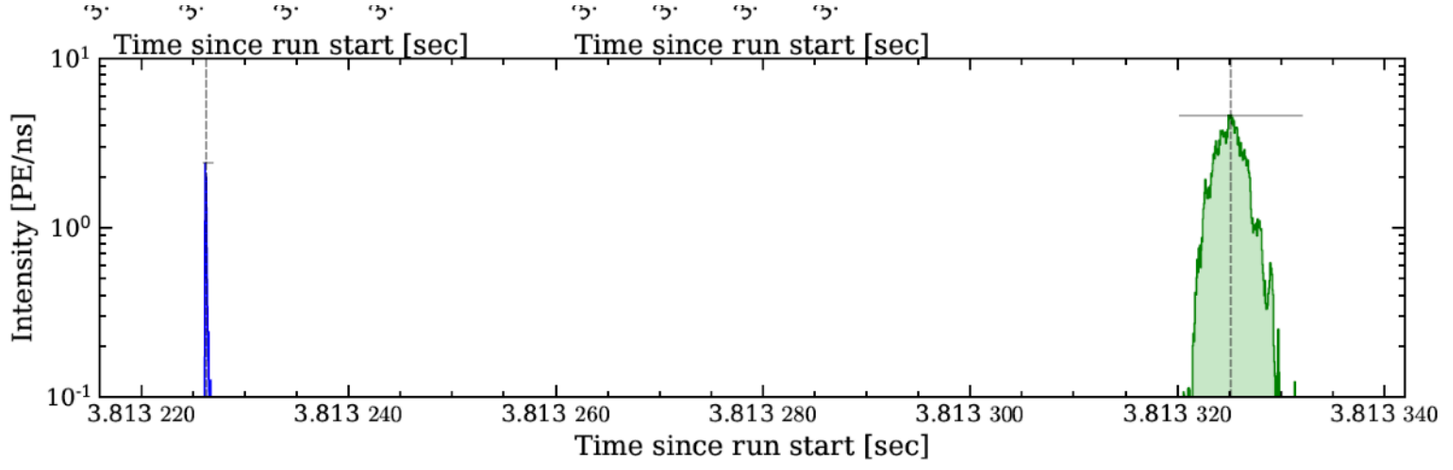

XENONnT performances: Cryogenics

Marco Selvi | selvi@bo.infn.it

Gas purification

Magnetically-coupled piston pump for high-purity gas applications

- Magnetically coupled piston pumps
- Stable performance with a flow of 100 slpm and compression of 1.5 bar

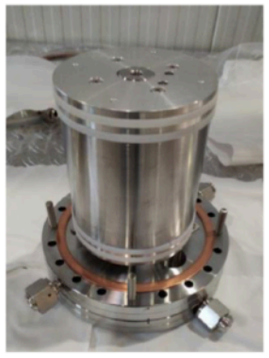

monolithic stainless-steel

Alternate polarity permanent neodymium bar magnets

Liquid purification

Liquid-phase purification for multi-tonne xenon detectors

- Novel liquid-phase purification system powered by cryogenic pumps
- Copper-impregnated spheres (Q5) for intense purification and ST707 pills filter for data taking period

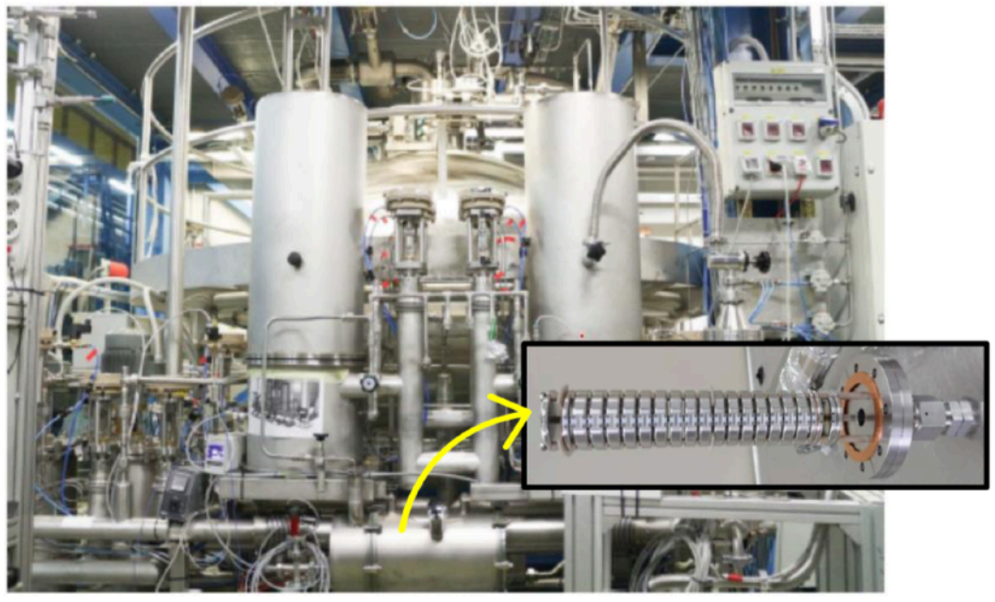

XENONnT performances: Cryogenics

Marco Selvi | selvi@bo.infn.it

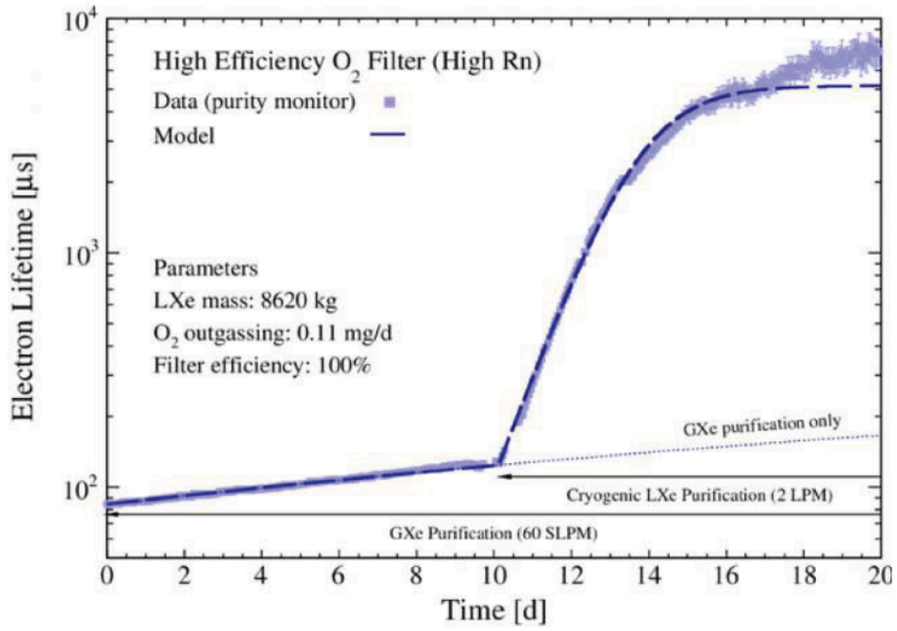

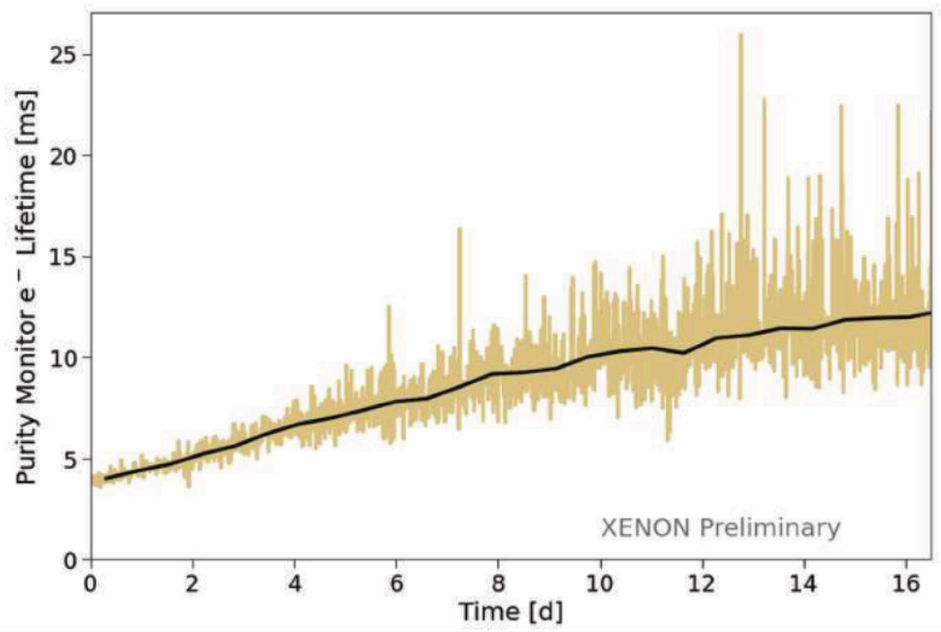

XENON1T

- 0.6 ms in SR1 ($0.9 \times \Delta t$ max)
- 1 ms after pump upgrade in SR2 ($1.4 \times \Delta t$ max)

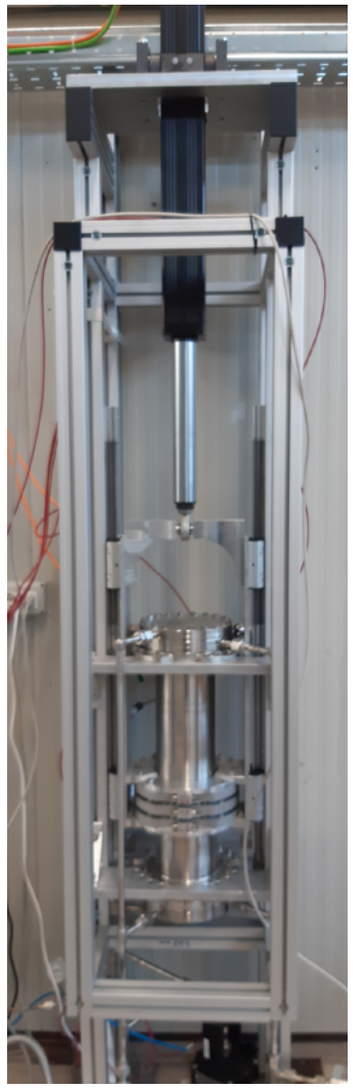

- High-flux purification (around 350 kg/h)
- Electron lifetime from 100 µs to 5 ms within 5 days (0.65 ms in XENON1T)
- e-lifetime during SR0 > 10 ms

XENONnT performances: Kr/Ar and Rn

Marco Selvi | selvi@bo.infn.it

Radon distillation

Design, construction and commissioning of a high flow radon removal system for XENONnT

- Novel distillation column to separate Rn from Xe in the gas phase thanks to its lower vapor pressure
- 1.7 μBq/kg ^{222}Rn achieved, expected further reduction to reach XENONnT goal of 1 μBq/kg

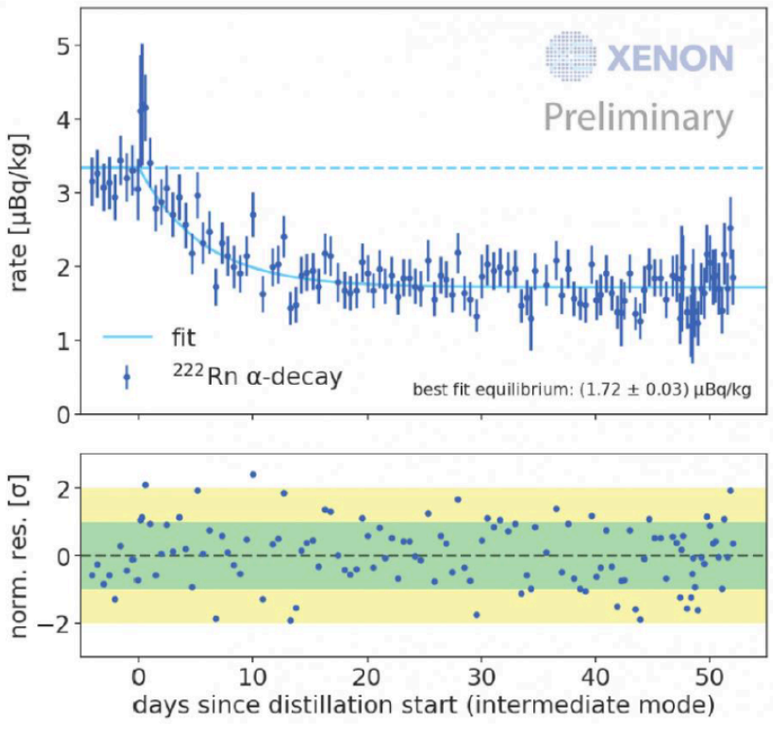

Krypton distillation

Application and modeling of an online distillation method to reduce krypton and argon in XENON1T

- Kr/Ar distillation based on their higher vapor pressure compared to Xe at -96 °C (goal 100 ppq)
- Inherited from XENON1T

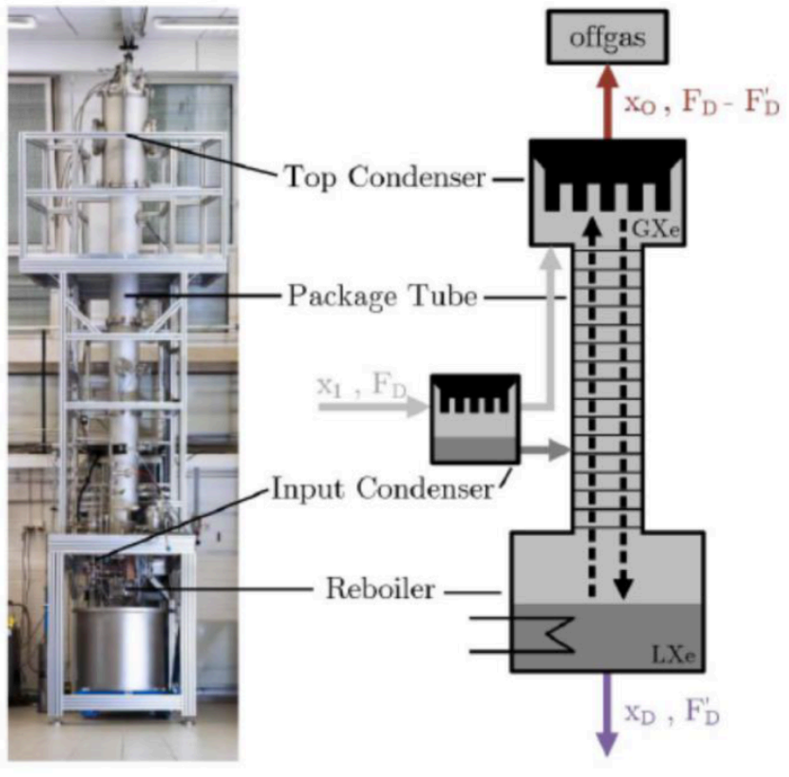

XENONnT Rn distillation

Key performance parameter

- liquid xenon inlet and outlet
- flow of 0.4 l/min LXe = 200 SLPM ≈ 70 kg/h
- radon reduction of factor 2 for sources within detector
- further reduction by gas extraction from cryogenics

Basic removal concept proven: EPJ C77 (2017) 358, arXiv:2009.13981

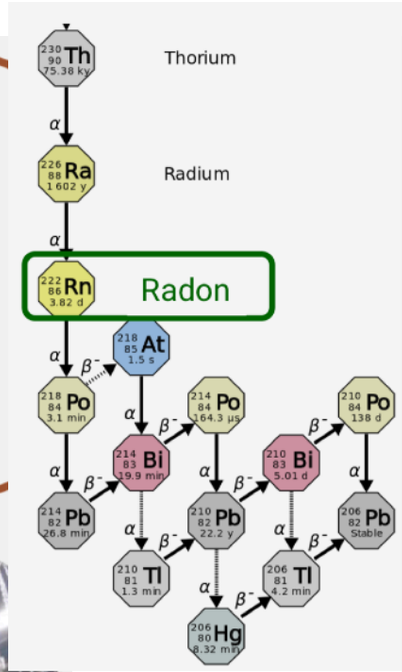

NEW RADON REMOVAL SYSTEM

ER background reduction

- Dedicated Rn cryogenic distillation column
- 1 μBq/kg ^{222}Rn level (goal)
- In XENON1T was
  13 μBq/kg (science run)
  4.5 μBq/kg (latest R&D run)

Expectation from radon emanation (J. Palacio T45.5) and radon removal system parameters

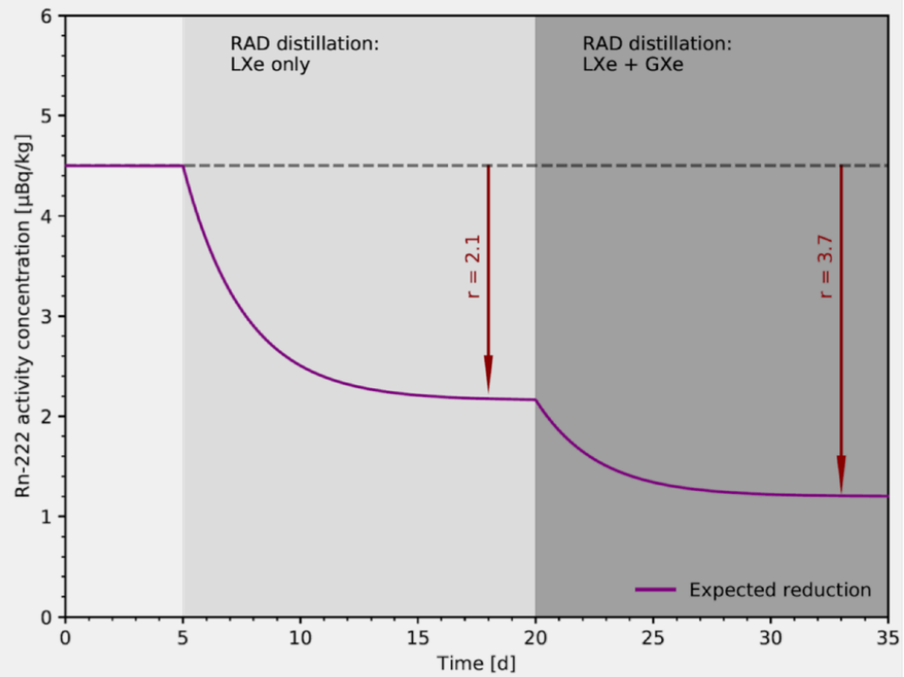

ER: Rn removal -> solar pp neutrinos

Marco Selvi | selvi@bo.infn.it

Radon Removal in XENONnT down to the Solar Neutrino Level, arXiv:2502.04209, accepted by PRX

The XENONnT experiment has achieved an unprecedented reduction of the ^{222}Rn activity concentration within its liquid xenon dual-phase time projection chamber to a level of $(0.90 \pm 0.01\,\text{stat.} \pm 0.07\,\text{sys.})\,\mu\text{Bq}\,\text{kg}^{-1}$, equivalent to about 1200 ^{222}Rn atoms per cubic meter of liquid xenon. This represents a 15-fold improvement over the ^{222}Rn levels encountered during XENON1T's main science runs and is a factor five lower compared to other currently operational multi-tonne liquid xenon detectors engaged in dark matter searches. This breakthrough enables the pursuit of various rare event searches that lie beyond the confines of the standard model of particle physics, with world-leading sensitivity. The ultra-low ^{222}Rn levels have diminished the radon-induced background rate in the detector to a point where it is for the first time lower than the solar neutrino-induced background, which is poised to become the primary irreducible background in liquid xenon-based detectors.

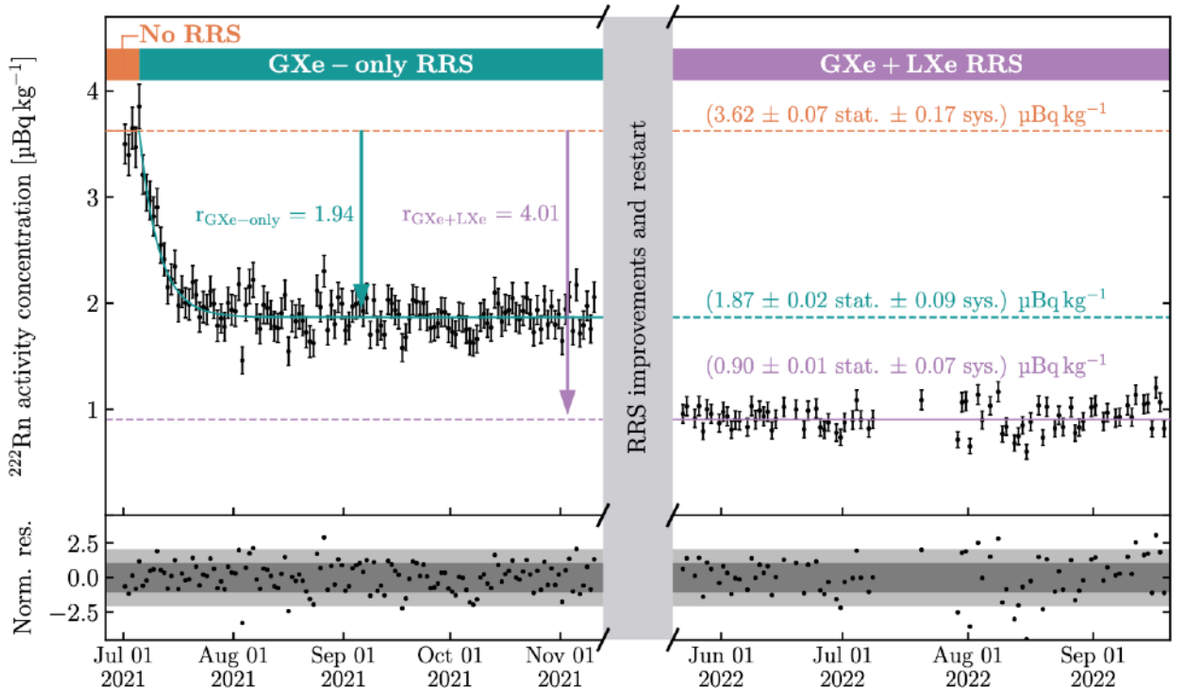

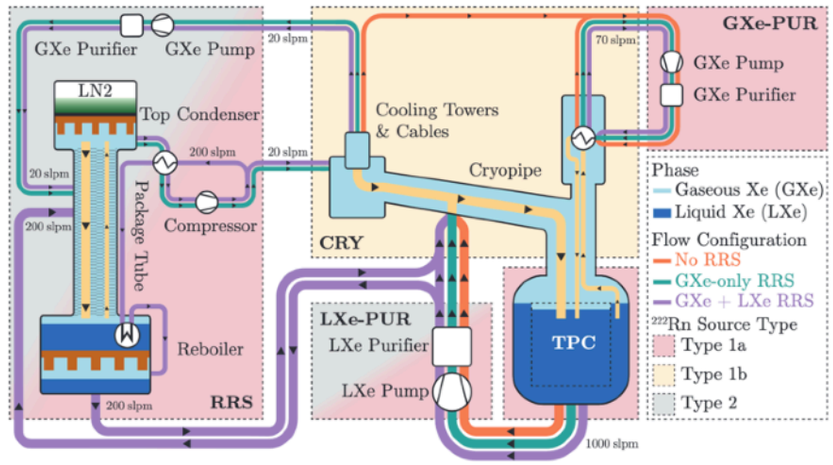

ER: Rn removal -> solar pp neutrinos

Marco Selvi | selvi@bo.infn.it

Radon Removal in XENONnT down to the Solar Neutrino Level, arXiv:2502.04209, accepted by PRX

The XENONnT experiment has achieved an unprecedented reduction of the ^{222}Rn activity concentration within its liquid xenon dual-phase time projection chamber to a level of $(0.90 \pm 0.01\,\text{stat.} \pm 0.07\,\text{sys.})\,\mu\text{Bq}\,\text{kg}^{-1}$, equivalent to about 1200 ^{222}Rn atoms per cubic meter of liquid xenon. This represents a 15-fold improvement over the ^{222}Rn levels encountered during XENON1T's main science runs and is a factor five lower compared to other currently operational multi-tonne liquid xenon detectors engaged in dark matter searches. This breakthrough enables the pursuit of various rare event searches that lie beyond the confines of the standard model of particle physics, with world-leading sensitivity. The ultra-low ^{222}Rn levels have diminished the radon-induced background rate in the detector to a point where it is for the first time lower than the solar neutrino-induced background, which is poised to become the primary irreducible background in liquid xenon-based detectors.

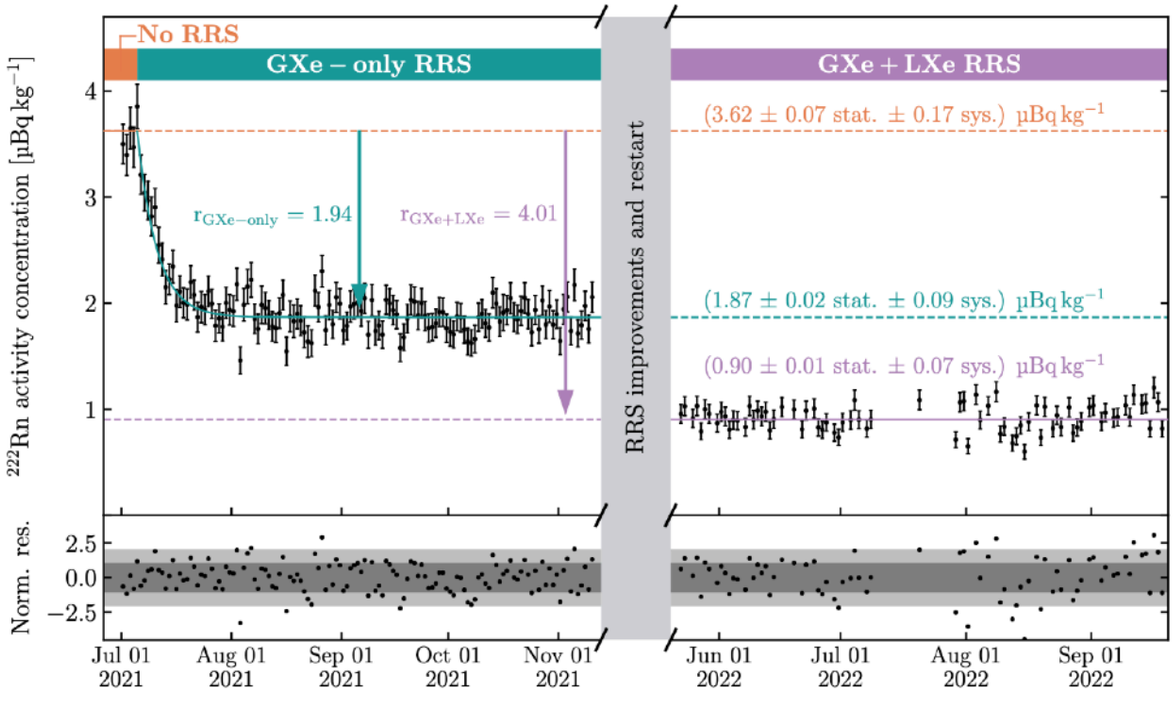

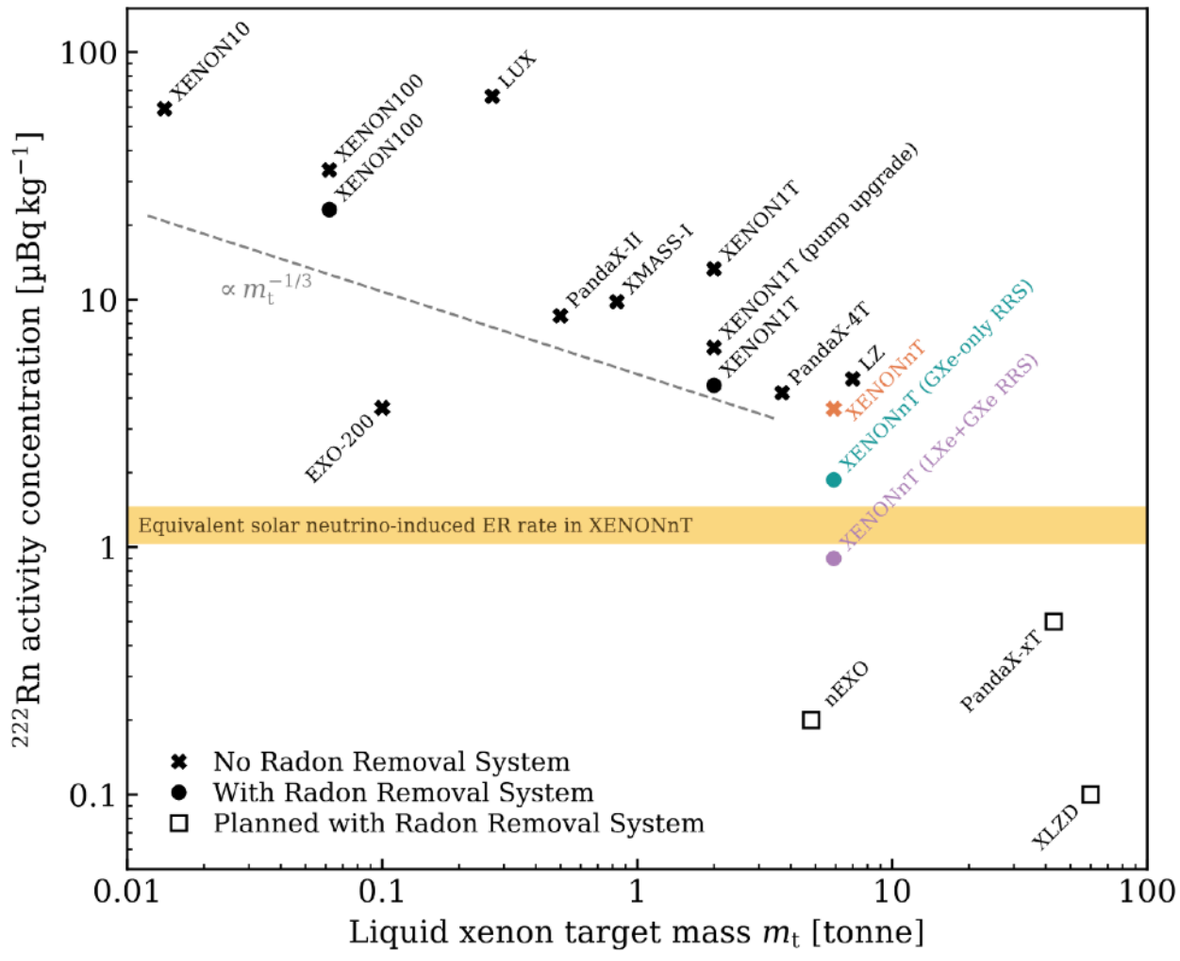

XENONnT nVeto

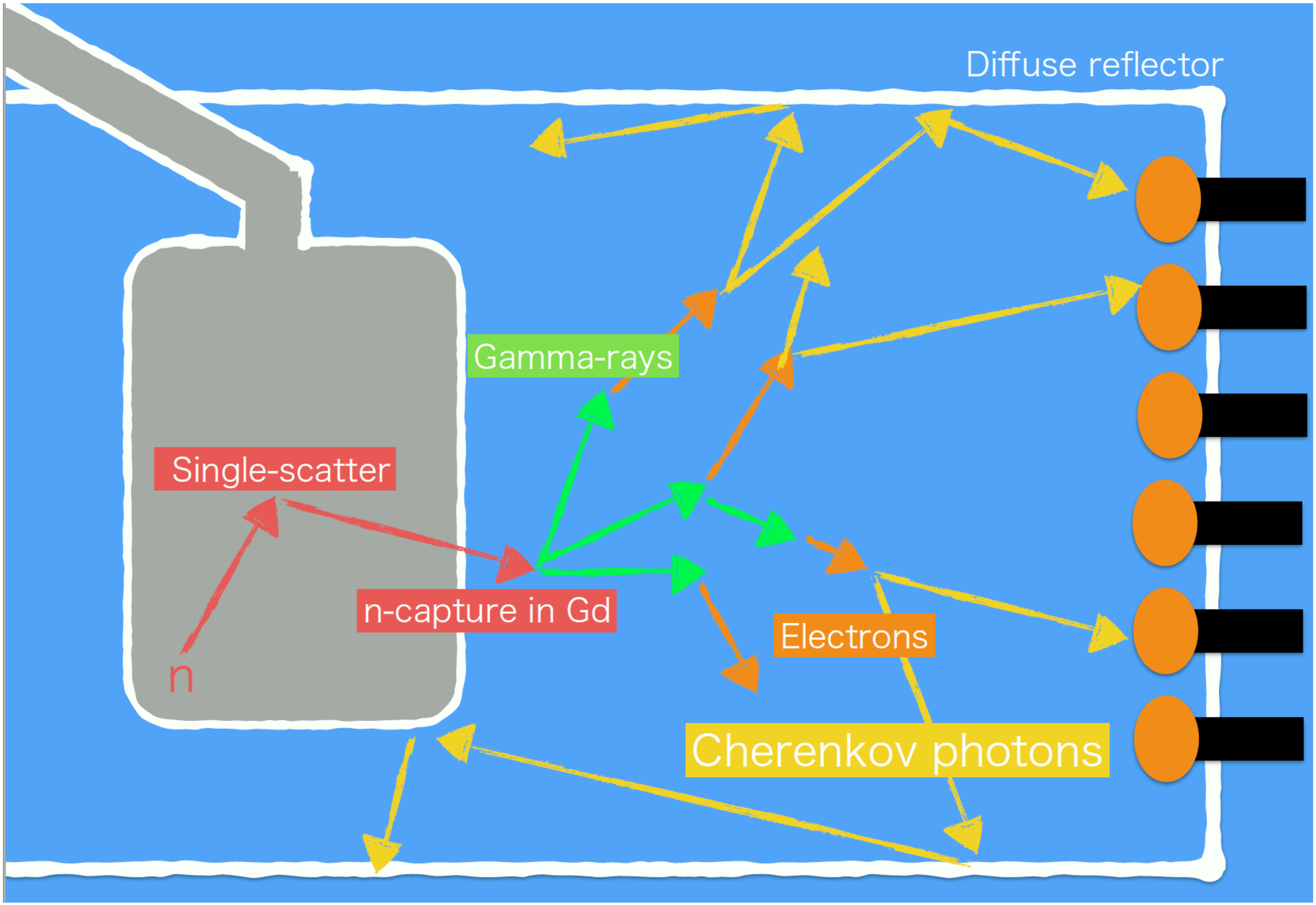

XENONnT nVeto

- Gd-loaded Water: 0.2% of Gd in mass
  -> 3.4 t of Gd-sulphate-octahydrate;
  (technology from EGADS-SK colleagues)

- Cerenkov light is seen by additional 120 8” PMTs placed in water around the cryostat;

- high-reflectivity foil to confine an inner nVeto region with high light collection efficiency.

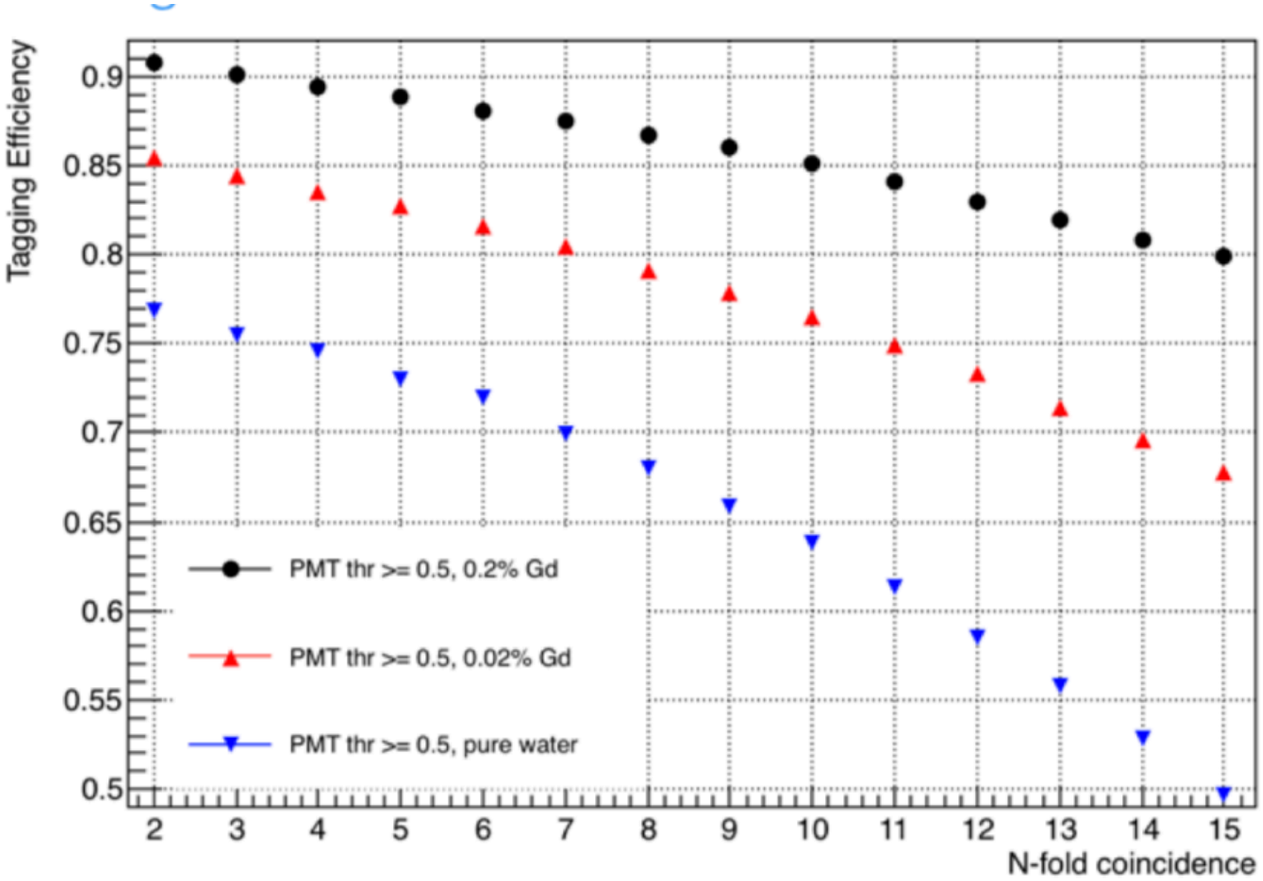

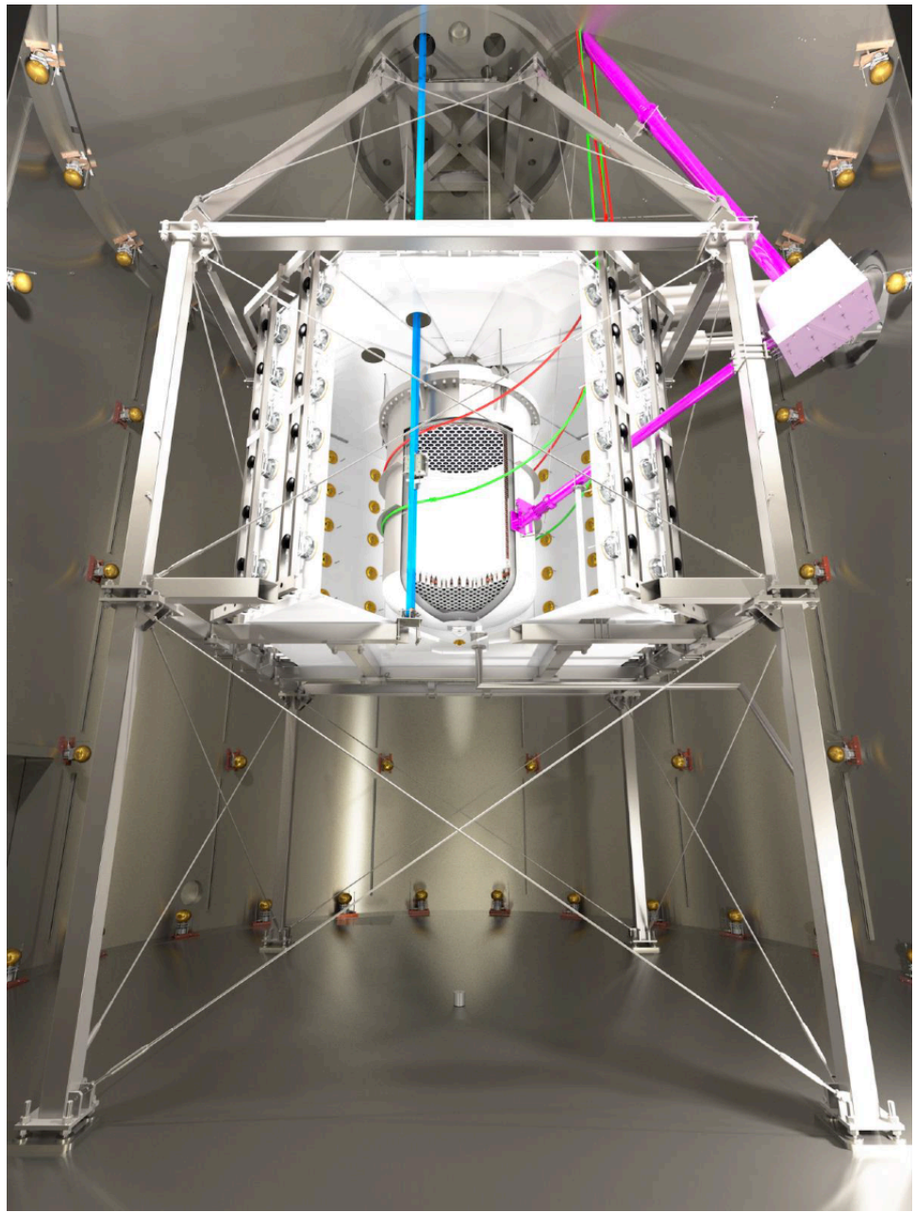

Neutron tagging efficiency:
85% with 0.2% Gd,
65% with pure water
(requiring a threshold of 10 PMTs in coincidence)

Making the nVeto:
https://www.youtube.com/watch?v=xb6aXrbGMR8

Gd-doped Neutron Veto (2023)

Gd-doped Neutron Veto (2023)

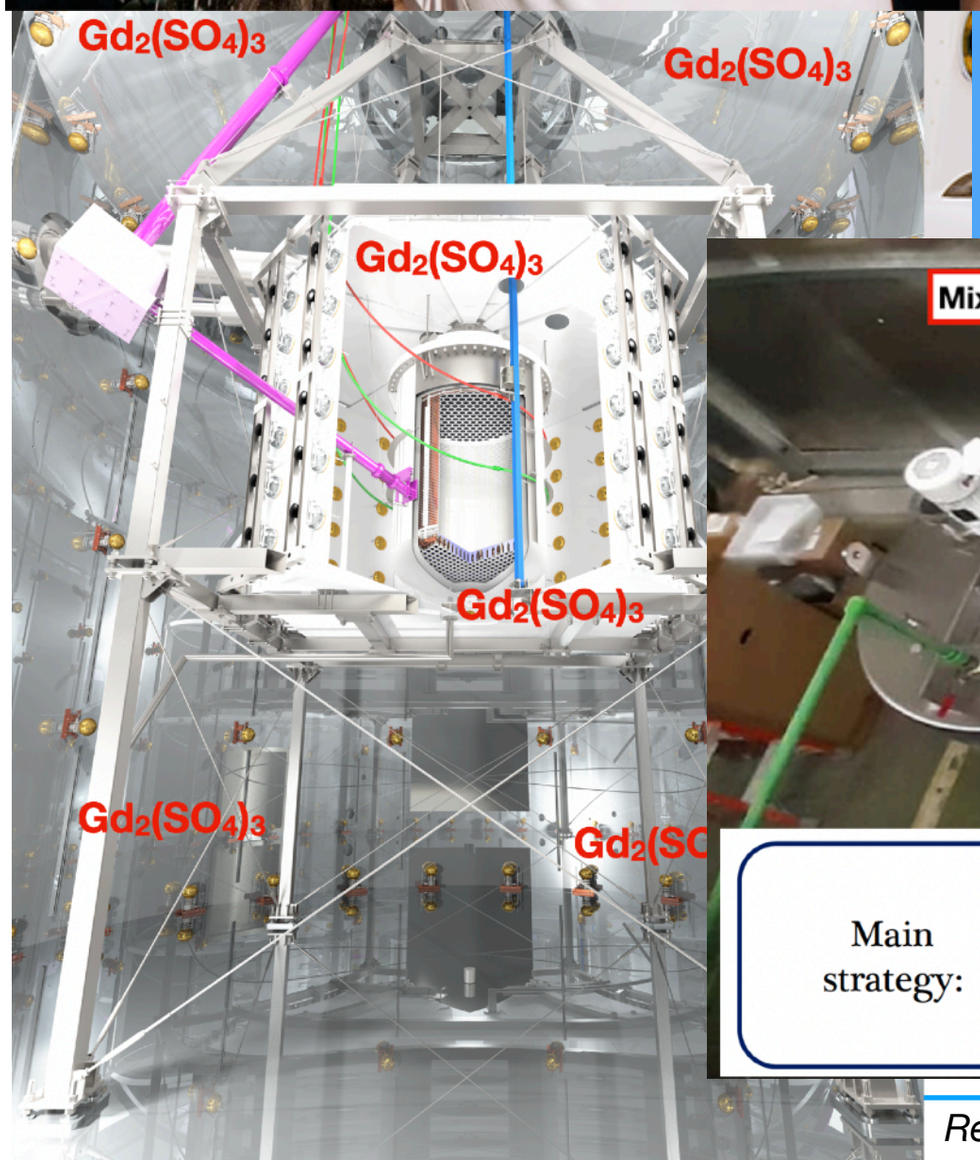

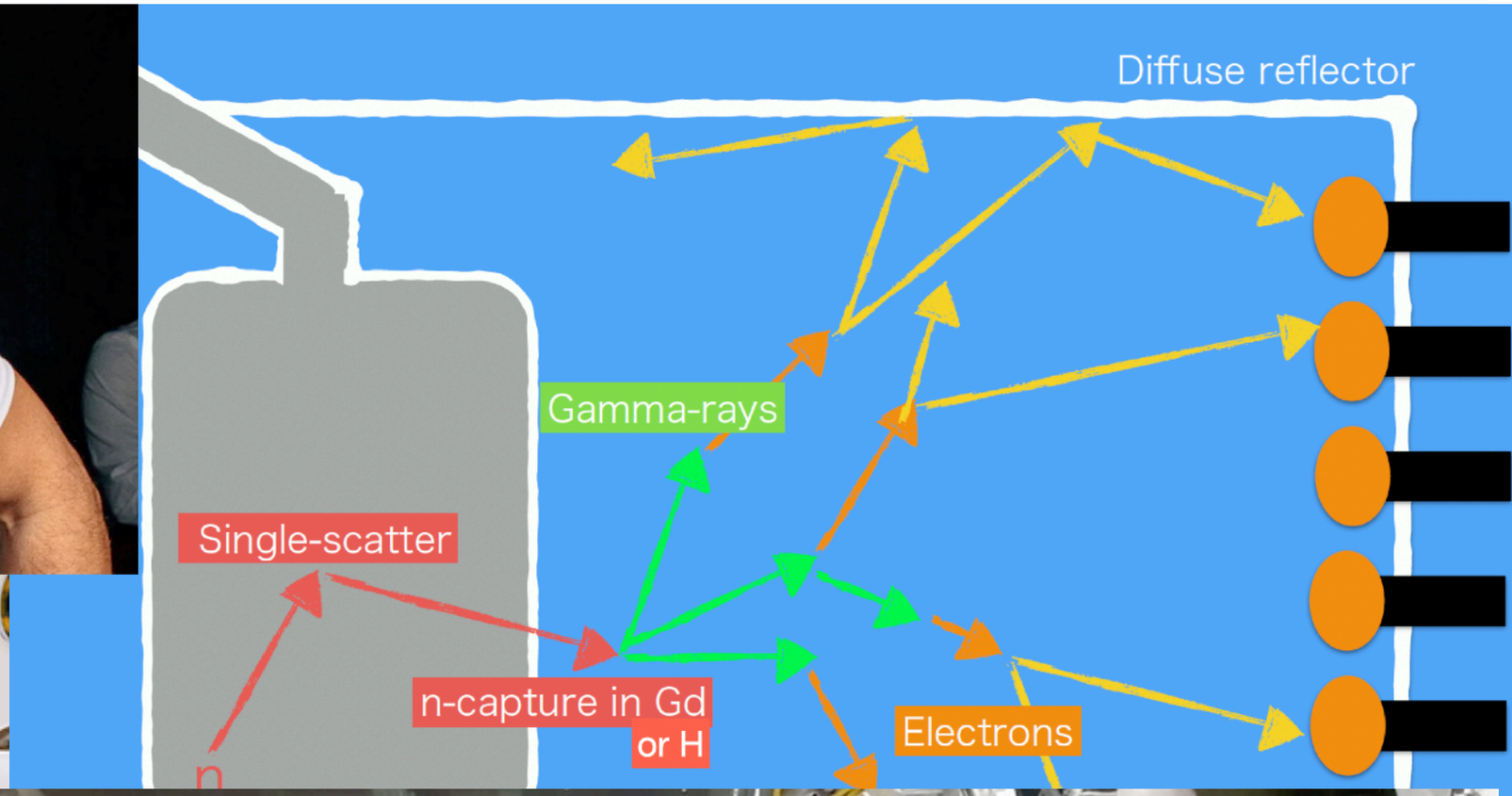

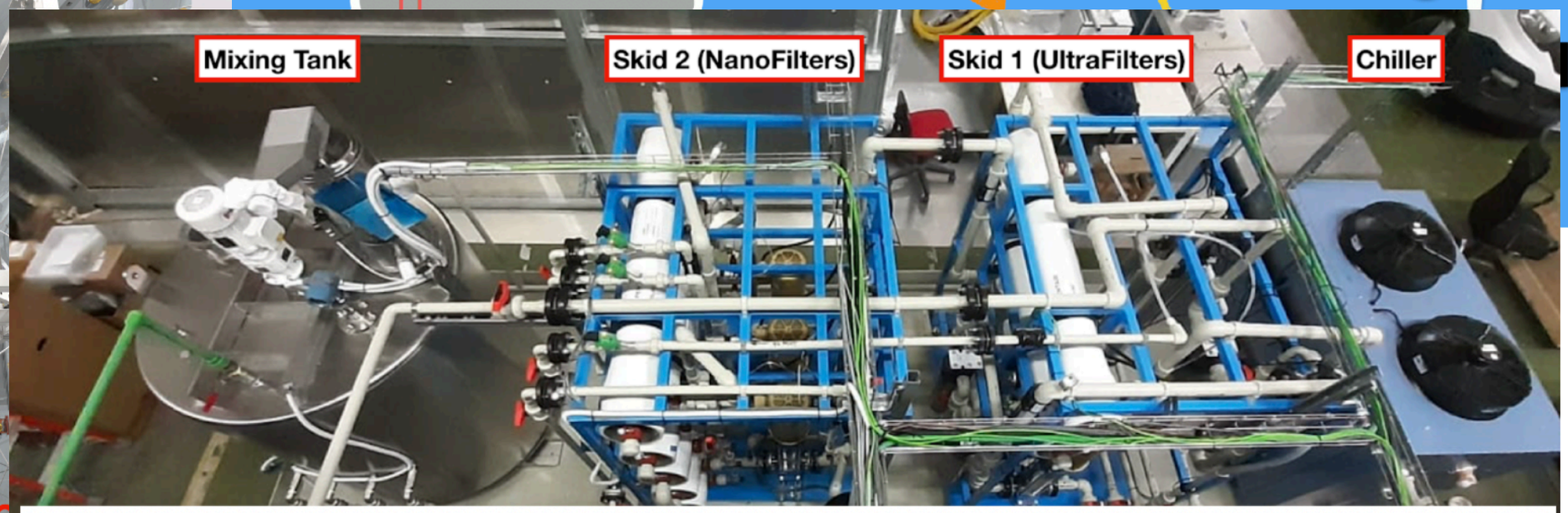

nVeto performance with GdWater

Marco Selvi | selvi@bo.infn.it

AmBe calibration with **source close** to **cryostat** (**~ 1 cm**) → events with **same** characteristics of **neutron** emitted from **detector materials**

Neutron **capture time** and **area spectrum** can be **estimated** by using **NV** only (**self-trigger**), by looking for NV events **following 4.4 MeV** signals from AmBe source in NV

At 500 ppm GdSO, **average** neutron **capture time** around **77 µs** (2x **shorter** than in **demi-water**) and **larger** average **area**, with a **10% increase** in neutron **captures.**

Tagging efficiency is estimated by **requiring coincidence** with **nuclear recoils** detected in the **TPC**
Neutron tagging efficiency with **500 ppm** of GdSO, in a **250 us** time-window, is about **77%** (about **53%** in SR0):
→ a **factor 2** neutron **background reduction** wrt SR0 with demi-water

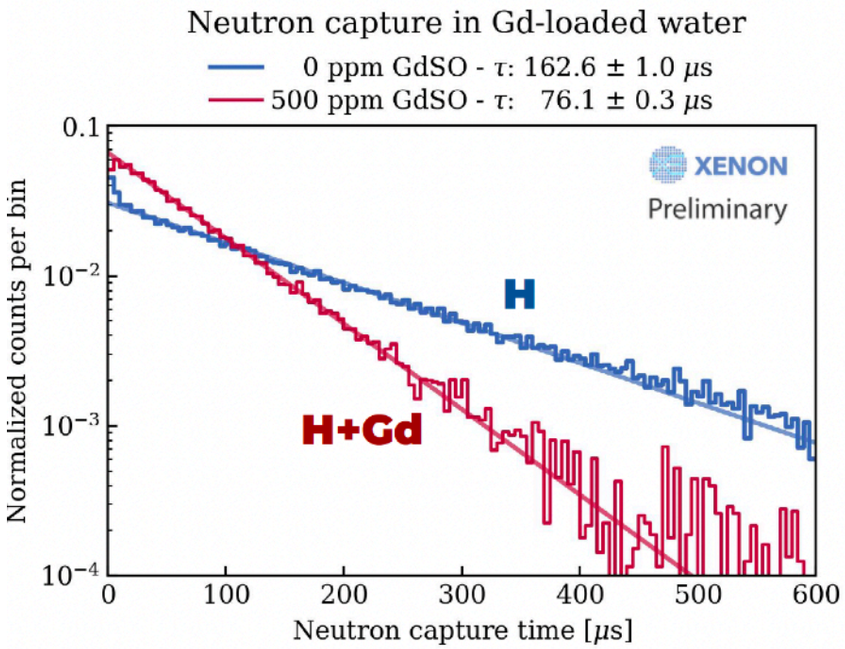

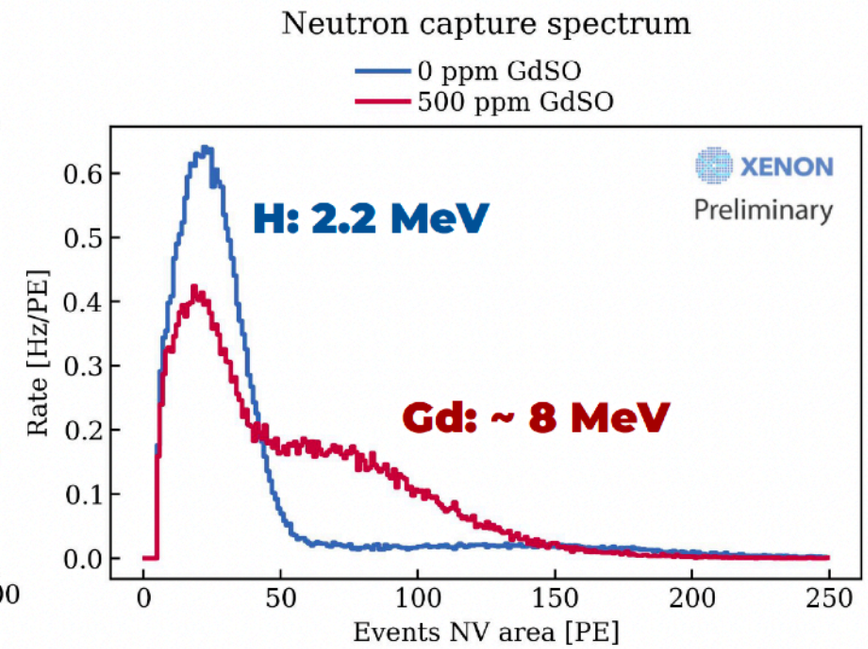

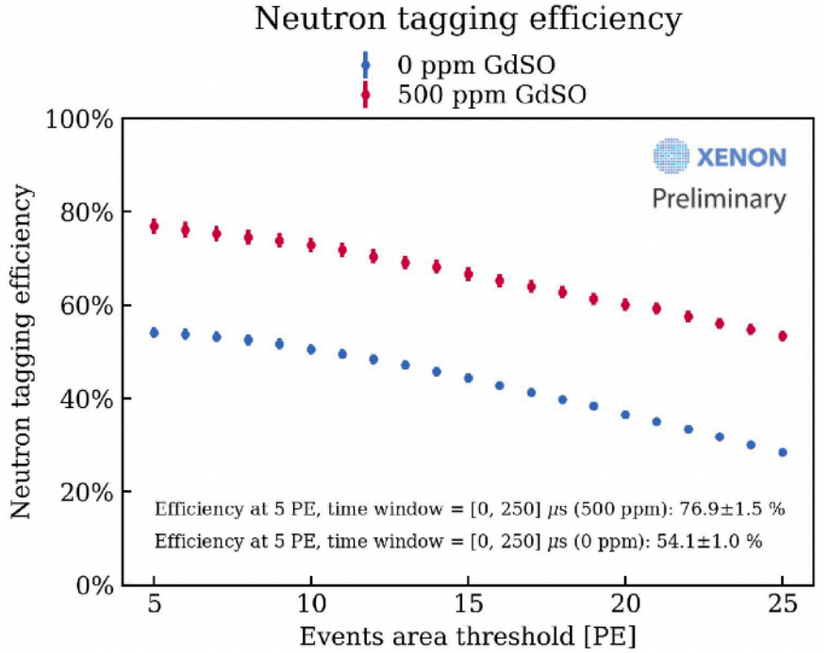

XENONnT Science Runs 0 and 1

Marco Selvi | selvi@bo.infn.it

Science Data Overview

Maxime Pierre
maxime.pierre@nikhef.nl

6 TAUP 2025

XENON

Fiducial Mass: about 4 tonne

Exposure: 3.1 tonne x year

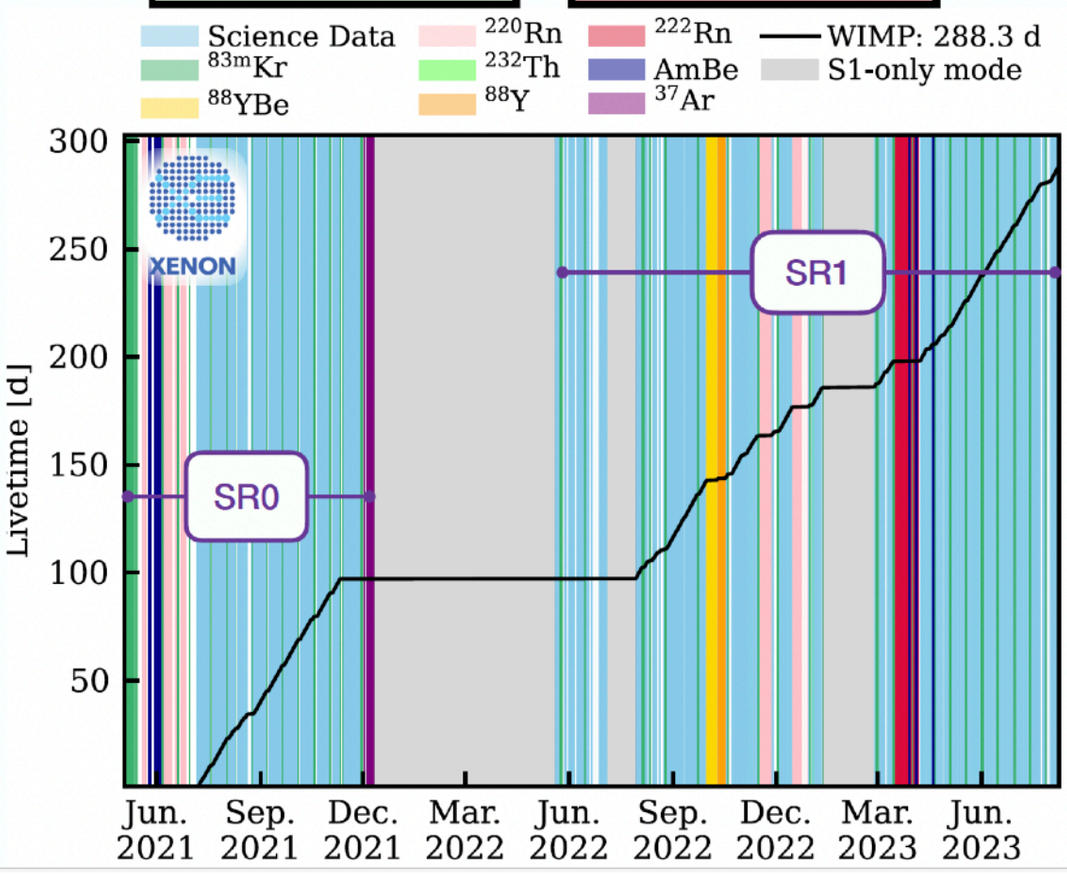

Stable Light (Charge) Yield with **variation < 1% (3%)**

Milestones Highlights

Continuous Rn online distillation

$^{222}Rn_{SR0}$: 1.9 μBq/kg

$^{222}Rn_{SR1}$: **0.9 μBq/kg**

Eur. Phys. J. C 82 (2022) 1104

Kr distillation

^{nat}Kr/Xe concentration **< 50 ppq**

Eur. Phys. J. C 77 (2017) 275

LXe Purification

Electron Lifetime **> 10 ms**

Eur. Phys. J. C 82 (2022) 860

Triggerless DAQ

DAQ shared between three detectors

Improve low-energy sensitivity

JINST 18, P07054 (2023)

I dati analizzati e i risultati pubblicati fino ad ora si riferiscono ai Science Run 0 e 1

XENONnT WIMP results (SR0+1)

Marco Selvi | selvi@bo.infn.it

SR0+1: WIMP Search **Unblinding**

Maxime Pierre
maxime.pierre@nikhef.nl

XENON

Blind analysis with 3.1 tonne x year exposure

- **Unbinned likelihood:** separate terms for SR0, SR1a, and SR1b and near and far-wire regions

- **Two steps unblinding in SR1 to identify ER leakage:**
  - ➡ Small region above NR median and E > 5 keVER
  - ➡ Followed by full unblinding

No excess over background observed

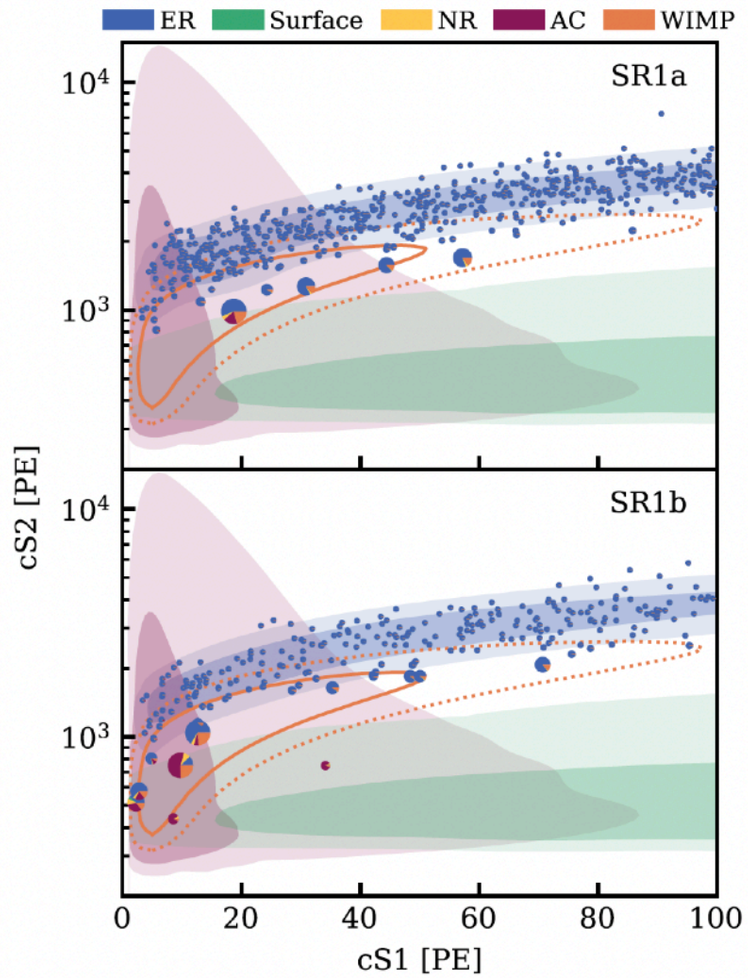

XENONnT WIMP results (SR0+1)

Marco Selvi | selvi@bo.infn.it

SR0+1: WIMP Search Results

Maxime Pierre
maxime.pierre@nikhef.nl

XENON

New limits on WIMP-nucleon cross-section. Improvement from SR0 by a factor ~1.5

Most stringent limit :
1.7 x 10^{-47} cm^2 @ 90% CL for WIMP mass of 30 GeV/c^2

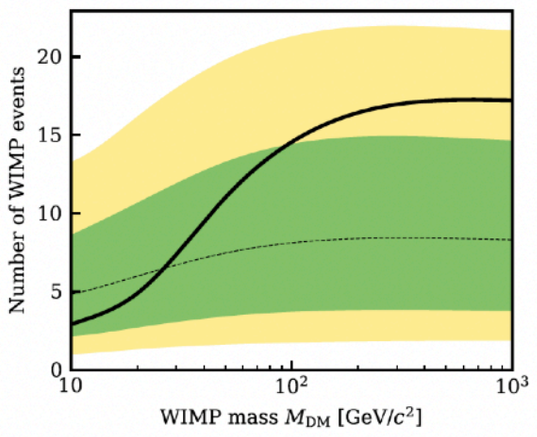

arXiv:2502.18005

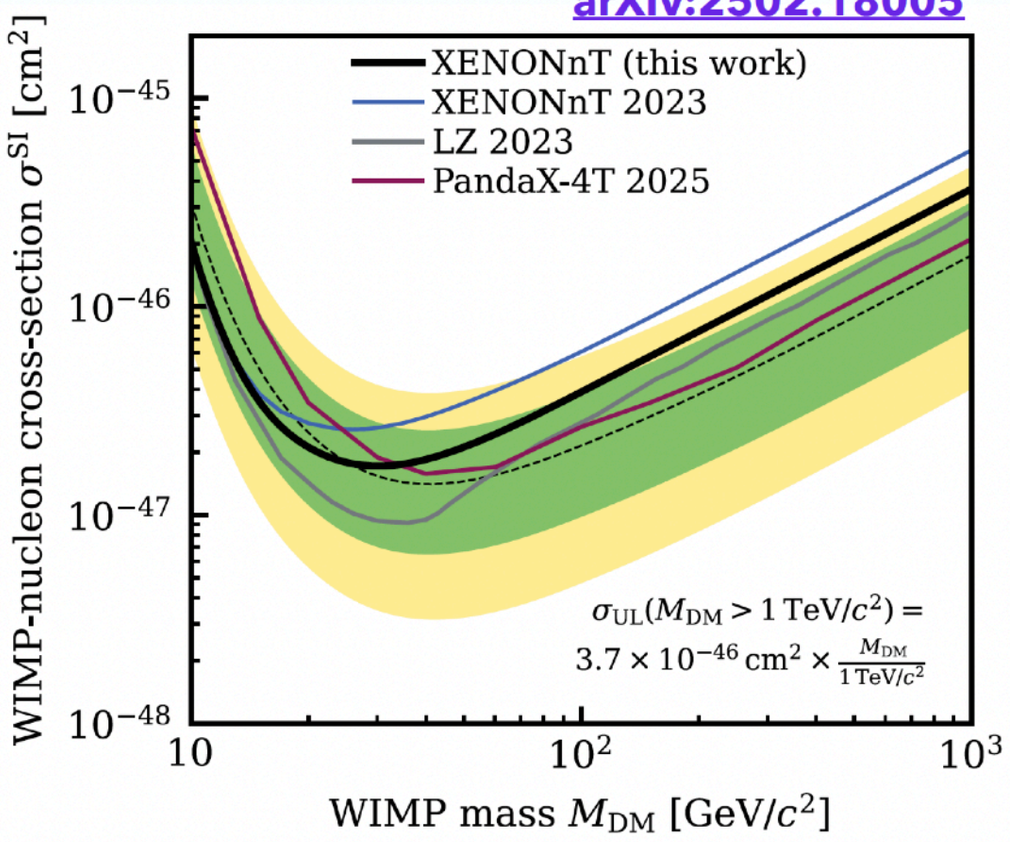

Marco Selvi | selvi@bo.infn.it

Phys.Rev.Lett. 133 (2024) 19, 191002
arXiv:2408.02877

SOLAR ^{8}B CEνNS

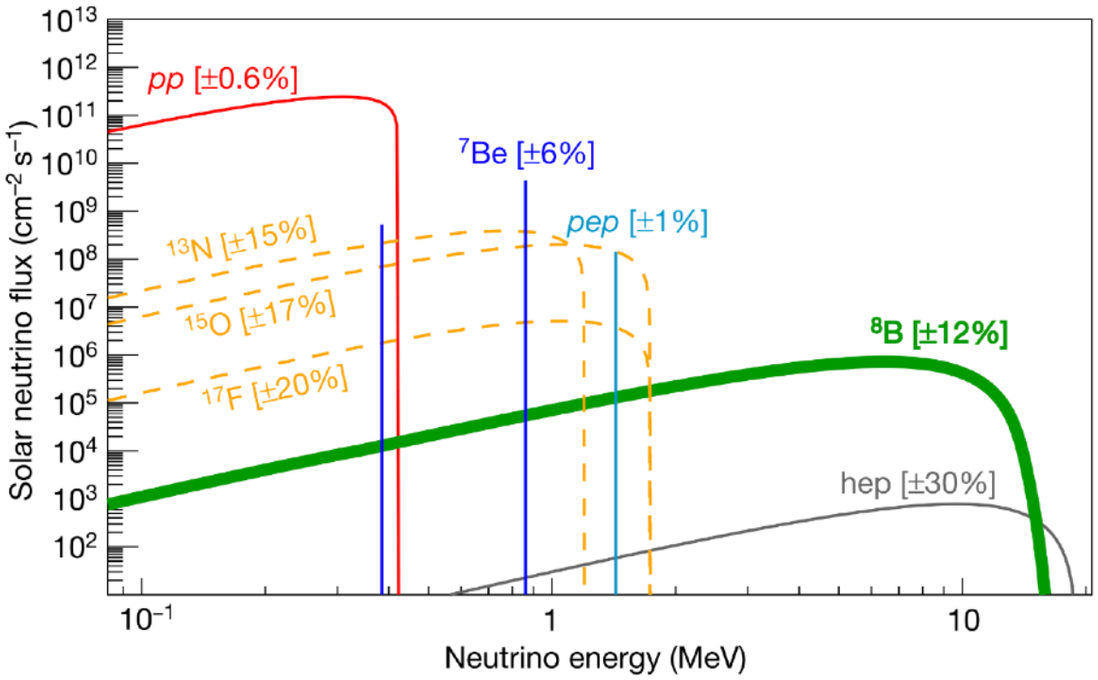

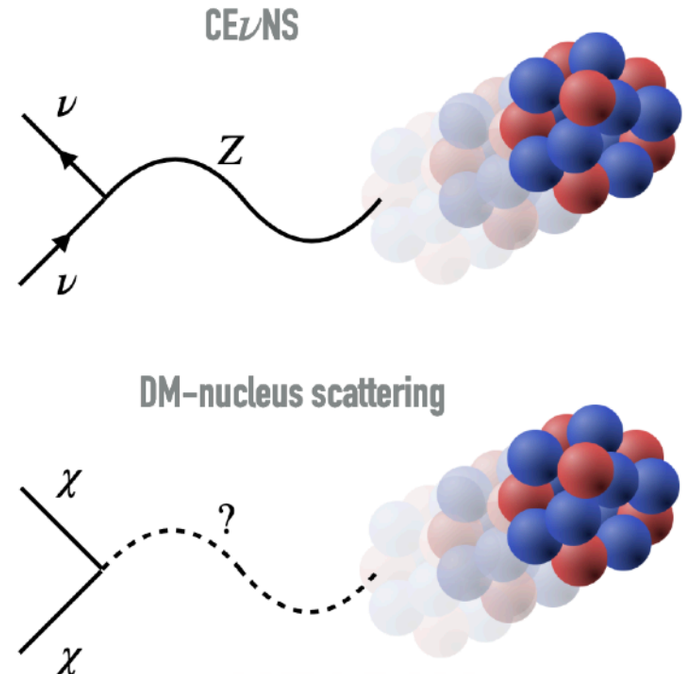

NEARLY INDISTINGUISHABLE

- CEνNS: Coherent Elastic Neutrino-Nucleus Scattering
  - First measured by COHERENT (2017) from a spallation neutron facility
  - Never measured in a xenon target
- ^{8}B CEνNS: Expected to have the largest detectable number of CEνNS events in xenon
  - Signature nearly indistinguishable from 5.5 GeV/c^2 WIMP with spin-independent $\sigma_{\mathrm{SI}} = 4.4 \times 10^{-45}$ cm^2 nuclear recoil

XENONnT 8B results

Marco Selvi | selvi@bo.infn.it

SOLAR ^{8}B CEνNS

- Nearly invisible in conventional 3-fold analysis that requires ≥ 3 detected photons
  - Can try to measure by **lowering energy threshold** in analysis
  - Need to be sensitive to nuclear recoil with energy ~1 keV_{NR}
- Goal: A **BLIND** search for ^{8}B CEνNS
- A measurement of ^{8}B CEνNS means:
  - Sensitivity to DM-like weak coherent scattering
  - And...

^{8}B CEνNS Typical recoil energy: ≤ 1.5 keV_{NR}

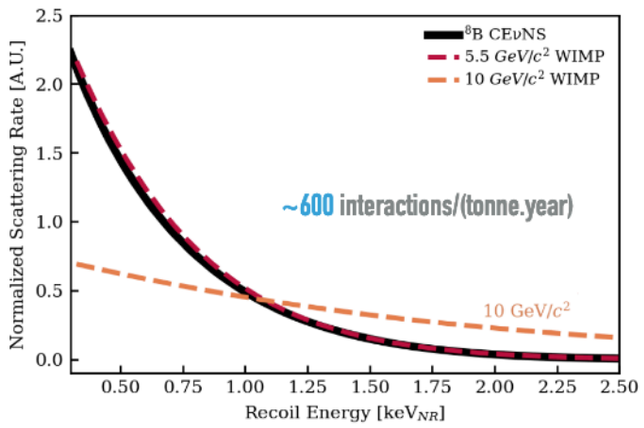

Conventional "3-fold analysis": detection efficiency ~ 1 %

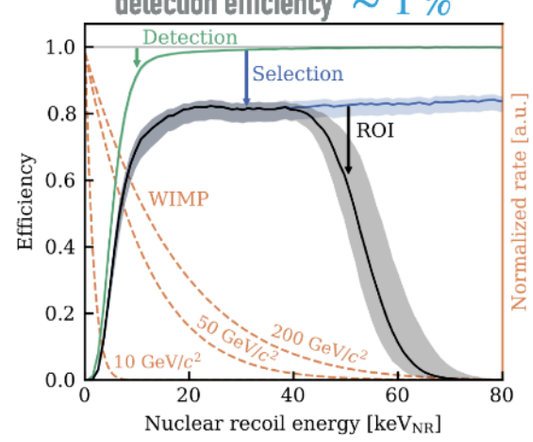

Accpetance with data-selection embedded

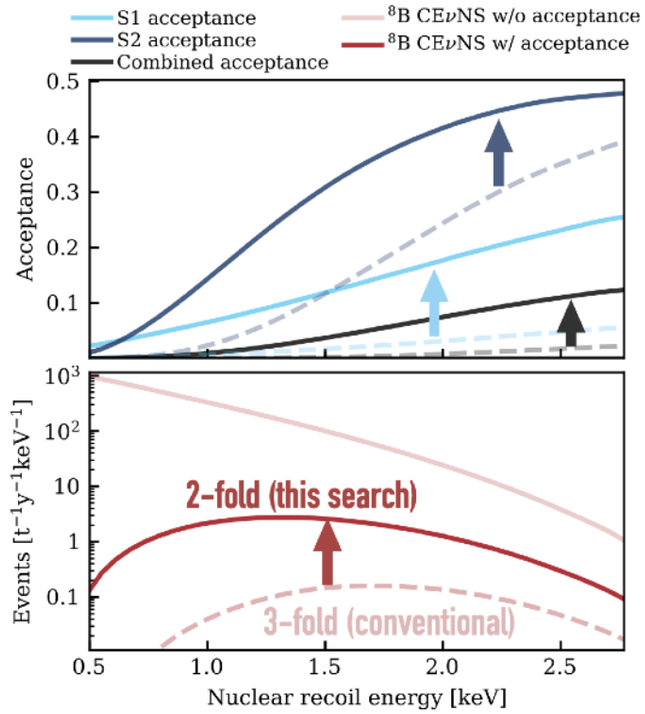

FIRST detected astrophysical ν in a dark matter detector
FIRST measured CEνNS from astrophysical ν source
FIRST measured CEνNS with a Xe target

~17 TIMES MORE EVENTS

Phys.Rev.Lett. 133 (2024) 19, 191002
arXiv:2408.02877

DOMINANT BACKGROUND: ACCIDENTAL COINCIDENCE

- **Accidental Coincidence (AC)**: Random unphysical pairing of isolated S1 and isolated S2
  - Isolated peaks are believed to be side products of high energy (HE) interactions
  - Exact physical mechanisms of isolated peaks are under investigation
  - Isolated-S1 Rate before mitigation: 15 Hz
  - Isolated-S2 Rate before mitigation: 150 mHz
- **Mitigated** by utilizing selections based on space&time correlation to previous HE interactions
  - Isolated-S1 rate after mitigation: 2.3 Hz
  - Isolated-S2 rate after mitigation: 25 mHz

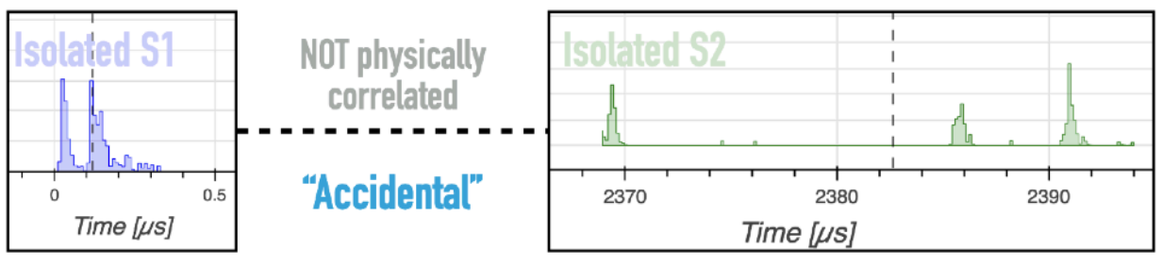

$\text{TimeShadow} \equiv \text{Max}(S2_{pre}/\Delta t_{pre})$ used in inference

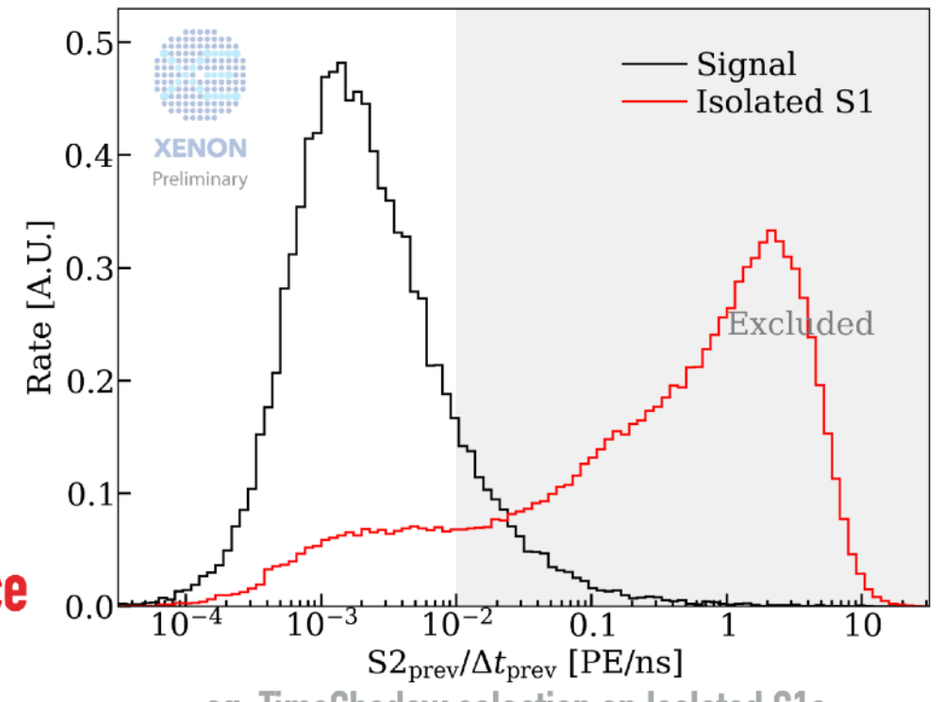

eg. TimeShadow selection on Isolated S1s

Phys.Rev.Lett. 133 (2024) 19, 191002
arXiv:2408.02877

FINAL PREDICTION BEFORE UNBLINDING

Component	Expectation	Best-fit
AC (SR0)	7.5 ± 0.7	
AC (SR1)	17.8 ± 1.0	
ER	0.7 ± 0.7	
Neutron	$0.5^{+0.2}_{-0.3}$	
Total background	$26.4^{+1.4}_{-1.3}$	
^{8}B	$11.9^{+4.5}_{-4.2}$	
Observed		

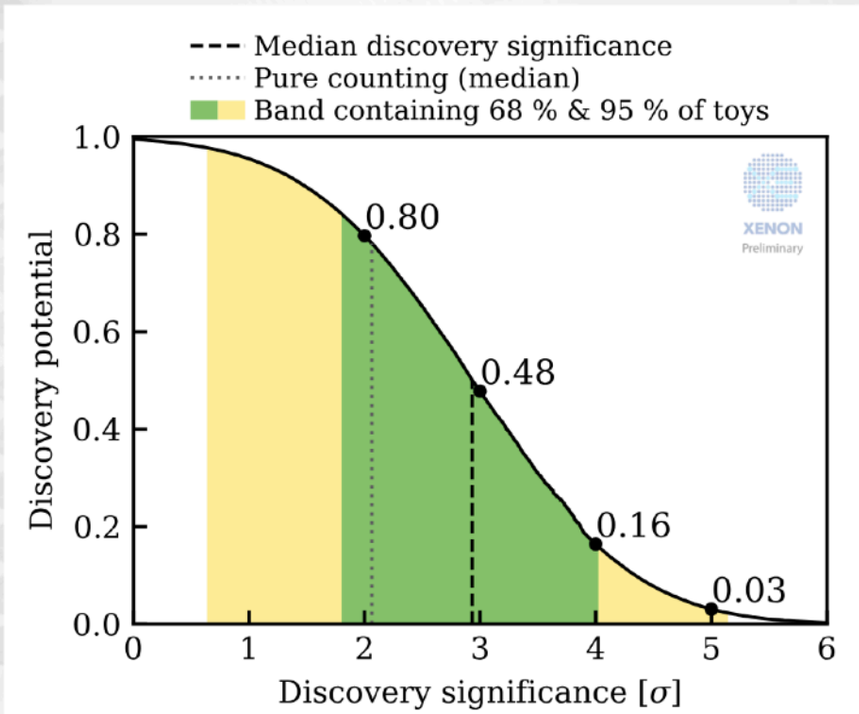

Total exposure: 3.51 ton year

Expect ^{8}B CEνNS: $11.9^{+4.5}_{-4.2}$ Events

$48\,\%$ probability to observe $>3\sigma$ significance

Phys.Rev.Lett. 133 (2024) 19, 191002
arXiv:2408.02877

XENONnT 8B results

Marco Selvi | selvi@bo.infn.it

BEST-FIT AFTER UNBLINDING

Component	Expectation	Best-fit
AC (SR0)	7.5 ± 0.7	7.4 ± 0.7
AC (SR1)	17.8 ± 1.0	17.9 ± 1.0
ER	0.7 ± 0.7	$0.5^{+0.7}_{-0.6}$
Neutron	$0.5^{+0.2}_{-0.3}$	0.5 ± 0.3
Total background	$26.4^{+1.4}_{-1.3}$	26.3 ± 1.4
^{8}B	$11.9^{+4.5}_{-4.2}$	$10.7^{+3.7}_{-4.2}$
Observed	37	

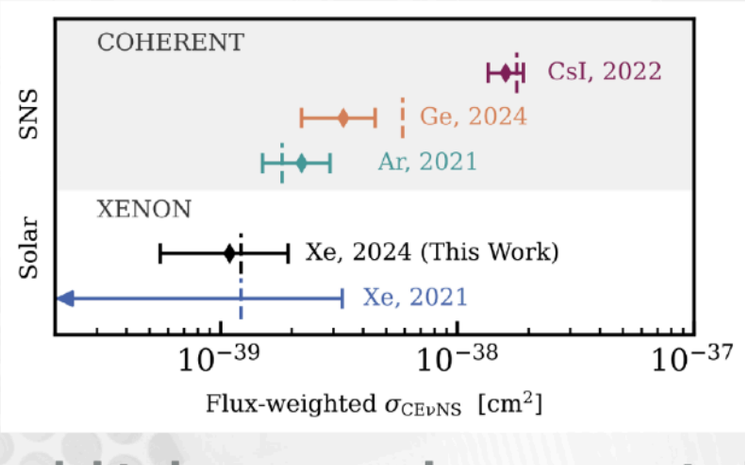

Flux-weighted $\sigma_{CE\nu NS}$ in agreement with SM

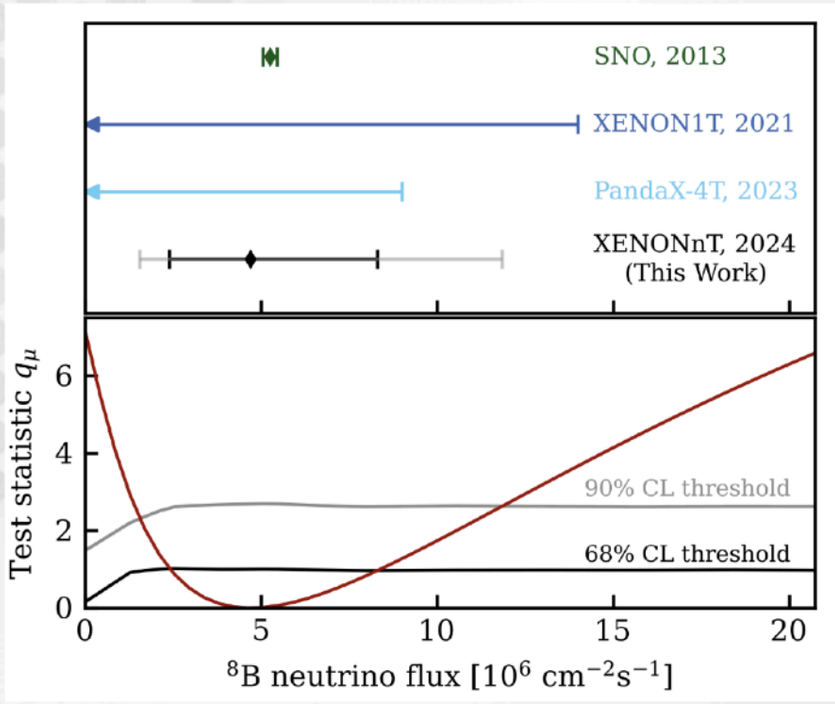

Flux measurement in agreement with SNO (2013)

Phys.Rev.Lett. 133 (2024) 19, 191002
arXiv:2408.02877

Electrode Replacement in the TPC

Marco Selvi | selvi@bo.infn.it

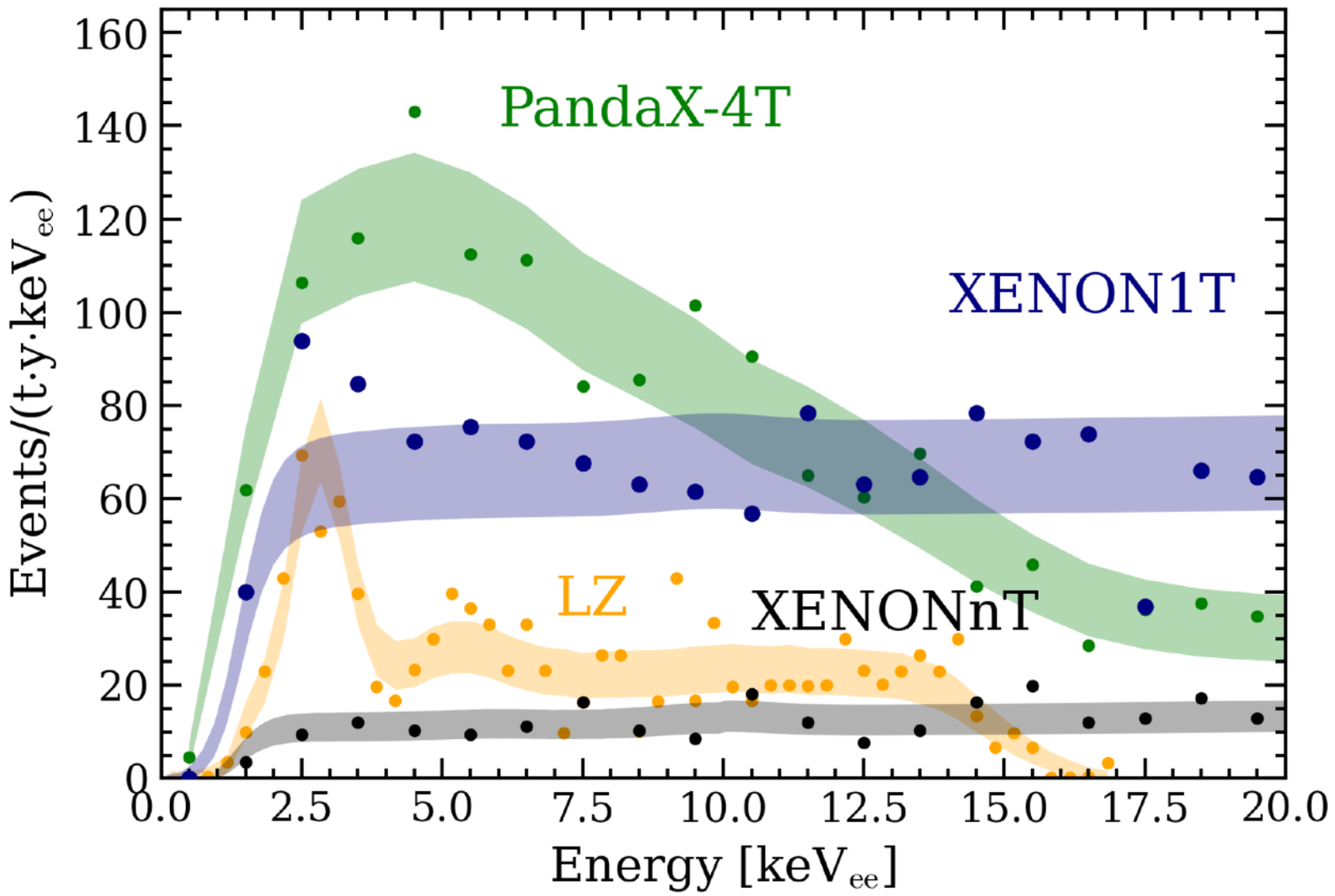

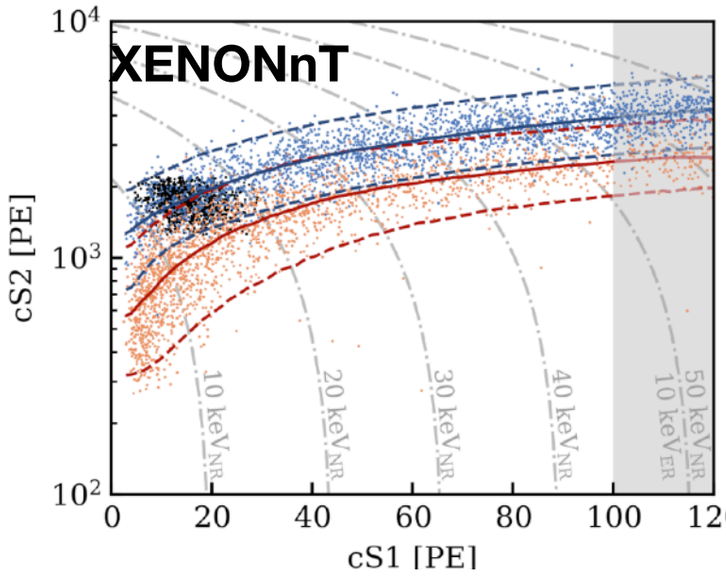

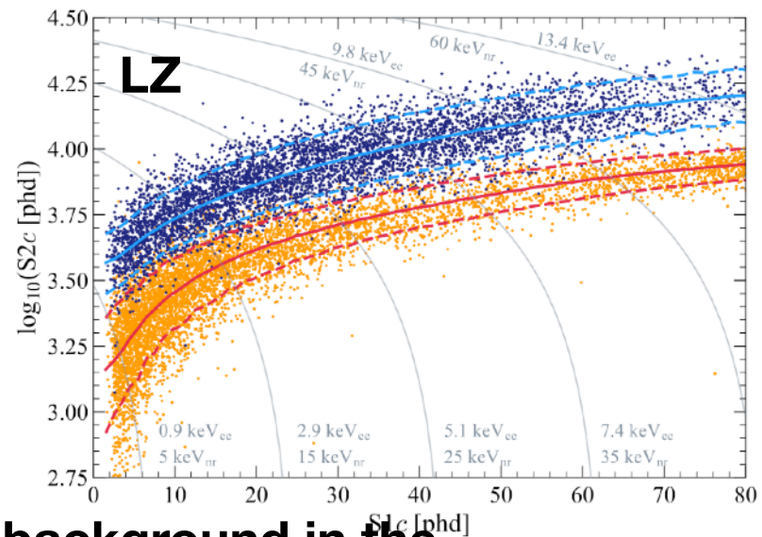

Despite the lower ER background, in XENONnT the most important background in the WIMP ROI comes from ER recoils leaking into the NR band, due to the lower E-field.

Electrode Replacement in the TPC

Marco Selvi | selvi@bo.infn.it

ER-NR Band Separation

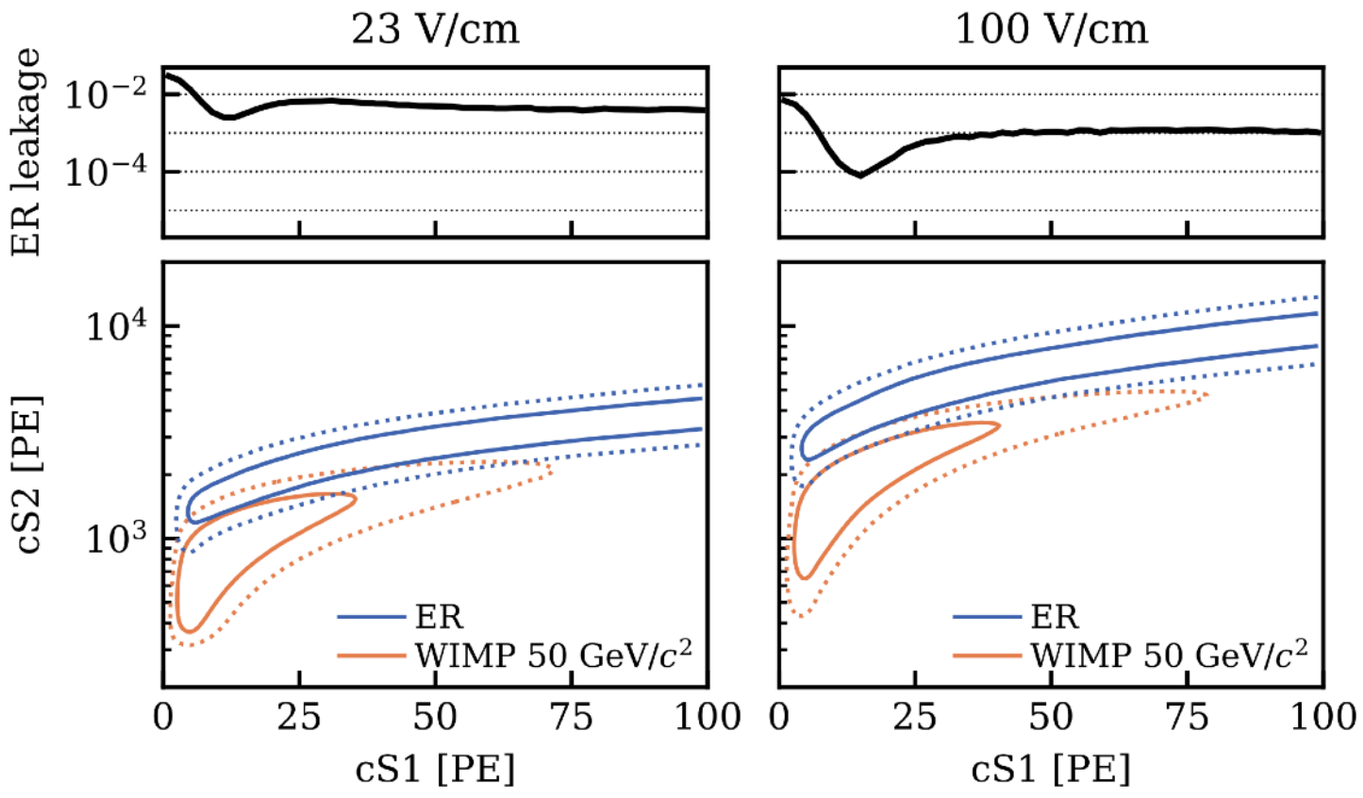

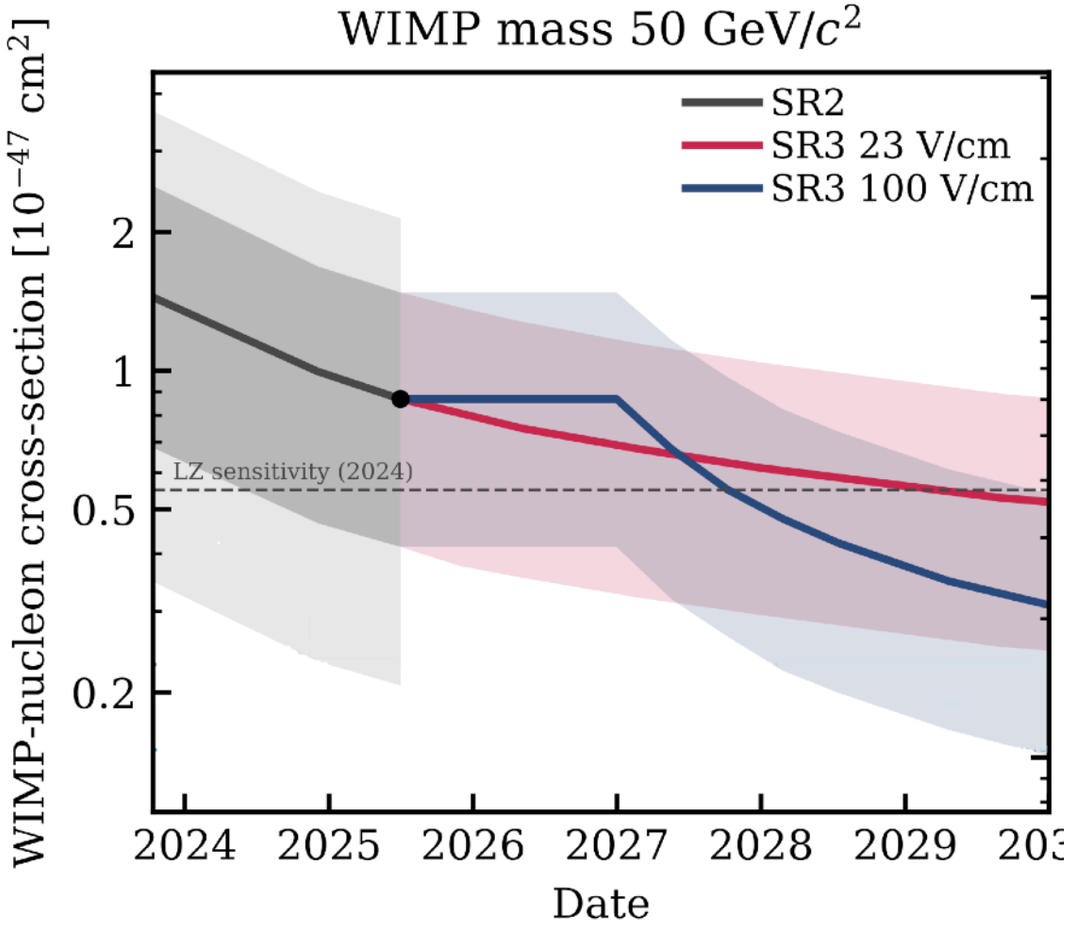

Fraction of ER background below NR median

New electrodes assembled and tested

Marco Selvi | selvi@bo.infn.it

Cathode (hexagonal mesh)

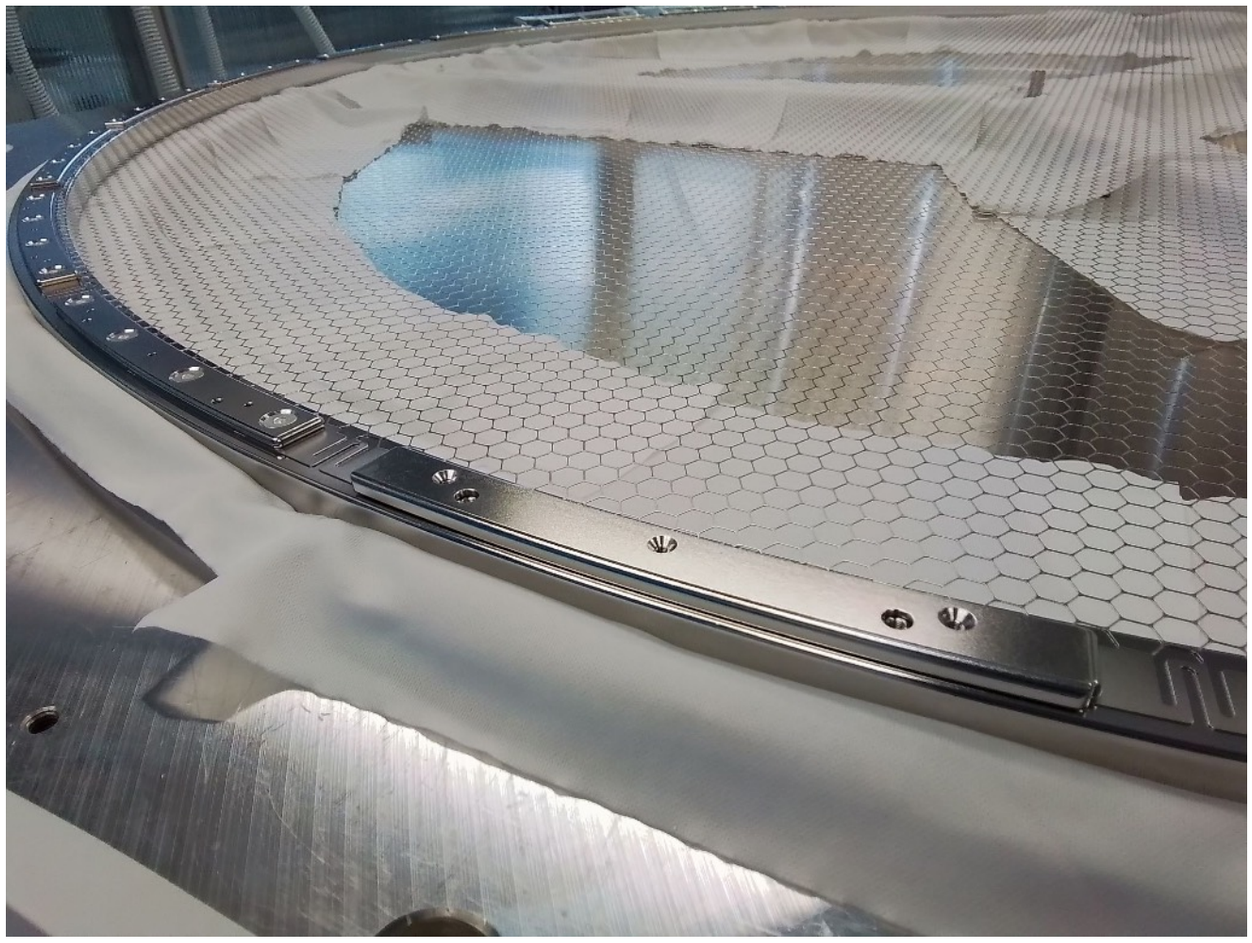

Anode (reinforced ring, higher wire tension)

Successfully tested in LXe in 2024.

next step beyond
XENONnT: XLZD

next-gen LXe exp.: XLZD

XLZD ~~Consortium~~ -> Collaboration

Leading Xenon Researchers unite to build next-generation Dark Matter Detector

SURF is distributing this press release on behalf of the DARWIN and LZ collaborations

July 20, 2021

Successful joint XLZD meeting June 27-29 at KIT
https://xlzd.org/
White paper (2203.02309)

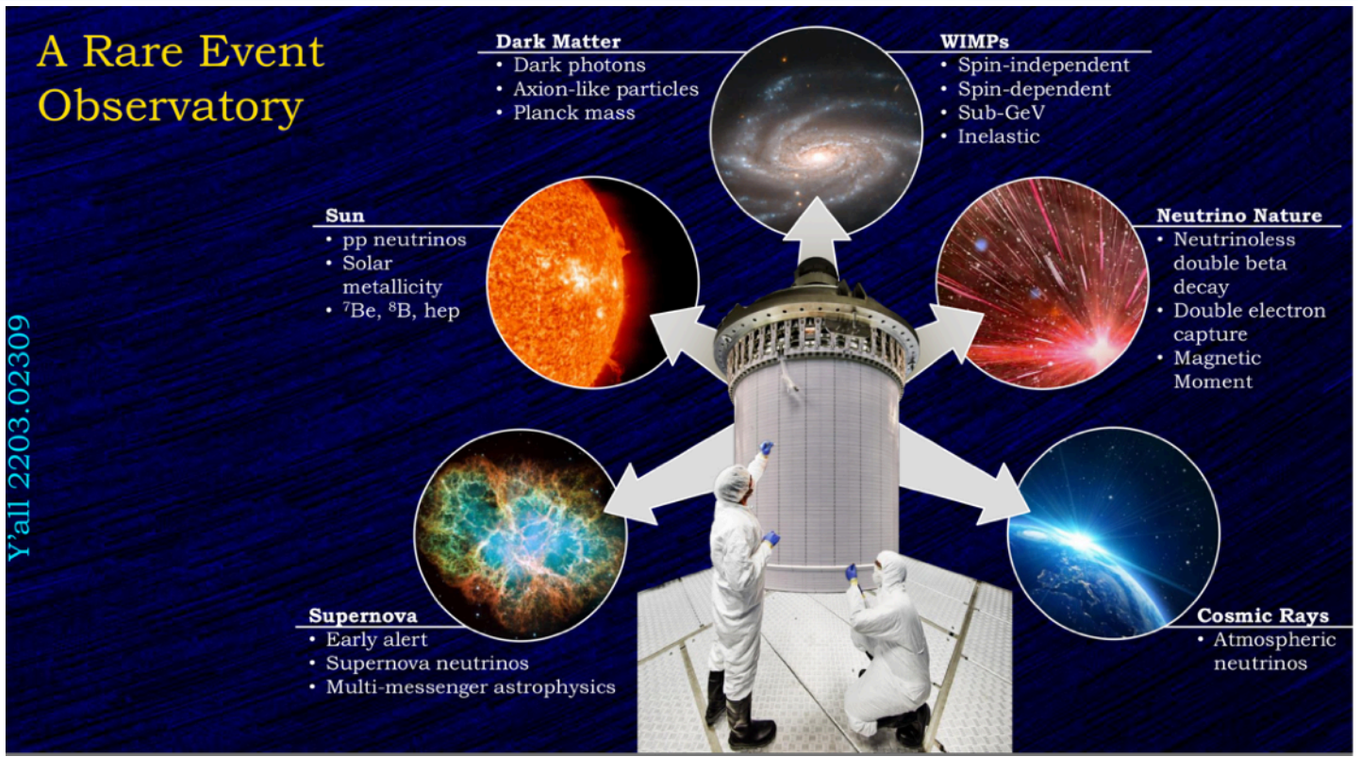

450 ricercatori (PhD excluded), 70 istituzioni, 16 nazioni
Spokespersons: Dan Akerib (LBNL), Marc Schumann (U. Freiburg)

Exec Committee: H. Araujo (Imperial), L. Baudis (Zurich), P. Decowski (NIKHEF),
T. Fruth (Sydney), H. Lippincott (UCSB), K. Ni (UCSD), K. Palladino (Oxford), M. Selvi (INFN Bologna), K. Valerius (KIT), M. Yamashita (Tokyo)

XLZD meeting in July 2025 @LNGS

XLZD -> next-gen LXe detector

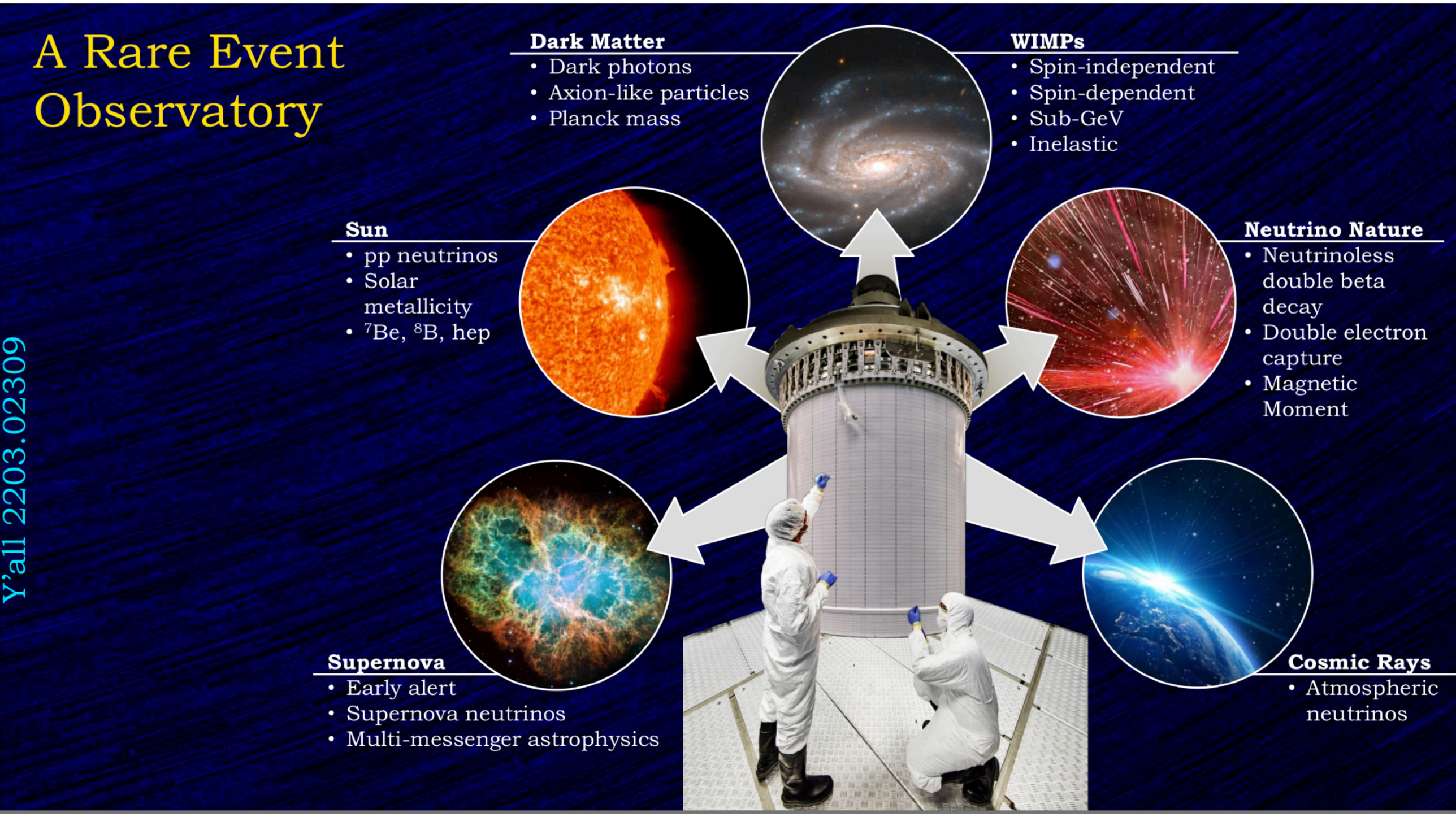

XLZD scale & goals

Early phase (<40 t active) | **Nominal (60 t active)** | **Opportunity (80 t active)**

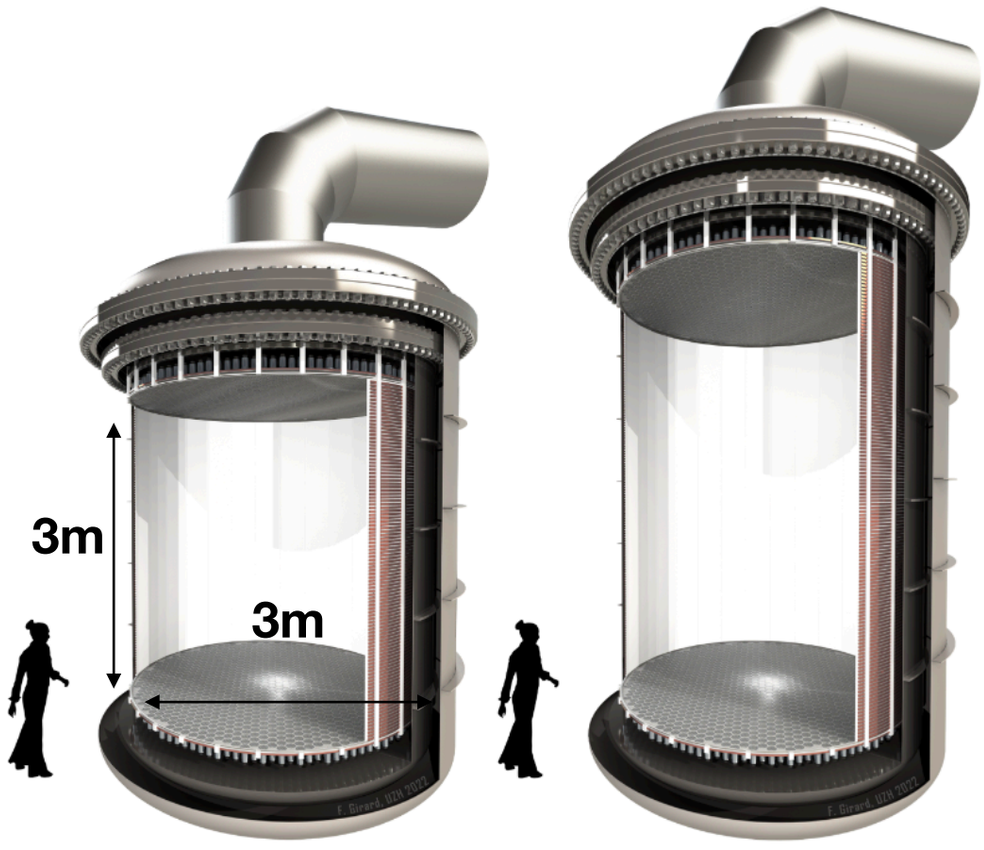

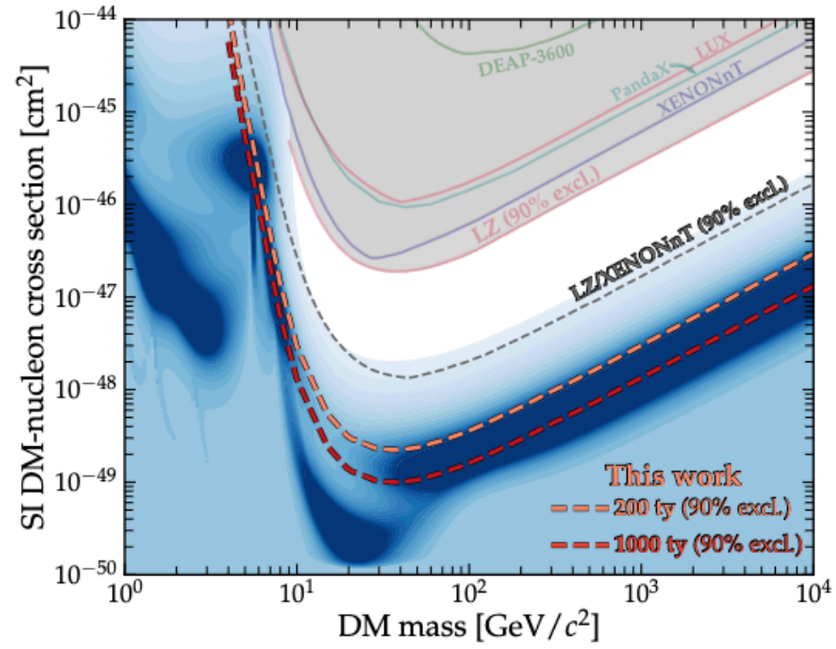

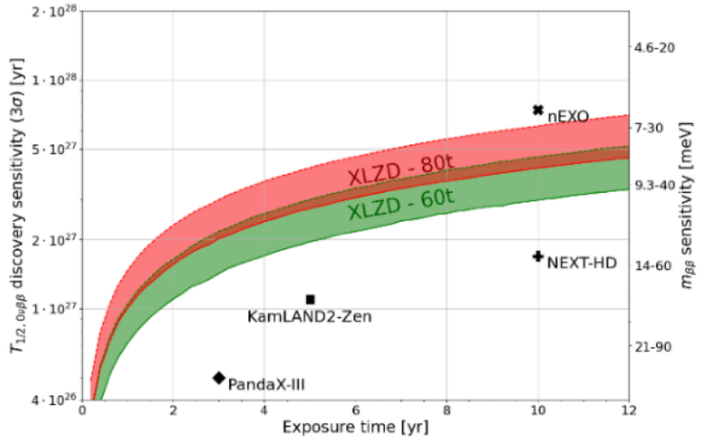

Figure 7: XLZD experimental strategy: the nominal system (left) features a LXe-TPC with 1:1 aspect ratio for 60 tonnes of active mass (~3 m in diameter and height); the nominal system could be readily upgraded to 80 tonnes (~3 m in diameter and ~4 m in height) of active mass should the xenon market allow a faster acquisition rate (right).

Sites for XLZD

Site shortlisting:

- Boulby (UK)
~~- Kamioka (Japan)~~
- LNGS (Italy)
- SNOLab (Canada)
- SURF (US)

Kamioka is too shallow, the others are fine.

LNGS is the only one where no excavation is needed.

Decision by 2026.

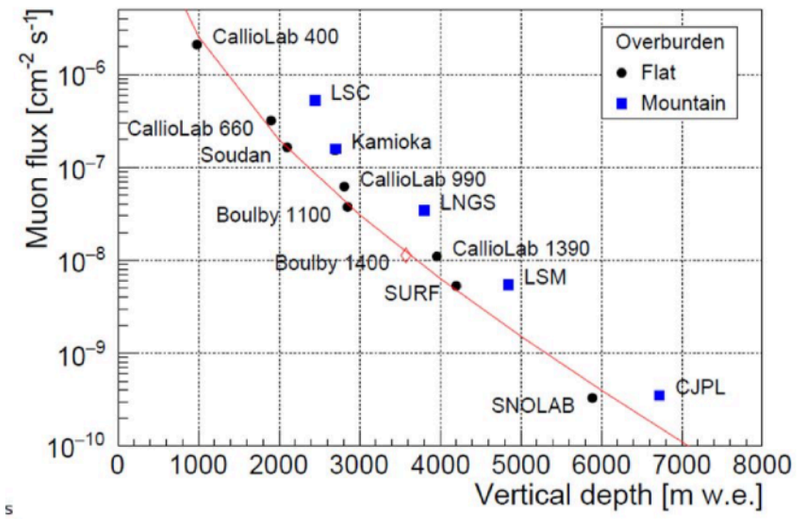

Table 2: Laboratory-related backgrounds – part I.

Laboratory	Muons flux /m^2/d	Muons $\langle E \rangle$ GeV	Neutrons cosmo.† /t/yr	Neutrons radio. 10^{-6}/cm^2/s	Neutrons thermal /cm^2/s
Kamioka	128	273	4.2×10^{-3}	*3.3	1.4×10^{-5}
BUL (Boulby)	32.3	261	1.3×10^{-3}	1.7	tbc
LNGS (Gran Sasso)	29.7	273	1.2×10^{-3}	‡0.6	$1.\times10^{-6}$
SURF (Sanford Lab)	4.6	283	2.0×10^{-4}	1.7	1.7×10^{-6}
SNOLAB	<0.29	310	1.3×10^{-5}	4.6	4.8×10^{-6}

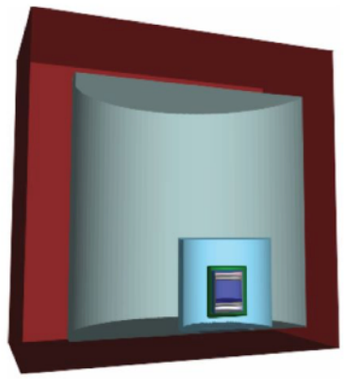

WIMP search

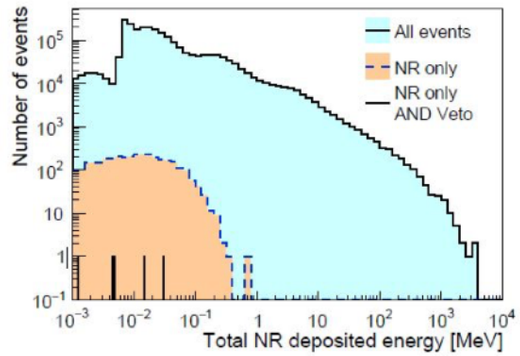

Xe137 activation for 0n2b search

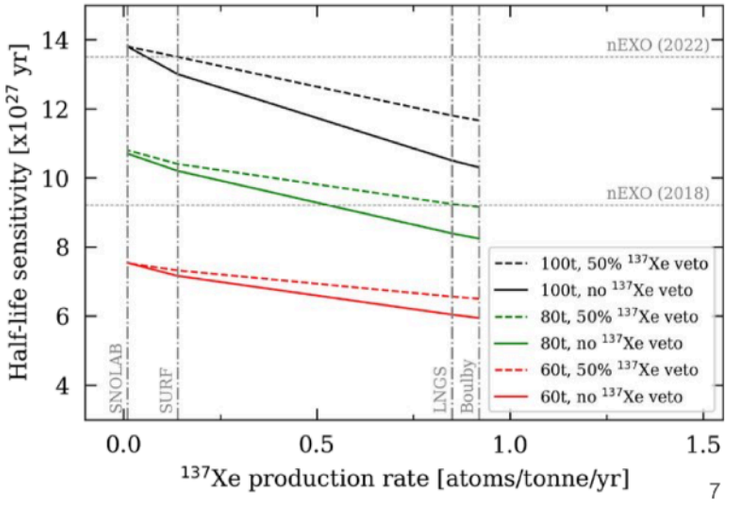

Design studies for XLZD @LNGS

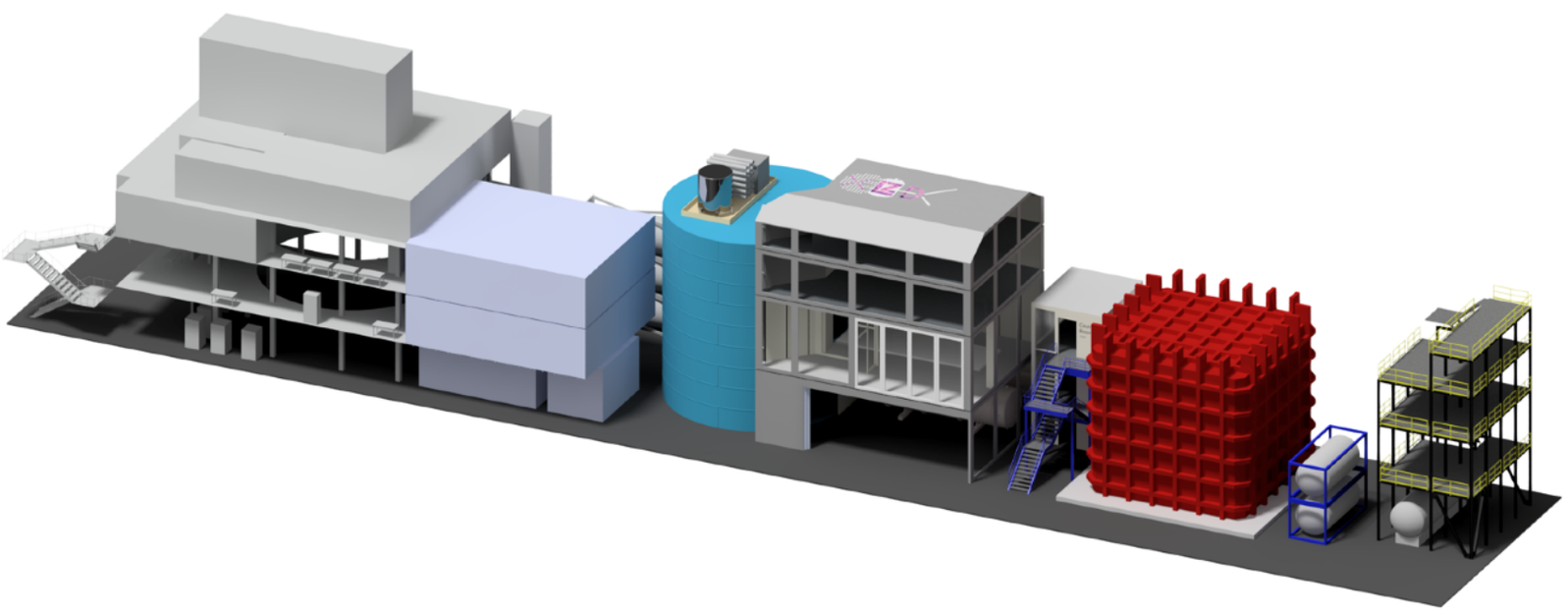

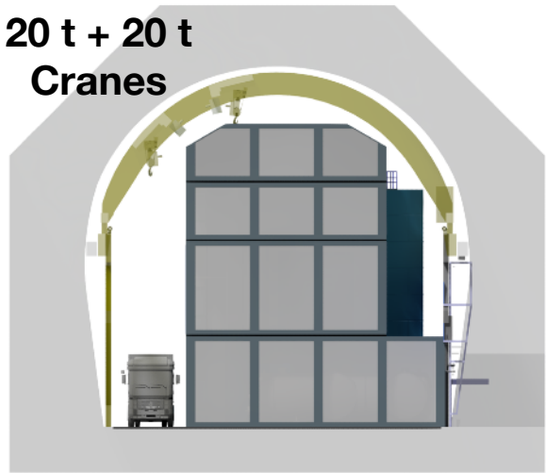

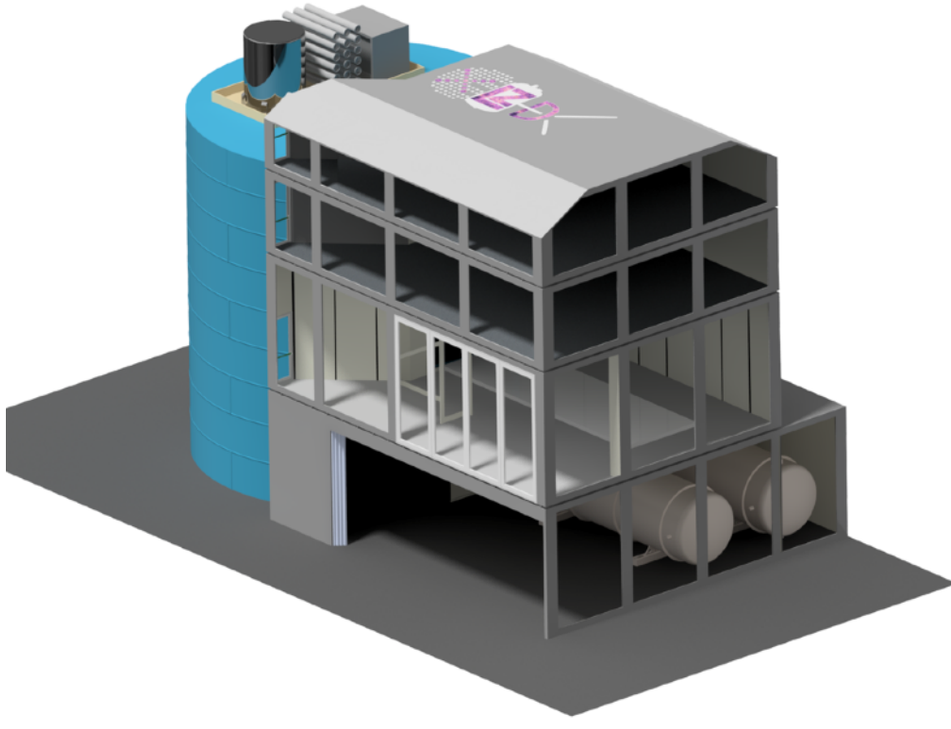

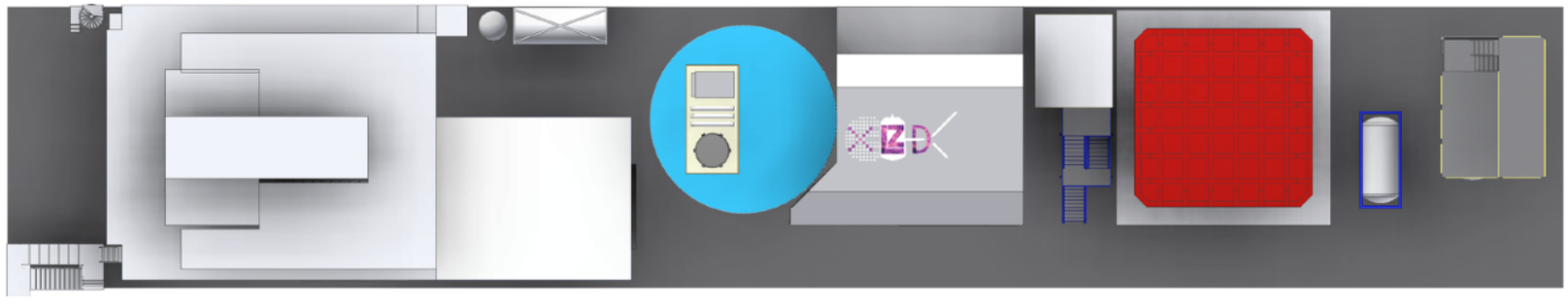

Direct Detection of WIMPs by 2035?

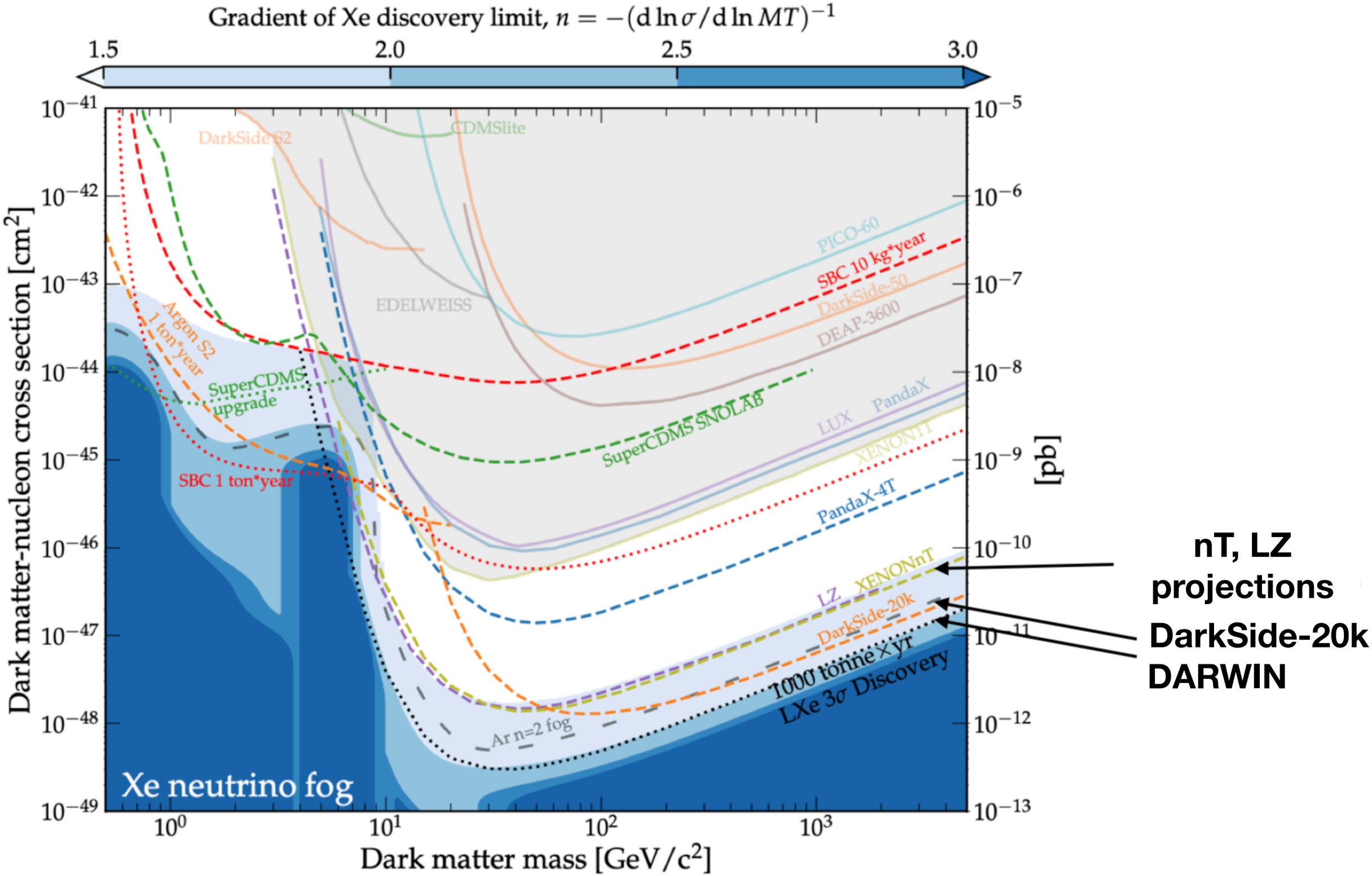

Istituto Nazionale di Fisica Nucleare

Thanks !

Marco Selvi
INFN Bologna

Direct Dark Matter Detection: Lectures for Master and PhD students

Istituto Nazionale di Fisica Nucleare

Thanks !

Marco Selvi
INFN Bologna

Direct Dark Matter Detection: Lectures for Master and PhD students